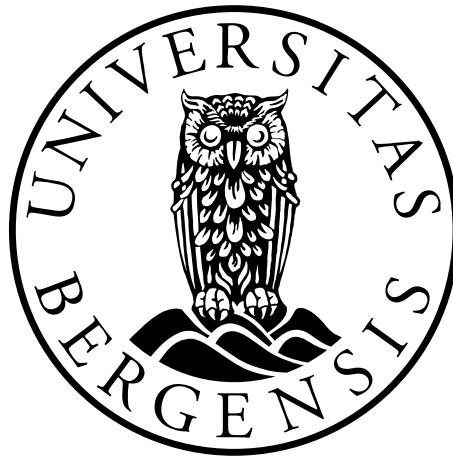


# Characterizing the Predictability of Seasonal Climate in Ethiopia

Diriba Korecha Dadi



Dissertation for the degree philosophiae doctor (PhD) in Meteorology  
University of Bergen, Norway

December 2013



## **Acknowledgements**

First of all, I thank my advisor Prof. Asgeir Sorteberg, for his continuous support during my PhD study. Asgeir is always accessible to advice, involve him in the study, share his knowledge, experience and propose new ideas throughout my study period. He also taught me comprehensive approaches on how to resolve climate prediction problems, overcome research challenges and provided me with the resources needed to accomplish my study successfully. My thanks also go to the National Meteorological Agency of Ethiopia for granting me permission to go for my study. I am also grateful to the staff members of Meteorological Forecast and Early Warning Directorate of NMA, with whom I have been working for the past decades. I would also like to thank Mr. Matheos Hunde, who initially informed me about the Ethiopian Malaria Prediction Systems Project

I wish to thank the staff, students and colleagues at the Geophysical Institute for good working environment. In particular, I want to thank my PhD fellows; Torleif Lunde, Ellen Viste and Dereje Tesfahun for their endless assistance and constant support they offered me during my stay in Bergen. Furthermore, I express my deepest gratitude for Prof. Bernt Lindtjørn, who has brought the idea of the Ethiopian Malaria Prediction Systems project (EMaPS) into existence and the project coordinator, extends his courage and moral thoughts throughout my study period. My study has been funded by the Norwegian Government, through the Ethiopian Malaria Prediction Systems Project.

Last, but not least, I thank my wife Tewabech Abelti and my daughter Deborah and my son Hundaol, for their strong courage leading a lonely life

during my absence. Tewabech has taken tough responsibility in taking care of the family, especially mentoring our kids, and encouraged me to concentrate on my study. I owe my special thanks to her for making my study become successful. Thanks also go to my parents, relatives and friends for their invariable courage.

Bergen, 10 December 2013

Diriba Korecha Dadi

## **Preface**

This synthesis and collection of papers constitute a thesis presented in partial fulfillment of the requirement for the degree philosophiae doctor (PhD) in Meteorology at the Geophysical Institute, University of Bergen, Norway.

The skills of real-time seasonal rainfall predictions issued by the National Meteorological Agency of Ethiopia have been verified. Spatially coherent homogeneous rainfall regions have also been developed. Multivariate statistical techniques have been employed to develop multiple regression and canonical correlation analysis models for the main rainy season in Ethiopia. Influences of regional and teleconnection of oceanic and atmospheric components have been examined on seasonal and annual time scales. An overview of drought episodes in all parts of Ethiopia during the recent decades has been examined using standard statistical techniques.

Both observational and reanalyzed data for the ocean and atmosphere have been used in this study. More emphasis is given for local observations in order to diagnose the teleconnection linkages that exist between ENSO phenomena and seasonal rainfall conditions, and documented their feedback on various temporal and spatial scales.

## **Abstract**

Ethiopia composes diversified topographic structures; undulated plateaus and mountains, rugged valleys and plains. The highlands and ever-green portions of the country are fringed by the Sahara and Arabian deserts as well as East African arid climates. In contrast, climate of the major parts of the country is influenced majorly by tropical features while partly interacted with inter-hemispheric weather systems. Ethiopia's climate is prone to both extended rainfall deficits and excesses. In extreme cases, these may lead to droughts, economic hardship and humanitarian disasters. Droughts are the most natural catastrophes that impose impending social and economic crisis in the history of Ethiopia that have been manifested in tampering agriculture and food security, livestock development, hydro-electricity production, transport, water resource management, health and public safety. Numerous evidences have been documented that when any one of these sectors become affected, the effect can spread quickly and a whole country may suffer. Skillful prediction of seasonal rainfall would therefore bring sound change in disaster risk reduction and prevention and economic benefit to the country that depends on rain-fed agriculture. It would enable timely actions to be taken by the government and the public in order to avert or minimize potential hunger, poverty and famine resulting from drought.

Since the issuance of the seasonal climate prediction has begun in Ethiopia, the National Meteorological Agency has gone through continuous improvement in order to enhance the skill of predicting seasonal rainfall anomalies for various occasions. However, there are a lot of constraints in quantifying the seasonal rainfall trends and homogenizing their spatial and temporal patterns. Although seasonal climatic features are complex in nature, this thesis has focused mainly on the characterization of the predictability of rainy seasons in Ethiopia. Four manuscripts are included. The first manuscript provides an overview of NMA's operational seasonal rainfall

prediction skills in various rainfall regimes of Ethiopia. The second manuscript provides spatially coherent homogeneous rainfall regimes as the main platform for developing region-specific climate prediction model. The third one deals with the construction of multivariate statistical seasonal rainfall based on ENSO indices for the main rainy season in major portions of Ethiopia. The fourth manuscript provides an overview of drought episodes in all parts of Ethiopia during the recent decades.

In the forecast verification manuscript (Paper I), we evaluated the skill of the National Meteorological Agency of Ethiopia's operational seasonal rainfall forecast for the February–May (FMAM) and June–September (JJAS) rainy seasons for the period 1999–2011. Our analysis showed that the forecasting system was biased toward the near-normal category. The ranked probability skill scores (RPSS) which computes the relative skill of the probabilistic forecast over that of the climatology is positive for all 16 forecasts series, indicating that the forecast has better skill as compared to chance. The results further suggested that the forecasting system has problems in capturing below normal rainfall events. This under-forecasting of dry events is of great practical importance. In contrast, the forecast showed slightly higher skills for above normal than below normal rainfall categories during both seasons and hence indicated that there is a greater reluctance to assign higher terciles for below normal than for above normal rainfall as a forecast for dry conditions would be considered more serious and may lead to initiation of drought preventive actions.

In the homogeneous rainfall classification (Paper II), we analysed a spatial and temporal rainfall patterns of Ethiopia based on 162 quality-controlled point stations and 717 grid-points generated from satellite rainfall estimate-merged with meteorological stations. Analysis of various clusters on the monthly rainfall data indicated the presence of distinct spatial rainfall patterns

over Ethiopia. Principal Component Analysis (PCA) was broadly categorized Ethiopia in three major rainfall regions that vividly identified the dominance of large rainfall dissimilarities and strong seasonality, which separate June–September (*Kiremt*) rain-benefiting from February–May (*Belg*) and October–January (*Bega*) rainfall regimes. The application of Cluster Analysis (CA), on the other hand identified twelve distinct rainfall regions for the country. The characteristic of each homogeneous rainfall region is the reflection of the typical seasonal cycle that prevails in Ethiopia. The identification of specific rainfall regions add values in the local seasonal climate forecasting, monitoring of climate variability and change on regional and national scales. In this study, the mountainous chains that bisect northwestern from the northeastern regions were well replicated in our spatial delineations. The formation of the dry corridors of the northern Rift Valley and southeastern lowlands are among the most interesting clearly depicted regional features, where understanding of the meteorological mechanisms may provide a benefit to realize the impact of rainfall variation on social and economic activities of the region.

In paper III, we examined the predictive potential for June–September rainy seasonal in Ethiopia using multivariate statistical approaches. The skill of a dynamical approach to predicting the El Niño–Southern Oscillation (ENSO), which impacts Ethiopian rainfall, was assessed. The study attempts to identify global and more regional processes affecting the large-scale summer climate patterns that govern rainfall anomalies. Multivariate statistical techniques are applied to diagnose and predict seasonal rainfall patterns using historical monthly mean global sea surface temperatures and other physically relevant predictor data. We showed that Ethiopia’s June–September rainy season is governed primarily by ENSO, and secondarily reinforced by more local climate indicators near Africa and the Atlantic and Indian Oceans, which revealed in this case that 67% (85%) of dry (wet) events are associated to El

Niño (La Niña) episodes. It is therefore scientifically judicious that rainfall anomaly patterns can be predicted with some skill within a short lead time of the summer season, based on emerging ENSO developments. We further identified that the ENSO predictability barrier in the Northern Hemisphere spring poses a major challenge to providing seasonal rainfall forecasts two or more months in advance.

In the drought analysis (Paper IV), meteorological observations were used to construct monthly time series for 14 homogeneous rainfall zones, covering all of Ethiopia during 1971–2010/2011. The Standardized Precipitation Index (SPI) was then calculated for each zone on time scales of 3, 4, 6, 9, 12, 24 and 48 months. The results indicate that 2009 was one of the driest years in Ethiopia since 1971, and that there has been a cluster of dry spring (locally known as *Belg*) seasons in most of the country during the last 10–15 years. Linear regression analysis confirmed a decline in precipitation in southern Ethiopia, both in the spring and in the summer (locally known as *Kiremt*). The trend analysis did not give us reason to draw any conclusions for central and northern Ethiopia, but the clustering of dry spring seasons during the last 10–15 years was apparent also in this part of the country.

## List of Publications

Korecha, D. and A. Sorteberg (2013): “Validation of operational seasonal rainfall forecast in Ethiopia”, *Water Resources Research*, VOL. 49, 7681–7697, doi: 10.1002/2013WR013760.

Korecha, D. and A. Sorteberg (2013): “Construction of Homogeneous Rainfall Regimes for Ethiopia”, *Submitted to International Journal of Climatology*.

Korecha, D. and A. Barnston (2007): “Predictability of June–September rainfall in Ethiopia”, *Monthly Weather Review*, 135:628–650.

Viste, E., D. Korecha and A. Sorteberg (2012): “Recent drought and precipitation tendencies in Ethiopia”, *Theoretical Applied Climatology*. doi: 10.1007/s00704-012-0746-3.

## Table of Contents

### Acknowledgments

### Preface

### List of Publications

<b>1</b>	<b>Introduction</b>	<b>11</b>
1.1	Background .....	11
1.2	Motivation .....	12
1.3	Objectives .....	17
<b>2</b>	<b>Background</b>	<b>19</b>
2.1	The country Ethiopia .....	19
2.2	Climate of Ethiopia .....	22
2.2.1	General Features .....	22
2.2.2	Rainfall seasons and mean circulation systems	26
2.3	Climate Prediction .....	42
2.3.1	Background .....	42
2.3.2	Seasonal climate predictability skill in Ethiopia ...	46
<b>3</b>	<b>Data</b>	<b>49</b>
3.1	Climate Data .....	49
3.2	Atmospheric and Oceanic indices .....	51
<b>4</b>	<b>Summary Results from the Papers</b>	<b>53</b>
4.1	Paper I: Seasonal rainfall forecast Validation .....	53
4.2	Paper II: Construction of Homogeneous Rainfall Regimes .....	56

4.3	Paper III: Predictability of June–September Rainfall .....	58
4.4	Paper IV: Drought in Ethiopia – an overview of Precipitation .....	60
	<b>References</b>	62
	Paper I: Validation of operational seasonal rainfall forecast in Ethiopia	73
	Paper II: Construction of Homogeneous Rainfall Regimes for Ethiopia	124
	Paper III: Predictability of June–September rainfall in Ethiopia	177
	Paper IV: Recent drought and precipitation tendencies in Ethiopia	230

# **1 Introduction**

## **1.1 Background**

The rainfall pattern of the tropical regions is strongly characterized by seasonality, with dry and short rainy seasons on the one side, and wet and long rainy seasons on the other side of the year. One of the physical causes that produce a seasonal cycle is the differential variation of solar radiation and meridional and zonal migration of weather producing systems. The position and intensity of the meteorological systems impacts the amount and distribution of climatic elements such as; rainfall, temperature, humidity and wind.

From a practical point of view, knowing the seasonality of climate and the underlying characteristics of a given region help policy-makers to foresee how weather and climate may influence the ever growing social and economic strive. In this regard, efforts have been made worldwide to investigate the seasonal variations of climates that commonly prevail at local, regional and global scales. Among these global initiatives, researches and scientific explorations to improve the weather forecasting and climate predictions capabilities have remained on the top of a global agenda. Despite the fact that a lot of improvements have been made in scaling-up climate prediction methods, predictability and reliability of seasonal forecasts are not yet reached a satisfactorily level.

In Ethiopia, there are three distinct seasons; broadly prevailing on annual timescale where each season has its own particular feature in terms of spatial climatic distributions and temporal variations. Much of the Ethiopian economic

performances depend on rain. For instance, rain-fed agricultures of the country perform better under timely onset and cessation of the rainy season as well as low intra-seasonal variability of rainfall. Similarly, agro-pastoralists and pastoralists also require a stable rainy season with minimum tolerance to extreme climatic events. Water resources for day-to-day activities and hydropower energy generation depend on the seasonal rainfall performance and also waterborne diseases, malaria and meningitis are strongly influenced by spatial and temporal variability in parameters such as; rainfall, temperature, relative humidity, sunshine duration, pressure gradient and wind.

The construction of weather and climate prediction schemes and the evaluation and checking of their skills are therefore important to several aspects of Ethiopian society. However, lack of comprehensive understanding on the terrain complexities and their impacts on the seasonal climatic distributions diffuse the selection of climate prediction models to make reliable prediction for the country. The overall aim of this thesis is therefore to undertake scientific studies on the seasonality of rainfall over Ethiopia, establish spatial coherent homogeneous rainfall regions, perform an in-depth evaluation on the performance of the National Meteorological Agency (NMA) seasonal rainfall forecasting system and examine the progress that have been made toward the development of improved seasonal rainfall prediction system.

## **1.2 Motivation**

The strong seasonal rainfall variation, which has affected much of Ethiopia in recent years, added to potential climate effects associated with increasing

climate-related disasters, have provoked speculations about the predictability skill of Ethiopia climate in the future. The impact of false alarm from the failure of seasonal rain differs among the rainfall regimes and directly corresponds with the degrees of their reliability. In particular, the failure of the *kiremt* rains creates heightened stresses in the major crop producing regions and big water dams regions of the country. It causes severe shortages in terms of water and food crops, and subsequently leading to increased hardship for millions of people and livestock mortality in the dry regions. On this background, this thesis is motivated, particularly to investigate the predictability nature of seasonal rainfall, temporal and spatial tendencies of droughts across various climatic regions of Ethiopia.

An investigation on the natural disaster over Ethiopia reveals that the country has experienced large climate-related hazards historically. For example, NMSA (1996) documented the chronology of Ethiopian droughts and famines since 253-242 BC to 1992. In recent years, a case study made in parts of Ethiopia by Stefan and Krishnan (2000) suggested that 50 percent below average rainfall would give a poverty rate of about 60 percent. Webb et al. (1992) also suggested that the worst recent droughts were caused due to at least two consecutive years of poor rainfall. Although climate variability and the associated socio-economic impacts have continued, the level to which it imposes nationwide influence has declined in recent years. For example, the beginning of issuing seasonal forecast in Ethiopia has contributed for the inclination of mitigating likelihood of climate-related impacts on various social and economic sectors. In fact, it is hard to say how much economy and social losses have been saved by using seasonal forecast. Furthermore, evidence of similar causes in the Ethiopian context is still inconclusive. Nevertheless, we believe that climate-based early warning would play a significant role in reducing societal incidences partly due to climatic extremes.

Seasonal climate forecasting techniques are broadly categorized into two; empirical/statistical, and numerical/dynamical modeling techniques, of which the former have historically been more widely developed (Murphy et al., 2001). Murphy et al. (2001) have further documented that seasonal climate forecasting is one of the promising development for early warning on climate hazards. Tropical and subtropical countries have made the forecast in the monitoring and disaster preparedness for droughts and floods associated with El Niño Southern Oscillation (ENSO). Mutai et al. (1998) have found for East Africa a promising seasonal forecast skill for the OND (October-December) short rains using multiple regression techniques and predictors based on eigenvectors of global sea surface temperature (SST). ENSO-based rainfall forecast in Ethiopia also showed potential skills in predicting seasonal anomalies (Bekele 1997; Gissila et al. 2005; and Diro et al. 2010). Prediction of the onset and cessation dates of the rainy season is also a key issue in countries which rely on rain-fed agriculture for better explanation of the growing season of a given area (Camberlin and Diop 2003). In the case of Ethiopia, the use of seasonal rainfall forecast could play a noticeable role in order to scaling-up crop productivity during the main rainy season (Yemenu and Chemedda 2010). The prospect of using Regional Climate Models (RCM) to provide advance information about higher-order weather statistics, such as wet and dry spell distributions, that are relevant to agriculture (Sun et al. 2005), is a promising area for further research in the African context.

Hansen (2002) suggested that opportunities for the use of seasonal climate forecasts arise in which there is a combination of climate predictability, response, and decision capacity. Similarly, Millner and Washington (2011) emphasized that the economical use of seasonal forecasts became viable when the products meet the users' need. Thus, the value of seasonal

forecasts may increase by tailoring the forecast categories to the user's needs. Yemenu and Chemedda (2010) further documented that despite encouraging efforts in developing skillful potential forecasts, they are not widely used in part because of poor performance and lack of relevance to specific users' decision problems, and in part because of various economic and behavioral causes.

Another societal benefit of seasonal climate prediction is its application in monitoring and forecasting disease outbreak during the rainy or dry seasons. Thomson et al. (2005) acknowledged how seasonal climate predictions are recently in use to forecasting disease risks such as; malaria epidemic. Because it was known that malaria epidemics was often preceded by one month of anomalous high minimum temperatures in the preceding three months prior to the outbreak (Abeku et al 2003 and 2004). As the need for climate information from the health sector increases, the National Meteorological Agency (NMA) adopted the Grover-Kopec et al. (2006) approach to prepare and disseminate a monthly health bulletin for malaria monitoring in Ethiopia. Equally, the seasonal climate forecast has contributed enormously in water resource management, particularly, in hydropower generation (Block 2011). In this regard, Block (2011) further showed that tailoring the rain forecast to highlight critical dry forecasts would minimize poor-decision on hydropower management.

Generally, the uses of seasonal climate prediction for various social and economic sectors persuade my research attention towards the evaluation of past forecasting systems, the exploration of new prediction systems and to contribute towards the creation of improved climate predictability in Ethiopia. In this thesis, my study largely centered on the techniques that enable to,

- Identify climatic systems that influence seasonal rainfall over Ethiopia,
- Document the benefit of research and study on the advancement of seasonal climate predictions,
- Identify the gaps in generating user-tailored seasonal climate information, which could improve decision-making and societal benefits, especially in the long-term,
- Identify the local and regional factors for the preparation of local-specific seasonal climate. Because until recently most of the operational seasonal forecasts are prepared for vast regions, which reduce their spatial resolution and possibility to be used at local level,
- Examine and identify the severity of drought tendencies, and
- Apply suitable verification techniques that enable to verify seasonal climate forecasts on routinely basis.

The scientific motivation for this thesis is therefore to evaluate the impact of regional and global circulation features and their predictability potentials as well as their link to the seasonal rainfall cycle in Ethiopia. Much of the earlier seasonal forecasting systems partly concentrated on subjectivity and relied on ENSO information. Emphasis is therefore given here to examine the time lag relationship between Ethiopian June-September (main rainy season) rainfalls and build multivariate statistical model that enable to predict the seasonal rainfall pattern. Developing homogeneous rainfall regions and show how they can provide in-depth knowledge on the local climates for exploring specific climate features is also another task of this thesis. Besides, this thesis is aimed to evaluate the predictability skill of NMA's seasonal forecasting system and drought severities and tendencies.

### 1.3 Objectives

This study concentrated on the scope of seasonal climate prediction of rainfall in Ethiopia. Seasonal climate prediction started in 1987 after the worst drought of 1984 occurred in Ethiopia. During earlier days, the seasonal forecast was aimed to provide rainfall outlook for the main rainy season so that the government can undertake appropriate actions on disaster prevention and preparedness for the expected climate-related hazards in advance. After the use of climate prediction for early monitoring on droughts was realized, NMA established the long-range forecast unit. This unit was intended to prepare and disseminate seasonal climate forecasts on the national scale. During the past two decades, the request for seasonal forecasts have significantly expanded and has ultimately become core inputs for early planning and decision making mainly for annual agricultural practice, water resource management, vector-borne diseases monitoring, disaster preparedness and prevention. Despite the critical need for one season to year-long climate forecasts from policy makers, planners and general public, the improvement on NMA's seasonal forecasting methods has shown slow progress. In this regard, the seasonal forecasting system should be verified and evaluated using standard forecast verification methods. If NMA's seasonal forecasts do not meet the need of the user community it will loss trust from the public.

The main objectives of this thesis are:

- Evaluate and verify NMA's seasonal forecasting system for the two rainy seasons (February-May and June-September) and identify regions and temporal rainfall events that are forecasted better (weaker) than the climatology (Paper I).

- Develop and establish spatially-coherent homogeneous rainfall regimes in Ethiopia (Paper II).
- Construct skillful seasonal models for June-September rainy season in Ethiopia using multivariate statistical method, with sufficient lead time (Paper III).
- Document the meteorological component of Ethiopian drought episodes and evaluate their spatial and temporal tendencies(Paper IV)

## **2 Background**

### **2.1 The country Ethiopia**

Ethiopia is located within 3.30°N–15°N and 33°E–48°E, in the Horn of Africa (Fig. 1). It covers an area of about 1.14 million square kilometers (944,000 square miles), with the total population of more than 85 million (MoFA 2013). The country's topography consists of high and rugged plateaus and the peripheral lowlands. From a topographic view point, the country confines the Great African Rift Valley that bisects Ethiopia into the eastern and western escarpments. It gradually slopes up from the lowland edges of Rift Valley to the eastern and western escarpments into the southern, central, western and northern mountains. Major parts of the country are made up of a wide plateau and mountains of various heights (Fig. 2). Elevations in the country range from the 160 meters below sea level (northern exit of the Rift Valley) to over 4600 meters above sea level (of northern mountainous regions). The highest mountains are concentrated on the northern and southern plateaus of the country (MoWR 2013). The climatic condition of the country results in high rainfall during the rainy season, which in turn causes perennial and seasonal rivers and stream flows. However, as rainfall is seasonal, the volume of discharges of rivers, both local and trans-boundaries are subject to seasonal variations (MoWR 2013).

Ethiopia leads an agrarian economy, in which pure farming, mixed farming and livestock herding (pastoralists) are common practice. Consistent increasing in population as well as over-exploitation of natural resources such as; natural forest, swampy lands for agriculture and an alarming expansion of

urbanization impose strong influence on agricultural led economic pathway development of the country. The agricultural sector supports 85% of the population and hence is central to the livelihoods of the rural poor in Ethiopia (Conway et al. 2007; Deressa 2006). The agricultural practices currently held in the country mainly depend on the seasonal rainfall as only a small fraction of the agriculture is irrigated and a significant declining in annual agricultural production have been observed during drought years (Lemi 2005).

Ethiopia is repeatedly affected by floods and droughts. During the twentieth century, prolonged droughts often followed by seasonal floods partly stagnated the country's economic growth while exacerbated societal dispute, migration and famines. NMA (2007) documented some of the climate related hazards in Ethiopia include droughts, floods, heavy rains, strong winds, frost and heat waves. There have been traditional and modern coping mechanisms including changes in cropping and planting practices as well as declining of consumption levels through the collection of wild foods, use of inter-household transfers and loans, increased petty commodity production, temporary and permanent migration in search of employment, grain storage, sale of assets such as livestock and agricultural tools, mortgaging of land, credit from merchants and moneylenders, use of early warning, food appeal and aid (NMA 2007).



Fig. 1: Location of Ethiopia.

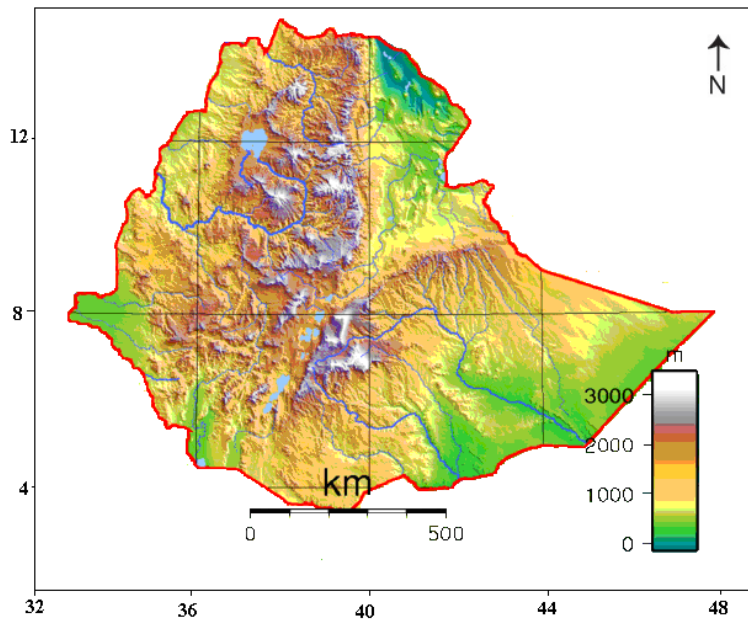


Fig. 2: Topographic map of Ethiopia (Wikipedia 2013)

## **2.2 Climate of Ethiopia**

### **2.2.1 General Features**

Ethiopia experiences a typical warm and moist tropical climate, with hot and semiarid dominate the north-eastern lowland regions. Mean annual temperatures range between 15 and 20°C in the highlands. In contrast, the low-lying regions experience 25-30°C. The seasonal rainfall progression is mostly influenced by the north/south ward migration of the Inter-Tropical Convergence Zone (ITCZ). Most parts of the country receive substantial rainfall amounts between June and September (Fig. 3a-d). Indeed, some parts of central, northeast and eastern Ethiopia receive relatively less rainfall between March to May (Fig. 3b and c). For the southern and southeastern regions of Ethiopia, March-May and October-December are the major and small rainy seasons, respectively (Fig. 3f).

Ethiopia, with its vast and complex topography (Fig. 2) experiences a wide diversification of climates, which vary from typically tropical in the lowlands and Rift Valley regions to cool temperate-type in the northern and southern mountainous regions. Plateaus and ragged mountains play great roles in dictating the climatic features of the country. For instance, the southeastern lowland plains are the major passage of southwesterly cross equatorial moisture during the northern hemisphere summer season, which is carried by southwesterly winds from the Indian Ocean to southwest regions and partly also flow into other portions of Ethiopia. The closeness of this region to the ocean and lying under the highway passage of moisture flow, the regions could have received plentiful rains during the northern hemisphere summer season if topographic feature enabling the condensation of water was present. Similarly, the northeastern lowlands lay underneath of the passage

of cloud storms that emerge both from Yemen high grounds and Arabian Sea into the northeastern highlands, while traversing to the western escarpments of the Rift Valley (Fig. 3b). As a result of few topographic barriers these regions are the dry corridor of the country. In contrast, the southwestern regions, where the country's tropical rainfall forests remain partially intact receive maximum amount of rainfall throughout the year.

The atmospheric systems that induce strong influence on the rainfall and temperature patterns of Ethiopia have widely been documented by many authors. For instance, Kassahun (1987) elaborated the major weather systems that trigger various climate patterns over Ethiopia on monthly timescale. Tadesse (1994), Segele and Lamb (2005), and Gissila et al. (2004) also studied on rainfall variability of the June-September rainy season from regional and global perspectives. Diro et al. (2009) described some of the weather systems that produce spring rains (February-May, small rainy season) over Ethiopia. Even though NMSA (1996) documented the major weather systems controlling the country's climate, further scientific investigation is needed on how local and regional climate features responded to the major atmospheric phenomena.

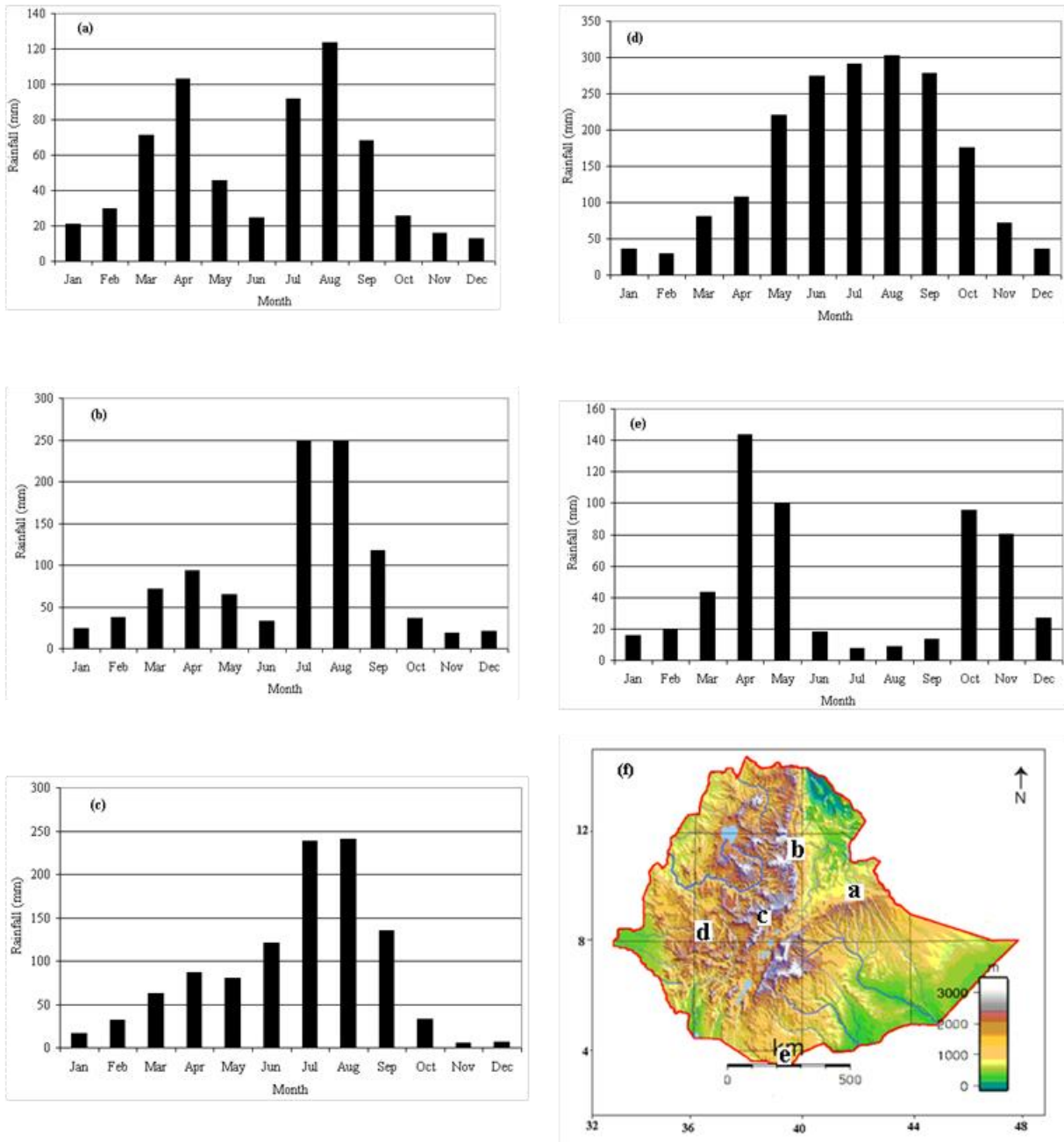


Fig. 3: Seasonal rainfall cycle over (a) Eastern, (b) Northern, (c) Central, (d) Western and (e) Southern sector of Ethiopia. Figure (f) shows geographical location of the regions, underlying with the topographic map

As the climate of mountainous region such as Ethiopia is rather complex, it has been the topic of many studies and several classification systems. The Ethiopian traditional system uses altitude and mean daily temperature to divide the country into five climate zones (Gemechu 1977). Both the Köppen and the Thornthwaite classification systems have also been applied (Gonfa 1996). The most useful for agricultural purposes is the agroclimatic zones which used the water balance concept, the length of the growing season (including onset dates) at certain probability levels (NMSA 1996). In this regard, three distinct zones can be identified namely; the area without a significant growing period (N), areas with a single growing period (S) and area with a double growing period (D) (Fig. 4). This information could be able to form the basis on which the seasonal forecast is built with particular emphasis on the specific user-tailored agricultural sector in each region.

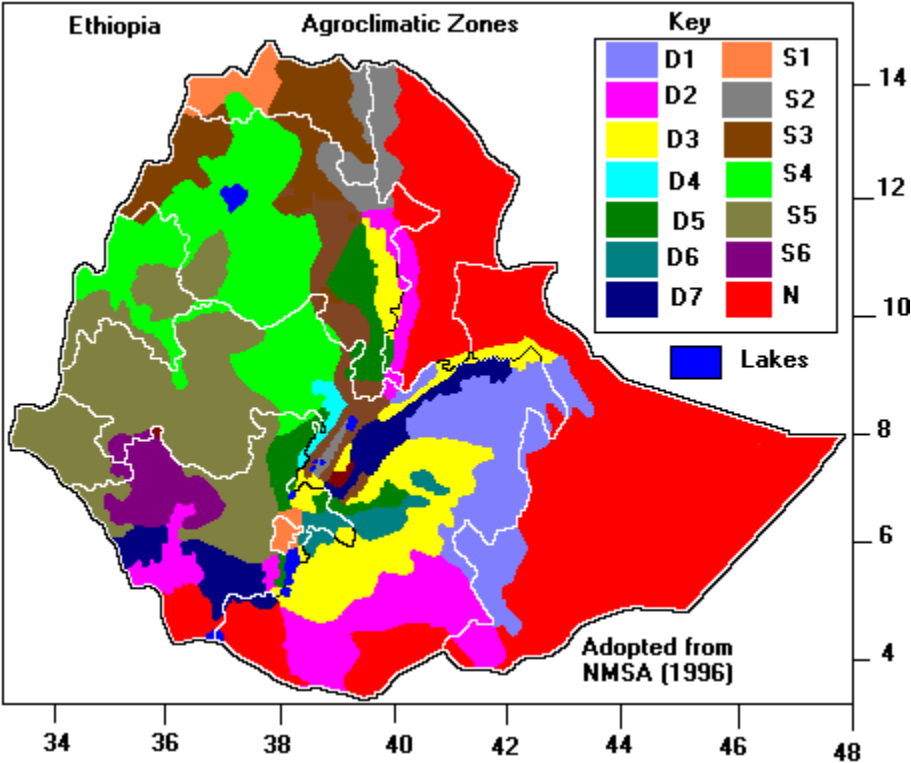


Fig. 4: Agroclimatic zones of Ethiopia

## 2.2.2 Rainfall seasons and mean circulation systems

### i) General

Ethiopia has three climatological rainy seasons namely; February–May (FMAM, *Belg*), June–September (JJAS, *Kiremt*) and October–January (ONDJ, *Bega*) seasons (Seleshi and Demarée 1995; Shanko and Camberlin 1998; Tsegay 1998 and 2001; Gissila et al. 2004; Segele and Lamb 2005; Diro et al. 2010). NMA uses these seasonal classifications for routine seasonal climate forecasting and monitoring of climatic features. However, over some parts of the country uninterrupted rainy season continue for successive two to three seasons. The wet season, which spans from March to November over southwestern Ethiopia, broadly exemplifies these circumstances. Rift Valley and the adjoining escarpments generally, experience two rainy seasons; small (March-May) and main (June-September) rainy seasons, which are interrupted by dry months. The northern and southern portions on the other hand, receive intensive rains when Inter-tropical Convergence Zone (ITCZ) takes its seasonal position over north and south Ethiopia, respectively. To examine some of the meteorological systems that govern the seasonal climate patterns of Ethiopia, NCEP/NCAR reanalysis (Kalnay et al. 1996) data were composited for FMAM (February-May), JJAS (June-September) and ONDJ (October-January) seasons.

As shown in Fig. 5a, maximum mean annual rainfall amounts of 1750 to 2500mm are observed over the southwest-northwest sectors of Ethiopia. This is because ITCZ and its meridional trough cause rains over these regions during *kiremt* (JJAS) season. The reversal of southerly monsoon winds across the western sector of Indian Ocean also played a role in modulating the seasonal cycle of Ethiopian rainfall climatology (Riddle and Cook 2008; Segele et al. 2009). An intrusion of southwesterly wind flows

associated with the southwest monsoon (Fig. 5b) and the subsequent ITCZ shifting northward as well results in summer rains across the northern half of Ethiopia. In contrast, when ITCZ shifts northwards, southern and southeastern regions remain dry throughout the *kiremt* season, with seasonal rainfall totals of less than 100 mm (Fig. 5b).

One of the underlying factors for the dryness of southern Ethiopia is the strong southerly flow that diverges into two components when it reaches the periphery of the region; most portions form the southwesterly Low Level Jets (LLJ), and become the major components of the southwest monsoon system (Fig. 5b right panel). Southerly flows (Fig. 5b) also reach the northern Ethiopia and form a converging inflow over the high grounds and hence produce abundant rains over the northern half of the country. In contrast, when southerly moisture influxes weaken, the northerly flow becomes dominant and pushes the rainfall-belt to progress towards west and southward (Fig. 5c and 5d). This is clearly seen from the vertically integrated moisture fluxes, which was computed from ERA Interim reanalyzed data. ERA-Interim is the European Centre for Medium Range Weather Forecasts (ECMWF) latest global atmospheric reanalysis (Simmons et al, 2006). It can be seen that a large part of the moisture transport comes from the north, and this flow meets the southerly flow make the convergence zone (see Fig. 5b-5d). Viste and Sorteberg (2012) also found that the amount of moisture brought into the Ethiopian highlands from the north is 46%, which is higher than that comes from the south.

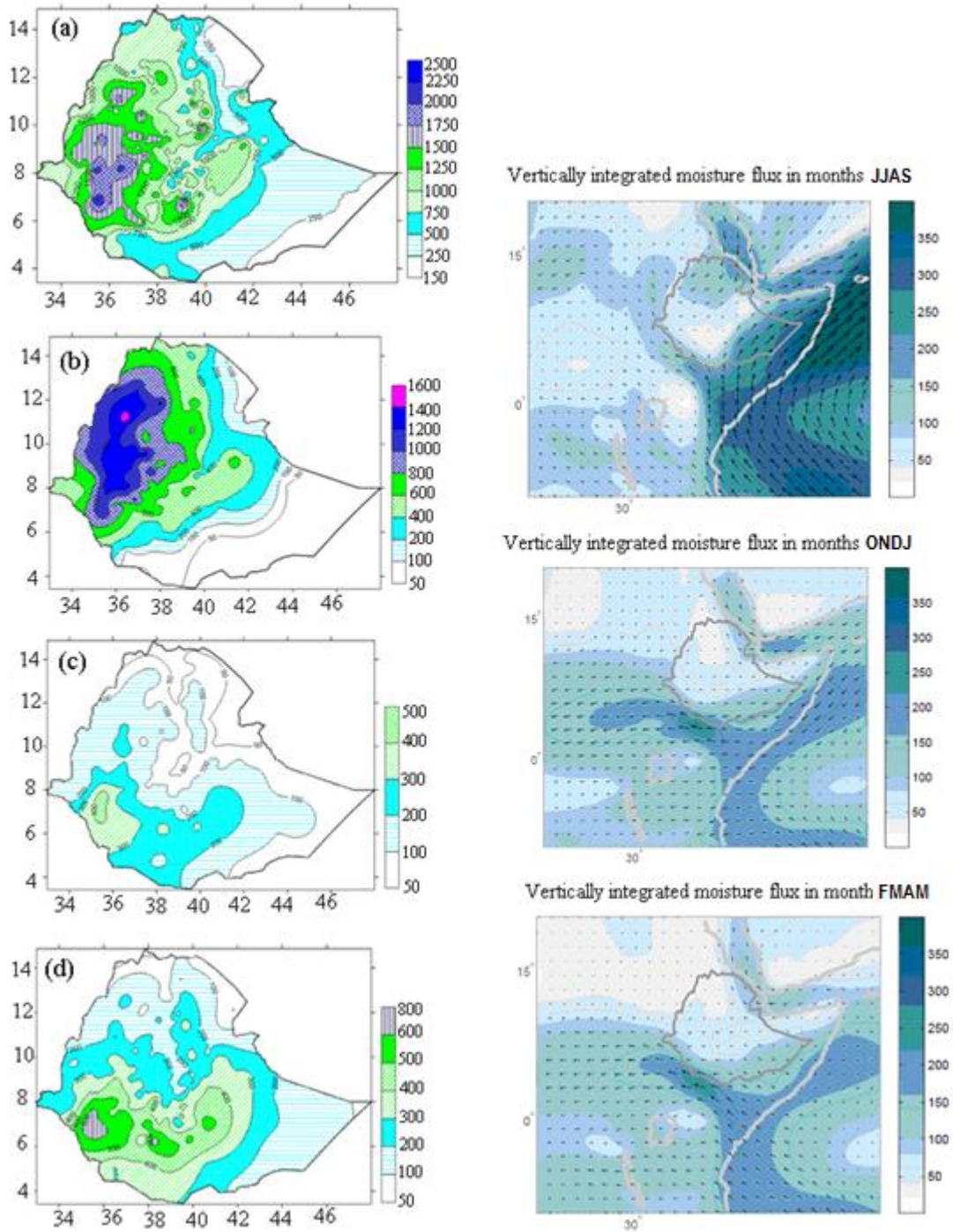


Fig. 5: Spatial interpolation of station-based total rainfall climatology (mm) from 1971-2000. (a) annual, (b) *Kiremt* (JJAS), (c) *Bega* (ONDJ) and (d) *Belg* (FMAM). Seasonal climatological values of vertically integrated ERA interim moisture transports in kg/ms (1989-2009) are depicted on the right panel for each season. The light colors represent the lowest values of both

elements. The months are represented as JJAS for June-September; ONDJ for October-January and FMAM for February-May).

## **ii) Roles of St. Helena and Mascarene high pressure systems**

Semi permanent high pressures and seasonal heat low pressure systems play substantial roles in modulating the climate of particular place on the Earth's surface. In order to demonstrate the degree of their influence, position and intensity of surface level pressure belts are then identified for each season. Fig. 6a, 7a and 8a show the location of Azores High over northwest coast of Africa, St. Helena and Mascarene high pressure centers over southern Atlantic and Indian Oceans during FMAM, JJAS and ONDJ seasons, respectively. Some of the pressure belts always remain within their respective position despite the fact that the role of each pressure system varies from season to season. The intensification of the southern hemisphere high-pressures and the orientation of the main mountain ridges boosts moisture fluxes and hence widespread rainfall over Ethiopia (Kassahun 1987). Camberlin (2009) suggested that from the end of June, because of the deepening in the Indian monsoon low further east, the south-westerly flow associated with the Indian southwest monsoon spills over the Ethiopian highlands to reach the southern Red Sea, where it channeled until it joins the main Indian monsoon flow in the Arabian Sea.

## **iii) Role of Inter-Tropical Convergence Zone (ITCZ)**

The inter-hemispheric migration of ITCZ follows the Sun's position, and hence its location and intensity changes over the course of the year. The cooling of the North Atlantic Ocean (partly covering the Azores high pressure region),

combined with the warming of the Southern Hemisphere oceans (including the Indian Ocean; St. Helena and Mascarene high pressure regions) is likely to have resulted into a reduced northward excursion of the ITCZ and/or more rainfall over the tropical oceans than over the African continent (Camberlin 2009). It implies that the weakening of Southern Hemisphere high pressure areas (St. Helena and Mascarene) negatively affected the ITCZ, which in turn disturbed seasonal rainfall performance over Ethiopia. Besides, Camberlin (2009) has shown that the South Atlantic warming is not only a component of that of the southern hemisphere, but it also occasionally has a separate incidence on monsoon depth, like in 1984 where the devastating drought which affected Ethiopia and the Sahel regions can be exceptionally related to high Sea Surface Temperature (SST) in the Gulf of Guinea of the Equatorial Atlantic Ocean.

Due to its temporal fluctuation and variation, it is difficult to locate ITCZ at seasonal mean chart. It, however, generally retreats towards the equator during FMAM and ONDJ, but it is organized and located around 10 to 20°N during JJAS season. The Sahel region and Ethiopia JJAS rainfall is relatable with the position and intensity of this feature. As a result, southern and southeastern Ethiopia receives rains in September-November (small) and March to May (main rain season for these regions). Camberlin and Philippon (2002) pointed that the southward extension of the subtropical westerly jet has played important role on the variability of Ethiopian spring (Feb-May) rainfall.

#### **iv) Roles of Low-Level Jet and easterly perturbation**

Findlater (1977) explored the formation of low-level jet (LLJ) during the northern hemisphere summer over western Indian Ocean, bordering to the East African coast (Fig. 7b). He further documented that over eastern Africa coast the low-level jet streams centered at about 1-1.5 km and lie in the middle of the daytime convective layer. Low-level wind flows with its core centered in 850hPa over the Indian Ocean partly intrude into the Ethiopian highlands while the large portion of this feature forms strong southwesterly flow towards south Asia during the northern hemisphere summer season (Fig. 7b). For Ethiopia's JJAS rainy season, low level flows play vital role in transporting moisture into the country. In the FMAM and ONDJ seasons, low-level flows reverses into northerly and northeasterly flow over Ethiopia, which mostly transport dry and cold air into the large parts of northern, eastern and central Ethiopia (Fig. 6c and 8c). Sometimes within these low-levels, wet weather disturbances formed due to moist easterly flow along the horn of Africa.

#### **v) Roles of African Easterly Jet and mid-latitude troughs**

Using NCEP/NCAR reanalysis, the 600hPa mid tropospheric levels, 600hPa and 500hPa are plotted to show the wind climatology for the three seasons of Ethiopia. During the June-September rainy season, the African Easterly Jet is depicted at 600hPa although its direct impact on Ethiopia's summer rain has not yet known (Fig. 7c). Equator-ward penetrations of mid-latitude low pressure systems are sometime identified at 500hPa during FMAM and ONDJ as it emerges from the plot of vector wind reanalysis. Fig. 6b and 8b show the climatological pattern of vector wind. Over the tropical region this field is smooth with few features. Therefore, it is difficult to identify the position of prominent features affecting Ethiopian climate.

## **vi) Roles of Subtropical Western Jet (STWJ) and Tropical Easterly Jet (TEJ)**

Ethiopian rainfall is also affected by upper-level systems such as; the Tropical Easterly Jet (TEJ) and African Easterly Jet (AEJ) during the main rainy season and the Subtropical Westerly Jet (STWJ) during small rainy and dry seasons (e.g., Diro et al. 2009). Many authors (e.g., Camberlin and Philippon 2002; Nicholson and Grist 2003; Segele and Lamb 2005) documented the location and intensity of these jets, which modulate convection and thus rainfall over northern half of Ethiopia. Fig. 6d, 7d and 8d show the mean subtropical westerly jets and tropical easterly jet. TEJ originates from Southeast Asia as part of the Indian summer monsoon, with the maximum winds found in July-August at 150hPa near 10-15°N over Sudan, with velocities decreasing from 25 to 10 m/s from east to west Sudan (Hulme and Tosdevin 1989; Segele and Lamb 2005). It plays an important role in facilitating deep cloud formation and steering monsoon cloud clusters, which are formed over the Arabia region into the Ethiopian high grounds. On the regional scale, Pedgley (1969) pointed out that most weather storms developed over Ethiopia drift westward because of TEJ of the upper troposphere although they often decay before reaching the Nile Plains. In contrast, subtropical westerly jet that is formed around the 200hPa pressure level oscillates north and southwards. In particular, during the short rainy seasons (i.e. FMAM and ONDJ for Ethiopia), Camberlin and Philippon (2002) have shown the existence of an upper level trough over the Red Sea. Upper-level trough emerges from the northern hemisphere cold and moist region contributes to above normal FMAM rains over northeast, central, east and Rift Valley regions, while it causes unseasonal rains during November-January, which is the main crop harvesting period over Ethiopia.

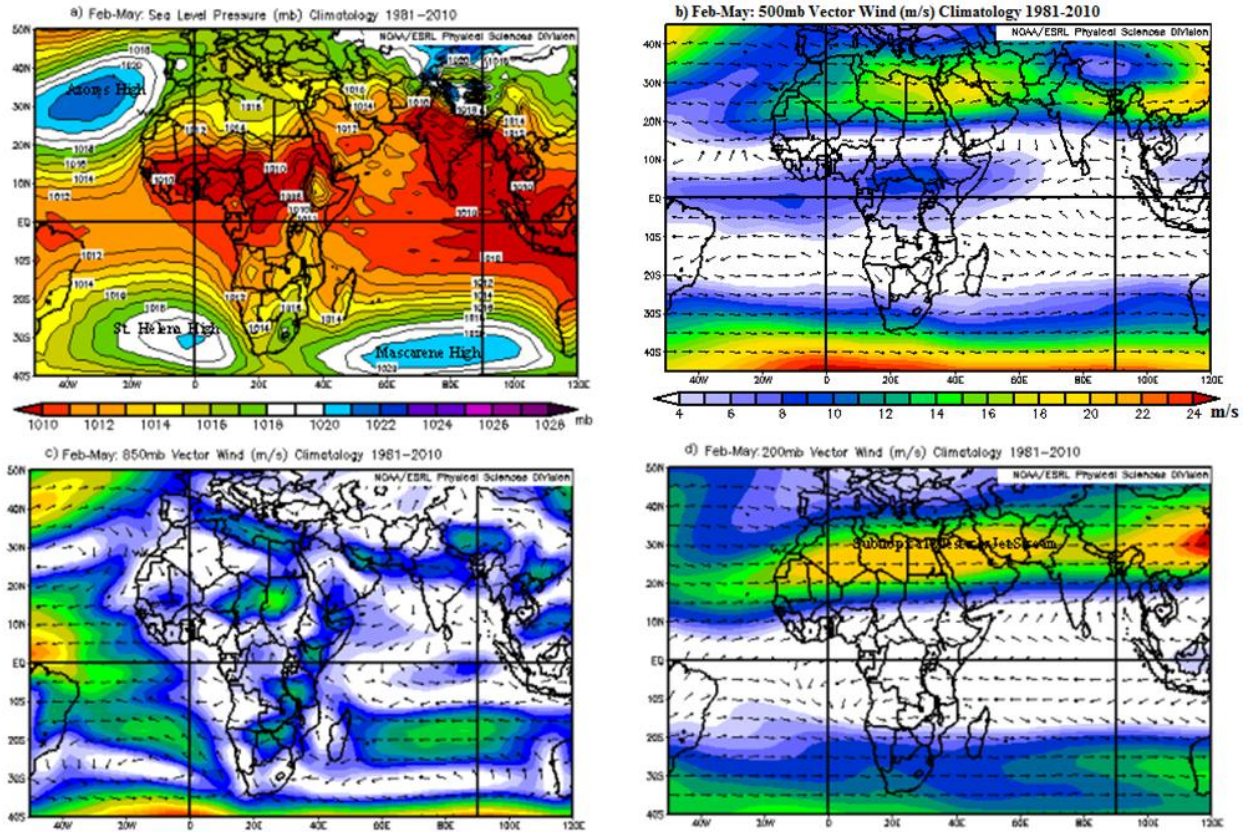


Fig. 6: NCEP reanalysis\* climatology of Feb-May 1981-2010, a) sea level pressure (mb), b) 500mb vector wind (m/s), c) 850mb vector wind (m/s or  $\text{m}\cdot\text{sec}^{-1}$ ) and d) 200mb vector wind (m/s).

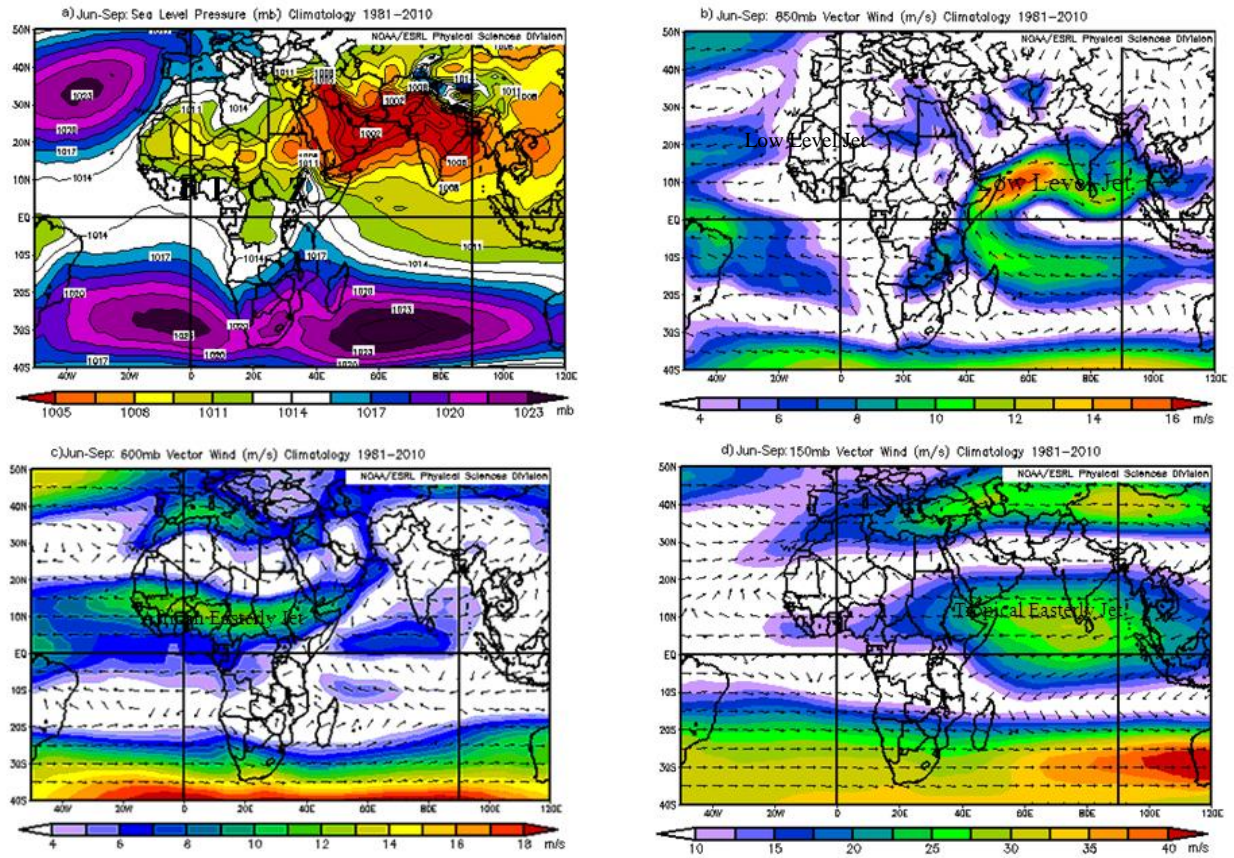


Fig. 7: NCEP reanalysis\* climatology of June-September 1981-2010, a) sea level pressure (mb), b) 600mb vector wind (m/s), c) 850mb vector wind (m/s) and d) 200mb vector wind (m/s).

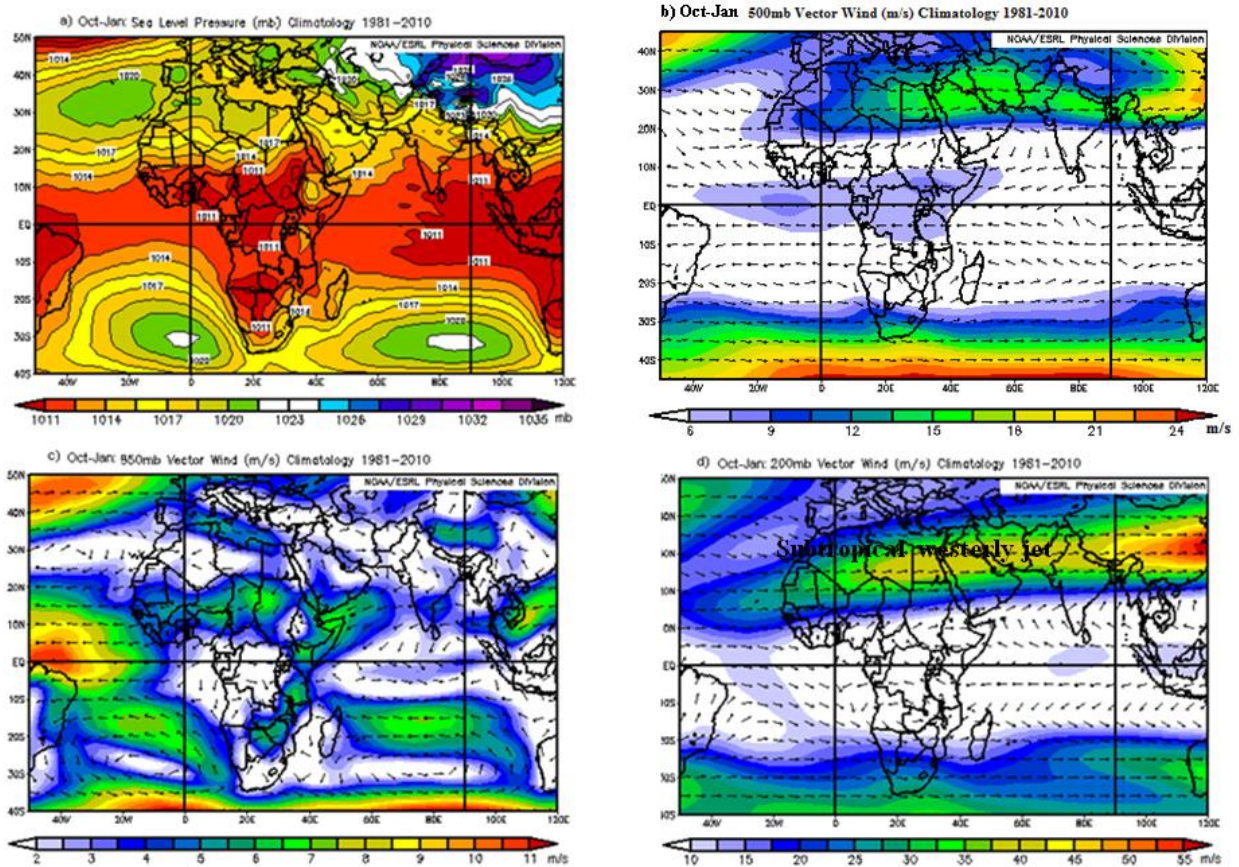


Fig. 8: NOAA/NCEP reanalysis\* climatology of October-January 1981-2010, a) sea level pressure (mb), b) 850mb vector wind (m/s), c) 500mb vector wind (m/s) and d) 200mb vector wind (m/s).

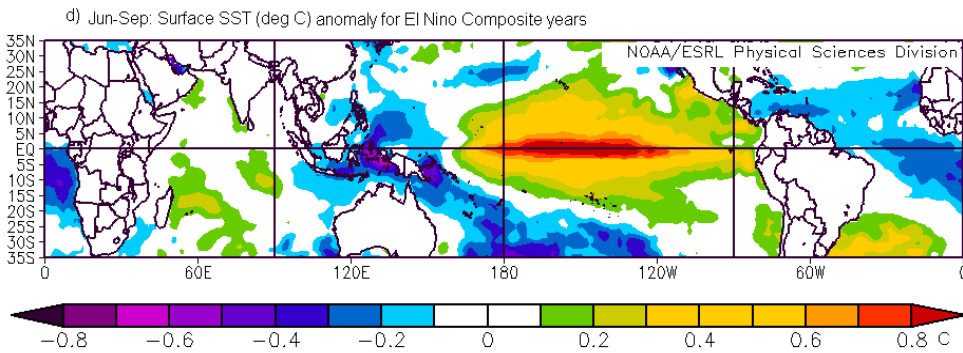
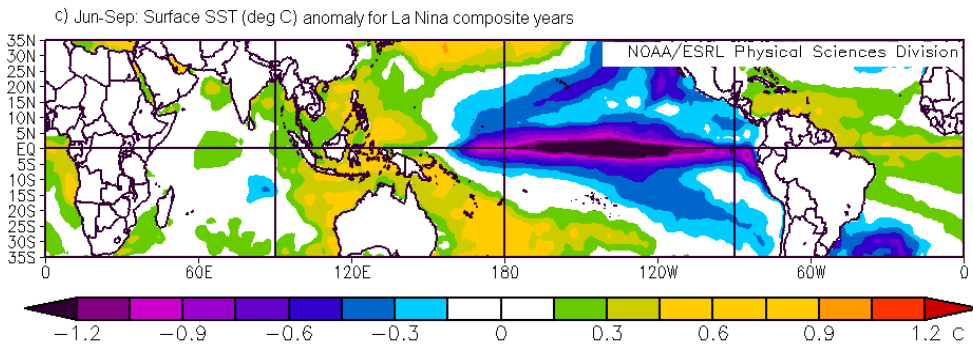
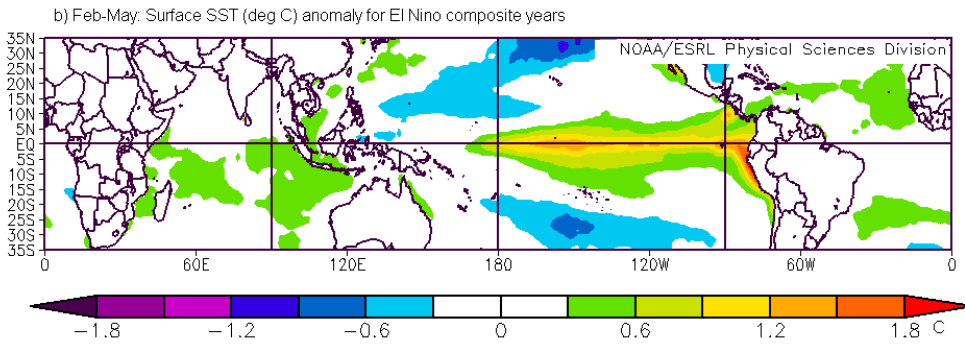
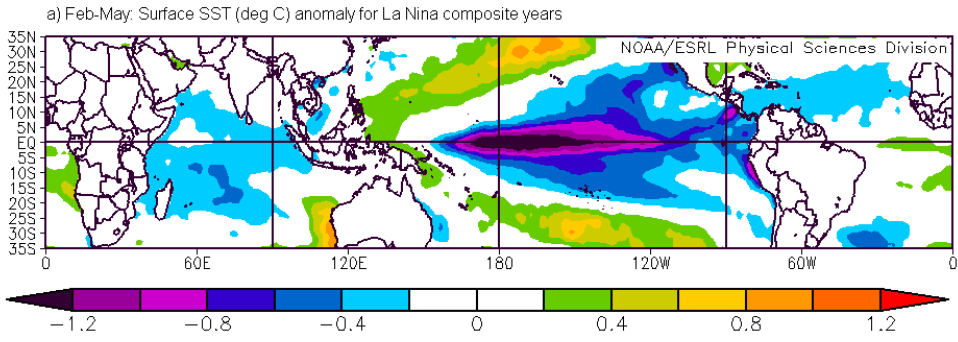
\*NOAA/NCEP Reanalysis data and map room were explored from the NOAA/OAR/ESRL PSD, Boulder, Colorado, USA; <http://www.esrl.noaa.gov/psd/>.

### vii) Role of ENSO

NOAA (2013) defines ENSO state (e.g., El Niño or La Niña) as a departure from normal of the sea surface temperature (SST) in the Niño 3.4 region of magnitude  $0.5^{\circ}\text{C}$  or more, lasting for at least five running three-month periods over the tropical Equatorial Pacific Ocean. The main ENSO signal is found

during the northern summer (Camberlin 2009), at which time a negative correlation is found with the Niño 3.4 index, depicting lower than normal rainfall in the years of higher sea-surface temperatures (SST) in the eastern equatorial Pacific (i.e., El Niño years). It is argued that each ENSO state (El Niño, neutral or La Niña) has had its own influence on the rainy or dry season. For each season the NCEP Reanalysis data were used to compute composite SST anomalies for La Niña and El Niño years (Fig. 9).

Okumura and Deser (2010) have shown that there is a strong asymmetry in the duration of El Niño and La Niña. In this case, they have pointed out that both El Niño and La Niña typically begin in late spring–summer and intensify through the equatorial cold season. They also noted that most El Niño events terminate rapidly after peaking toward the end of the year. In contrast, many La Niña events persist through the following spring–summer and re-intensify in winter; some even last through a third year and again strengthen during winter.



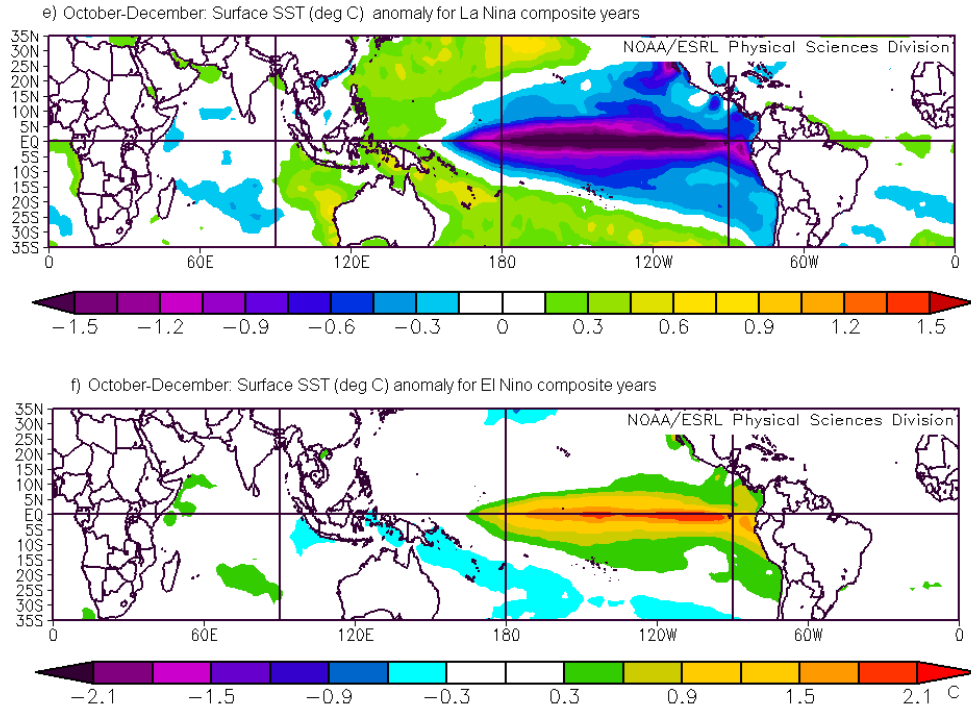


Fig. 9: Surface NOAA Oceanic Indices of SST composite anomalies ( $^{\circ}\text{C}$ ) for some La Niña and El Niño years during 1981-2010; a) and b) for February to May; c) and d) for June to September and e) and f) for October-December seasons. Anomalies are computed from 1981-2010 SST climatology.

The impact of ENSO on Ethiopian rainfall are widely documented (e.g., Degefu 1987; Seleshi and Demarée 1995; NMSA 1996; Bekele 1997; Camberlin 1997; Tsegay 2001; Gissila et al. 2004; Segele and Lamb 2005; Diro et al. 2011). Most of these documents showed that the warm phase of ENSO (El Niño) is associated with suppressed rains during the main wet season (JJAS) over north and central Ethiopia. It may cause severe drought and sometimes famine. On the other hand, it enhances rainfall in FMAM and ONDJ seasons, which mainly affects various parts of Ethiopia. In contrast, La Niña has an opposite impacts on the seasonal rainfall; flood in JJAS and drought in FMAM and ONDJ seasons.

During JJAS, suppressed rainfall has been observed to accompany El Niño over much of Ethiopia, often with economic catastrophe. As shown in Fig. 9 (for 1970 onward), lower tercile all-Ethiopian JJAS seasonal rainfall occurred in 1965, 1972, 1979, 1982, 1984, 1987, 1990, 1991, 1995, 1997, and 2002. More than half of these summers coincided with El Niño events; none occurred during La Niña. Upper tercile rainfall conditions occurred in 1961, 1964, 1970, 1973, 1974, 1975, 1977, 1978, 1981, 1988, 1994, 1996, 1998, 1999, and 2003; more than half of these matched La Niña events, while only one (1994) occurred with El Niño.

The effect of ENSO on rainfall is seen in composite analyses for selected individual stations by month. JJAS monthly rainfalls are averaged for El Niño, La Niña, or near-neutral conditions, using the classification system of the NOAA/Climate Prediction Center (CPC). Here, all months of any year are assigned the ENSO phase existing during JJAS of that year, so that impacts of ENSO events occurring during the Belg and Bega seasons are not directly represented. Mean monthly rainfalls seem to be enhanced during La Niña years in regions where JJAS is the major rainy season, due to greater duration of the rainy season (Segele and Lamb 2005), and increased rainfalls during individual months of the rainy season. Examples of stations from different parts of Ethiopia having a clear ENSO influence are shown in Fig. 10.

Fig. 11 illustrates the geographical distribution of the correlation between the SST in the Niño 3.4 index region and Ethiopian JJAS rainfall at the 78 stations, based on 1970–2004, keying SST to individual months prior to summer (Fig. 11a–c) and SST during JAS (Fig. 11d). The association of summer rainfall with ENSO in early pre-summer months (January–April) is weak, and increases as the time of the ENSO state approaches the beginning of the rainfall season. Statistically significant ( $\geq 0.34$ ) negative correlations are found between JJAS rainfall totals and Niño 3.4 SST occurring nearly

simultaneously (in JAS) mainly in the northern half of the country but also in the southern highlands and southwest Ethiopia (Fig. 11d). In the climatologically dry southeastern lowlands, associations with ENSO are weak. The moderate negative simultaneous correlations (-0.4 to -0.6 at some locations) imply that rainfall forecasts would have useful skill levels if the summer Niño 3.4 SST could be predicted beforehand. Correlations between JJAS rainfall and Niño 3.4 SSTs of pre-season months may be of some use only for May, where some correlations are stronger than -0.4. The lack of a stronger relationship between the May ENSO state and rainfall is not surprising, as the ENSO condition may change in either direction between April and June (Tziperman et al. 1998). For example, high Niño 3.4 SST in May could be due to an El Niño that had matured earlier and would likely dissipate before July, or to a newly emerging El Niño that was absent in February and March. Predicting ENSO is known to be difficult during the northern spring. Later we will discuss an indicator of summer ENSO based on the change of the May SST anomaly from that of a few months earlier.

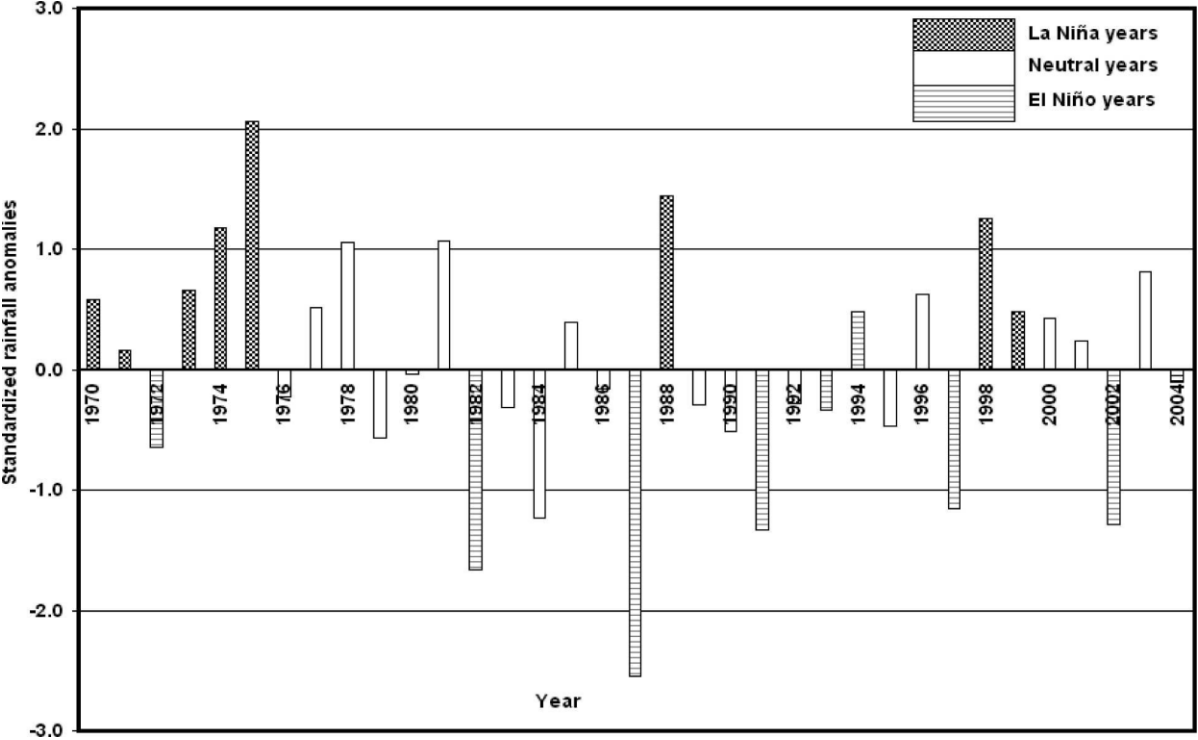


Fig. 10: Standardized JJAS rainfall anomalies of all-Ethiopian rainfalls for the 1970–2004 period. Years having El Niño, La Niña, and neutral conditions during JJAS, based on the NOAA/CPC ENSO classification, are denoted by the patterns inside the bars.

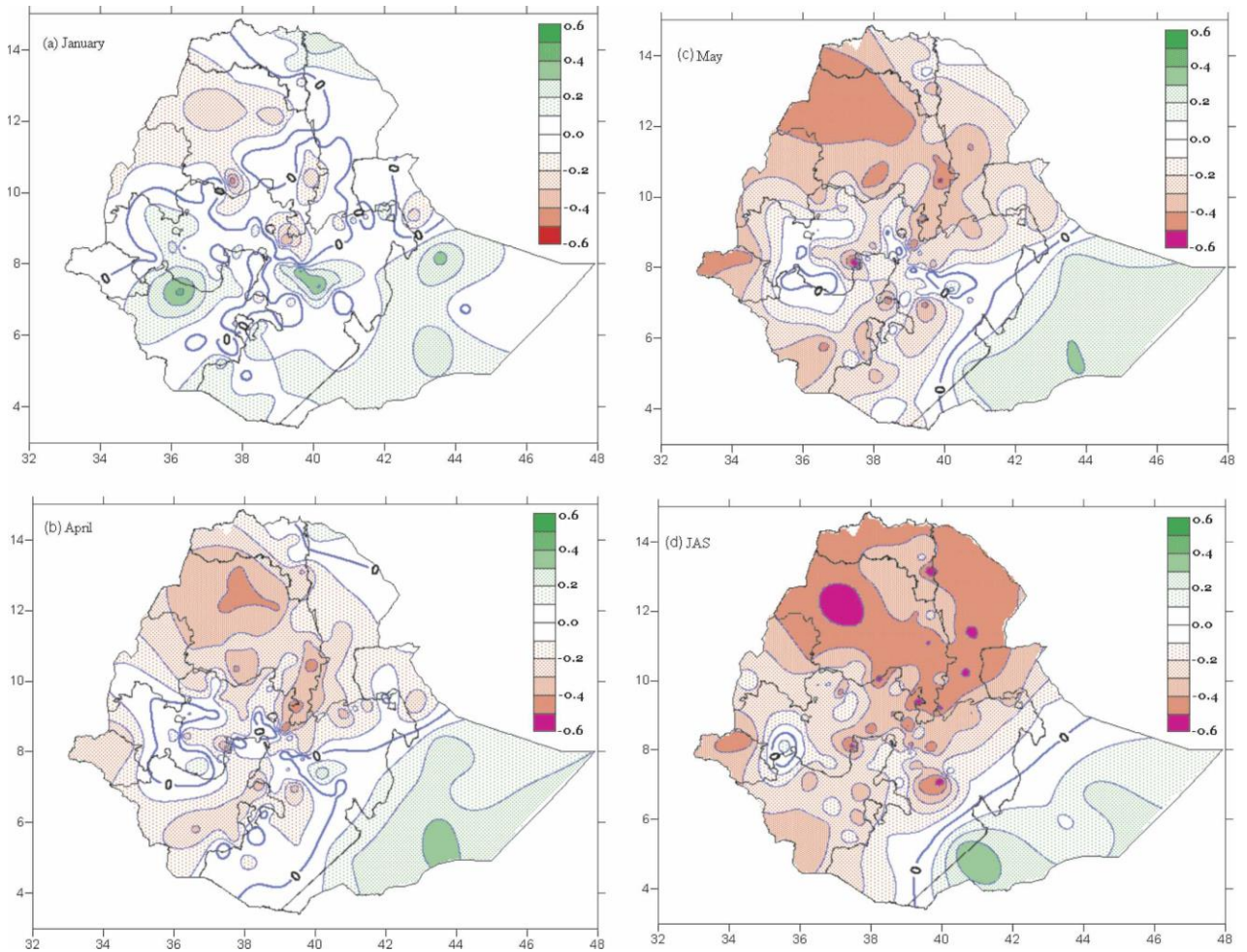


Fig. 11: Spatial distribution of correlation between JJAS rainfall for 78 stations in Ethiopia and Niño 3.4 SST in (a) January, (b) April, (c) May, and (d) JAS. Computed for 1970–2004, values of 0.34 or greater in magnitude are statistically significant at the 95% confidence level.

## **2.3 Climate Prediction**

### **2.3.1 Background**

American Meteorological Society's Glossary of Meteorology (AMS 2013) defines climate prediction as the method by which climate of a region is predicted during some future period of time. Climate predictions prepared in the form of probabilities of anomalies of climate (e.g., temperature, rainfall), with lead times up to several seasons. This could be done using either by simple climatological and persistence approaches or by employing the most sophisticated Ocean-Atmosphere coupled multilayer general circulation models. The predictability skill of climate under consideration, however, need due attention before they are in use for operational purposes. The motive of this section is not reviewing the overall development of climate prediction science but it entails to provide highlight on some of the key issues revolving around predictability skill of tropical climates and its time evolution. Hastenrath (1986) clearly underscored that large interannual variations of rainfall are an intrinsic part of tropical climate and can have severe impacts on human. He further noted that World Meteorological Organization (WMO) and the U.S. National Climate Program (National Climate Program Office, NOAA) showed their interest in declaring climate prediction as a central objective. Charney and Shukla (1981) pointed out that climatic variability in the tropic should be more predictable because it was in large part of slowly varying anomalies of lower boundary of the atmosphere.

Since the middle of the twentieth century, many environmentalists have tirelessly campaigned to bring the issue of environmental change to the attention of international society. In the late nineteen seventies and early eighties the connections between day-to-day activities and climate change

and shorter-term environmental abnormalities were explained. For shorter timescales, scientists have introduced techniques to improve environmental monitoring of institutions across the globe. Also, forecasting of short-range weather variations has attained successful for many regions with various lead times depending on the predictability, which may vary seasonally. However, there were few accomplishments in long-range climate predictions despite some efforts made by Sir Gilbert Walker (Cane 2000) near the turn of twentieth century. Studies leading to significant progress in weather forecasting had taken place in the 1960s by Bjerknes (Cane 2000). An introduction of physical modeling on the climate scale, which encompassed the predictability of sea surface temperature (SST) over the eastern tropical Pacific Ocean, was first established by Zebiak and Cane (1987). These significant breakthroughs laid the cornerstone for the predictability of seasonal climates over many tropical, and some extra tropical, regions.

Importance of ocean SST and its physical forcing for climate anomaly patterns was investigated for a particular region. For instance, Zeng (2003) presented evidences that global sea surface temperature is a major forcing for climate in the Sahel region. Using principal components analysis, Giannini et al. (2003) also showed the low-frequency variability of Sahel rainfall is closely related to a largely tropical sea surface temperature anomaly pattern that spans the Pacific, Atlantic, and Indian oceans. Further expansion in climate modeling can provide good evidence for the short and long-term rainfall variations observed over the region. Progress in climate modeling arguably improves the prediction skill for tropical climate, despite the fact that some of the techniques need enormous to implement in the developing nations. However, some of the model methods may be shortened to portable but nonetheless skillful simplified dynamical model or statistical (or empirical) models are needed for smaller spatial scales.

Various statistical techniques have widely applied to modeling rainfall variability on different timescales. Osman and Shamseldin (2002) examined the influence of ENSO and the Indian Ocean SST on rainfall variability in the central and southern regions of Sudan. They have shown that the driest year highly correlated with the warm phase of ENSO and Indian Ocean SST, and so that developing quantitative rainfall prediction models using ENSO and Indian Ocean SST is possible. Unganai and Mason (2002) applied an analysis of variance approach to assess the predictability of long-range prediction of Zimbabwe summer rainfall. They found that close to 70% of the total variance in Zimbabwe summer rainfall is potentially predictable at long-range time scale. Using a statistical approach, Mason (1998) assessed the seasonal forecasting of South African rainfall using a non-linear discriminant analysis. Barros and Silvestri (2002) applied canonical correlation analysis in the study of the relation between rainfall in southeastern South America and SST in the subtropical south-central Pacific Ocean. Besides, Nazemosadat and Cordery (2000) have shown statistically that ENSO induces significant rainfall anomalies in northwestern Iran in autumn, making possible rainfall prediction because the summer SOI was good indicator of the behavior of the autumn ENSO state, and thus rainfall, well in advance. Delsole and Shukla (2002) showed the potential of statistical methods in selecting skillful linear prediction models based on global parameters such as ENSO, NAO, and others, for predicting Indian monsoon rainfall. Also Gissila et al. (2004) and Diro et al. (2011a) found out that statistical model making use of the correlation between SST in the Pacific and Indian Oceans and rainfall in various part of Ethiopia in forecasting seasonal rainfall anomalies. Diro et al. (2011b) further applied two atmospheric climate models, HadAM3 and HiGAM on various dataset to evaluate the seasonal rainfall over Ethiopia. Their finding suggested that both models are capturing the different seasonal cycles in different regions of the country.

Dynamical downscaling of climate modeling technique uses fairly high resolution Regional Climate Model (RCM), driven by the output of a relatively low resolution General Circulation Models (GCM), to simulate small-scale features over a limited region (Hansen et al. 2011). The use of regional models to downscale seasonal climate in Africa has been able to provide climate information with useful local detail, including sensible extreme events (Sun et al. 1999; Sylla et al. 2009). Pohl et al. (2011) further documented the capacity of Weather Research and Forecasting Model (WRF) to simulate some atmospheric variables, such as rainfall over Equatorial East Africa. They have shown that several model configurations have capable to simulate regional climate with reasonable accuracy despite biases toward wet and dry conditions over some regions.

In climate prediction, proper setting up of spatial domains and zoning is essential to identify regions resembles in internal characters and their response to external factors. Configuring global or regional models in atmospheric variables means parameterization of the model for external boundary condition forcing. Accuracy of climate prediction model is then verified against observed or climatological values. Documentation of the skill of climate prediction techniques over long historical period is therefore required to evaluate contribution of the method contribute to operational forecasts. Climate prediction is realizing climate patterns and identifying prospective external factors that influence the climate of a given region. Besides, it is also a tool to develop and make suitable test on the skill of developed climate models and performing routine forecast verification. In forecast verification scheme, forecast producers evaluate their forecasts whether they have skill of capturing ground truth for a given timescale. Relevance of the forecast verification also helps in boasting confidence among the users in the utilization of forecast information.

In Ethiopia, an onset and cessation of seasonal rainfall vary considerably within few kilometers distance due to altitudinal variations, orientation of mountain chains and their physical influence on atmospheric flow. Topographic variation, on the other hand, is a good opportunity to regionalize the country's rainfall pattern. Flohn (1987), for example, noted that Ethiopian mountains created a distinct climatic division across the source region of the Blue Nile and its tributaries. Diverse topography and strong seasonal variation over the other parts of the country also indicate the potential physical justifications to delineate rainfall patterns on various spatial scales. Thus, delineating the country into homogeneous rainfall zones is primarily to characterize the rainfall variability on a similar spatial scale to provide local-specific seasonal climate predictions. Some of the rainfall homogenous zoning methods were widely discussed by many authors (e.g., Goossens 1985; Puvaneswaran and Smiths 1993; Gadgil et al. 1993, Nicholson 1994; Basalirwa 1995; Basalirwa et al. 1999; Gissila et al. 2004; Diro et al. 2009).

### **2.3.2 Seasonal climate predictability skill in Ethiopia**

The seasonal forecasting systems and techniques used by NMA have been documented in several papers (e.g., Bekele 1997; Korecha and Barnston 2007; Diro et al. 2011a). As seasonal climate predictors, NMA uses indices of sea surface temperatures (SSTs) over the tropical Pacific Ocean, the Southern Oscillation Index (SOI), the Multivariate ENSO Index (MEI as described by Wolter and Timlin (1998]) and the ENSO (El Niño-La Niña) outlook obtained from NOAA/CPC. Historical and current Niño 3.4 SSTs (the Niño 3.4 region is located in the central equatorial tropical Pacific Ocean) are

used to select years with ENSO evolution similar to the current year. Rainfall prediction for the current year is then based on rainfall observed in these analog years. Monthly SSTs are compared for several months in advance of the season to be predicted.

By considering the current and future ENSO states, the best three analog years are selected from the primarily listed similar years. This procedure is done using graphical and rank correlation techniques. Following these steps, the seasonal rainfall of each station is calculated for each analog year that the station rainfall in each analog year is expressed as a percentile of the full climatology using a percentile statistical approach. Station-based seasonal rainfall percentiles (following Gibbs and Maher 1967) are then used to calculate tercile categories (0–33; 34–66, and 67–100%) for each homogeneous rainfall region. NMA's seasonal rainfall forecast is then prepared as a probability of the regional seasonal rainfall being below, near, and above the climatological normal. The tercile rainfall categories, which are more commonly known as the probabilities, refer to the likelihood that the region-averaged rainfall will be below, near, or above average as the anomalies in seasonal (4 month) rainfall are often large in geographical scale. This forecast format is motivated by the simplicity of the forecast presentation and is used by many operational seasonal forecast centers. Finally, NMA issues the seasonal rainfall forecast for each season (FMAM, JJAS, and ONDJ), 1–2 weeks prior to the normal onset date of each season.

The relative skills of the probabilistic forecasts (RPSS) were assessed over that of climatology and ENSO-RPSS are calculated for FMAM and JJAS. The results reveal that the forecast to have slightly better skill than climatology with RPSS values up to 8–9% in a few regions during the FMAM season over the regions experiencing bimodal rain types, while in the case of JJAS the

RPSS is somewhat lower (4–6% in five of the eight regions). Although the RPSS indices are weak, they are all positive, indicating the presence of some predictability skill for both seasons over Ethiopia.

In order to evaluate the performance of seasonal rainfall forecast in Ethiopia, yearly national RPSS values for the period 1999–2011 are calculated for the FMAM and JJAS seasons (Fig. 12). The values are computed by averaging RPSS of each station (thus, it is bias to the regions with many stations). The results showed that the forecast system has positive skill on a national level except for the dry FMAM season of 2002 and 2009 and during JJAS 2000, 2004, 2005, and 2010. The highest skills (above 10%) are found in 2005 and 2011 for the FMAM season and during 2002 and 2009 for JJAS. With few exceptions the nationally averaged RPSS scores are slightly positive (Fig. 12).

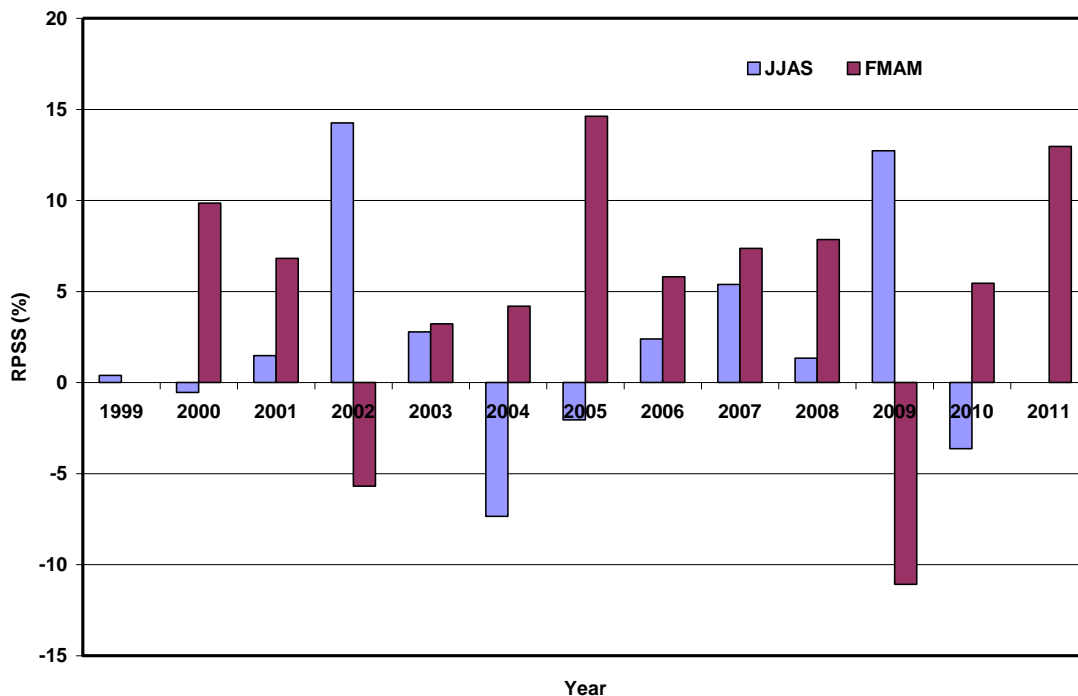


Fig. 12: Mean yearly RPSS values for FMAM and JJAS seasons for Ethiopia. Negative (positive) values indicate poor (good) forecast skill.

## **3 Data**

### **3.1 Climate Data**

Meteorological observations began in Ethiopia at few sites around the middle of 19<sup>th</sup> Century. Since the beginning of 20<sup>th</sup> Century few stations from central, northern and southwestern Ethiopia have continued to recording rainfall and temperature despite many missing values (Conway et al. 2004). However, meteorological stations networks significantly increased after 1950s when the importance of weather information realized for water and agricultural sectors. In present days, NMA and partner institutions are administering more than one thousand meteorological stations (Fig. 13) of different classes, representing various climatic regimes of the country (NMA 2013). Climate data used in the analysis of the predictability skill and develop prediction model, create homogeneous rainfall zones, perform forecast verification on seasonal rains and evaluate the severity of drought and its tendencies are based on Ethiopian historical monthly rainfall data. Daily rainfall data from the same source are also in use during quality checking, filling missed data and for the case study over Ethiopia. Long-term monthly climatological rainfall values for Ethiopian meteorological stations and seasonal rainfall forecast products also extracted from NMA's data bank. Besides, NMA's newly assembled satellite rainfall estimate merged with station rainfall data, which have duration of 1983 to present are also widely used.

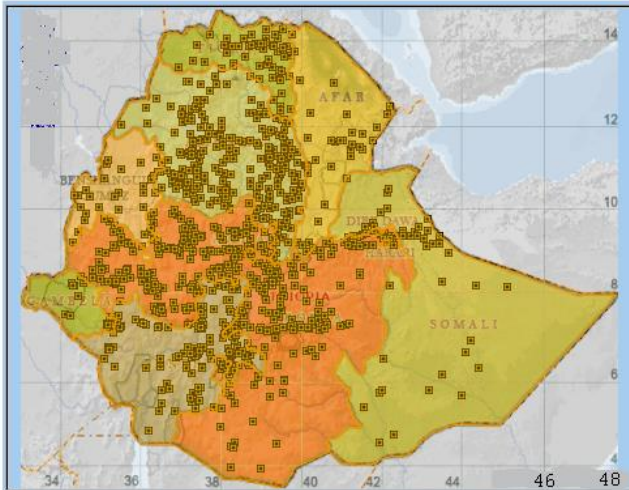


Fig. 13: Spatial distribution of Ethiopian meteorological stations (NMA 2013). Background of the map shows Regional administrative regions of Ethiopia.

Quality controls on climate data were critically performed based on WMO (1986) method for meteorological station data. At beginning, daily rainfall recorded at each station was checked against nearby principal stations and inspected if there are suspected outliers. The quality of monthly rainfall totals then validated and rechecked before the seasonal totals were calculated. In Paper II, the period 1971-2000 were used as climatological base in creating seasonal and annual mean national rainfall maps, which was consistent with that of NMA's official climatological maps. The proportion of missing data used in this paper is low, with few stations having at most 10% of missing data. Missing months were estimated by interpolating data from the highly correlated stations within a reasonable distance away. Similar quality control was also done for the rainfall data (for the periods, 1951-2010/11), which were also used in the same paper I as well as Paper IV. Along the border regions, where there are scarce national data, we used some neighboring stations from the Nile Basin data set available at Geophysical Institute (GFI/UIB), especially for Paper II. In Paper IV, for each homogeneous rainfall zones constructed in Paper I, a time series of monthly

precipitation for January 1970–May 2011 was made, based on monthly data for 238 gauge stations obtained from NMA. Furthermore, merged station-satellite data, which have duration of 1983-2010, extracted at the 162 station locations and 717 random locations are also examined for the validity and stability of rainfall classification as well as in quantifying the performance of seasonal rainfall in Ethiopia. The monthly climatology of each station was calculated and averaged over the stations in the zone to produce the zone climatology.

### **3.2 Atmospheric and Oceanic Indices**

The National Centers for Environmental Prediction (NOAA/NCEP) and National Center for Atmospheric Research (NCAR) have cooperated to perform data analysis assimilation on global atmospheric fields using historical data from 1948 to the present. The NCEP/NCAR Reanalysis is a project (Kalnay et al. 1996) used to reanalyze historical meteorological data using state-of-the art global data assimilation systems and a database as complete as possible. Climatological patterns were drawn and analyzed for 2.5° by 2.5° grid for three seasons over Ethiopia. For spatial analysis, we used an algorithm available in Earth System Research Laboratory Physical Science Division (NOAA/ESRL/PSD) and generate seasonal climatology and anomaly maps of some oceanic and atmospheric field for the selected constant pressure levels (NCAR 2013).

For Paper III, we used global SST from the National Oceanic and Atmospheric Administration/National Climatic Data Center (NOAA/NCDC) Extended Reconstructed Sea Surface Temperature version 2 (ERSSTv2) historical dataset (Smith and Reynolds 2004), with 2° by 2° resolution for the

period 1970–2004. For Paper I and II, improved Extended Reconstructed SST version 3 (ERSST.v3) have been used from NOAA/NCDC (Smith et al. 2008). Classification of ENSO into El Niño, La Niña or neutral state made according to NOAA's ENSO category. NOAA defines non-neutral ENSO state as a departure from normal of the SST in the Niño-3.4 region of magnitude 0.5°C or more, lasting for at least five running three-month periods. In Paper IV, we used ERA-Interim reanalysis data in order to describe anomalies in the moisture flux field in the spring and summer of 2009. ERA-Interim is produced by the European Centre for Medium-Range Weather Forecasts at a resolution of about 0.75° latitude and longitude, with 60 vertical levels and a 4-D variational assimilation system (Simmons et al. 2006; Uppala et al. 2008; Berrisford et al. 2009).

## **4 Summary Results from the Papers**

This thesis aims to examine the performance of seasonal forecast, spatial coherence of rainfall regimes and propose skillful prediction models for the main rainy season in Ethiopia. The results as generated from the present study have been presented in four papers.

The first manuscript provides an overview of NMA's operational seasonal rainfall prediction skills in various rainfall regimes of Ethiopia. The second manuscript provides spatially coherent homogeneous rainfall regimes as the main platform for developing region-specific climate prediction model. The third paper deals with the construction of multivariate statistical seasonal rainfall based on ENSO indices for the main rainy season in the major portions of Ethiopia. The fourth manuscript provides an overview of drought episodes and precipitation tendencies in all parts of Ethiopia during the last decades.

### **4.1 Paper I: Seasonal rainfall forecast Validation**

Korecha D. and Sorteberg A. (2013): Validation of operational seasonal rainfall forecast in Ethiopia. Published online in the *Water Resources Research*, VOL. 49, 7681–7697, doi: 10.1002/2013WR013760.

This paper is aimed to evaluate the skill of National Meteorological Agency of Ethiopia seasonal rainfall forecast issued for February-May (FMAM) and June-September (JJAS) rainy seasons during the period 1999 to 2011.

The verification techniques we employed for this study are able to assess both the direction and magnitude of seasonal rainfall forecast biases. The results reveal that the forecast under-forecast below average rainfall in all regions in the FMAM and JJAS seasons. In contrast, the forecast was substantially biased toward the near average category in all regions both in FMAM and JJAS. In general, above average rainfall occurred on average 28% of the cases during period 1999 to 2011 as compared to the reference climatological base period (1971-1998). The bias of the prediction system towards near average indicates lack of forecast sharpness in predicting events deviating from the normal.

When the skill of a seasonal forecast is further examined, the probabilistic value assigned for each category shows that near average rainfall forecast category was forecasted to be the most probable event, while the below and above average categories were forecasted as the most likely is less frequent. NMA's forecasting system sometimes forecasts the above average category as most probable for low rainfall years. This under-forecast of severe dry events may be a result of the fact that there is a greater reluctance to assign high probabilities for below average than for above average rainfall since in many parts of the country a warning of dry conditions would be considered more serious than wet conditions.

The aggregated RPSS for each homogeneous rainfall region shows positive, but low predictability skills. The RPSS values for FMAM are slightly higher

than for the JJAS season, indicating that the short rainy season has been predicted slightly better than the main rainy season. On spatial scale, among the eight homogeneous rainfall regions, the forecast skill is above the climatology only for three of them (eastern parts of the country) during the FMAM season. For the JJAS season, however, the forecast system exceeds the climatological chance (0.33) in four of the eight homogeneous regions (two regions in the west and two in the south).

The results further show that the forecast attains slightly better skill than climatology with RPSS values up to 8-9% in a few regions during the FMAM season, while in the case of JJAS the RPSS is somewhat lower (4-6% in 5 of the eight regions). We argue that although the RPSS indices are weak, they are all positive, indicating the presence of some predictability skill for both seasons over Ethiopia. When RPSS of ENSO climatology is compared with the forecast issued by chance (assigning equal chances for the three tercile rainfall categories), ENSO information alone can indicate the direction of the seasonal rainfall anomalies particularly during JJAS season for northern Ethiopia. The results further indicate that a stronger weight on ENSO information into the seasonal predictability scheme would improve the forecast skill in parts of Ethiopian during the rainy seasons.

Overall, the RPSS results indicate that NMA's seasonal rainfall forecasts have modest positive skill compared to climatology while compared to an ENSO climatology the seasonal forecast performs poorly, particularly over the central and northern regions in JJAS. The results also show that more weight on ENSO information into the seasonal predictability scheme would improve the forecast skill for JJAS rainy season.

Based on the overall study results we suggest that NMA should work further to make appropriate improvement on the predictability of seasonal rainfall systems, especially for below normal rainfall categories. Therefore, further work on identifying the underlying rain-producing systems and examine closely their physical linkage with larger scale surface indices. Merging heterogeneous rainfall regions into one region may also distort the level of seasonal forecasting skill over various parts of Ethiopia. In this regard, further research on how to separate the country into useful rainfall regions may be beneficial to improve the forecast quality.

## **4.2 Paper II: Construction of Homogeneous Rainfall Regimes**

Korecha, D. and Sorteberg, A., 2013: Construction of Homogeneous Rainfall Regimes for Ethiopia. Submitted to *International Journal of Climatology*.

In the second paper of this thesis, monthly rainfall totals recorded over 162 meteorological stations from Ethiopia for the period 1951-2009 were examined in order to reconstruct spatially-coherent but independent homogeneous rainfall regions. Homogeneous rainfall classifications were further validated and modified based on merged station-satellite rainfall data of fine spatial resolution (of 10-km). Moreover, temporal rainfall patterns of Ethiopia were examined to know how sub-continental rainfall anomalies such as the Sahel and all-India, correlate with all-Ethiopia rainfall index. Results show that all-Ethiopia rainfall time series is strongly correlated with both the Sahel and all-India summer rains. Results from this study therefore, suggest that the scientific findings on the Sahel and India rainfall, which are well documented and more comprehensively studied than that of the Ethiopian

rainy seasons, can be beneficial for understanding and make use of the all-Ethiopia rainfall variability.

A national rainfall index, which was computed for all-Ethiopia rainfall time series based on the 250 stations, indicates that Ethiopia on average (for the period 1971– 2000) receives 1115 mm of rainfall annually. From this crude mean value, which is biased toward regions with a dense station network; 655, 310 and 150 mm rainfall totals are the climatological values for *Kiremt* (Jun-Sep), *Belg* (Feb-May) and *Bega* (Oct-Jan) seasons, respectively. It follows that each of this season contributes 59%, 28% and 13% (*Kiremt*, *Belg* and *Bega*, respectively) to the mean annual rainfall totals. Large scale atmospheric circulation anomalies related to sea surface temperature anomalies such as El Niño or La Niña events combined with regional and local atmospheric circulation anomalies induced significant anomalies in Ethiopian rainfall. It has been observed that El Niño and La Niña usually suppress and enhance *Kiremt* (summer) rains while they behave differently in the case of *Bega* (winter) and *Belg* (spring) seasons.

Regions of strong principal components (PC1) loading receive maximum rains in June-September, and small rains during March-April-May, while the region often receives less rain showers in December-January. PC2 and PC3 loadings show distinct seasonality of rainfall patterns for southwest-west and south-southeast regions, respectively. The two PC loadings clearly emphasize the non-*Kiremt*-rain benefiting region of south-southeast in contrast to the *Kiremt*-rain benefiting regions of the western and northern half of the country. The K-means cluster analysis (CA) method created twelve rainfall clusters and the stations that are grouped in each cluster match well geographically and exhibit the same seasonal rainfall characteristics. Results from CA clearly showed the presence of rainfall dissimilarities across the

regions. Hence, the presence of numbers of rainfall clusters suggest that rainfall patterns over Ethiopia vary with short distance, while modulated by topographic variation and orientation, large-scale atmospheric circulation systems, moisture track and local dynamical conditions.

Thus the results presented in this study confirm that much of the large scale meteorological systems known to influence the Ethiopian rainfall distribution are fairly used in justifying the dissimilarities of twelve homogeneous rainfall regions. Besides, the study reveals that local rainfall variations that are recurrently influencing various social and economic practices can be more identified on the present homogeneous rainfall regime than those based on earlier regional classification. It is believed, however, that further detailed spatial analysis of rainfall on various time scales is needed to obtain finer information relevant for localized societal activities.

### **4.3 Paper III: Predictability of June–September rainfall**

Korecha, D. and Barnston A., 2007: Predictability of June–September rainfall in Ethiopia. Published on the *Monthly Weather Review*, 135:628–650.

In this study, the predictability of main rainy season (JJAS) over Ethiopia was examined using multivariate statistical techniques for the period 1970-2004. This study shows the presence of strong teleconnection linkage between major JJAS rain-benefiting regions of Ethiopia, which was consistent with previous findings. Lag relationship calculated between JJAS rainfall and spring months SSTs showed promising results for seasonal rainfall prediction.

As a result, the northern hemisphere spring barrier is more than halfway traversed by the end of May and a moderately skillful summer forecast can be made at this short lead time. When and if ENSO can be better predicted through this difficult time of year, longer lead forecasts could be made for Ethiopian summer rainfall. Pre-summer ENSO state, and its direction and rate of evolution, could be used as a simple statistical precursor during the summer season ahead, and consequently the summer seasonal rainfall.

Seasonal rainfall teleconnections to SST regions other than the tropical Pacific are considerably weaker and of smaller spatial scale, and include the Indian and Atlantic Oceans both during and preceding summer. Pertinent to examining the linkage of all-Ethiopian JJAS to SST and SOI indices, the main finding is that northern summer ENSO condition is overwhelmingly the single most important factor governing the JJAS rainfall across Ethiopia, excluding the southern/southeastern lowlands. SST anomalies in the Atlantic and Indian Oceans appear to matter far less. More regional climate and weather processes were not investigated here, but could be tied into this larger scale. Skillful predictions of Ethiopian summer rainfall hinge upon the best possible forecasts of the summer ENSO state from an earlier time. Useful summer rainfall predictions are thus potentially achievable using global dynamical or statistical models.

The Canonical Correlation Analysis (CCA) defines spatial pattern relationships between global SST and JJAS Ethiopia station rainfalls. The simultaneous SST–rainfall patterns strongly confirm the impact of ENSO, and indicate a lesser role for SSTs near the source regions of monsoonal low-level systems near southwest India and in South Atlantic. These conclusions also apply to the CCA using leading May SSTs.

#### **4.4 Paper IV: Drought in Ethiopia – an overview of precipitation**

Viste, E., Korecha D. and Sorteberg A., 2012: Recent drought and precipitation tendencies in Ethiopia. Published online in the *Theoretical Applied Climatology*. doi: 10.1007/s00704-012-0746-3.

This paper aims to quantify the meteorological component of drought episodes in Ethiopia since 1971. The standardized precipitation index (SPI), a statistical measure that indicates how unusual an event is, making it possible to determine how often droughts of certain strength are likely to occur. All drought measures were calculated based on accumulated precipitation at several time scales. Long-time drought was considered at time scales of 12 and 24 months, and the 4-month indices for May and September were used to describe the spring and summer seasons, respectively.

Analysis of gauge-based precipitation data for 14 Ethiopian climatic zones during 1971–2011 justifies the international concern about the recent dryness. Some of the last years have been among the driest in this period, and in southern Ethiopia, precipitation has declined, both in the spring (February–May) and the summer season (June–September). Dry spring seasons have characterized the period since 1999, affecting most of Ethiopia. The largest relative precipitation deficits have appeared in the southern Ethiopia, where this is the main rainy season. The rest of the country has also experienced extremely dry springs during the last decade, but no general, long-lasting trend can be assumed based on this data set.

The spring seasons of 2008 and 2009 were extremely dry in about half of the zones, and in 2009, the dry spring was followed by a dry summer. As a result, 2009 was one of the few years with drought conditions in all of Ethiopia, both on seasonal and annual scales. On the national level, 2009 was the second driest year in the record, after 1984, and drier than 2002. In the southern highlands, 2009 was the driest year in the record, whereas in the rest of the country, previous droughts were more extreme. In the three southernmost zones, where the spring season is the most important rainy season, the linear regression equation we develop show a decline in precipitation both in the spring (2.6 mm/year), the summer (2.2 mm/year), and annually (5.4 mm/year). In the rest of the country, those zones where the summer rains are most important, the linear regression analysis does not give us a reason for suggesting a corresponding decrease, neither on seasonal nor annual scale.

The spatial drought pattern from year to year varies, to a large extent reflecting the variation in the seasonal precipitation cycle between the zones. Ethiopian precipitation exhibits great spatial variation, both in the average year, and when it comes to interannual variability. This affects the drought patterns. In a few years, mainly 1984 and 2009, drought conditions prevailed in all of Ethiopia, on both seasonal and annual time scales. In most historic drought years, the problem was of a more local or regional character, affecting only some parts of the country, and not necessarily in the same season. Due to this variation, there were no years without at least mild annual drought in at least one zone. If the tendency of dry springs persists in the future, the risk of serious drought years may increase in all of Ethiopia; in the south because the spring is the main rainy season. In northern and central Ethiopia, where the summer is the main rainy season, the outcome is less obvious. But unless physical mechanisms act against it, an increase in spring

droughts increases the probability of the occasional dry summer having been preceded by a dry spring. As a result, droughts may more frequently last throughout the agricultural growth season, as in the two driest years during 1971– 2010: 1984 and 2009.

## References

- Abeku, T. A., G. T. van Oortmorssen, G. Borsboom, S. J. de Vlas and J. D. Habbema (2003).** Spatial and temporal variations of malaria epidemic risk in Ethiopia: factors involved and implications. *Acta Trop.* **87**(3): 331-340.
- Abeku, T. A., S. J. de Vlas, G. Borsboom, A. Tadege, Y. Gebreyesus, H. Gebreyohannes, D. Alamirew, A. Seifu, N. D. Nagelkerke, J. D. Habbema (2004).** Effects of meteorological factors on epidemic malaria in Ethiopia: A statistical modeling approach based on theoretical reasoning. *Parasitology*, **128**: 585-593.
- AMS (2013).** American Meteorological Society meteorological glossary. <http://amsglossary.allenpress.com/glossary>.
- Barros, V. y G. Silvestri, 2002:** On the relation between sea surface temperature at the subtropical south-central pacific and precipitation in southeastern South America. *J. Clim.*, **15**: 251-267.
- Basalirwa, C. P. K. (1995).** Delineation of Uganda into climatological rainfall zones using the method of principal component analysis. *Int. J. Climatol.* **15**: 1161-1177.

- Basalirwa, C. P. K., J. O. Odiyo, R. J. Mngodo and E. J. Mpeteta (1999).** The climatological regions of Tanzania based on the rainfall characteristics. *Int. J. Climatol.* **19**: 69–80.
- Bekele, F. (1997).** Ethiopian use of ENSO information in its seasonal forecasts, *Internet J. Afr. Studies*, No. 2. [Available online at <http://www.ccb.ucar.edu/ijas/ijasno2/bekele.html>.]
- Berrisford, P., D. Dee, K. Fielding, M. Fuentes, P. W. Kállberg S. Kobayashi, S. M. Uppala (2009).** The ERA-Interim archive. ERA report series, vol 1. ECMWF, Reading.
- Block, P. (2011).** Tailoring seasonal climate forecasts for hydropower operations. *Hydrol. Earth Syst. Sci.*, **15**: 1355–1368.
- Camberlin, P. (1997).** Rainfall anomalies in the source region of the Nile and their connection with the Indian summer monsoon. *J. Climate*, **10**: 1380–1392.
- Camberlin, P. (2009).** Nile Basin Climates. In “*The Nile: Origin, Environments, Limnology and Human Use*”, Dumont, Henri J. (Ed.), *Monographiae Biologicae*, Springer, 307-333.
- Camberlin, P. and M. Diop (2003).** Application of daily rainfall principal component analysis to the assessment of the rainy season characteristics in Senegal. *Clim Res*, **23**: 159–169.
- Camberlin, P. and N. Philippon (2002).** The East African March–May Rainy Season: Associated Atmospheric Dynamics and Predictability over the 1968–97 Period. *Journal of Climate* **15**(9): 1002–1019.
- Cane, M. A. (2000).** Understanding and Predicting the World’s Climate System: Applications of Seasonal Climate Forecasting in the Agricultural and Natural Systems, *Kluwer Academic Publishers*, 29-50. *University Press*, 735 pp.

- Cane**, M. A. and D. Verschuren (2011). Reduced Interannual Rainfall Variability in East Africa During the Last Ice Age. *Science* 333, 743; DOI: 10.1126/science.1203724.
- Charney**, J., and J. Shukla (1981). Predictability of monsoons. Monsoon dynamics, Sir J. Lighthill and R. P. Pearce, Eds., pp. 99-104, *Cambridge*
- Conway**, D. (1996). The Impacts of Climate Variability and Future Climate Change in the Nile Basin on Water Resources in Egypt. *International J. Water Resources Development*, **12**(3): 277-296.
- Conway**, D., L. Schipper, M. Yesuf, M. Kassie, A. Persechino, A., B. Kebede (2007). Reducing vulnerability in Ethiopia: addressing the issues of climate change: Integration of results from Phase I. Norwich: Overseas Development Group, University of East Anglia.
- Conway**, D., C. Mould and W. Bewket (2004). Over one century of rainfall and temperature observations in Addis Ababa, Ethiopia. *Int. J. Climatol.*, **21**: 77-97.
- Degefu**, W. (1987). Some aspects of meteorological drought in Ethiopia. Drought and Hunger in Africa: Denying Famine a Future, M. H. Glantz, Ed., *Cambridge University Press*, 23–36.
- DelSole**, T., and J. Shukla (2002). Linear prediction of Indian monsoon rainfall. *J. Climate*, **15**: 3645-3658.
- Deressa**, T. T. (2006). Measuring the economic impact of climate change on Ethiopian agriculture: Ricardian approach. CEEPA Discussion Paper No. 21. Pretoria: University of Pretoria (<http://econ.worldbank.org>).
- Diro**, G. T., D. I. F. Grimes, E. Black, A. O'Neill and E. Pardo-Iguzquiza (2009). Evaluation of reanalysis rainfall estimates over Ethiopia. *Int. J. Climatol.*, **29**: 67–78.

- Diro**, G. T., D. I. F. Grimes and E. Black (2010). Teleconnections between Ethiopian summer rainfall and sea surface temperature: part II. Seasonal forecasting. *Clim. Dyn.*, **37**(1-2): 121-131.
- Diro**, G. T., D. I. F. Grimes and E. Black (2011a). Teleconnections between Ethiopian summer rainfall and sea surface temperature: part II. Seasonal forecasting. *Clim Dyn*, **37**: 121–131.
- Diro**, G. T., T. Toniazzo and L. Shaffrey (2011b). Ethiopian Rainfall in Climate Models. C.J.R. Williams, D.R. Kniveton (eds.), *African Climate and Climate Change*, 51, Advances in Global Change Research, 43: DOI 10.1007/978-90-481-3842-5\_3,
- Findlater**, J. (1977). Observational aspects of the low-level cross-equatorial jet stream of the western Indian Ocean. *Pure and Applied Geophysics*, **115**(5-6): 1256-1262.
- Gadgil**, S., M. Rajeevan and R. Nanjundiah (2005). Monsoon prediction – Why yet another failure? *Current Science*, **88**(9): 1489-1400.
- Gadgil**, S., Yadumani and N. V. Joshi (1993). Coherent rainfall zones of the Indian region. *Int. J. Climatol.* **13**: 547-566.
- Gemechu**, D. (1977). Aspects of climate and water budget in Ethiopia. *Addis Ababa University Press*, 77pp.
- Giannini**, A., R. Saravana, and P. Chang (2003): Oceanic forcing of Sahel rainfall on inter-annual to inter-decadal time scales. *Science*, **302**: 1027–1030.
- Gissila**, T., E. Black, D. I. F. Grimes, and J. M. Slingo (2004). Seasonal forecasting of the Ethiopian summer rains. *Int. J. Climatol.*, **24**: 1345–1358.

- Gonfa, L.** (1996). Climate classification of Ethiopia. NMSA, Addis Ababa, Ethiopia.
- Goossens, C. R.** (1985). Principal component analysis of Mediterranean rainfall. *Int. J. Climatol.* **15**: 1161-1177.
- Grover-Kopec, E. K., M. B. Blumenthal, P. Ceccato, T. Dinku, J. A. Omumbo and S.J. Connor** (2006). Web-based climate information resources for malaria control in Africa. *Malaria Journal*, **5**(38) doi: 10.1186/1475-2875-5.
- Hansen, J. W.** (2002). Realizing the potential benefits of climate prediction to agriculture: Issues, approaches, challenges. *Agric. Syst.*, **74**: 309–330.
- Hansen, J. W., S. J. Mason, L. Sun and A. Tall** (2011). Review of seasonal climate forecasting for agriculture in sub-Saharan Africa. *Expl. Agric.*, **47**(2): 205–240.
- Hastenrath, S.** (1986). On Climate Prediction in the Tropics. *Bull. Amer. Meteor. Soc.*, **67**: 696-702.
- Hulme, M. and N. Tosdevin** (1989). The tropical easterly jet and Sudan rainfall: a review. *Theoretical and Applied Climatology*, **39**: 179-187.
- Kalnay, E., M. Kanamitsu, R. Kistler, W. Collins, D. Deaven, L. Gandin, M. Iredell, S. Saha, G. White, J. Woollen, U. Zhiu, M. Chelliah, W. Ebisuzaki, W. Higgins, J. Janowiak, K. Mo, C. Ropelewski, J. Wang, A. Leetmaa, R. Roeynolds, R. Jenne, and D. Joseph** (1996). The NCEP/NCAR 40-year reanalysis project. *Bull. Amer. Meteorol. Soc.*, **77**: 437-471.
- Kassahun, B.** (1987). Weather systems over Ethiopia. *Proc. First Tech. Conf. on Meteorological Research in Eastern and Southern Africa, Nairobi, Kenya, UCAR*, 53–57.

- Lemi, A.** (2005). Rainfall probability and agricultural yield in Ethiopia. *Eastern Africa Social Science Research Review*, **21**(1): 57-96.
- Mason, S. J.** (1998) Seasonal forecasting of South African rainfall using a non-linear discriminant analysis model. *Int. J. Climatol.* **18**: 147–164.
- Millner, A.** and R. Washington (2011). What determines perceived value of seasonal climate forecasts? A theoretical analysis. *Global Environmental Change*, **21**: 209–218.
- MoFA** (2013). <http://www.mfa.gov.et/>: Federal Democratic Republic of Ethiopia, Ministry of Foreign Affairs, Addis Ababa, Ethiopia.
- MoWE** (2013). <http://www.mowr.gov.et/>: Federal Democratic Republic of Ethiopia, Ministry of Water and Energy, Addis Ababa, Ethiopia.
- Mutai, C. C., M. N. Ward and A. W. Colman** (1998). Towards the prediction of the East Africa short rains based on sea-surface temperature-atmosphere coupling. *Int. J. Climatol.*, **18**: 975–997.
- Nazemosadat, M. J. and I. Cordery** (2000). On the relationships between ENSO and autumn rainfall in Iran. *Int. J. Climatol.*, **20**: 47–61. doi: 10.1002/(SICI)1097-0088.
- NCAR** (2013). National Centers for Environmental Prediction (NOAA/NCEP) and National Center for Atmospheric Research (NCAR), Earth System Research Laboratory Physical Science Division (NOAA/ESRL/PSD). [www.esrl.noaa.gov/psd/data/reanalysis/reanalysis.shtml](http://www.esrl.noaa.gov/psd/data/reanalysis/reanalysis.shtml).
- Nicholson, S. E.** (1994). Recent rainfall fluctuations in Africa and their relationship to past conditions over the continent. *The Holocene*, **4**, 121-131.

- Nicholson**, S. E. and J. P. Grist (2003). The Seasonal Evolution of the Atmospheric Circulation over West Africa and Equatorial Africa. *Journal of Climate* **16**(7): 1013–1030.
- NMA** (2007). Climate change National Adaptation Programme of Action (NAPA) of Ethiopia. National Meteorological Services Agency, edited by Abebe Tadege, Addis Ababa, Ethiopia
- NMA** (2013). <http://www.ethiomet.gov.et/>: National Meteorological Agency, Addis Ababa, Ethiopia.
- NMSA** (1996). Climatic and agroclimatic resources of Ethiopia. National Meteorological Services Agency of Ethiopia. *Meteorological Research Report Series*, **1**(1): 1–137.
- NMSA** (2001). Initial National Communication of Ethiopia to the United Nations Framework Convention on Climate Change. June 2001, Addis Ababa, Ethiopia.
- NOAA** (2013). <http://www.esrl.noaa.gov/psd/>: National Oceanic and Atmospheric Administration, USA.
- Okumura**, Y. M. and C. Deser (2010). Asymmetry in the Duration of El Niño and La Niña. *J. Climate*, **23**: 5826-5843.
- Osman**, Y. Z., and Y. A. Shamseldin (2002). Quantitative rainfall prediction models for Central and Southern Sudan using El Niño–Southern Oscillation and Indian Ocean Sea Surface Temperature indices. *Int. J. Climatol.*, **22**: 1861–1878.
- Pedgley**, D. E. (1969). Diurnal variation of the incidence of monsoon rainfall over the Sudan. *Meteorological Magazine*, **98**: 97-106.

- Pohl**, B., J. Crétat and P. Camberlin (2011). Testing WRF capability in simulating the atmospheric water cycle over Equatorial East Africa. *Clim. Dyn.*, **37**: 1357–1379.
- Puvaneswaran**, K. M. and P. A. Smithson (1993). An Objective Classification of Homogeneous Rainfall Regimes in Sri Lanka. *Theor. Appl. Climatol.* **48**: 133-145.
- Riddle**, E.E., K. H. Cook (2008). Abrupt rainfall transitions over the Greater Horn of Africa. Observations and regional model simulations. *J. Geophys. Res.*, **113**: 1-14.
- Segele**, Z. T., and P. J. Lamb (2005). Characterization and variability of Kiremt rainy season over Ethiopia. *Meteor. Atmos. Phys.*, **89**: 153–180.
- Segele**, Z. T., P. Lamb, and L. Leslie (2009). Large-scale atmospheric circulation and global sea surface temperature associations with Horn of Africa June–September rainfall, *Int. J. Climatol.*, 29, 1075–1100.
- Shanko**, D., and P. Camberlin (1998). The effect of the southwest Indian Ocean tropical cyclones on Ethiopian drought. *Int. J. Climatol.*, **18**: 1373–1378.
- Seleshi**, Y. and G. R. Demarée (1995). Rainfall Variability in the Ethiopian and Eritrean Highlands and its Links with the Southern Oscillation Index. *Journal of Biogeography* **22**(4/5): 945–952.
- Simmons**, A. J., S. M. Uppala, D. Dee and S. Kobayashi (2006). ERA-Interim: new ECMWF reanalysis products from 1989 onwards. *ECMWF News Letter*, **110**: 25–35.
- Smith**, T. M., R. W. Reynolds, T. C. Peterson and J. Lawrimore (2008). Improvements to NOAA’s Historical Merged Land–Ocean Surface Temperature Analysis (1880–2006). *J. Climate*, **21**: 2283-2296.

- Smith**, T. M. and R. W. Reynolds (2004). Improved extended reconstruction of SST (1854–1997). *J. Climate*, **17**: 2466–2477.
- Stefan**, D. and P. Krishnan (2000). Vulnerability, seasonality and poverty in Ethiopia. *J. Development Studies*, **36**(6): 25-53
- Sun**, L., D. F. Moncunill, D. F., H. Li, A. D. Moura, and F. Filho (2005). Climate downscaling over Nordeste, Brazil, Using the NCEP RSM97. *J. Climate*, **18**: 551–567.
- Sun**, L., F. H. M. Semazzi, F. Giorgi and L. Ogallo (1999). Application of NCAR regional climate model to eastern Africa: Part II: Simulations of interannual variability of precipitation. *J. Geophysical Res.* **104**: 6549–6562.
- Sylla**, M. B., A. T. Gaye, J. S. Pal, G. S. Jenkins and X. Q. Bi (2009). High resolution simulations of West Africa climate using regional climate model (RegCM3) with different lateral boundary conditions. *Theor Appl Climatol.* **98**: 293–314.
- Tadesse**, T. (1994). The influence of the Arabian Sea storms/depressions over the Ethiopian weather. *Proc. Int. Conf. on Monsoon Variability and Prediction*, WCRP-84 and WMO Tech. Doc. 619, Geneva, Switzerland, World Meteorological Organization, 228–236.
- Thomson**, M. C., S. J. Mason, T. Phindela and S. J. Connor (2005). Use of rainfall and sea surface temperature monitoring for malaria early warning in Botswana. *Am. J. Trop. Med. Hyg.*, **73**: 214–221.
- Tsegay**, W., 1998: El Niño and drought early warning in Ethiopia. *Internet J. Afr. Studies*, No. 2. [Available online at <http://www.ccb.ucar.edu/ijas/ijasno2/georgis.html>.]
- Tsegay**, W., 2001: The case of Ethiopia: Impacts and responses to the 1997-98 El Niño event. *Once Burned, Twice Shy? Lessons Learned from the*

1997-98 *El Niño*, M. H. Glantz, Ed., United Nations University Press, 88–100.

**Tziperman**, E., M. A. Cane, S. E. Zebiak, Y. Xue, and B. Blumenthal (1998).

Locking of El Niño's peak time to the end of the calendar year in the delayed oscillator picture of ENSO. *J. Climate*, **11**: 2191–2199.

**Unganai**, L.S. and S.J. Mason (2002) Long-range predictability of Zimbabwe summer rainfall. *Int. J. Clim.* **22**: 1091-1103.

**Uppala**, S. M., D. Dee, S. Kobayashi, P. Berrisford, A. J. Simmons (2008).

Towards a climate data assimilation system: status update of ERA-Interim. ECMWF Newsletter. ECMWF, Reading.

**Viste**, E., Sorteberg A. (2012). Moisture transport into the Ethiopian

highlands. *Int. J. Climatol.*, Published online in Wiley Online Library, DOI: 10.1002/joc.3409.

**Webb**, P., J. V. Braun, and Y. Yohannes (1992). Famine in Ethiopia: Policy

implications of coping failure at national and household levels. *International Food Policy Research Institute*, 167 pp.

**Wikipedia** (2013). <http://en.wikipedia.org/>:

**WMO** (1986). Guidelines on quality control. World Meteorological Organization, *WMO/TD WCP-85*, 56 pp.

**Wolter**, K., and M. S. Timlin (1998). Measuring the strength of ENSO events:

How does 1997/98 rank?, *Weather*, 53(9), 315–324.

**Yemenu**, F. and D. Chemedda (2010). Climate resources analysis for use of

planning in crop production and rainfall water management in the central highlands of Ethiopia, the case of Bishoftu district, Oromia region. *Hydrol. Earth Syst. Sci. Discuss.*, **7**: 3733–3763

**Zebiak**, S. E. and M. A. Cane (1987). A model El Niño–Southern Oscillation.  
*Mon. Wea. Rev.*, **115**: 2262–2278.

**Zeng**, Ning (2003). Drought in the Sahel. *Science*, **302**: 999-1000.

## **Paper I**

### **Validation of operational seasonal rainfall forecast in Ethiopia**

Korecha D. and Sorteberg, A. (2013)

This manuscript is published online in *Water Resources Research*, VOL. 49, 7681–7697, doi: 10.1002/2013WR013760.

# Validation of operational seasonal rainfall forecast in Ethiopia

Diriba Korecha<sup>1, 2</sup> and Asgeir Sorteberg<sup>2, 3</sup>

1 National Meteorological Agency of Ethiopia, Addis Ababa, Ethiopia

2 Geophysical Institute, University of Bergen, Bergen, Norway

3 Bjerknes Centre for Climate Research, University of Bergen, Bergen, Norway

## Abstract

Operational rainfall forecasts using the analog method have been issued in Ethiopia since 1987. We evaluate the performance of the forecast system for February–May and June–September rainy seasons over the period 1999–2011. Verification is performed using rainfall data obtained from Ethiopian meteorological stations covering eight homogeneous rainfall regions used in the forecasts. The results reveal that forecasts issued by the National Meteorological Agency (NMA) of Ethiopia, for the past 12 years have a weak positive skill for all eight regions compared with climatology. In terms of ranked probability skill scores, the values are all lower than 10% indicating that the forecast skill is modest. The results further suggest that the forecasting system has bias toward forecasting near-normal conditions and has problems in capturing below average events. In contrast, the forecast has some positive skills in ranking the wet years of February–May season, particularly over the regions where there is high seasonal rainfall variability with significantly positive rank correlations for the above average years. For the main season, however, the forecast is not able to rank wet years or dry

years. The extreme low and high rainfall events are mostly missed by the forecast scheme. The results indicate rather low forecast skill for extreme rainfall events in both seasons. Generally, the results indicate that NMA's forecasts have low but positive skill as it is common with results from other forecasting systems for the Greater Horn of Africa region. The under-forecasting of dry events is the most serious shortcoming of the system.

## **1 Introduction**

With irrigation covering only 1% of the soil that feeds more than 85 million people, the link between rainfall and agricultural yield is close in Ethiopia. It has been documented that food shortage and scarcity of water have led to local and nationwide famines, mainly due to the complete or partial failure of short and long rainy seasons over various parts of Ethiopia [e.g., NMSA, 1996]. The failure of seasonal rainfall is often caused by either misplacement or weakening of large-scale seasonal rain-producing systems. Attempts have been made to model these systems and factors out that could cause such failures in rainfall and numerous statistical and dynamical prediction models have been developed worldwide [Goddard et al., 2003; Barnston and Mason, 2011].

Annual rainfall characteristics of Ethiopia are classified into three rainy seasons as documented by many authors [Gissila et al., 2004; Segele and Lamb, 2005; Korecha and Barnston, 2007]. These distinct seasons are; the dry (October–January), the small rainy (February–May), and the main rainy (June–September) seasons. The seasons are locally defined as Bega (October–January), Belg (February–May), and Kiremt (June–September). Although delineation of distinct regions and rainy seasons are difficult due to

the complex topography of the country and high rainfall variability, the present forecast verification is done based on the existing homogeneous rainfall regimes.

Variation of rainfall depends mainly on an advection of moist air and the location and intensity of rain bearing systems over the vicinity of Ethiopia. For instance, the westward propagation of weather disturbance developing over the Indian Ocean and Arabian Sea as well as southerly moisture flow are widely known rain-producing features for the eastern African subregion, including Ethiopia [e.g., Nicholson, 2000; Segele and Lamb, 2005]. In Kiremt, the rain-producing systems and their features are mostly associated with the establishment of synoptic and planetary scale systems such as Inter-tropical Convergence Zone (ITCZ), southwest monsoon components, and short-lived weather disturbances forming over the Arabian region [Camberlin, 1997; Segele et al., 2009a; Diro et al., 2011; Wolff et al., 2011].

Seleshi and Demaree [1995] indicated that the Indian Ocean is one of the main moisture sources for Ethiopian rainfall. Similarly, Camberlin [1997] argued that the Kiremt rains (June–September) of Ethiopia rely on moisture advection from the Congo Basin through the southwesterly monsoon. Mohamed et al. [2005] also indicated that the oceanic sources of atmospheric moisture over the Nile basin are the Atlantic and the Indian Oceans. In contrast to the Kiremt rain, eastward traversing of midlatitude frontal systems often triggers unseasonal rain during reasonably dry seasons (October–April) over portions of northern, central, and eastern Ethiopia [Kassahun, 1987; Nicholson, 2000]. The skill of the predictability of seasonal rainfall therefore depends on an extent toward which the prediction systems could quantify the depth and the flow of moisture, regional, and global systems as well as the atmospheric dynamics that initiate seasonal rains.

Statistical relationships between the Ethiopia rainfall and other meteorological parameters or sea surface temperatures have been investigated in a number of papers [e.g., Degefu, 1987; Segele and Lamb, 2005; Korecha and Barnston, 2007; Diro et al., 2011]. By assessing the lag-time correlations of SSTs with seasonal rainfalls of various regions over Ethiopia, the National Meteorological Agency (NMA) has issued seasonal forecasts three times a year since 1987 as documented by Korecha and Barnston [2007].

The role of the El Niño Southern Oscillation (ENSO) on the Ethiopian seasonal rainfall is well documented and associated hazards often coincide with the occurrence of major ENSO events [NMSA, 1996; Camberlin, 1997; Bekele, 1997; Tsegay, 1998; Gissila et al., 2004; Segele and Lamb, 2005; Korecha and Barnston, 2007; Diro et al., 2011]. More recently, Araya and Stroosnijder [2011] documented how various ENSO events disturbed the onset and cessation of seasonal rainy season over northern Ethiopia. In association to mitigating river floods, Wang and Eltahir [1999] underscored the importance of ENSO information for forecasting precipitation over Ethiopia. Moreover, Block and Rajagopalan [2007] pointed out that ENSO phenomenon is the main driver of the interannual variability in seasonal precipitation in the Blue Nile basin, with El Niño (La Niña) events generally producing drier (wetter) than normal conditions. Furthermore, Elagib and Elhag [2011] provided evidence of an ENSO footprint on seasonal rains over about two-thirds of the area of the Sudan. It is, therefore, broadly argued that Ethiopian seasonal rainfall performance is strongly linked to ENSO.

Since the beginning of seasonal climate prediction in Ethiopia, NMA has gone through continuous improvement in order to enhance the skill of predicting

strong seasonal rainfall anomalies for various parts of the country. In recent years, research papers have proposed various statistical techniques to predict the major rainy season in Ethiopia [Gissila et al., 2004; Korecha and Barnston, 2007; Segele et al., 2009a, 2009b; Diro et al., 2009, 2011]. However, to what extent these forecast techniques are of better quality than the NMA forecasting system is unknown. This is due to the fact that few attempts have been made to assess the skill of the operational seasonal rainfall forecasts issued by NMA or other regional and international climate prediction centers for Ethiopia. To address this we here attempt to assess the skill of the NMA's operational seasonal predictions in order to provide a benchmark against which new climate prediction systems can be measured.

The main objective of the present study is, therefore, to verify the skill of seasonal rainfall forecast that have been issued by NMA for the period 1999–2011 for the February–May and June–September rainy seasons. Although ONDJ (October–January) is the dry season over the Kiremt-rain-benefiting regions of Ethiopia, it may have better predictability [e.g., Indeje et al., 2000], it will not be considered in this study.

The paper is arranged as follows: in section 2, the seasonal rainfall forecasting systems used by NMA are presented. The database (archive of forecasts and observations) and validation techniques are explained in section 3. Section 4 describes and discusses results. Conclusions and recommendations are given in section 5.

## **2 Seasonal Rainfall Forecasting System at National Meteorological Agency (NMA)**

### **2.1. Background**

The seasonal forecasting systems and techniques used by NMA have been documented in several papers [e.g., Bekele, 1997; Korecha and Barnston, 2007; Diro et al., 2011]. In this section, some of the essential components of seasonal forecasting and procedures used by NMA are briefly described. As seasonal climate predictors, NMA uses indices of sea surface temperatures (SSTs) over the tropical Pacific Ocean, the Southern Oscillation Index (SOI), the Multivariate ENSO Index (MEI as described by Wolter and Timlin [1998]) and the ENSO (El Niño-La Niña) outlook obtained from NOAA/CPC. Historical and current Niño 3.4 SSTs (the Niño 3.4 region is located in the central equatorial tropical Pacific Ocean) are used to select years with ENSO evolution similar to the current year. Rainfall prediction for the current year is then based on rainfall observed in these analog years. Monthly SSTs are compared for several months in advance of the season to be predicted (Figures 1 and 2). For example, in order to predict rainfall of the June–September (JJAS) season, Niño 3.4 SSTs for January–May of the current year are compared with SSTs for the same months in 1970, 1971, etc., and analogs (years with similar ENSO evolution) are identified. By considering the current and future ENSO states, the best three analog years are selected from the primarily listed similar years (Figure 2). This procedure is done using graphical and rank correlation techniques. Following these steps, the seasonal rainfall of each station is calculated for each analog year that the station rainfall in each analog year is expressed as a percentile of the full climatology using a percentile statistical approach. Station-based seasonal rainfall percentiles [following Gibbs and Maher, 1967] are then used to calculate tercile categories (0–33; 34–66, and 67–100%) for each

homogeneous rainfall region. NMA’s seasonal rainfall forecast is then prepared as a probability of the regional seasonal rainfall being below, near, and above the climatological normal (in this case, the mean from 1970 to the year under consideration). The tercile rainfall categories, which are more commonly known as the probabilities, refer to the likelihood that the region-averaged rainfall will be below, near, or above average as the anomalies in seasonal (4 month) rainfall are often large in geographical scale. This forecast format is motivated by the simplicity of the forecast presentation and is used by many operational seasonal forecast centers. Figure 2 (top right plot) shows an example of an official NMA rainfall outlook for the JJAS 2010 rainy season. Finally, NMA issues the seasonal rainfall forecast for each season (FMAM, JJAS, and ONDJ), 1–2 weeks prior to the normal onset date of each season (Figure 1).

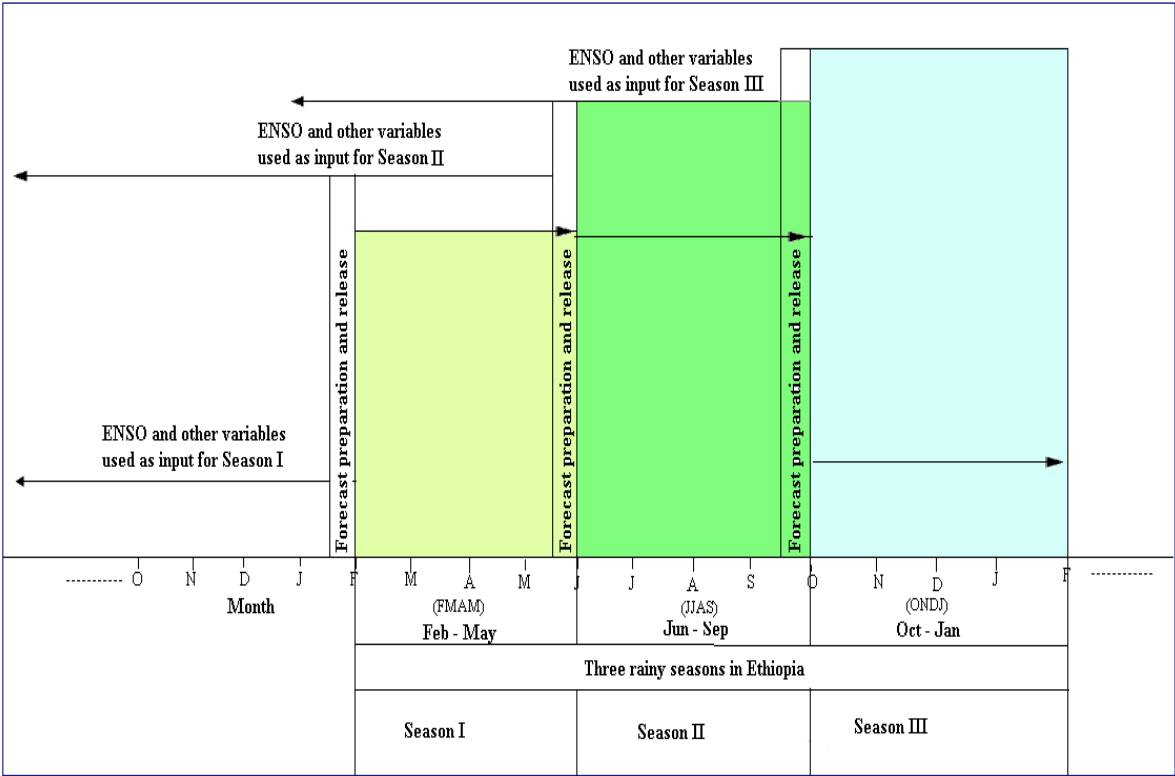


Figure 1. Seasonal rainfall forecasting system of the National Meteorological Agency of Ethiopia.

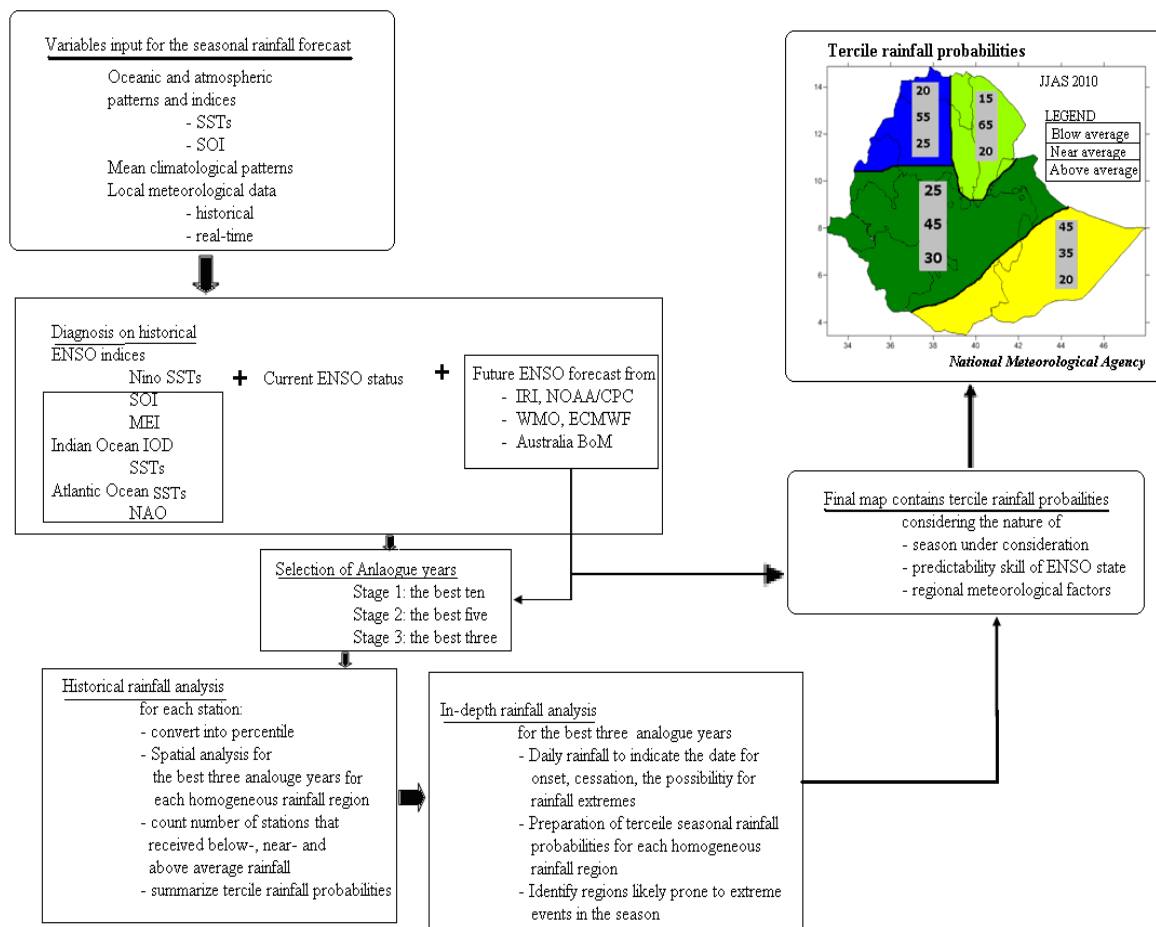


Figure 2. Schematic diagram showing analytical steps in the preparation of seasonal rainfall forecast by the National Meteorological Agency of Ethiopia.

## 2.2. Justification for Analog Forecasting Method

The use of analog methods to generate climate forecasts is an attractive idea, not the least because of its conceptual simplicity, and many meteorological institutions around the world either still use the analog forecasts or have done until recently [WMO, 2002]. The analog methods used to forecast rainfall anomalies directly, or through the intermediary of an anomaly flow pattern. In some cases, they are used more indirectly, e.g., the Australian Bureau of Meteorology determines analog years of the Southern Oscillation Index (SOI)

as a first step to subsequent analyses [Drosdowsky, 1994]. The techniques involve searching of the historical data, identifying previous periods that resembled the immediate past period, and predicting the following season's rainfall anomalies on the basis of what happened on those previous occasions. Analog forecasting techniques have been used in climate forecasting for a long time. Namias [1968] reviews the early history, and Nicholls [1980] presents a somewhat more recent view [Brett and Thompson, 2006]. There were also revivals of interest in the use of analog forecasting techniques at the end of the 1980s, particularly in the United States and New Zealand, with the papers [e.g., Barnston and Livezey, 1989; Chapman and Walsh, 1991; Livezey et al., 1994; Brett and Thompson, 2006]. In their comparative study, Barnett and Preisendorfer [1978] found that the use of climate systems evolution in defining an analog sometimes gave a superior prediction and at other seasons and lead times gave a worse result.

In identifying the predictors for Ethiopia rainy seasons, previous researches guide the selection of the most appropriate predictors from the historical archives. In this regard, a number of observational studies have identified the use of Equatorial Eastern Pacific Ocean SSTs as potential predictors of Ethiopia rainfall anomalies with some lead-time in advance [Korecha and Barnston, 2007]. For instance, during the El Niño/La Niña events, Ethiopia experiences less/more rainfall in the northern half and more/less in the south and southeast regions during the Kiremt season. Shanko and Camberin [1998] have found that Indian Ocean sea surface temperatures have an important influence on Ethiopia seasonal rainfall. They have found that higher SSTs in the Eastern Indian Ocean, for instance, generate a lot of tropical cyclones, which are resulted in drier conditions in the north, east, and south of the country during Bega and Belg seasons.

Various teleconnection patterns are linked to Indian, Atlantic, and Pacific Oceans, where they produce different climatic anomalies in various parts of Ethiopia [Segele and Lamb, 2005; Diro et al., 2011]. Thus, when predicting Ethiopia seasonal rains, it is important to allow for seasonality and regional rainfall feedback to various teleconnection indices. However, ENSO-indices have well been identified as the potential pre-season indicators and thus became the basis for the analog forecasting techniques in Ethiopia [Korecha and Barnston, 2007]. ENSO indices are being retained year round, but allowing these indices to be weighted differently from season to season as well as from region to region, depending on the direct linkage between regional rainfall pattern and SST anomalies. The analog forecast methodology is therefore now run operationally at the National Meteorological Agency. As part of NMA's long years' early warning program on the monitoring of climate variability, national seasonal rainfall outlook forums usually convene three times a year to discuss seasonal climate anomalies over Ethiopia since 1996. A range of guidance material is used, and the analog seasonal climate prediction method that identifies 3–5 analog years is a very useful prediction tool in providing tercile rainfall probabilities for each season in Ethiopia.

The National Meteorological Agency of Ethiopia has therefore integrated an analog forecasting technique in its seasonal climate prediction system. The major significant analog forecasting technique currently used in NMA is its dependence on the scientific innovations and explorations of ENSO. The technique has improved seasonal rainfall predictions and has better consideration of oceanic longer time memory of SST anomalies, and has been used in the countries where the computing facility is very weak. It is also widely used in the tropical regions as the predictability skill of seasonal rain is relatively dependable. Hence, examining of national rainfall anomalies on the basis of ENSO-teleconnection, as well as the extent of the extremity of

droughts and flooding can be resolved. This can give a unique opportunity for NMA to provide timely early warnings on the adverse effect of climatic anomalies within the reasonable lead time. This is unique and to the best of our knowledge, no other climate prediction technique has used such simple, less expensive computer facility and makes use of few indices because it is too expensive to run the state-of-art of modern general circulation models. So, this guarantees NMA's seasonal climate prediction technique is well maintained and acquired the modest capacity in capturing the drier and wetter occasions without using any other advanced climate prediction models. Thus, this is the superior point of the current analog forecasting technique of NMA.

NMA has divided Ethiopia into eight homogeneous rainfall regions. The classification is based on; typical rain-producing systems affecting the region and spatial and temporal response of respective region to major atmospheric and oceanic circulation systems. Although some authors [Gissila et al., 2004; Diro et al., 2008, 2009] have proposed modifications to the NMA homogeneous rainfall regions, NMA still uses the originally defined eight rainfall zones for the preparation of seasonal rainfall forecast (Figure 3). Although, NMA has been issuing the seasonal forecasts for many years, the overall statistical performance of these forecasts has not yet been comprehensively documented. Bekele [1997] made qualitative forecast verification on the seasonal rainfall forecasts issued for the period 1987–1996 and claimed a seasonal rainfall forecast percent correct score of 75% or more. From the qualitative forecast assessment, we noted that under-forecast of severe dry events may be a result of the fact that there is a greater reluctance to assign high probabilities for below average than for above average rainfall since in many parts of the country a warning of dry conditions would be considered more serious than wet conditions. In this paper, we revisit assessment of the forecasts using an objective verification approach.

## **3 Database and Verification Technique**

### **3.1. Database**

This verification is made for two rainy seasons over Ethiopia; February to May and June to September for the period 1999–2011. Monthly rainfall data from NMA meteorological stations (Figure 3) are used. Numbers of meteorological stations used in this study varies between 115 and 226. The period 1970–1998/99 is regarded as base period against which the observed seasonal rainfall in each verification year is compared. Missing data for any months are excluded from the verification analysis so as to avoid artificial data filling for the season under consideration. Seasonal rainfall forecasts that are available only in tercile rainfall probabilities maps (Figures 4a and 4b) obtained from NMA’s seasonal climate prediction records. The spatial delineation of zones with the same set of forecast probabilities varied from year to year. The forecast maps have therefore been recast using the NMA’s eight homogeneous rainfall regions (Figure 3), employing the method described in the next section. Meteorological stations used for the forecast verification are also organized in their respective homogeneous regions. To indicate the state of ENSO, we use the ENSO indices from NOAA/CPC data set as described by Korecha and Barnston [2007].

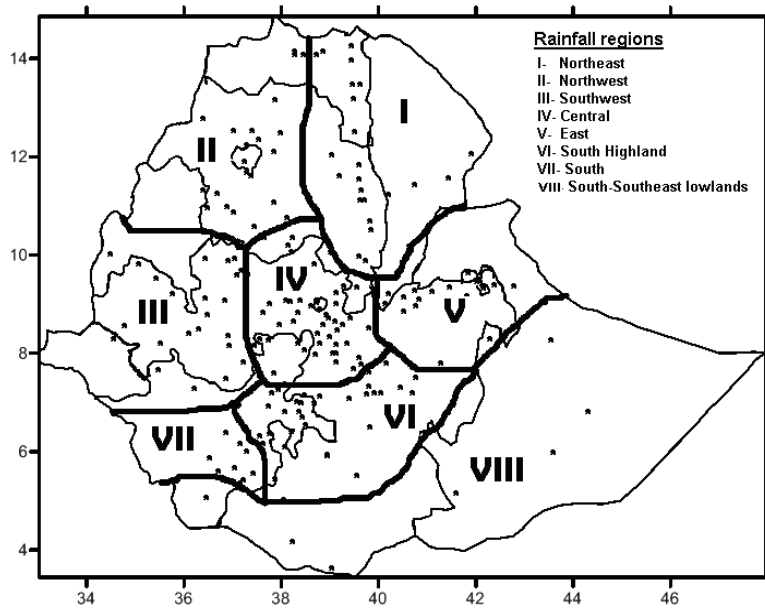


Figure 3. Homogeneous rainfall regions currently used for the preparation of seasonal rainfall forecast in Ethiopia. Meteorological stations used in this study are marked as “\*”

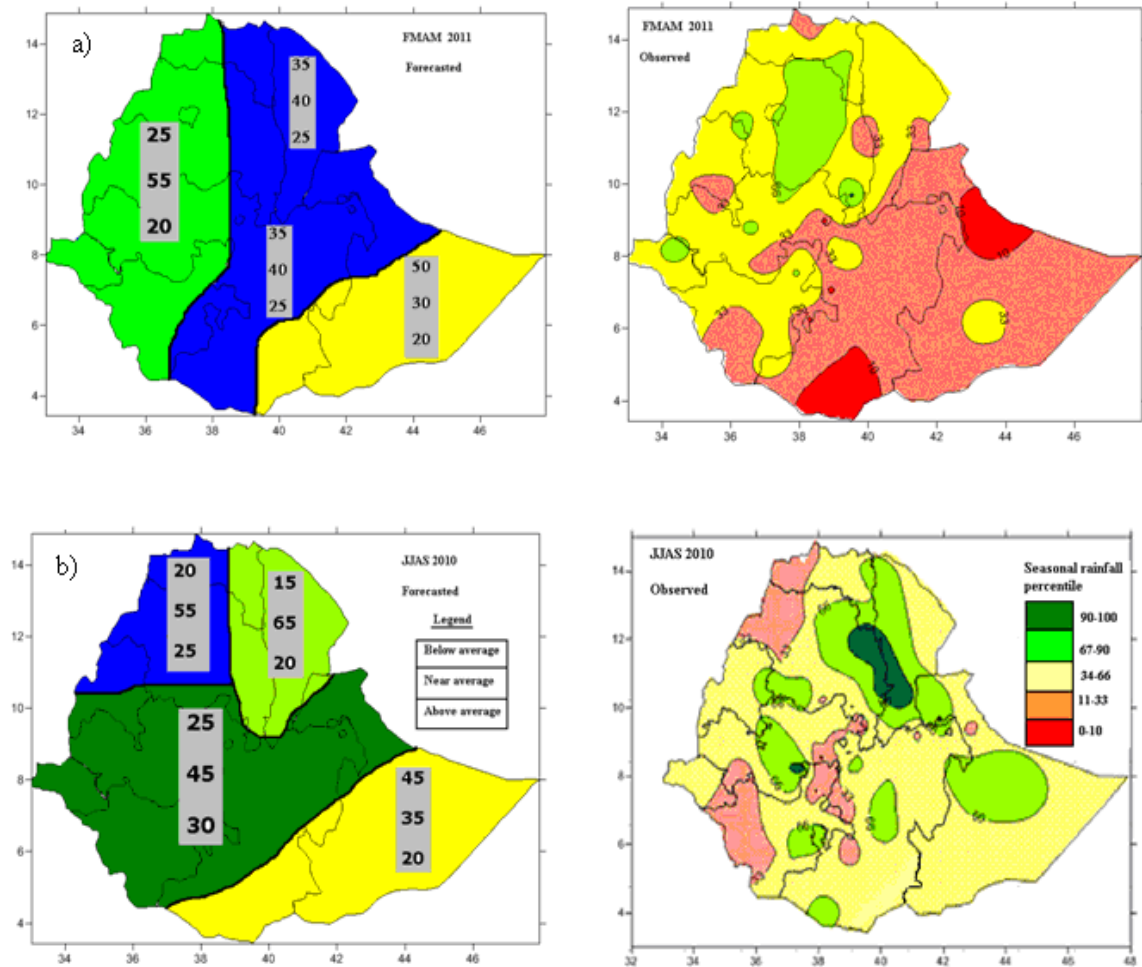


Figure 4. Examples of tercile observed and probability forecasts for seasonal rainfall over Ethiopia. The two paired maps show forecasted (observed) rainfall probabilities for a) FMAM and b) JJAS rainy seasons. Here, the maps are presented as prototype. The seasonal rainfall forecast issued for the period 1999-2011, which did not display here have similar configuration.

### 3.3 Verification Technique

In the preparation of seasonal rainfall forecasts, NMA uses eight homogeneous rainfall regions (Figure 3). The tercile rainfall probabilities for

the eight regions are however, as we can see from Figures 4a and 5c often merged into fewer regions in the presentation of the forecast. In order to verify the forecast we split the merged regions into the eight original homogeneous rainfall regions based on Figure 3. This is achieved by superimposing Figure 3 on the forecasts maps for each year. When two or more forecast zones occupy one homogeneous region, the forecast probabilities for the zone that covered substantial portions of the region are assigned to the whole of the homogeneous region. This is done for the periods 1999–2010 for the June–September main rainy season and for 2000–2011 for the small February–May rainy season. Meteorological stations used for this verification processes (see section 3.1) are then grouped into their respective region. Seasonal rainfall totals for each station are then ranked in comparison to the values in the base years. For example, JJAS rainfall totals recorded at station “X” in 1999 is ranked within 1970–1999 rainfall time series and its percentile rank is assigned, accordingly. Similarly, the seasonal rainfall time series for 1970–2000 are ranked and percentile rank is assigned for the year 2000, and so on until all years to be verified scheme are ranked according to the rainfall magnitude. This is done for all stations within the region. The tercile observed frequency of occurrence for a given season are then calculated based on the number of stations having its seasonal rainfall ranked in the upper third (above normal), lower third (below normal), or in between (near normal) for the given year.

Various verification techniques are described in the literature [e.g., Murphy, 1988; Jolliffe and Stephenson, 2003; Goddard et al., 2003; Barnston et al., 2010; Barnston and Mason, 2011]. Based on the format of our data set, we employ the following verification techniques to examine the bias, association, accuracy, and skill of the forecasting systems.

First, we use a diagram presentation to compare the forecasted and observed seasonal rainfall probabilities for each tercile category. The diagram indicates how well the predicted probabilities of an event correspond to their observed probability for each category. The measure does not say if the seasonal predicted rainfall is strongly deviated to other tercile categories.

Second, in order to assess any directional bias, which is a systematic tendency to assign too much or too little probabilities to particular tercile

categories, we computed the directional bias (DB) as 
$$DB = \frac{\sum_{k=1}^n f_k}{\sum_{k=1}^n o_k} - 100$$

where  $f_k$  and  $o_k$  are the average forecasted and observed seasonal rainfall probabilities for the years 1999 to 2011 for station k in each region, respectively. The three tercile categories used in this particular case are below, near and above normal rainfall probabilities. If there is no directional bias the result is always zero. In contrast, if the forecast probabilities are too high, DB will be negative and vice versa.

Third, the spearman rank correlation test [Jolliffe and Stephenson, 2003] was applied to measure the statistical association between the forecasted and observed relative frequencies of rainfall categories in each tercile. Spearman correlation coefficient (SRC) is defined as the Pearson correlation coefficient between the ranked variables:

$$SRC = 1 - \frac{6 \sum_{i=1}^n D_i}{n(n^2 - 1)}$$
 , where  $D_i$  represents the difference between ranks of pair of data values for  $n$  observations. More specifically,  $D_i$  is the difference between the highest rainfall tercile probability assigned for the forecast and the corresponding actual rainfall percentile for the  $i^{\text{th}}$  year. The higher/lower value of  $SRC$  (approaches to 1) indicates if the forecast is able to rank the years within a tercile correctly. For example if the forecast is able to assign high probabilities of a wet season to a year that was extremely wet and a lower probability of a wet season to a year that was less wet, the forecast will have good skill.

In addition to the above verification measures, we also use the ranked probability skill scores (RPSS) to the three forecast categories collectively [Goddard et al., 2003]. RPSS computes the relative skill of the probabilistic forecast over that of climatology, in terms of the forecast ability to assign high probabilities to the actual outcome and is defined as the difference in ranked probability score between the forecast and a chosen reference forecast [Goddard et al., 2003; Wilks, 2006; Barnston et al., 2010]. Thus, the RPSS measures the improvement of the multicategory probabilistic forecast relative to a reference forecast (usually the long term or sample climatology). It is similar to the 2-category Brier skill score, in that it takes climatological frequency into account. When RPSS is computed, the probabilities of the three forecast categories; below, near, and above averages are arranged in ascending order. The ranked probability score (RPS) is then calculated

$$RPS = \sum_{k=1}^N (f_k - o_k)^2$$
 where  $o_k$  is an indicator which is 1 if the forecasted and observed category coincided (for example, both have below average rainfall as the most probable category) or 0 otherwise.  $f_k$  is the predicted probability

in forecast category  $k$  (for  $k=1, 2$  or  $3$ ) for each station and forecast year, and  $N$  is the number of forecast categories (in this case  $N=3$ ). Low RPS indicates high skill, and vice versa. The RPSS is thus calculated as:

$$RPSS = \frac{RPS - RPS_r}{0 - RPS_r} = 1 - \frac{RPS}{RPS_r}$$

where,  $RPS_r$  represents the RPS value obtained from climatological forecasts. In our case, climatological value is 0.33 (any of the three terciles; below, normal and above normal are equally likely to occur).

In addition to using climatology as a reference, also we use ENSO as a reference to see if the forecast beats a pure ENSO-based forecast. The way this is done is that rainfall recorded at each meteorological station was ranked within 1970–2011. Then based on ENSO phases (El Niño, Neutral, and La Niña) numbers of stations within a region were stratified into terciles (below, near, and above average). For the 41 years of JJAS (1970–2010), 10(9) years are classified as El Niño (La Niña), and 22 years as neutral. Similarly, for 42 years of FMAM (1970–2011), 6(10) years are classified as El Niño (La Niña), and 26 years as neutral.

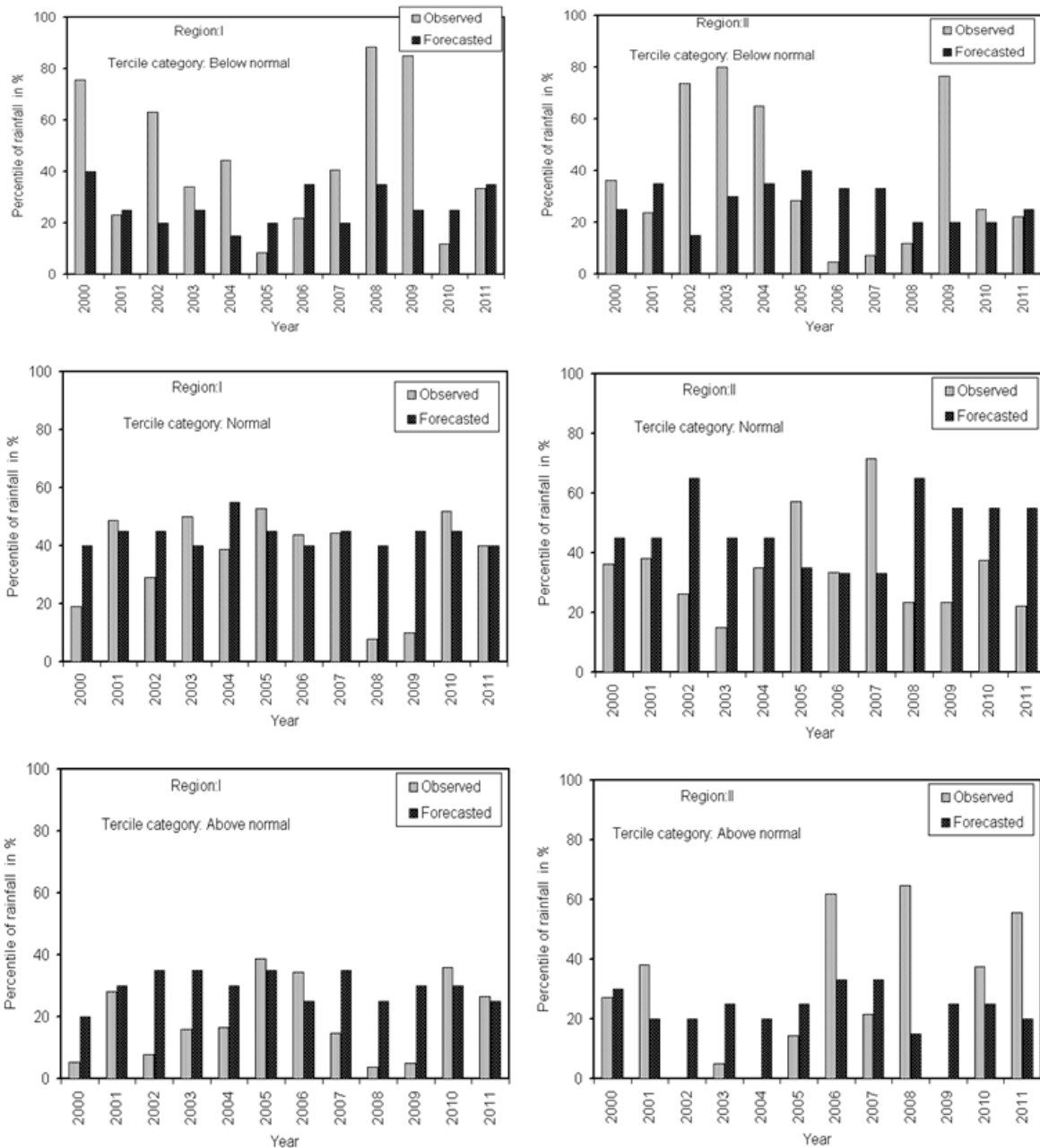


Figure 5. Comparison of observed and forecasted the tercile rainfall probabilities over the two homogeneous rainfall regions in Ethiopia. Below, near and above average rainfall probabilities are paired in the diagrams in order to identify the discrepancy between observed and forecasted rainfall during Feb-May season.

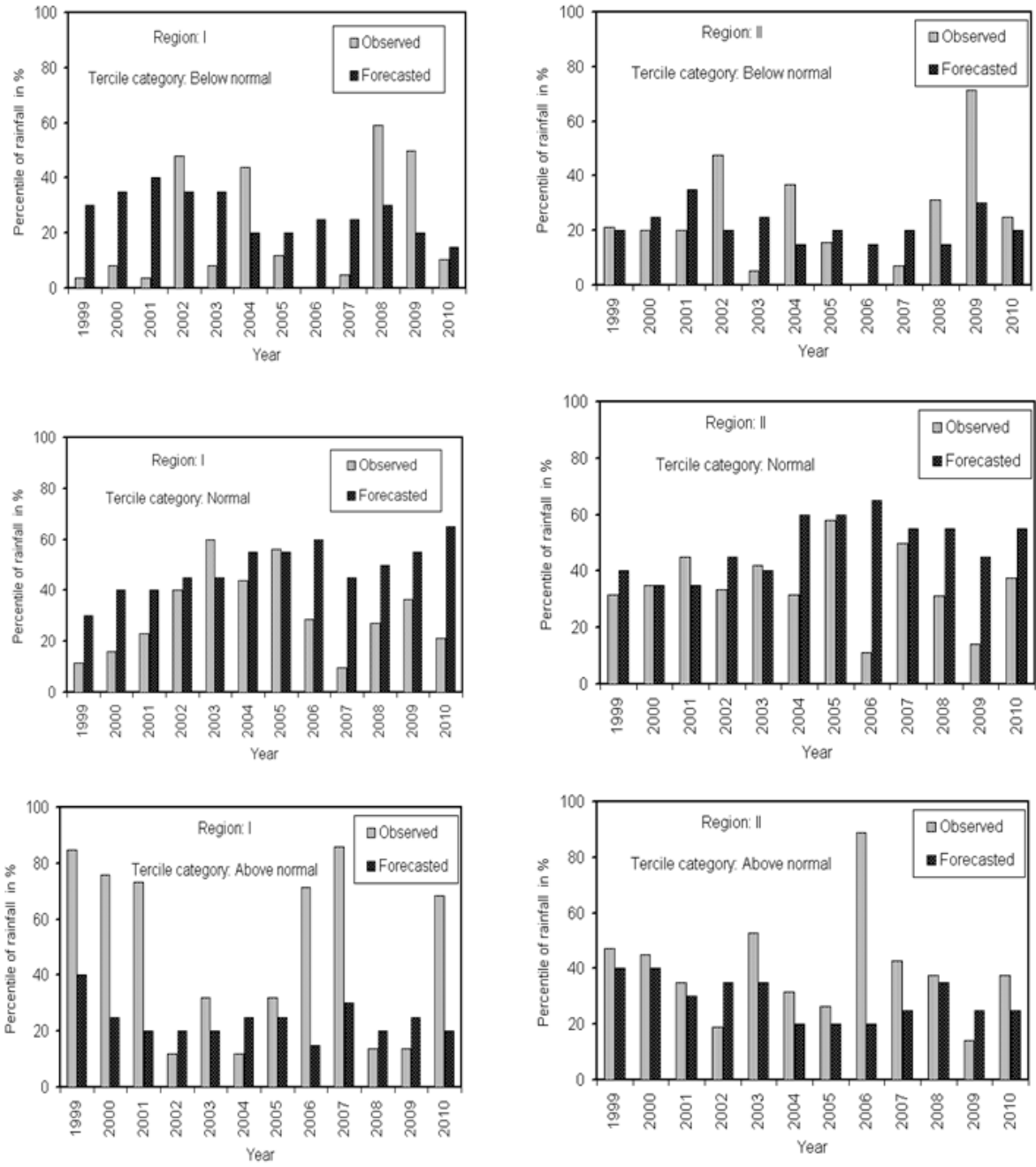


Figure 6. Comparison of observed and forecasted the tercile rainfall probabilities over the two homogeneous rainfall regions in Ethiopia. Below, near and above average rainfall probabilities are paired in the diagrams in order to identify the discrepancy between observed and forecasted rainfall during Jun-Sep rainy season.

## 4 Results and Discussion

### 4.1. Categorical Forecast Skill

The seasonal forecasts were evaluated to see if there is any directional bias. It can be seen from Table 1a that the forecast under-predict below average rainfall in all regions in the FMAM season. The under-forecasted value ranges from 27 to 45%. The same tendency for under-forecasting dry conditions is seen in JJAS (Table 1b). In contrast, the forecast was substantially biased toward the near average category in all regions both in FMAM and JJAS (Tables 1a and 1b). In general, above average rainfall occurred on average 28% (not shown in Tables 1a and 1b) of the cases during period 1999–2011 as compared to the reference climatological base period (1971–1998). Whilst, the near average forecast probabilities remained above 45% exceeding the actual “probabilities” (Tables 1a and 1b). The bias of the prediction system toward near average indicates that lack of forecast sharpness in predicting events deviating from the normal.

Table 1. The bias in forecast probabilities for 3 tercile categories. (a) FMAM rainfall forecasts (b) JJAS rainfall forecasts. Numbers with symbol “↓” indicate that the forecast system was under forecasted of observed rainfall is being under-forecasted by the forecast while “↑” indicates over-forecasting.

a)

Rainfall region	Directional skill of the seasonal forecast (%)		
	Below average	Near Average	Above average
I	<b>-40↓</b>	<b>20↑</b>	<b>52↑</b>

II	<b>-27↓</b>	37↑	11↑
III	<b>-38↓</b>	66↑	<b>-13↓</b>
IV	<b>-34↓</b>	38↑	4↑
V	<b>-43↓</b>	32↑	<b>45↑</b>
VI	<b>-45↓</b>	52↑	40↑
VII	<b>-31↓</b>	36↑	<b>-32↓</b>
VIII	<b>-30↓</b>	74↑	<b>-13↓</b>

b)

Rainfall region	Directional skill of seasonal forecast (Forecasted/Observed)%-100		
	Below average	Near Average	Above average
I	31↑	57↑	<b>-50↓</b>
II	12↑	40↑	<b>-23↓</b>
III	<b>-35↓</b>	48↑	<b>-11↓</b>
IV	<b>-28↓</b>	36↑	<b>-16↓</b>
V	<b>-2↓</b>	52↑	<b>-39↓</b>
VI	<b>-32↓</b>	32↑	2↑
VII	<b>-32↓</b>	52↑	<b>-9↓</b>
VIII	<b>-5↓</b>	6↑	<b>-4↓</b>

<sup>a</sup> Numbers with symbol “↓” indicate that the forecast system was under forecasted of observed rainfall is being under-forecasted by the forecast, while “↑” indicates over-forecasting.

To further examine the skill of the seasonal forecasts, the probabilistic value assigned for each category is plotted with the observed rainfall percentile in Figures 5 and 6 (only shown for Regions I and II). Each paired bar diagrams show the comparison of the forecasted versus observed rainfall percentiles for each tercile categories. The near average rainfall probabilities were forecasted to be the most probable event in the order of 40–50% of the time (Figure 5), while the below and above average categories were forecast less frequently (22–33% and 24–30% of the time, respectively). From Figures 5 and 6, we observe that large numbers of stations with the lower tercile are not forecasted by the forecast system correctly. For instance, there is a large departure between forecasted and observed rainfall in 2002 and 2009, when many regions experienced deficient rainfalls. On average, the below normal rainfall probability forecast was the highest in 46% (ranging from 40 to 70% depending on the region) of the observed below normal rainfall events, while below normal rainfall probability was wrongly assigned as the most probable in 54% of the events. NMA's forecasting system sometimes forecasts the above average category as most probable for low rainfall years. This under-forecast of severe dry events may be a result of the fact that there is a greater reluctance to assign high probabilities for below average than for above average rainfall since in many parts of the country a warning of dry conditions would be considered more serious than wet conditions.

Above normal rainfall probability forecast was the highest in 52% (ranging from 30 to 60% depending on the region) of the observed above normal rainfall events with a false alarm rate of 41% (Figure 6). In particular, the wet events of 2003, 2006, and 2007 were not predicted correctly. The extreme low and high rainfall events are mostly missed by the forecast scheme. Hence, the results indicate that low forecast skills were attained for strong rainfall events both for the two seasons.

## 4.2. Spatial Forecast Skill

Forecast biases, standard deviations of the forecast and observed rainfall probabilities and the rank probability scores skill (RPSS) were computed for each homogeneous rainfall region in Ethiopia for the FMAM and JJAS rainy seasons between 1999 and 2011 (Tables 2a and 2b). The standard deviations show that strong interannual rainfall variability is marked, with higher standard deviations of the probabilities of the observed rainfall over each region much higher than the standard deviations of the forecasts probabilities (Tables 2a and 2b). This indicates that the forecasts issued for the seasonal rainfall varied much less than the actual rainfall.

The aggregated RPSS for each homogeneous rainfall region shows positive, but low predictability skills. The RPSS values for FMAM are slightly higher than for the JJAS season mainly over the Belg rain-benefiting regions (Table 2). This indicates that the short rainy season has been slightly better predicted than the main rainy season over the regions that experience bimodal rain type. But the difference is only 0.09, which is unlikely to be significant. To investigate whether the forecasting system has skills in all homogeneous rainfall regions, the hit rate of the seasonal rainfall forecast over each region is shown in Figure 7. As we noticed in the previous sections, the forecast skill varied from region to region in addition to its seasonal variation. Among the eight homogeneous rainfall regions, the forecast is above 0.33 only for three of them (eastern parts of the country) during the FMAM season. For the JJAS season, the forecast system exceeds the climatological chance (0.33) in four of the eight homogeneous regions (two regions in the west and two in the south).

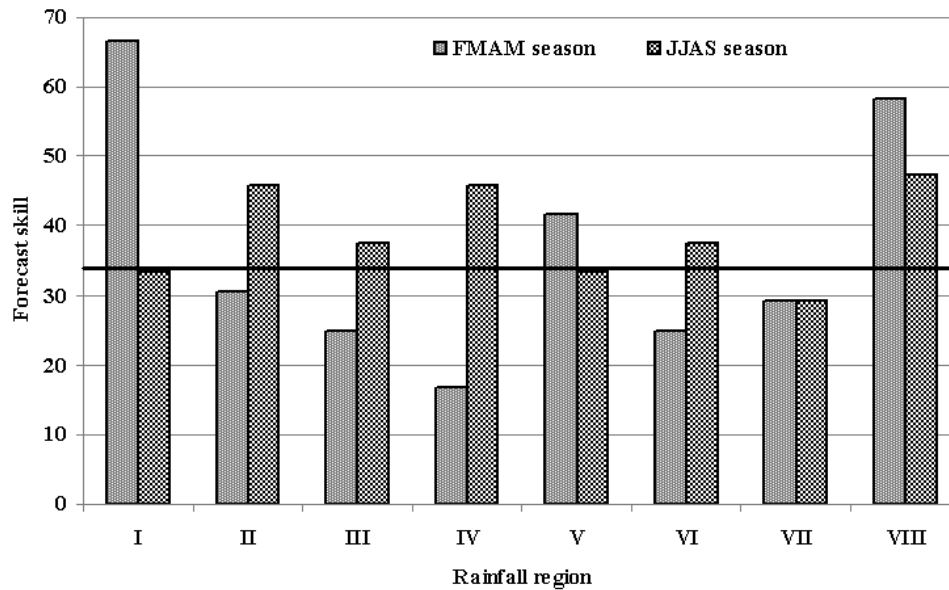


Figure 7. Seasonal forecast hit rate, for FMAM and JJAS seasons, scores probabilities given for an event mostly occurred for below, near and above average rainfall category. Horizontal black line represents the forecast skill obtained by chance or climatology. The skill of a forecast is evaluated based on distance between the hit and the level that is reached by chance (33%).

Table 2. Statistical values for skill of Ethiopia seasonal rainfall forecasts over the homogeneous rainfall regions during 1999–2011 for a) FMAM, b) JJAS seasons. Forecast probabilities issued for each tercile category are verified against the observed relative frequency at each region. Biases, the difference between the average forecasted and observed probabilities are computed along with the standard deviations for observed (SDo) and forecasted (SDf) and are also included. RPSS are computed based on both individual station and regional rainfall performance for each homogeneous rainfall region.

a) FMAM season

Rainfall probability				Measure of discrepancy			
Region	Category	Observed	Forecasted	Bias	SD <sub>o</sub>	SD <sub>f</sub>	RPSS
I	Below	0.44	0.26	-0.18	0.28	0.08	0.09
	Normal	0.36	0.44	0.08	0.16	0.04	
	Above	0.20	0.30	0.10	0.13	0.05	
II	Below	0.38	0.28	-0.10	0.28	0.08	0.02
	Normal	0.35	0.48	0.13	0.16	0.11	
	Above	0.27	0.24	-0.03	0.24	0.11	
III	Below	0.41	0.25	-0.16	0.25	0.07	0.06
	Normal	0.29	0.49	0.19	0.15	0.07	
	Above	0.30	0.26	-0.04	0.20	0.07	
IV	Below	0.39	0.26	-0.13	0.31	0.05	0.08
	Normal	0.32	0.44	0.12	0.16	0.05	
	Above	0.29	0.30	0.01	0.26	0.05	
V	Below	0.46	0.26	-0.20	0.35	0.07	0.05
	Normal	0.34	0.45	0.11	0.19	0.04	
	Above	0.20	0.29	0.09	0.22	0.05	
VI	Below	0.51	0.28	-0.23	0.31	0.07	0.06
	Normal	0.29	0.44	0.15	0.18	0.06	
	Above	0.20	0.28	0.08	0.26	0.05	
VII	Below	0.41	0.28	-0.13	0.30	0.07	0.02
	Normal	0.19	0.44	0.25	0.16	0.09	
	Above	0.40	0.28	-0.12	0.33	0.08	

VIII	Below	0.46	0.33	-0.13	0.28	0.11	0.08
	Normal	0.25	0.42	0.17	0.15	0.10	
	Above	0.29	0.25	-0.04	0.33	0.08	

b) JJAS season

Rainfall probability				Measure of discrepancy			
Region	Category	Observed	Forecasted	Bias	SD <sub>o</sub>	SD <sub>f</sub>	RPSS
I	Below	0.21	0.28	0.07	0.22	0.08	0.03
	Normal	0.31	0.49	0.18	0.16	0.10	
	Above	0.48	0.24	-0.24	0.31	0.06	
II	Below	0.25	0.22	-0.03	0.20	0.06	0.00
	Normal	0.35	0.49	0.14	0.13	0.01	
	Above	0.40	0.29	-0.11	0.19	0.08	
III	Below	0.34	0.22	-0.12	0.17	0.07	0.04
	Normal	0.33	0.48	0.15	0.11	0.10	
	Above	0.33	0.30	0.03	0.16	0.07	
IV	Below	0.30	0.22	-0.08	0.19	0.08	0.05
	Normal	0.37	0.50	0.13	0.08	0.09	
	Above	0.34	0.28	-0.05	0.18	0.06	
V	Below	0.27	0.26	-0.01	0.18	0.05	0.02
	Normal	0.32	0.49	0.17	0.12	0.05	
	Above	0.41	0.25	-0.16	0.20	0.05	
VI	Below	0.38	0.26	-0.12	0.26	0.05	0.06

	Normal	0.36	0.48	0.12	0.16	0.06	
	Above	0.26	0.26	0.00	0.18	0.06	
VII	Below	0.42	0.29	-0.14	0.29	0.03	0.06
	Normal	0.31	0.47	0.16	0.22	0.06	
	Above	0.27	0.25	-0.02	0.34	0.06	
VIII	Below	0.30	0.29	-0.02	0.27	0.07	0.05
	Normal	0.42	0.45	0.03	0.19	0.09	
	Above	0.27	0.26	-0.01	0.29	0.06	

<sup>a</sup> Forecast probabilities issued for each tercile category are verified against the observed relative frequency at each region. Biases, the difference between the average forecasted and observed probabilities are computed along with the standard deviations for observed (SDo) and forecasted (SDf) and are also included. RPSS are computed based on both individual station and regional rainfall performance for each homogeneous rainfall region.

The relative skills of the probabilistic forecasts were assessed over that of climatology and ENSO RPSS are then calculated and presented in Table 2 for FMAM and JJAS. Table 2 shows the forecast to have slightly better skill than climatology with RPSS values up to 8–9% in a few regions during the FMAM season over the regions experiencing bimodal rain types, while in the case of JJAS the RPSS is somewhat lower (4–6% in five of the eight regions). Although the RPSS indices are weak, they are all positive, indicating the presence of some predictability skill for both seasons over Ethiopia.

Figures 8a and 8d show the spatial RPSS patterns with climatology as the reference in both rainy seasons. Spatial RPSS patterns indicate that the forecast system performs better than climatology in much of the country, however the values are low. The FMAM season (Figure 8a) has the highest forecast skill with values above 10% over south Ethiopia (Figure 8a). In contrast, for the JJAS season the RPSS was worse than climatology over the southwestern lowlands and eastern portions of the country (Figure 8d). Overall, in many regions the forecast skills are slightly higher over the Belg-rain-benefiting regions in FMAM compared to JJAS. This is possibly related to the persistent nature of rainfall producing systems and their strong spatial variability during the spring season. In contrast, JJAS rainfall is more predictable with relatively higher RPSS over the Kiremt is mainly the main rainy season.

Figures 8c and 8f show the maps of RPSS for ENSO climatology and climatological references. When RPSS of ENSO climatology is compared with the forecast issued by chance (assigning equal chances for the three tercile rainfall categories), ENSO information alone can indicate the direction of the seasonal rainfall anomalies particularly during JJAS season for northern Ethiopia. For this study, ENSO climatology is computed based on the Oceanic Nino Index of NOAA as documented in NOAA [2013]. The results indicate that injection of more weight of ENSO information into the seasonal predictability scheme would improve the forecast skill in parts of Ethiopia during the rainy seasons, a conclusion also drawn by Korecha and Barnston [2007].

As the above analysis indicated, the ENSO information alone provided some skills in predicting seasonal rains. This would, therefore, further lead us to investigate the quality of the seasonal forecast by considering ENSO

climatology. Results from Figure 8b show that in FMAM the forecasting system have better skills in regions I, III, and VII, while ENSO climatology was better in regions IV, VI, and V (Figure 8b). In JJAS, the ENSO climatology outperforms the NMA forecast over the major portions of the country (Figure 8e) with the exception of the dry southeastern parts. The underperformance of the seasonal forecast could emerge probably due to the fact that either the forecast system has given too little weight to the ENSO cycle or it has underestimated the ENSO impact over the aforementioned regions.

Overall, the RPSS results indicate that NMA's seasonal rainfall forecasts have modest positive skill compared to climatology. In contrast, when the forecast is compared to ENSO climatology, it performs poorly, particularly over the central and northern regions in JJAS.

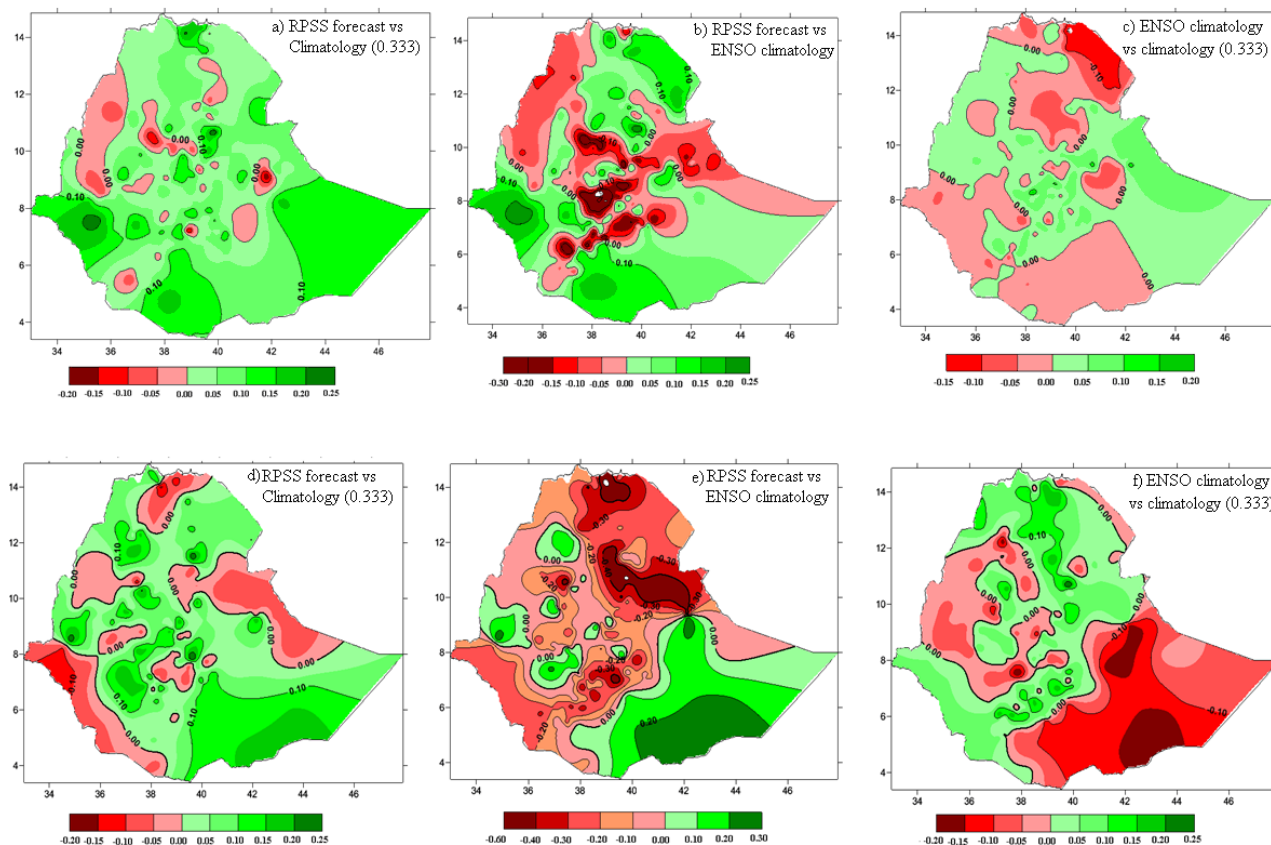


Figure 8. Spatial distribution of RPSS averaged for the study periods. RPSS are computed for FMAM (a-c) and JJAS (d-f) seasons separately based on point meteorological stations. Three RPSS are analyzed in order to evaluate the skills of NMA'S seasonal forecast versus climatological reference and ENSO climatology (b and d). Also ENSO climatology is compared against climatological references (c and f).

### 4.3 Variation of Forecast Skills With Seasons

In order to assess if the forecast is cable to rank the years within a tercile correctly, Tables 3a and 3b show the Spearman rank correlations between the observed and forecasted tercile categorical seasonal rains. Eight of the 48 forecast series considered (eight regions, three categories, and two

seasons) have a significant positive correlation. Most of the significant values were noticed for the above average rainfall forecasts during FMAM, which have statistically significant values for the regions in the south (regions III, VI, VII, and VIII, Figure 3). In general, the correlations in the JJAS season (Table 3) are weaker than in FMAM. The weak capabilities of the forecast to be able to rank the years within a tercile correctly were partly due to the fact that the system is biased toward the near normal rainfall category.

The frequency of stations having seasonal rainfall of below, near, and above normal categories each year on a national scale is presented in Figure 9. It should be noted that the national rainfall index is biased toward regions with a dense station network. For the FMAM season 2000, 2002–2004, 2008–2009, and 2011 were severe drought years (Figure 9a), in line with the analysis of Viste and Sorteberg [2012]. In contrast, Figure 9b shows JJAS rainfall performance in tercile categories. Unlike, FMAM which experienced a higher number of years with deficient rains, the JJAS seasons over the period 1999–2010 seemed relatively stable; severe droughts occurred only in 2002 and 2009, when more than 60% of meteorological stations recorded below average rainfall.

Yearly national RPSS values for the period 1999–2011 are calculated for the FMAM and JJAS seasons (Figure 10). The values are computed by averaging RPSS of each station (thus, it is bias to the regions with many stations). The results showed that the forecast system has positive skill on a national level except for the dry FMAM season of 2002 and 2009 and during JJAS 2000, 2004, 2005, and 2010. The highest skills (above 10%) are found in 2005 and 2011 for the FMAM season and during 2002 and 2009 for JJAS. With few exceptions the nationally averaged RPSS scores are slightly positive.

Table 3. The association between forecasted and observed (a) FMAM and (b) JJAS seasonal rainfall Probability for each forecast Category <sup>a</sup>.

a) FMAM season

Rainfall region	Correlation between observed and forecasted rainfall probability		
	Below average	Near average	Above average
I	0.16	0.17	0.20
II	-0.22	-0.53**	-0.03
III	0.33	0.26	<b>0.57**</b>
IV	<b>0.64**</b>	0.01	0.08
V	0.30	0.34	0.17
VI	0.37	-0.12	<b>0.41*</b>
VII	0.16	-0.39*	<b>0.42*</b>
VIII	<b>0.40*</b>	<b>0.40*</b>	<b>0.52**</b>

b) JJAS season

Rainfall region	Correlation between observed and forecasted rainfall probability		
	Below average	Near average	Above average
I	-0.28	0.38	0.34

II	0.00	-0.21	0.27
III	0.10	0.21	-0.49*
IV	-0.18	-0.20	-0.17
V	-0.37	0.20	-0.25
VI	-0.25	-0.23	0.18
VII	-0.01	0.10	<b>0.42*</b>
VIII	-0.33	-0.34	0.21

<sup>a</sup> Correlations are computed using Spearman rank correlations (

$$SRC = 1 - \frac{6 \sum_{i=1}^n D_i}{n(n^2 - 1)}).$$

Values indicated \* and \*\* are statistically significant at 90 and 95% probability levels, respectively.

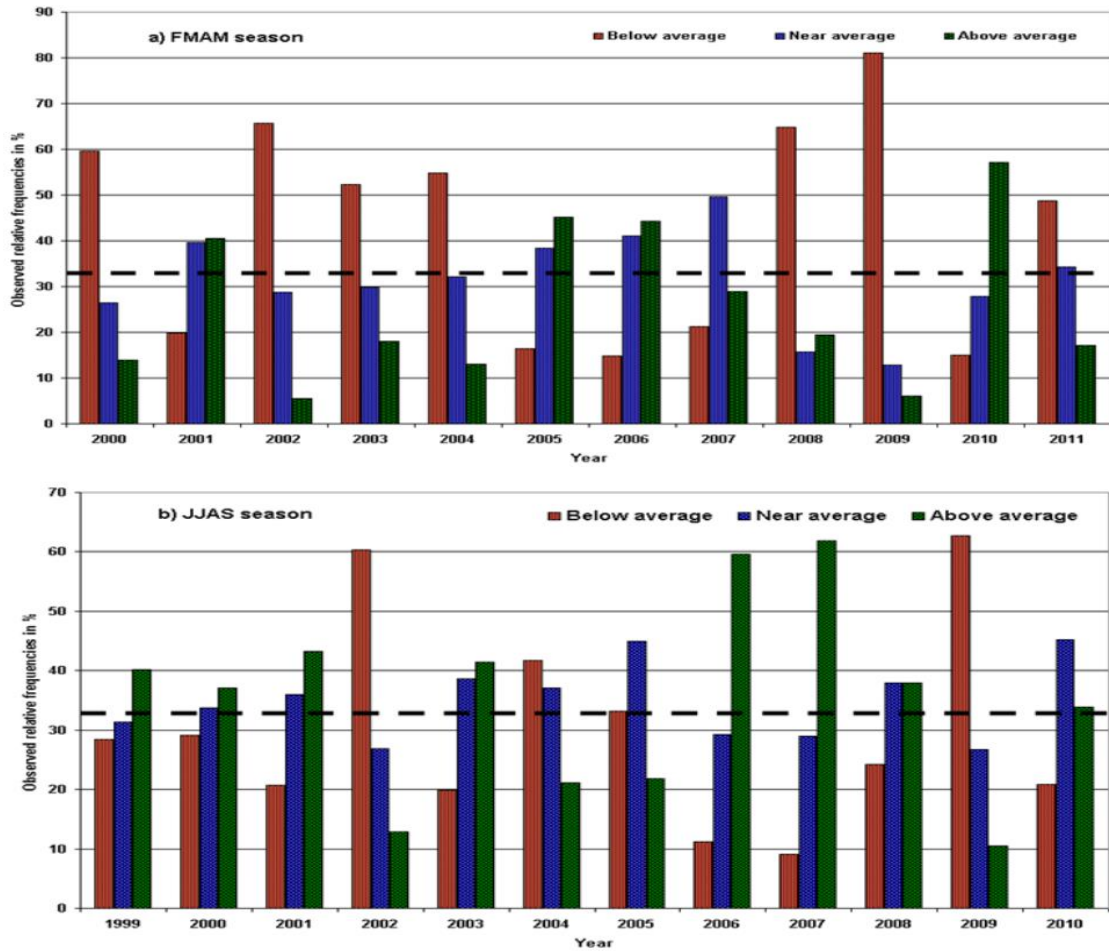


Figure 9. Nationalized tercile seasonal rainfall categories for: (a) FMAM and (b) JJAS rainy seasons. The dash line represents the climatological buffer zone (33.3%), which divides the degree of dryness or wetness of each season on the national scale.

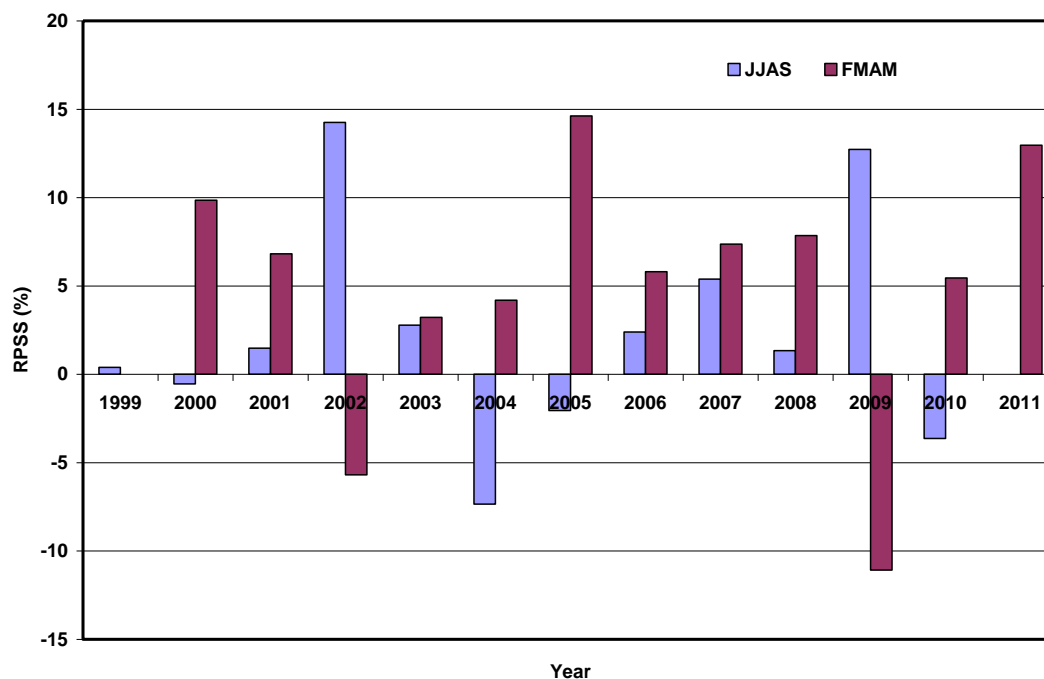


Figure 10. Mean yearly RPSS values for FMAM and JJAS seasons for Ethiopia. Negative (positive) values indicate poor (good) forecast skill.

#### 4.4 Reproducibility of Analog Climate Prediction Method

The techniques of using the historical analogs to formulate a forecast, known as analog prediction method has been used to varying degree of success by different researchers [Agarwal et al., 2001]. Agarwal et al. [2001] further stated that this method is based on the premise that interseasonal changes in the climate system occur similarly from one instance to another, such that when the system is in the same state it was for the same season in some past years, a sequences of events similar to those which occurred in the past instance may be expected now also. For instance, Penland and Sardeshmuckh [1995] have reasoned that SST alone contains all of the relevant dynamics to a large extent, and thus there is sufficient ground to use

SST observations for making predictions for up to nine months. Besides, conceptual simplicity, the main advantage of empirical prediction methods like analog techniques is that predictions are made using observed data alone, whereas in the case of coupled models the predicted SST fields may be affected by the way different physical process (e.g., air-sea coupling) have been parameterized in the model [Agarwal et al., 2001].

Hammer et al. [2000] stated that the more historical data available the better the analog years could be identified that enable to capture possible climatic fluctuations and direction of change in climate variables. Development in good practices of climatic factors would also facilitate inclusion of effects of potential climate variation, which may underline trends in historical data that need to be considered when using historical analogs. The point remains, however, that of appropriate methods to derive analog years in order to connect forecasts and applications need to be viewed as an essential component of forecasting research and development [Hammer et al., 2000]. The issuing of forecast as simple probability statements is better, but provides only general information. In this regard, defining analog years enable the policy makers to capture climatic variability in a way that could formulate riskiness of alternatives decisions and to be evaluated by examining each year in the analog set separately.

Hammer et al. [2000] further pointed out, averages are often a far less meaningful static of the probability distribution of outcomes than some consideration of the likelihood of exceeding some critical system state be it profit or land condition. Hammer et al. [2000] also noted that trends and phases of the ENSO have also been employed to provide seasonal climate outlook maps and tercile rainfall probabilities, from which forecast maps that describe the chances of rainfall in the above, average, or below average can

be generated. With this understanding, the analog prediction method that has been verified in the case of Ethiopia contains a lot of scientific and application merits. In previous sections, it has been well articulated that in order to predict anomalies of rainfall amounts for the future season, analog method searches for a similar time evolution of seasonal rainfall in the historical data set.

Pacific warm (El Niño) and cold (La Niña) episodes based on a threshold of  $\pm 0.5^{\circ}\text{C}$  for the Oceanic Niño Index (ONI as computed based on 3 month running mean of ERSST.v3b SST anomalies in the Niño 3.4 region (5N–5S, 120–170W) have been used as the main database in order to identify more resemblance analog years with the ongoing features from the historical episodes or non-episodes [NOAA, 2013]. To demonstrate the reproducibility of analog prediction method, we use 760 grid box from the gridded rainfall data set that haven't generated by blending observed rainfall data from coarse stations with satellite rainfall estimates [Dinku et al., 2011; NMA, 2013]. Gridded data set has records back to 1983. We assemble gridded rainfall data into each homogeneous rainfall zone and compute regional rainfall totals for the period 1983–2010. The linear correlation coefficient is then computed for each homogeneous rainfall region based on rainfall total and ONI for simultaneous and lags seasons. In order to investigate the response of regional rainfall to ENSO episodes, the correlation values are plotted against the 3 month running season (Figure 11). For the sake of clarity, the results reveal that there is a strong linkage between seasonal rainfall and ENSO episodes. We therefore strongly argued that ENSO-based analog years selection is scientifically sound and can further be explored as well as adopted for the tropical regions. Figures 11a and 11b depicted the analog methods that are reasonably skillful in indicating the direction of seasonal rainfall conditions for both rainy seasons in Ethiopia. One of the limitations of analog prediction method, however, is in fact the shortening of lag time

relationship exists between ENSO and Ethiopian rainfall. It can be expected that the accuracy of the present prediction method will improve as other global indices include in the selection of analog years with time.

Generally, the analog prediction technique employed in Ethiopia has been compared with the existing regional and international model products (not shown here). The results revealed that the present method has the potential to predict most of anomalous years during February–May and June–September rainy seasons, specifically over the regions where rainfall is typically deficient. This argument could be further substantiated by considering simultaneous relationship that exists between February–May and June–September seasons. It is depicted that ENSO episodes enhance/suppress February–May/June–September (Figure 11). For instance, with the exception of northwest (Regions II, RII) and southwest Ethiopia (Regions III, RIII), El Niño usually increases the likely of above average seasonal rainfall during February–May (Figure 11a). In contrast, El Niño increases the likelihood of below average rainfall during June–September season over the major portions of Ethiopia (Figure 11b). As far as the scientific merit of analog prediction method is concerned, this method has potential particularly over the tropical regions where ENSO is strongly teleconnected with seasonal rainfall feature. This is clearly evidenced from our analysis as depicted in Figure 11. The method is therefore, highly recommended and reproducible for the regions that have similar rainfall pattern like Ethiopia, specifically where the climate models suffers a lot for its poor performance in capturing seasonal rainfall variation. It seems fairly certain that the method will be superior in the field of seasonal climate prediction by providing more reliable forecast even in the arena of newly emerging complex computational technologies. Because it is very impractical to run expensive climate models with the existing limited computing facilities and expertise in Ethiopia.

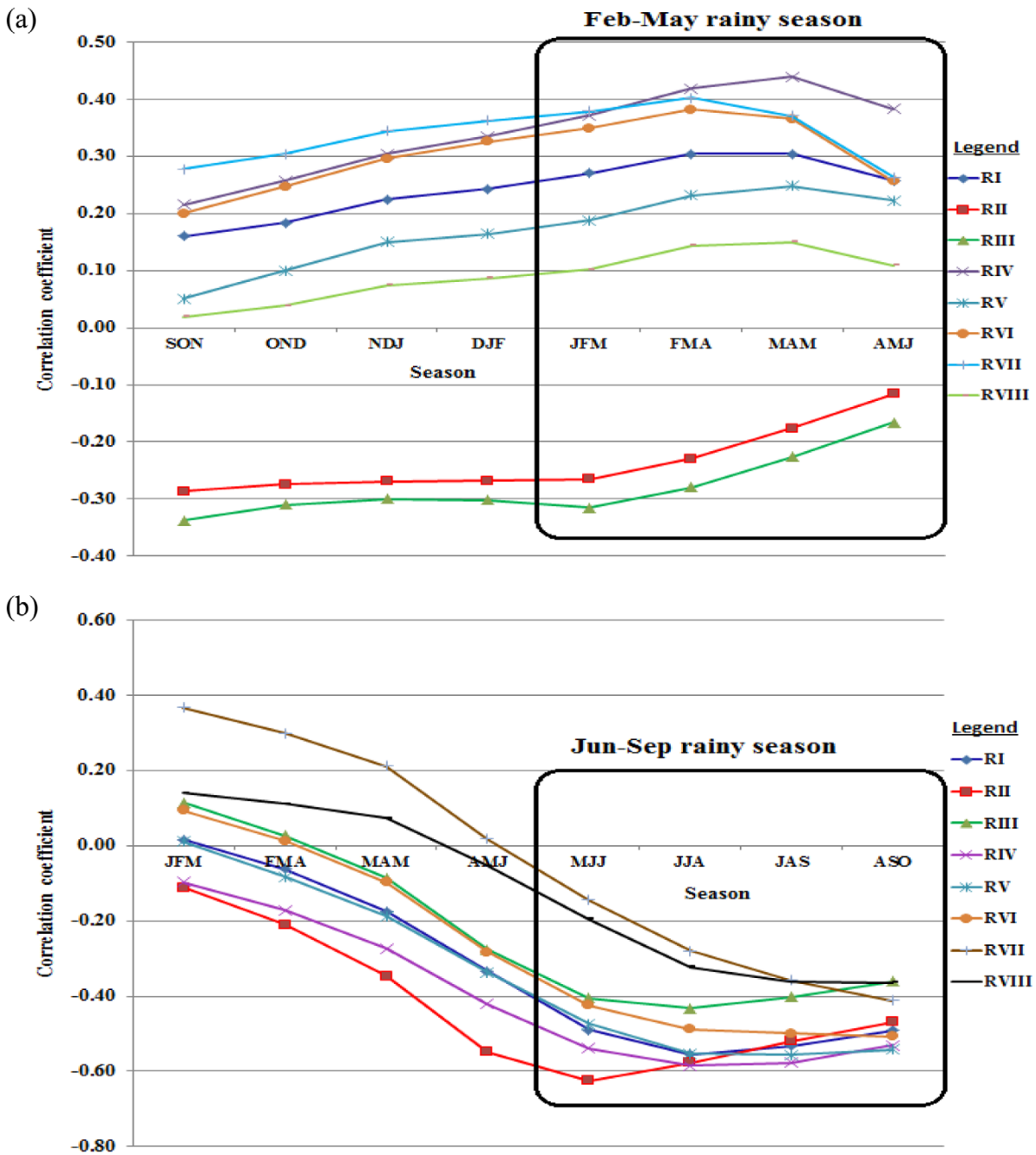


Figure 11. Correlation between seasonal rainfall totals of each rainfall regime and Niño 3.4 Sea Surface Temperature (SST) as computed for Ocean Niño Index (ONI). ONI is computed as an overlapping of consecutive months (e.g., JJA means June–August) as documented by NOAA [2013]. The linear correlation coefficient is computed between seasonal ((a) FMAM and (b) JJAS) rainfall totals (NMA, 2013) and ONI for the same season and preceding months.

## 5 Conclusions and Recommendations

In the present study, we evaluated the skill of the National Meteorological Agency of Ethiopia's operational seasonal rainfall forecast for the February–May (FMAM) and June–September (JJAS) rainy seasons for the period 1999–2011. Our analysis shows that the forecasting system is biased toward the near-normal category. The hit rate for forecasting the correct tercile is above 33.3% (the value that may be obtained by chance) for 8 out of 16 forecasts series. The ranked probability skill scores (RPSS) which computes the relative skill of the probabilistic forecast over that of the climatology is positive for all 16 forecasts series, indicating that the forecast has skill compared to chance. However, the values are all lower than 10% thus the forecasts skill generally ranges from weak to moderate, depending on the season and regions under question.

The results further suggest that the forecasting system has problems in capturing below normal rainfall events. This is particularly pronounced during the February–May rainy season. This under-forecasting of dry events is of great practical importance. The forecast showed slightly higher skills for above than below normal rainfall categories during both seasons and indicate that there is a greater reluctance to assign higher terciles for below normal than for above normal rainfall as a forecast for dry conditions would be considered more serious and may lead to initiation of drought preventive actions.

The forecast has some skill in ranking the wet years of the FMAM season, where four of the eight regions have significantly positive rank correlations for the above normal years. In the JJAS season, the forecast is not capable of

ranking neither the wet nor dry years. The seasonal difference in skill found in this study was also noted by Batte and Deque [2011]. The predictability skill results computed over the Greater Horn of Africa varied between the MAM (March–May) and SON (September–October) seasons, and suggested that seasonal rainfall predictability was higher for SON than MAM [Batte and Deque, 2011].

In the above validation, it may seem that the forecast is not performing too well, but is not worse than other seasonal forecast attempts. The RPSS values that are computed for NMA's forecast systems seem to be comparable to the values computed for IRI's prediction scheme as documented by Goddard et al. [2003] and Barnston et al. [2010], the CFS seasonal forecast [Sooraj et al., 2012], the ENSEMBLES project [Batte and Deque, 2011], and African RCOF forecasts [Mason and Chidzambwa, 2008].

We have already pointed to the importance of ENSO as potential indicator for the Ethiopian rainfall. When RPSS of ENSO climatology is compared with the forecast issued by chance and ENSO information alone had some skill in indicating the direction for the seasonal rainfall anomalies particularly during JJAS season for the northern Ethiopia. The results show that more weight on ENSO information into the seasonal predictability scheme would improve the forecast skill for JJAS rainy season. However, the information from ENSO alone is limited, particularly, due to the seasonality of ENSO and its predictability barrier during the northern hemisphere spring [Webster and Hoyos, 2010]. In order to make considerable improvements in the forecast some of the underlying factors other than ENSO are needed to be identified. In this case, Ng'ongolo and Smyshlyaev [2010] have shown that the phase of the QBO prior to the East African March–May (MAM) seasonal rainfall is a useful predictor for the seasonal rainfall. They argued that this finding is

useful particularly in the case of the East African long rains, which is FMAM in this case, for which ENSO provides only limited skill.

We suggest that NMA should work further to make appropriate improvement on the predictability of seasonal rainfall systems, especially for below normal rainfall categories. From a practical use, quantifying and providing accurate forecast for this category would be very beneficial for the user communities. The present RPSS analysis shows that the predictability skill for the June–September rainy season is poor. Therefore, work on identifying the underlying rain-producing systems and examine closely their physical linkage with larger-scale surface indices such as ENSO or circulation indices (QBO) which have been shown to have some predictability skill on the seasonal scale should be conducted. Moreover, the selection of homogeneous rainfall regions is important as this is the spatial scale for which the forecast is issued for. Merging heterogeneous rainfall regions into one region may also distort the level of seasonal forecasting skill over various parts of Ethiopia. In this regard, further research on how to separate the country into useful rainfall regions may be beneficial for the forecast quality.

Major advantages of NMA's ENSO-based forecasting technique over the other prediction methods are that it automatically finds out closely matching patterns from the corresponding historical occasions. This feature considerably minimizes data processing requirements. The skills demonstrated with this fairly simple method are high and have immense potential for practical purposes. It is argue that the on-going statistical and dynamical climate prediction models will improve with time with the wealth of understanding of the climatic factors and would be able to simulate and produce skillful extended-range forecasts of the Ethiopian intraseasonal rainfall variability. For the time being, however, a judicious and practical way

is to use the existing NMA's ENSO-based analog methods for seasonal predictions, with reasonably a few weeks in advance.

Finally, in addition to relying on the existing analog method NMA should explore the possibility to improve the forecast by using other dynamical and statistical forecast techniques that uses the seasonal forecast information from available global modeling systems.

### **Acknowledgements**

This work was carried out with the support from the Ethiopian Malaria Prediction System (EMaPS) project funded by the Norwegian Programme for Development, Research and Education (NUFU), NUFUPRO-2007/10121. The authors thank the National Meteorological Agency of Ethiopia for allowing the first author to carry out this research and for providing Ethiopia rainfall data.

### **References**

- Agarwal, N., C.M. Kishtawal, and P. K. Pal (2001), An analogue prediction method for global sea surface temperature, *Curr. Sci.*, 80(1), 49–55.
- Araya, A., and L. Stroosnijder (2011), Assessing drought risk and irrigation need in northern Ethiopia, *Agric. Forest Meteorol.*, 151, 425–436.

- Barnett, T. P., and R. W. Preisendorfer (1978), Multifield analog prediction of short-term climate fluctuations using a climate state vector, *J. Atmos.Sci.*, 35, 1771–1787.
- Barnston, A. G., and R. E. Livezey (1989), An operational multifield analog/antianalog prediction system for United States seasonal temperatures.Part II : Spring, summer, fall, and intermediate 3-month period experiments, *J. Clim.*, 2, 513–541.
- Barnston, A. G., and J. S. Mason (2011), Evaluation of IRI’s seasonal climate forecasts for the extreme 15% tails, *Wea. Forecasting*, 26, 545–555.
- Barnston, A. G., J. S. Mason, G. A. DeWitt, L. Goddard, and X. Gong (2010), Verification of the First 11 years of IRI’s seasonal climate forecasts,*J. Appl. Meteorol. Climatol.*, 49, 493–520.
- Batte, L. E., and M. D. Deque (2011), Seasonal predictions of precipitation over Africa using coupled ocean-atmosphere general circulation models: Skill of the ENSEMBLES project multimodel ensemble forecasts, *Tellus, Ser. A*, 63, 283–299.
- Bekele, F. (1997), Ethiopian use of ENSO information in its seasonal forecasts, *Internet J. Afr. Studies*, No. 2. [Available at <http://www.ccb.ucar.edu/ijas/ijasno2/bekele.html>.]
- Block, P., and B. Rajagopalan (2007), Interannual variability and ensemble forecast of upper Blue Nile basin Kiremt season precipitation, *J. Hydrometeorol.*,8(3), 327–343.
- Brett, A. M., and G. Thompson (2006), Analogue forecasting of New Zealand climate anomalies, *Int. J. Climatol.*, 26, 485–504.
- Camberlin, P. (1997), Rainfall anomalies in the source region of the Nile and their connection with the Indian summer monsoon, *J. Clim.*, 10, 1380–1392.

- Chapman, W. L., and J. E. Walsh (1991), Long-range prediction of regional sea ice anomalies in the Arctic, *Wea. Forecasting*, 6, 271–288.
- Degefu, W. (1987), Some aspects of meteorological drought in Ethiopia, in *Drought and Hunger in Africa: Denying Famine a Future*, edited by M. H. Glantz, pp. 23–36, Cambridge, Cambridge Univ. Press.
- Dinku, T., K. Asefa, K. Hailemariam, D. Grimes, and S. Connor (2011), Improving availability, access and use of climate information, *WMO Bull.*, 60(2), 80-86.
- Diro, G., E. Black, and D. Grimes (2008), Seasonal forecasting of Ethiopian spring rains, *Meteorol. Appl.*, 15, 73–83.
- Diro, G., D. Grimes, E. Black, A. O'Neill, and P. Iguzquiza (2009), Evaluation of reanalysis rainfall estimates over Ethiopia, *Int. J. Climatol.*, 29, 67–78.
- Diro, G. T., D. I. F. Grimes, and E. Black (2011), Teleconnections between Ethiopian summer rainfall and sea surface temperature: Part II. Seasonal forecasting, *Clim. Dyn.*, 37, 121–131.
- Drosowsky, W. (1994), Analogue (non-linear) forecasts of the Southern Oscillation index time series, *Wea. Forecasting*, 9, 78–84.
- Elagib, N. A., and M. M. Elhag (2011), Major climate indicators of ongoing drought in Sudan, *J. Hydrol*, 409, 612–625.
- Gibbs, W. J., and J. V. Maher (1967), Rainfall deciles and drought indicators, *Bur. Meteorol. Bull.*, 48, 33p.
- Gissila, T., E. Black, D. I. F. Grimes, and J. M. Slingo (2004), Seasonal forecasting of the Ethiopian summer rains, *Int. J. Climatol.*, 24, 1345–1358.

- Goddard, L., A. G. Barnston, and S. J. Mason (2003), Evaluation of the IRI's "Net Assessment" seasonal climate forecasts: 1997–2001, *Bull. Am. Meteorol. Soc.*, 84, 1761–1781.
- Hammer, G. L., N. Nicholls, and C. Mitchell (2000), Applications of seasonal climate forecasting in agricultural and ecosystems, *Atmos. and Oceanic Sci. Libr.*, Kluwer Acad, P.O. Box 17, 3300 AA Dordrecht, The Netherlands.
- Indeje, M., F. H. M. Semazzi, and L. J. Ogallo (2000), ENSO signals in East African rainfall seasons, *Int. J. Climatol.*, 20, 19–46.
- Jolliffe, I. T., and D. B. Stephenson (2003), Forecast Verification: A Practitioner's Guide in Atmospheric Science, edited by I. T. Jolliffe and D. B. Stephenson, pp. 1–12, Wiley, Chichester.
- Kassahun, B. (1987), Weather systems over Ethiopia, paper presented at the first international Technical Conference on Meteorological Research in Eastern and Southern Africa, pp. 53–57, Nairobi, Kenya, UCAR.
- Kharin, V. V., and F. W. Zwiers (2003), Improved seasonal probability forecasts, *J. Clim.*, 16, 1685–1701.
- Korecha, D., and A. Barnston (2007), Predictability of June–September rainfall in Ethiopia, *Mon. Weather Rev.*, 135, 628–650.
- Livezey, R. E., A. G. Barnston, G. V. Gruza, and E. Y. Ran'kova (1994), Comparative skill of two analog seasonal temperature prediction systems: Objective selection of predictors, *J. Clim.*, 7, 608–615.
- Mason, S. J., and S. Chidzambwa (2008), Position paper: Verification of African RCOF forecasts, Tech. Rep. 09-02, International Research Institute for Climate and Society, Columbia University, New York, USA.

- Mason, S. J., and A. P. Weigel (2009), A generic forecast verification framework for administrative purposes, *Mon. Weather Rev.*, 137, 331–349.
- Mohamed, Y. A., B. J. J. M. van den Hurk, H. H. G. Savenije, and W. G. M. Bastiaanssen (2005), Hydroclimatology of the Nile: Results from a regional climate model, *Hydrol. Earth Syst. Sci.*, 9, 263–278.
- Murphy, A. H. (1988), Skill scores based on the mean square error and their relationships to the correlation coefficient, *Mon. Weather Rev.*, 116, 2417–2424.
- Namias, J. (1968), Long range weather forecasting—History, current status, and outlook, *Bull. Am. Meteorol. Soc.*, 49, 438–470.
- Ng'ongolo, H. K., and S. P. Smyshlyaev (2010), The statistical prediction of East African rainfalls using quasi-biennial oscillation phases information, *Nat. Sci.*, 12, 1407–1416, doi:10.4236/ns.2010.212172.
- Nicholls N. (1980), Long-range weather forecasting—Value, status and prospects, *Rev. Geophys. Spec. Phy.*, 18, 771–788.
- Nicholson, S. E. (2000), The nature of rainfall variability over Africa on time scales of decades to millennia, *Global Planet. Change*, 26, 137–158.
- NMA (2013), National Meteorological Agency of Ethiopia [Available at [http://www.ethiometmaprooms.gov.et:8082/maproom/Climatology/Clim ate\\_Forecast/](http://www.ethiometmaprooms.gov.et:8082/maproom/Climatology/Clim ate_Forecast/)].
- NMSA, (1996), Climatic and agroclimatic resources of Ethiopia, *Natl. Meteorol. Serv. Agency of Ethiopia, Meteorol. Res. Rep. Ser.*, 1(1), 1–137.
- NOAA (2013), Cold and Warm Episodes by Season, National Oceanic and Atmospheric Administration (NOAA). [Available at

[http://www.cpc.ncep.noaa.gov/products/analysis\\_monitoring/ensostuff/ensoyears.shtml](http://www.cpc.ncep.noaa.gov/products/analysis_monitoring/ensostuff/ensoyears.shtml)].

Penland, C., and P. D. Sardeshmukh (1995), The optimal growth of tropical sea surface temperature anomalies, *J. Clim.*, 8, 1999–2024.

Shanko, D., and P. Camberlin (1998), The effect of the southwest Indian Ocean tropical cyclones on Ethiopian drought, *Int. J. Climatol.*, 18, 1373–1378.

Segele, Z. T., and P. J. Lamb (2005), Characterization and variability of Kiremt rainy season over Ethiopia, *Meteorol. Atmos. Phys.*, 89, 153–180.

Segele, Z. T., P. Lamb, and L. Leslie (2009a), Large-scale atmospheric circulation and global sea surface temperature associations with Horn of Africa June–September rainfall, *Int. J. Climatol.*, 29, 1075–1100.

Segele, Z. T., P. Lamb, and L. Leslie (2009b), Seasonal-to-Interannual variability of Ethiopia/Horn of Africa monsoon. part I: Associations of wavelet-filtered large-scale atmospheric circulation and global sea surface temperature, *J. Clim.*, 22, 3396–3421.

Seleshi, Y., and G. R. Demar\_ee (1995), Rainfall variability in the Ethiopian and Eritrean highlands and its links with the Southern Oscillation Index, *J. Biogeogr.*, 22, 945–952.

Sooraj, K. P., H. Annamalai, A. Kumar, and H. Wang (2012), A comprehensive assessment of CFS seasonal forecasts over the tropics, *Wea. Forecasting*, 27, 3–27. doi:<http://dx.doi.org/10.1175/WAF-D-11-00014.1>.

Tsegay, W. (1998), El Niño and drought early warning in Ethiopia, *Internet J. Afr. Studies*, No. 2. [Available at <http://www.ccb.ucar.edu/ijas/ijasno2/georgis.html>].

- Wang, G., and E. A. B. Eltahir (1999), Use of ENSO information in medium- and long-range forecasting of the Nile floods, *J. Clim.*, 12, 1726–1737.
- Webster, P. J., and C. D. Hoyos (2010), Beyond the spring barrier?, *Nat. Geosci.*, 3, 152–153.
- Wilks, D. S. (2006), *Statistical Methods in the Atmospheric Sciences*, 2<sup>nd</sup> ed., 648 pp., Academic.
- WMO (2002), Long-range forecasting progress report for 2001, WMO/TDNo. 1150, LRFPP Rep. Ser. 8, pp. 89, World Meteorol. Organ.
- Wolff, C., G. H. Haug, A. Timmermann, J. S. S. Damst\_e, A. Brauer, D. M. Sigman, M. A. Cane, and D. Verschuren (2011), Reduced interannual rainfall variability in East Africa during the last ice age, *Science*, 333, 743–746.
- Wolter, K., and M. S. Timlin (1998), Measuring the strength of ENSO events: How does 1997/98 rank?, *Weather*, 53(9), 315–324.

## **Paper II**

### **Construction of Homogeneous Rainfall Regimes for Ethiopia**

Korecha, D. and Sorteberg, A. (2013)

Last version of this manuscript submitted to the *International Journal of Climatology*, 2013.

# Construction of Homogeneous Rainfall Regimes for Ethiopia

Diriba Korecha<sup>1,2</sup> and Asgeir Sorteberg<sup>2,3</sup>

<sup>1</sup>National Meteorological Agency of Ethiopia, Addis Ababa, Ethiopia

<sup>2</sup>Geophysical Institute, University of Bergen, Norway

<sup>3</sup>Bjerknes Centre for Climate Research, University of Bergen, Norway

## Abstract

Monthly rainfalls recorded over 162 meteorological stations for the period 1951-2009 are investigated to examine the spatial and temporal rainfall patterns in Ethiopia. Mean annual and seasonal rainfall are computed, and their spatial patterns are analyzed. Among the three seasons currently recognized in Ethiopia: June-September, February-May and October-January contributes 59%, 28% and 13% for the mean annual rainfall, respectively. To identify the coherent regions of seasonal rainfall variability, Principal Component Analysis (PCA) is applied on monthly rainfall data. The results reveal that the first three principal components (PCs), which accounts for 67% of the total variance, separate the major parts of Ethiopia in terms of bi-modal and mono-modal type of *Kiremt* (June-September) and Belg (February-May) rains. Also, when Cluster Analysis (CA) is applied on the same data set, additional homogeneous rainfall regions are identified. Results from CA suggest that when stations are further regrouped into the manageable number of clusters, each cluster represents coherent rainfall distribution, with similar geographical locations. After applying PCA and CA on monthly rainfall of 162 meteorological stations over Ethiopia, and considering the country's intra-annual rainfall variability, climatological patterns and topography of the

country, fourteen homogeneous rainfall regions are identified. However, when rainfall station-based classifications were compared with results from merged station-satellite rainfall data, the homogeneous rainfall regimes became twelve. We found that the homogeneous rainfall regimes are spatially more stable, coherent and robust to capture temporal and spatial rainfall variability across the country. Besides, each rainfall region behaves distinctively and reflects the seasonality of rainfall, which includes onset and cessation of seasonal rains, rain-type and exposure of each region to seasonal and intra-annual rainfall variations.

**Key words:** Ethiopia, homogeneous, PCA, ENSO, rainfall season, ITCZ

---

## 1. Introduction

In Ethiopia, an onset and cessation of seasonal rainfall vary considerably within few kilometers distance due to altitudinal variations, orientation of mountain chains and their physical influence on atmospheric flow. Topographic variation, on the other hand, is a good opportunity to regionalize the country's rainfall pattern. Flohn (1987), for example, noted that Ethiopian mountains created a distinct climatic division across the source region of the Blue Nile and its tributaries. Block (2011) and Block and Rajagopalan (2007) also noticed climatic peculiarity of northwestern region of Ethiopia. Diverse topography and strong seasonal variation over the other parts of the country also indicate the potential physical justifications to delineate rainfall patterns on various spatial scales. Thus, the main task of delineating the country into homogeneous rainfall zones is primarily to characterize the rainfall variability on a similar spatial scale.

Several attempts have been made to regionalize spatial variation rainfall of Ethiopia into homogeneous rainfall zones. For example, Gissila et al. (2004) divided the country into five homogeneous rainfall zones for the summer (*Kiremt*) season. Whereas Diro et al. (2008 and 2011) modified these classifications and produced six rainfall zones. The differences existed between these two works were emerged due to variations in number of stations used and seasons. Gissila et al. (2004) classified summer season based on 19 rainfall stations, while Diro et al. (2008 and 2011) used 33 and 45 rainfall stations to categorize spring (*Belg*) and summer rains, respectively. In contrast, the National Meteorological Agency (NMA) has been using eight homogeneous rainfall regimes for operational seasonal predictions since 1999. Nevertheless, the variation in the number of rainfall clusters for Ethiopia has emerged due to the under-representativeness of regions where no or limited number of meteorological stations were available. These led to inconsistencies on operational climate forecasts and research activities. It is therefore, important to examine the previous works and improve number and spatial delineation of rainfall regimes by using more rainfall data and apply additional multivariate statistical techniques.

Principal Component Analysis (PCA) and Cluster Analysis (CA) are widely used to delineate spatial rainfall patterns (Ramos, 2001). For example, hierarchical clustering technique, which requires specific measures of similarity, is used to characterize the relationships among the different stations and search for stations that have related rainfall variability (Unal et al., 2003). Furthermore, Comrie and Glenn (1998) have documented that non-hierarchical K-means clustering technique can be applied to identify regions of similar rainfall patterns. In some cases, the combinations of

these techniques also employed to produce homogeneous rainfall regions. The objective of this study is therefore to analyze the Ethiopian rainfall from large to smaller scales and propose a new set of homogeneous rainfall regions. The analyses are based on monthly rainfall totals from three data sets of NMA. These are; 162 meteorological stations, merged station-satellite rainfall data (Dinku et al., 2011) extracted at the locations of the 162 stations, and the same data extracted at 717 randomly selected rainfall grid points. Initially thousand random points were selected from the merged station-satellite rainfall grids, and then points out the Ethiopian boundary were removed. The later two data sets cover the period 1983-2010.

The organization of this paper is as follows: In section 2, data and methodology are outlined. Section 3 provides the results, starting with improved rainfall climatology of Ethiopia using all available national stations (250 stations are used only for reconstructing rainfall climatology) and stations bordering Ethiopia (30 stations). It then followed by the discussion of larger scale seasonal rainfall variability and ending up with a detailed description of the proposed classification of rainfall stations into homogeneous regions. Conclusions are given in section 4.

## **2. Data and Methodology**

### **2.1. Data**

To classify Ethiopian rainfall patterns into homogeneous regions, monthly rainfall data of surface meteorological stations from National Meteorological Agency of Ethiopia was obtained for the period 1951-2009 (Figure 1b).

Stations used in the present analysis contained less than 15% missing values. Missing values are filled with mean monthly rainfall for the period 1971-2000. Because of a low number of stations and high proportion of missing data during 1950s and 1960s, most of our diagnostic analyses were based on the period 1970 to 2009 (Figure 1a). As documented by Korecha and Barnston (2007), the sensitivity of including estimated rainfalls for these stations were compared with the neighboring stations having full actual records. The two versions of rainfall data strongly correlated, and the largest absolute differences are nearly insignificant. All rainfall dataset were subjected to quality control tests before analysis was done in accordance with WMO (1986) procedures (King'uyu et al., 2000). Efforts were made to ensure that the extreme values within the data set are true events, rather than the errors. For the 162 stations used in this study, we first performed routine quality assessment procedures to evaluate the records of monthly value against daily rainfall data. For any data values, we examined each case separately against the data from the neighboring stations and identified the outliers using linear correlation analysis with the surrounding stations. We also examined the stations' histories and data consistency and evaluated any potential discontinuities and extremes caused either by relocation of stations or errors during observations. In this way, we obtained complete and reliable monthly records of rainfall for the 162 stations used in this study. Furthermore, merged station-satellite data, which have duration of 1983-2010, extracted at the 162 station locations and 717 random locations (Figure 1c) are also examined for the validity, verification and stability of homogeneous rainfall classification in Ethiopia.

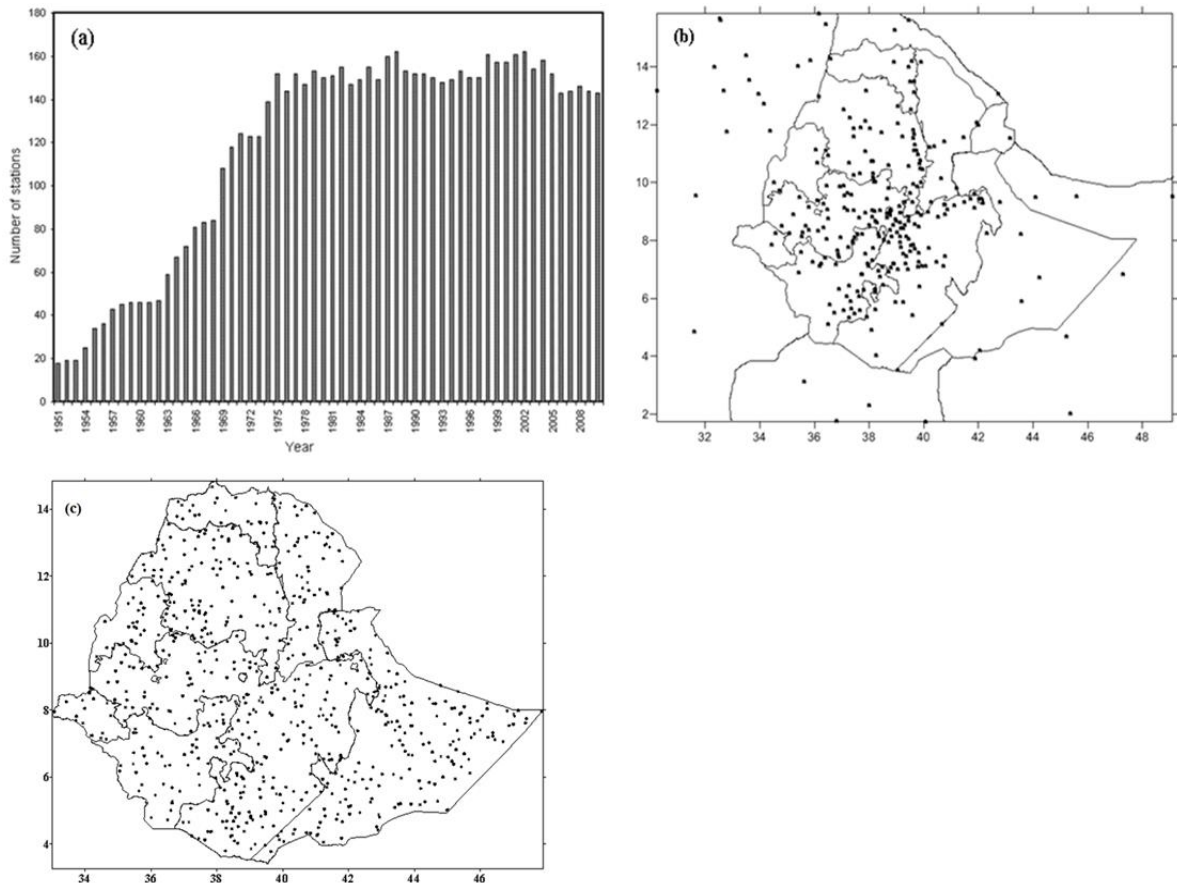


Figure 1. The number (a) and geographical distribution (b) of meteorological stations used in this study (c) location of random rainfall “station” extracted from the merged station-satellite grid points. Each dot represents position of meteorological station both from Ethiopia and neighboring countries. The lines in (b) and (C) indicate the regional administrative boundaries of Ethiopia.

## 2.2. Methodology

### 2.2.1. Classification techniques

To get a manageable number of and stable spatial rainfall clusters over Ethiopia, PCA and CA techniques were applied on standardized monthly

rainfall anomalies of the 162 stations, merged station-satellite rainfall data extracted at the 162 station locations and 717 random grid locations, separately. PCA and CA techniques have been employed in many rainfall classification studies and produced good results (e.g., Easterling, 1991; Gong and Richman, 1995; Baeriswyl and Rebetz, 1997; Buytaert et al., 2006; Littmann, T. 2000; Mazzoleni et al., 1992; Willmott, 1978). For instance, Littmann (2000) applied a hierarchical cluster analysis using the squared Euclidean distance and Ward's algorithm to classify weather types in the Mediterranean Basin. Similarly, Tennant and Hewitson (2002) applied Ward's clustering method on daily rainfall data in South Africa to construct homogeneous rainfall regions. Ellouze et al. (2009) also employed PCA techniques to classify South Tunisia rainfall into clusters. For the present study we therefore, adopted PCA and CA methods similar to those described above. General outline of the selection of rainfall zones is given in the flow chart (Figure 2).

In this study, correlation matrix, which represents the temporal correlation coefficients based on PCA, was applied on standardized monthly rainfall anomalies. Both orthogonal varimax and the oblique oblimin rotations (Morrison, 2005), which allow maximization of total variances for rainfall recorded at various meteorological stations in Ethiopia were used. The numbers of retained principal components (PCs) were determined by using the threshold point at which the eigenvalue drops to less than one as described by Ogallo (1988, 1989). It should be noted that while PCA technique identifies regions with similar variations, it does not provide any physical justification for the variation of meteorological elements such as rainfall over the substantial number of stations.

In the CA, thirty years of monthly rainfall data from 162 stations were used. Besides, we also used a newly-constructed data by merging station measurements with satellite estimates (Dinku et al., 2011). These gridded data cover the whole country at spatial resolution of 10km. Monthly values were extracted at the locations of the 162 stations as well as at 717 random locations. The main objective of including the new data set is to check the validity of the classification done with the 162 stations. This is very important particularly over data-sparse parts of the country (Figure 1b and 1c). The degree of similarity or dissimilarity between all possible pairs of rainfall stations in the rainfall data matrix were calculated using the hierarchical cluster analysis with Euclidean distance as the similarity measure. Details can be found in Soltani and Modarres (2006). In addition, a K-means cluster algorithm, which measures the proximity between groups using the Euclidean distance between groups centroid (Jobson, 1992; Jackson and Weinar, 1995), was applied. In the present study, the total spatial variances were computed for each identified cluster and K-means algorithm. The numbers of clusters are determined using hierarchical clustering (Ramos, 2001) and finally plotted on a dendrogram (Everitt, 1979). The number of clusters can be further decided based on the assumption that the ratio of the sum squared distances between stations in each cluster to the total sum squared distances between the clusters should be a minimum. Applications of CA and its K-means in rainfall clustering have widely been discussed by many authors (e.g., Romero et al., 1999; Unal et al., 2003). Running the cluster algorithm for the different number of clusters and using the above ratio indicated that the optimum number of clusters for Ethiopian rainfall was between twelve and fourteen. The results from the hierarchical and K-means clustering techniques were compared, and the serial correlations between the stations contained in the cluster and cluster averages were used to examine the stability of clustered stations.

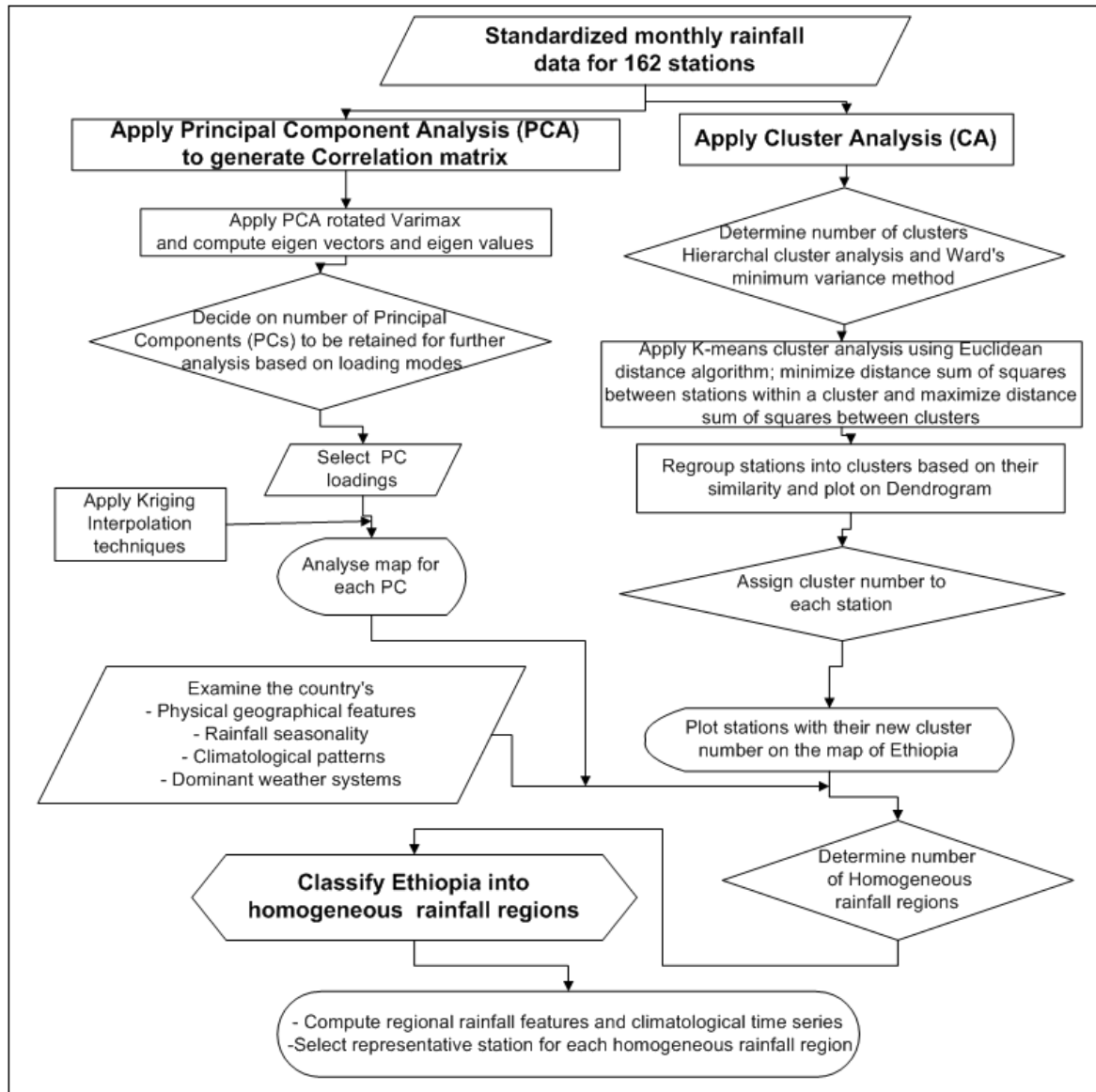


Figure 2. Flow chart showing the methodology applied in this study.

### 2.2.2. Spatial rainfall interpretation

Various interpolation methods have been proposed for the rainfall interpolation, which produce different results using the same rainfall data (Buytaert et al. 2006). Ashraf et al. (1997) listed some of these techniques, while stating that most of these techniques are applied to

interpolate and estimate an unknown rainfall pattern at the location having few or no observation computed as a linear combination of neighboring observations. According to Tabias and Sals (1985), kriging uses the interpolation weights as functions of semivariogram, which provides a measure of variance as a function of distance between data points. In the present study, we employed kriging interpolation method to map the spatial patterns of rainfall over Ethiopia.

### **2.2.3. All-Ethiopia rainfall index**

All-Ethiopia rainfall, which is nationally-aggregated based on stations data, was calculated in order to study how inter-annual and seasonal rainfall variations responded to regional and global meteorological indicators (e.g., El Niño/La Niña, Sahel and all-India rainfall indices). Two all-Ethiopia rainfall time-series data were constructed. The first time-series were constructed using only 18 stations, with complete data for the period (for the 1951-1960 periods, only 18 stations having full data set) 1951-2009. The second rainfall time-series data were computed by including additional stations having rainfall data in subsequent years for the same period. Statistical computations were made as follows: First, all-Ethiopia rainfall totals (mm) for each month were computed from averaging all stations in the country. Then, all-Ethiopia rainfall was aggregated into annual and seasonal totals for the period 1951-2009. In order to keep the stability of inter-annual and seasonal rainfall variability and accommodate many rainfall stations, the mean and standard deviation of rainfall were computed. Finally, the annual and seasonal rainfall totals for all-Ethiopia was standardized using mean and standard deviation of 1971-2000 climatological base periods. In order to examine the impacts of ENSO on Ethiopia, seasonal and annual rainfalls are also averaged for El

Niño, La Niña and near-neutral conditions as documented by Korecha and Barnston (2007).

### **3. Results**

#### **3.1. The rainfall climatology and moisture flux for Ethiopia**

For each season, Segele and Lamb (2005) and Korecha and Barnston (2007) computed and analyzed seasonal climatology for Ethiopia rainfall using 121 and 187 rainfall stations, respectively. In the present study, however, in addition to the 250 stations (1971-2000) within Ethiopia (Figure 1) 30 stations from the neighboring countries were used to minimize interpolation errors near the Ethiopian border. Our spatial rainfall climatology for 1971 to 2000 is comparable to previous studies (e.g., Segele and Lamb, 2005; Korecha and Barnston, 2007). In contrast, the inclusion of rainfall data from the neighboring countries and a larger substantial number of inland stations provides more details to the climatological rainfall characteristics of the country. This is particularly true for the northeastern, southern and southeastern Ethiopia, which had very few stations in previous studies.

As shown in Figure 3a, maximum annual rainfall amounts of 1750 to 2500mm are concentrated over the southwest-northwest sectors of Ethiopia. This is because the persistence of inter-tropical convergence zone (ITCZ) and its meridional trough cause substantial amounts of rainfall over these regions during *Kiremt* season. The reversal of southerly monsoon winds across the western sector of Indian Ocean also played a

significant role in modulating the seasonal cycle of Ethiopian rainfall climatology (Riddle and Cook, 2008; Segele et al., 2009). An intrusion of southwesterly wind flows associated with the southwest monsoon (Figure 3b) and the subsequent ITCZ shifting northward as well results in summer rains across the northern half of Ethiopia. In contrast, when ITCZ shifts northwards, southern and southeastern regions remain dry throughout the *Kiremt* season, with seasonal rainfall totals of less than 100 mm (Figure 3b).

One of the underlying factors for the dryness of southern Ethiopia is the strong southerly flow that diverges into two when it reaches the periphery of the region; most portions form the southwesterly Low Level Jets (LLJ), and become the major components of the southwest monsoon system (Figure 1b right panel). Southerly flows (Figure 3b) also reach the northern Ethiopia and form a converging inflow over the high grounds and hence produce abundant rains over the northern half of the country. In contrast, when southerly moisture influxes weaken, the northerly flow becomes dominant and pushes the rainfall-belt to progress towards west and southward (Figure 3c and 1d). This is clearly seen from the vertically integrated moisture fluxes, which was computed from ERA-Interim reanalyzed data. ERA-Interim is the European Centre for Medium Range Weather Forecasts (ECMWF) latest global atmospheric reanalysis (Simmons et al., 2006). It can be seen that a large part of the moisture transport comes from the north, and this flow meets the southerly flow make the convergence zone (see Figure 3b-1d). Viste and Sorteberg (2012) also found that the amount of moisture brought into the Ethiopian highlands from the north is 46% higher than from the south.

In subsequent months, wet and dry seasons prevail over portions of eastern, northern and southern regions while southwestern Ethiopia continues getting rainfall for an extended period (Kassahun, 1987). While *Kiremt* is the main rainy season in many regions, *Bega* (October-January) and *Belg* rains contribute one-third and two-thirds of the annual rainfall for the southern and southeastern Ethiopia, respectively (Figure 4a, 4b and 4c). For the *Bega* and *Belg* seasons, the seasonal rains show strong variability and are less reliable both from a temporal and spatial viewpoint, especially over the northern half of Ethiopia.

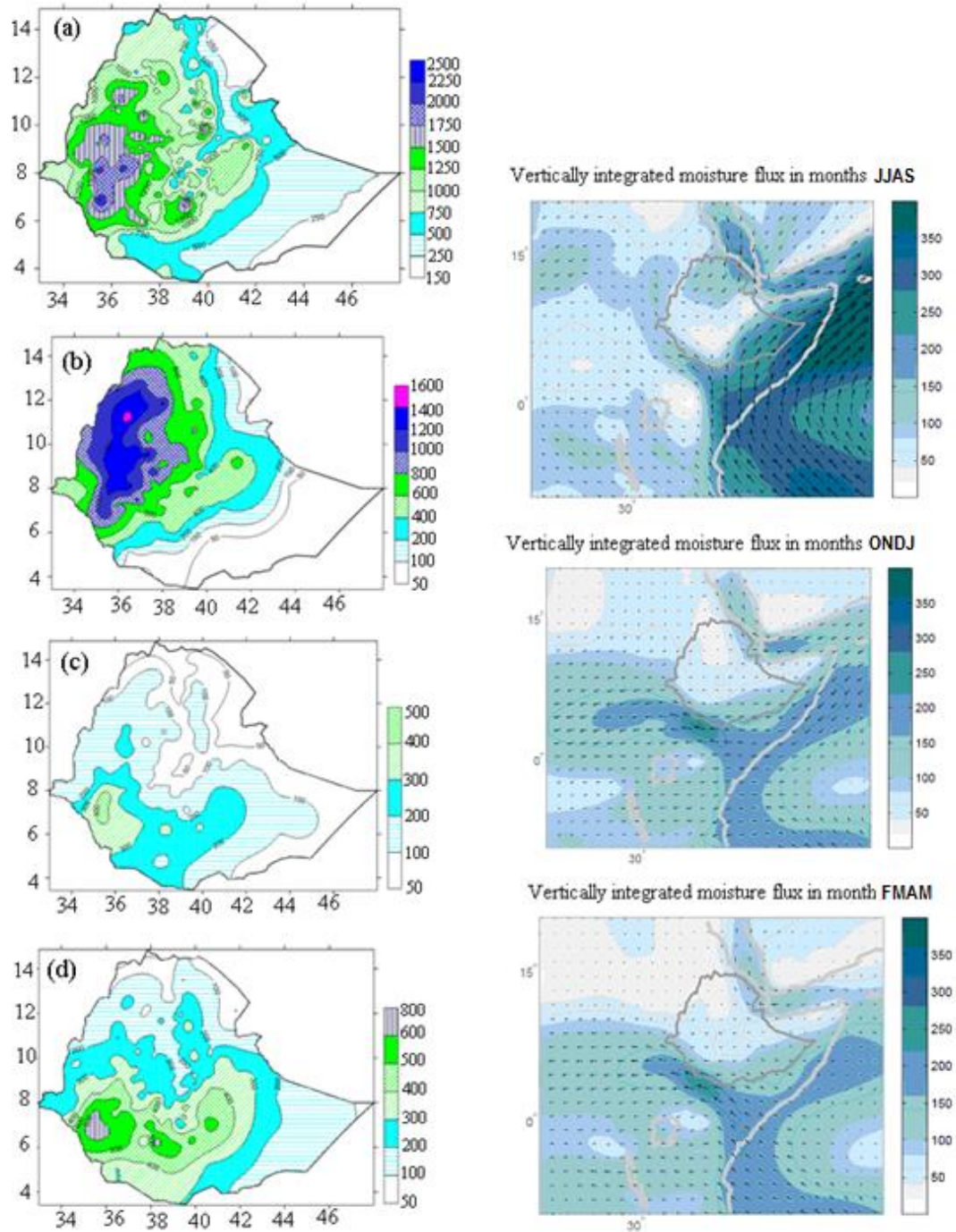


Figure 3. Spatial interpolation of station-based total rainfall climatology (mm) from 1971-2000. (a) annual, (b) Kiremt (JJAS), (c) *Bega* (ONDJ) and (d) *Belg* (FMAM). Seasonal climatological values of vertically integrated ERA interim moisture transports in kg/ms (1989-2009) are depicted on the right panel for each season. The light colors represent the lowest values of

both elements. The months are represented as JJAS for Jun-Sep; ONDJ for Oct-Jan and FMAM for Feb-May).

This is because major rain-bearing systems are associated with the passage of mid-latitude frontal systems and their interaction with the moist tropical air masses (Figure 3c and 3d). On the other hand, the southern half of the country receives relatively high rainfall totals due to its proximity to the movement of ITCZ during *Bega* and *Belg*, respectively (Figure 3c and 3d).

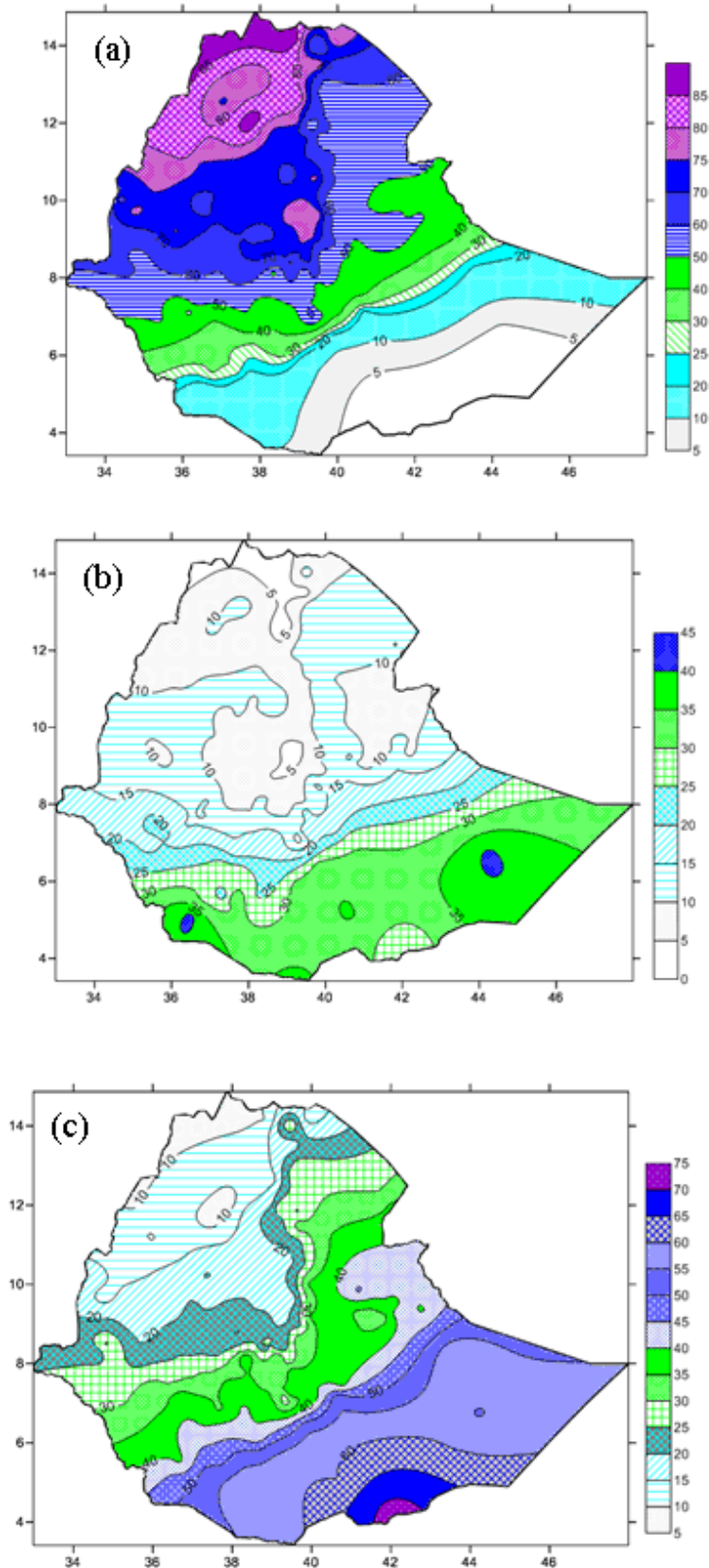
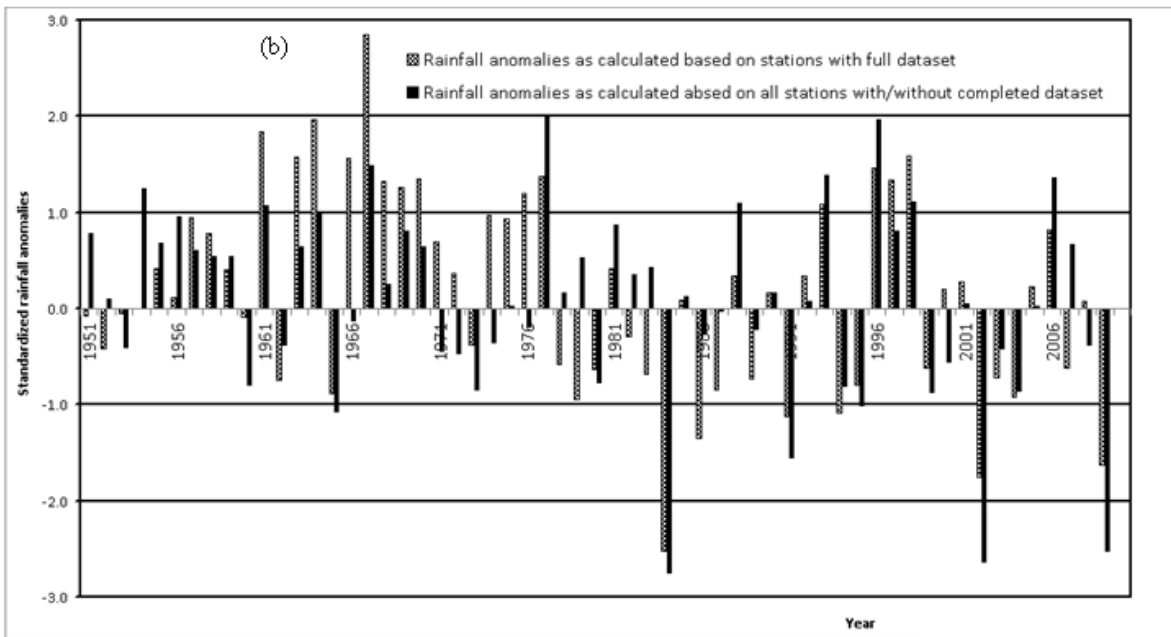
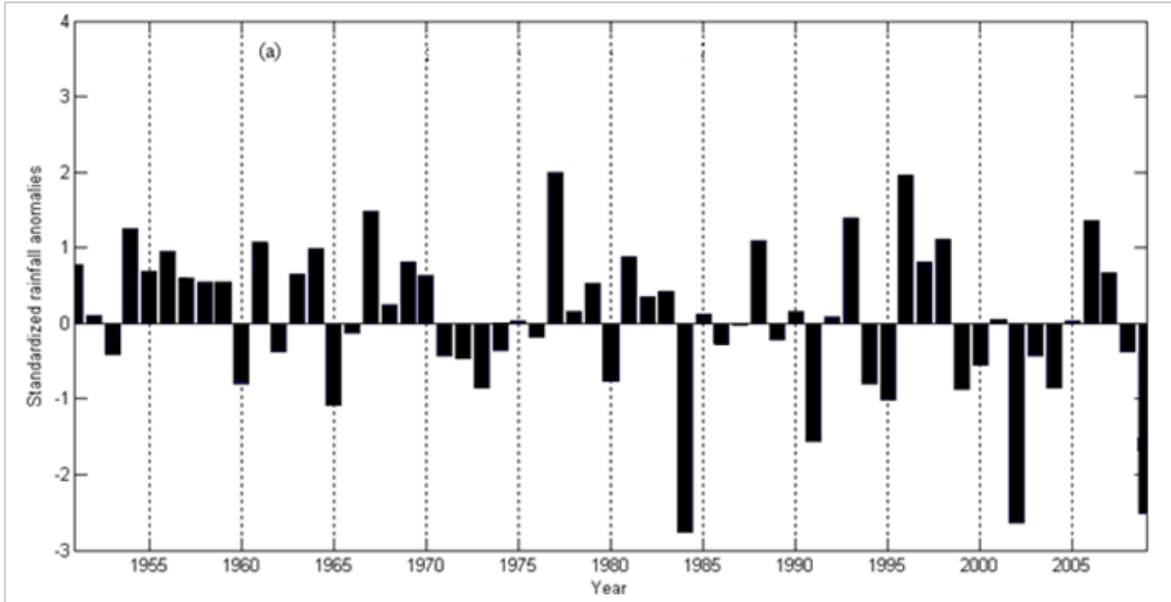


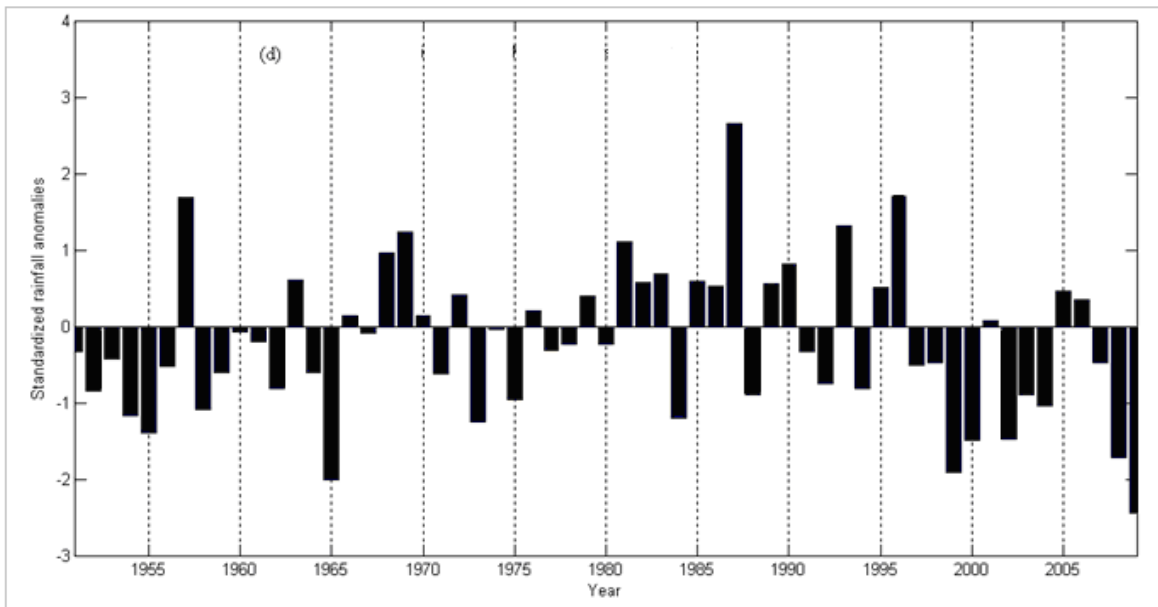
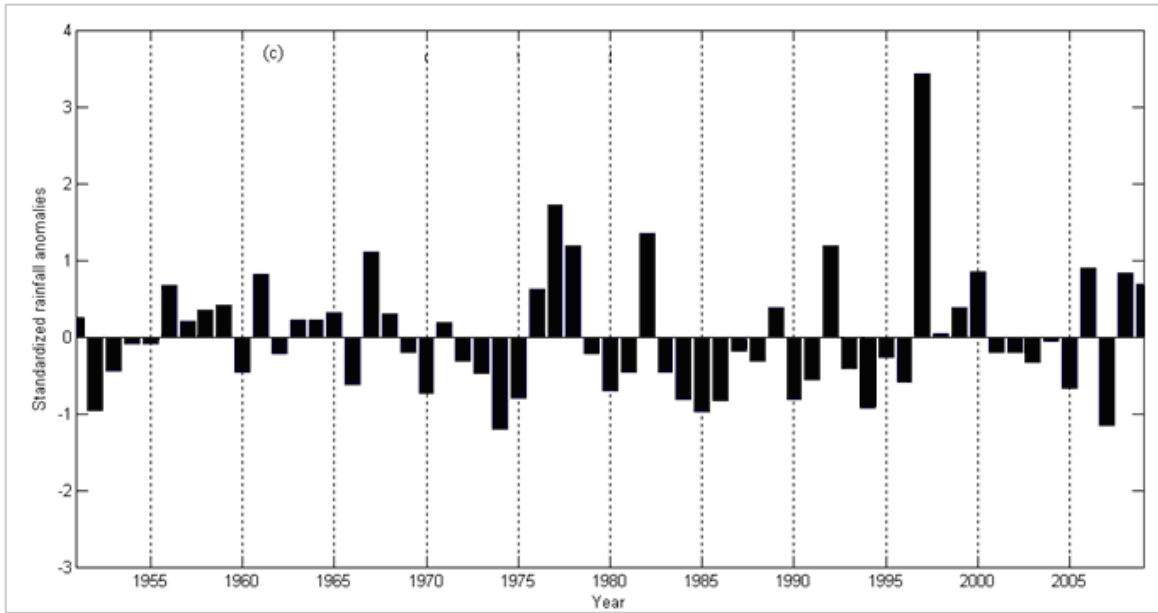
Figure 4. Percentage of mean annual rainfall (%) for (a) *Kiremt* (JJAS), b) *Bega* (ONDJ) and (c) *Belg* (FMAM) seasons for the period 1971-2000.

All-Ethiopia rainfall climatology, based on the 250 stations (Figure 1), indicates that Ethiopia on average receives 1115 mm of rainfall annually. From this crude mean value, which is biased toward regions with a dense station network; 655, 310 and 150 mm rainfall totals are the climatological values for *Kiremt*, *Belg* and *Bega* seasons, respectively. It follows that each of this season contributes 59%, 28% and 13%, respectively to the mean annual rainfall totals. On the monthly basis, the national rainfall average appears to have a mono-modal type rainy season, with peak in July and August (not shown). However, such representation camouflages regional rainfall patterns as there are at least two rainy seasons in Ethiopia, disconnected by dry periods in December-February, May-June and June-August.

### **3.2. All-Ethiopia rainfall variability**

All-Ethiopia rainfall indices were computed based on the available rainfall data for the period 1951-2009. On an annual time scale, the aggregated rainfall time series showed a relatively stable pattern with tendencies toward a somewhat wetter period in the 1950s and 1960s. From 1980 onwards, however, the national rainfall index became highly variable (Figure 5a and b.) with the three driest years being 1984, 2002 and 2009. Large scale atmospheric circulation anomalies related to sea-surface temperature anomalies such as El Niño or La Niña events combined with regional and local atmospheric circulation anomalies induced significant anomalies in Ethiopian rainfall. It has been observed that El Niño and La Niña usually suppress and enhance *Kiremt* rains while they behave differently in the case of *Bega* and *Belg* seasons (e.g., Korecha and Barnston, 2007). In a similar manner, we also examined the occurrence of extreme rainfall anomalies during each seasons, separately (see Figure 5c, 5d and 5e).





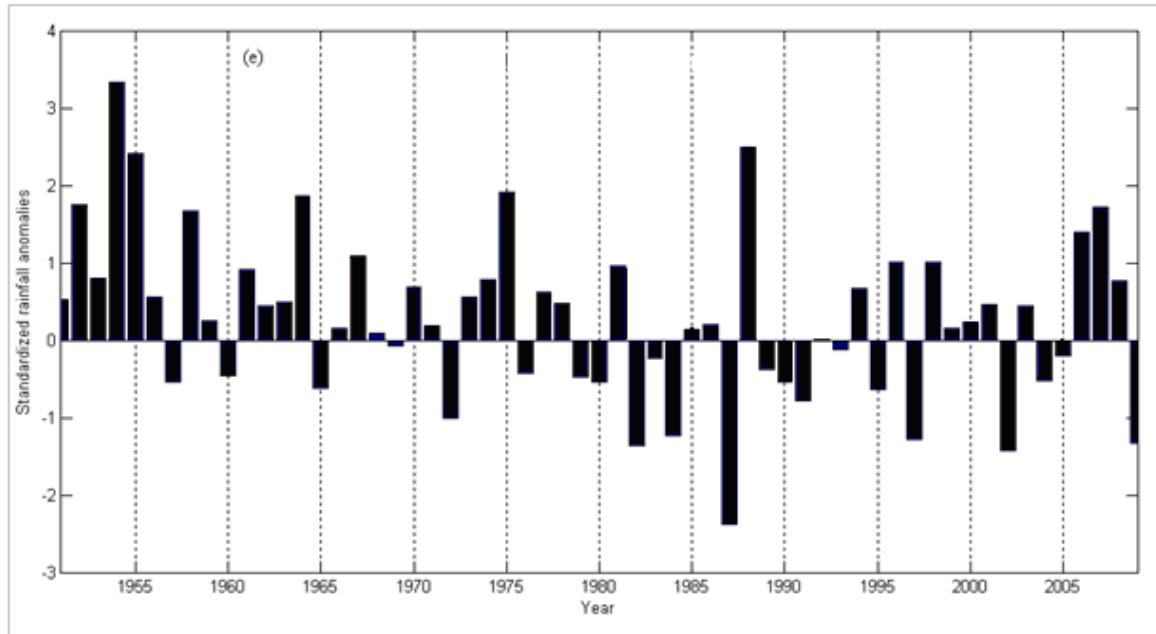


Figure 5. Standardized anomalies of the all Ethiopia rainfall for (a) and (b) Annual (with and without stations contained complete data set (18 and 18-162 stations, respectively)), (c) *Bega* (Oct-Jan), (d) *Belg* (Feb-May) and (e) *Kiremt* (Jun-Sep) (using all available stations). Figure 5b was included in order to show annual rainfall anomalies created only by considering all stations.

Continuous wet anomalies of 1950s and 1960s, and then weakening of rains, particularly during the major rainy seasons subsequently were coincided with the Sahel rainfall trend (Giannini et al., 2003). The correlation coefficient computed between all-Ethiopia *Kiremt* rains and rainfall indices of the Sahel (Giannini et al., 2003) and all-India were 0.83 and 0.60, respectively, indicating that these regions are widely influenced by similar large scale atmospheric circulation systems, such as ITCZ and Pacific SST anomalies. Flohn (1987) also showed the extension of positive spatial correlation within the Sahel-Sudan belt towards the western Ethiopia. On the other hand, Camberlin (1996) and Agnew and Chappell (1999) documented that for the long-range forecasting of the quality of the big rains in Ethiopia, the

connection with the India precipitation provides an interesting field of investigation. Based on the present study, we can therefore, argue that scientific findings on the Sahel and India rainfall, which are well documented and more comprehensive than that of the Ethiopian rainy seasons, can be beneficial for the understanding of all-Ethiopia rainfall variability.

Based on the standardized rainfall anomalies, Tables 1a and 1b show the ten wettest and driest years from 1951-2009 for the annual and three seasons. It was found (Table 1a) that among the driest years annually six of them coincided with moderate to severe El Niño, and two years were associated with La Niña and non-episodic events, respectively. In contrast, seven out of the ten wettest years had an association with non-episodes. In a similar manner, we also examined the occurrence of wet and dry anomalies during *Bega*, *Belg* and *Kiremt* seasons, separately (see Figure 5). In both *Bega* and *Belg* seasons, out of the first ten driest incidences, six occasions occurred during La Niña years. Whereas, the wettest *Bega* and *Belg* seasons occurred four times out of ten occasions during El Niño years (Table 1). In the case of *Kiremt* season, however, eight and six of the driest and wettest years (Table 1) coincided with El Niño and La Niña episodes, respectively.

**Table 1.** Extreme annual and seasonal rainfall anomalies in Ethiopia. (a) shows the 10 driest and (b) the wettest years annually and for all seasons in Ethiopia during the period 1951-2009. Anomalies are normalized by their standard deviation. † indicate El Niño episodes and <sup>a</sup> La Niña episodes.

a)

Annual		<i>Belg</i>		<i>Kiremt</i>		<i>Bega</i>	
Yr	Anom.	Yr	Anom.	Yr	Anom.	Yr	Anom.
1984	-2.75	2009	-2.44	1987 <sup>†</sup>	-2.38	1974 <sup>a</sup>	-1.21
2002 <sup>†</sup>	-2.63	1965	-2.01	2002 <sup>†</sup>	-1.43	2007 <sup>a</sup>	-1.15
2009 <sup>†</sup>	-2.52	1999 <sup>a</sup>	-1.91	1982 <sup>†</sup>	-1.37	1985	-0.97
1991 <sup>†</sup>	-1.55	2008 <sup>a</sup>	-1.71	2009 <sup>†</sup>	-1.33	1952	-0.96
1965 <sup>†</sup>	-1.07	2000 <sup>a</sup>	-1.48	1997 <sup>†</sup>	-1.29	1994 <sup>†</sup>	-0.92
1995 <sup>a</sup>	-1.01	2002 <sup>†</sup>	-1.48	1984	-1.24	1986 <sup>†</sup>	-0.84
1999 <sup>a</sup>	-0.88	1955 <sup>a</sup>	-1.39	1972 <sup>†</sup>	-1.01	1984 <sup>a</sup>	-0.82
2004 <sup>†</sup>	-0.86	1973 <sup>a</sup>	-1.25	1991 <sup>†</sup>	-0.79	1990	-0.82
1973 <sup>a</sup>	-0.85	1984	-1.20	1995 <sup>a</sup>	-0.63	1975 <sup>a</sup>	-0.81
1994 <sup>†</sup>	-0.81	1954 <sup>a</sup>	-1.17	1965 <sup>†</sup>	-0.63	1970 <sup>a</sup>	-0.74

b)

Annual		<i>Belg</i>		<i>Kiremt</i>		<i>Bega</i>	
Yr	Anom.	Yr	Anom.	Yr	Anom.	Yr	Anom.
1977 <sup>†</sup>	1.99	1987 <sup>†</sup>	2.66	1954	3.33	1997 <sup>†</sup>	3.42
1996	1.97	1996 <sup>a</sup>	1.70	1988	2.50	1977 <sup>†</sup>	1.71
1967	1.49	1957 <sup>†</sup>	1.69	1955	2.40	1982 <sup>†</sup>	1.35
1993 <sup>†</sup>	1.39	1993	1.32	1975	1.91	1992	1.19
2006 <sup>†</sup>	1.36	1969 <sup>†</sup>	1.23	1964	1.87	1978	1.19

1954 <sup>a</sup>	1.25	1981	1.11	1952	1.76	1967 <sup>a</sup>	1.10
1998 <sup>a</sup>	1.11	1968 <sup>a</sup>	0.96	2007	1.72	2006 <sup>†</sup>	0.90
1988 <sup>a</sup>	1.10	1990	0.81	1958	1.67	2000 <sup>a</sup>	0.84
1961	1.07	1983 <sup>†</sup>	0.68	2006 <sup>†</sup>	1.40	2008	0.83
1964 <sup>a</sup>	0.98	1963	0.60	1967	1.09	1961	0.82

### 3.3. Seasonal rainfall variability using principal components

In order to investigate the seasonal variability in rainfall, PCA (see subsection 1) was applied on the monthly rainfall data for the 1971-2000 periods. Moreover, the stability of classification is examined by applying PCA on station rainfall of 1961-1990 periods. The statistical results generated from 1961-1990 and 1971-2000 showed that the differences between the two base periods were not significant. Results of both unrotated and rotated PCA (using varimax and Oblimin techniques) were performed to identify large-scale modes of rainfall variations.

The first three PCs of rotated varimax, which were generated from 162 stations rainfall data, explained about 67% of the total rainfall variance. Each of these components depicts unique seasonal rainfall variations for northern half, southwestern, western and southern Ethiopia. The first PC (Figure 6a) accounts for 28% of total variance in the varimax-rotated PCAs depicting strong seasonal rainfall variability in central, northeast, north and northeast lowlands, with the highest loadings confined to the northeast escarpments. Regions of strong PC1 loading receive maximum rains in June-September (see Figure 3b), and small rains during March-

April-May (Figure 3d), while the region often receives fewer rain showers in December-January (Figure 3c). Unlike the western parts of the country, where the rain starts about March and continues through October, the seasonal rain in the northeastern Ethiopia starts in July and withdraws early September from these regions. Varimax-rotated PC2 and PC3 (26% and 13%) loadings show distinct seasonality of rainfall patterns for southwest-west and south-southeast regions, respectively (see Figure 6b and 6c). The two PC loadings clearly emphasize the non-*Kiremt*-rain benefiting region of south-southeast in contrast to the *Kiremt*-rain benefiting regions of the western and northern half of the country. Similar regional rainfall features were also identified from the PCA run ( the first three PCs have explained 77% and 80% of the total rainfall variance for merged station-satellite rainfall at 162 and 717 stations, respectively) on merged station-satellite rainfall data (not shown here).

On the larger geographical scales, the PCA results capture the mean seasonality in rainfall for the different regions of the country. However, there is a need for a further level of detail in order to capture the interannual and seasonal rainfall variability for different regions of Ethiopia as it will be addressed in the following section.

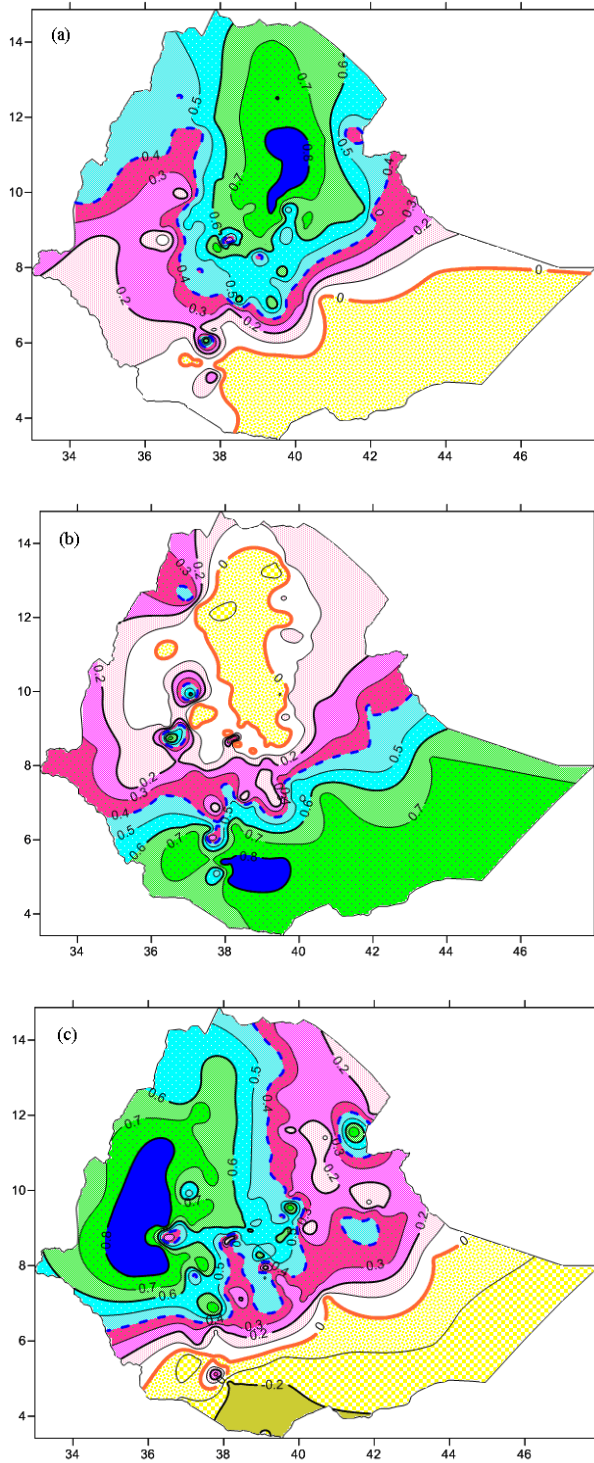


Figure 6. Spatial patterns of Ethiopian seasonal rainfall variations (computed on 162 meteorological stations) based on varimax-rotated principal component analysis for the period 1971-2000. Maps (a), (b) and (c) represent the first, second and third principal components, respectively.

### **3.4. Rainfall clusters produced from 162 rainfall stations using Cluster Analysis**

The spatial and temporal rainfall variability over Ethiopia were addressed by applying Ward's hierarchical and K-means cluster analysis techniques (for detail, see subsection 1). The K-means method created twelve rainfall clusters, which were further delineated into fourteen regions, and the stations that are grouped in each cluster were highly associated geographically and exhibited the same seasonal rainfall characteristics (Figure 7a). In contrast, each cluster has slightly shifted seasons or amplified their amplitudes. Generally, the presence of numbers of rainfall clusters suggests that rainfall pattern over Ethiopia vary with short distance, while modulated by topographic variation and orientation, large-scale atmospheric circulation systems, moisture track and local dynamical conditions.

### **3.5. Evaluation of the Classifications Using Merged Station-Satellite Data**

We have used 162 stations for delineating Ethiopia into 14 homogenous rainfall regimes (not shown). As some parts of the country have sparse rain gauge density, the creation of stable and coherent rainfall zones would be challenging. Thus, there is a need to evaluate the validity of the rainfall regimes, particularly over data-sparse parts of the country. This was accomplished using a new data set, which combines satellite rainfall estimates with rain-gauge data from over 600 stations. This data set goes back to 30 years at the grid resolution of 10km (Dinku et al., 2011). Evaluation of the homogeneous rainfall regions was done by comparing the

classification based on 162 stations and climatological characteristics of rainfall regimes in Ethiopia with classification based on the new data set. The use of the new data set is expected to improve stability and coherency of rainfall homogeneity, particularly over gauge-sparse regions of the country. Comparison was done using three data sets:

- a) Station rainfall data from the 162 stations for the period 1971-2000;
- b) Merged station-satellite rainfall data extracted at the 162 station locations for the period 1983-2010, and
- c) Merged station-satellite rainfall data extracted at 717 random locations across the country for the period 1983-2010.

The comparison of (a) and (b) is to see if the classification based on the merged rainfall data corresponds to the station data. The two classifications are similar, although the clusters with the merged data look more coherent (Figure 7 (a)). Likewise, comparison of (a) and (b) is to see if adding more “stations” would make any differences on rainfall homogenization. There are some significant differences between the two classifications (Figure 7 (a) and (b)). The main differences are over the regions with sparse of station network. On the other hand, the new classification also confirms some of the subdivisions we made in the first classification based on knowledge of local climate and topography. A good example would be the eastern and southern highlands.

The first fourteen homogeneous rainfall regions were delineated by consolidating multivariate rainfall statistics using data from the 162 stations, topography, climate and seasonal synoptic systems. However, the

classifications made using the 717 random points clearly demarcated some of the masked rainfall heterogeneity over the southeastern lowlands and the adjoining rangelands (Figure 7 (b)). The use of substantial number of points enabled us to merge the northeastern escarpments and the northern highlands into one homogeneous rainfall regime. The merging of two regions is in fact justifiable. One of the reasons would be the occurrence of rains over these regions as a result of southward penetration of troughs from westerly frontal systems during *Bega* and *Belg* seasons. Furthermore, this part of the country is widely known for its exposure to frequent droughts. Similarly, merging the southwestern lowlands and the southwestern tropical rainforest under the southwestern tropical rainforest rainfall region makes sense. The southeastern rangeland, which extends into the border area of southeast lowland, is also a result of using the new data set. Southeastern rangeland is a transition region between *Belg*-benefiting areas of south-southeast Ethiopia and southern and eastern highlands (Figure 8). The wide coverage of the new data set, including border regions (e.g., southeast, west and north Ethiopia) adds new information to the classifications (not shown). Thus, by incorporating valuable inputs both from the merged station-satellite rainfall data, we generate Figure 8, which represents twelve homogeneous rainfall regions in Ethiopia.

Figure 8, which shows homogeneous rainfall of Ethiopia has many advantages. Firstly, it is constructed based on high quality rainfall data, both at point stations and merged station- satellite rainfall estimates at finer spatial resolution. Secondly, all parts of Ethiopia are fairly represented. Thirdly, the merged data set represents the more recent inter-annual variability of rains than the station-based data. The merging of pocket places such as southern exit of Rift Valley, areas bordering with Djibouti and southern highlands with the neighboring regions is made based on the knowledge of local topography and climate. Figure 8 therefore, contains twelve homogeneous rainfall regions

in Ethiopia. The justification for these twelve rainfall regimes will be given in the next section. The corresponding regionally-aggregated mean monthly rainfall totals (for regions shown in Figure 8) are shown in Figure 9.

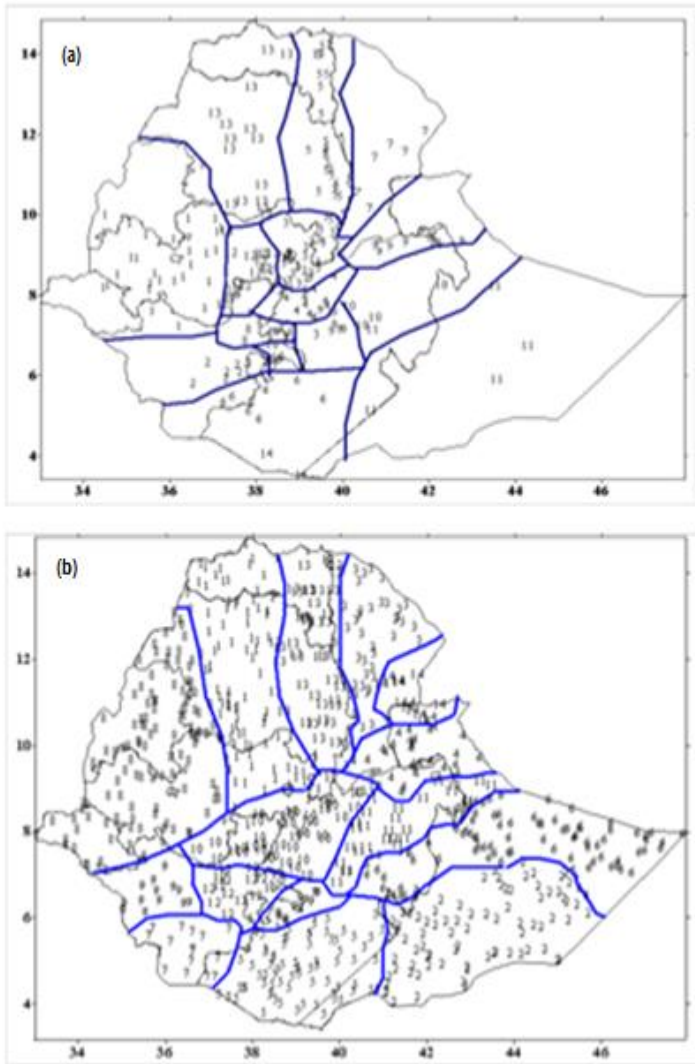


Figure 7. Geographical distributions of (a) 162 meteorological stations where the 1971-2000 monthly rainfall and merged station-satellite data extracted at the (1983-2010) and (b) merged station-satellite data extracted at 717 random locations (1983-2010) were classified using the K-means cluster method. Similar numbers indicate that stations belong to the same cluster.

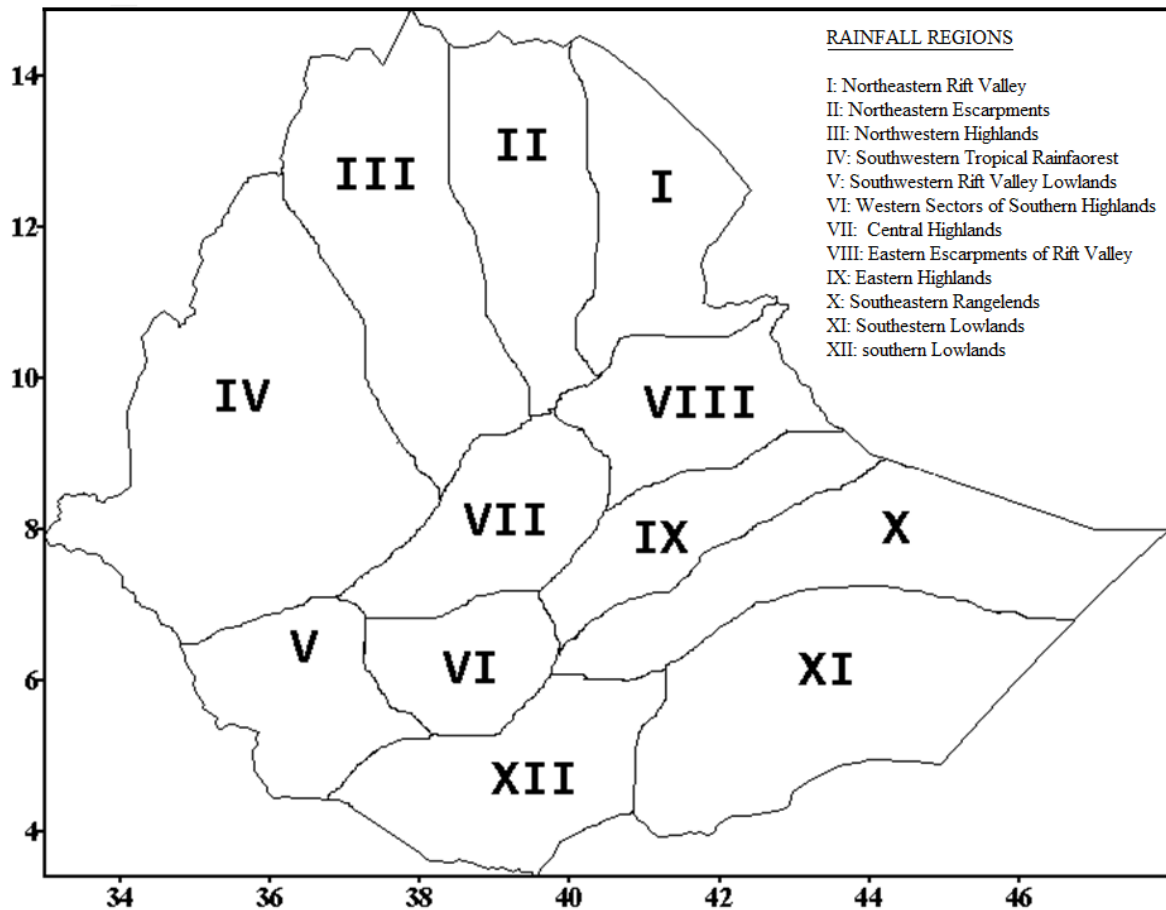


Figure 8. Homogeneous rainfall regions in Ethiopia based on outputs from stations, merged station-satellite rainfall data and knowledge of local climate and topography. In the classifying rainfall patterns into homogeneous regions, more information was used from station-satellite merged rainfall data. Roman number was used to represent each homogeneous rainfall region on the map of Ethiopia.

### 3.6. Justification for rainfall regions

PCA extracted three large rainfall regimes over Ethiopia, namely; the northeastern, southern and western region and the CA further classified the Ethiopian rainfall features into twelve clusters. PCA method allowed reduction

of the number of variables. By employing the method of Baeriswyl and Rebetez (1997), application of CA method (ascending hierarchical classification) on the 6 PCs divides Ethiopia into twelve rainfall regimes, which are characterized by a particular rainfall region.

Each rainfall cluster represents stations that have fairly coherent features in terms of seasonal cycle and amplitude. Combining the PCA and CA analysis suggest it is possible to identify distinct regions that have mono-modal or bi-modal type rainy season(s). When common climatological patterns and physical geographical features are superimposed on clusters, twelve distinct homogeneous rainfall regions emerge (Figure 8). We will discuss on the rainfall characteristics of each rainfall region (see Figure 8) in the subsequent subsections.

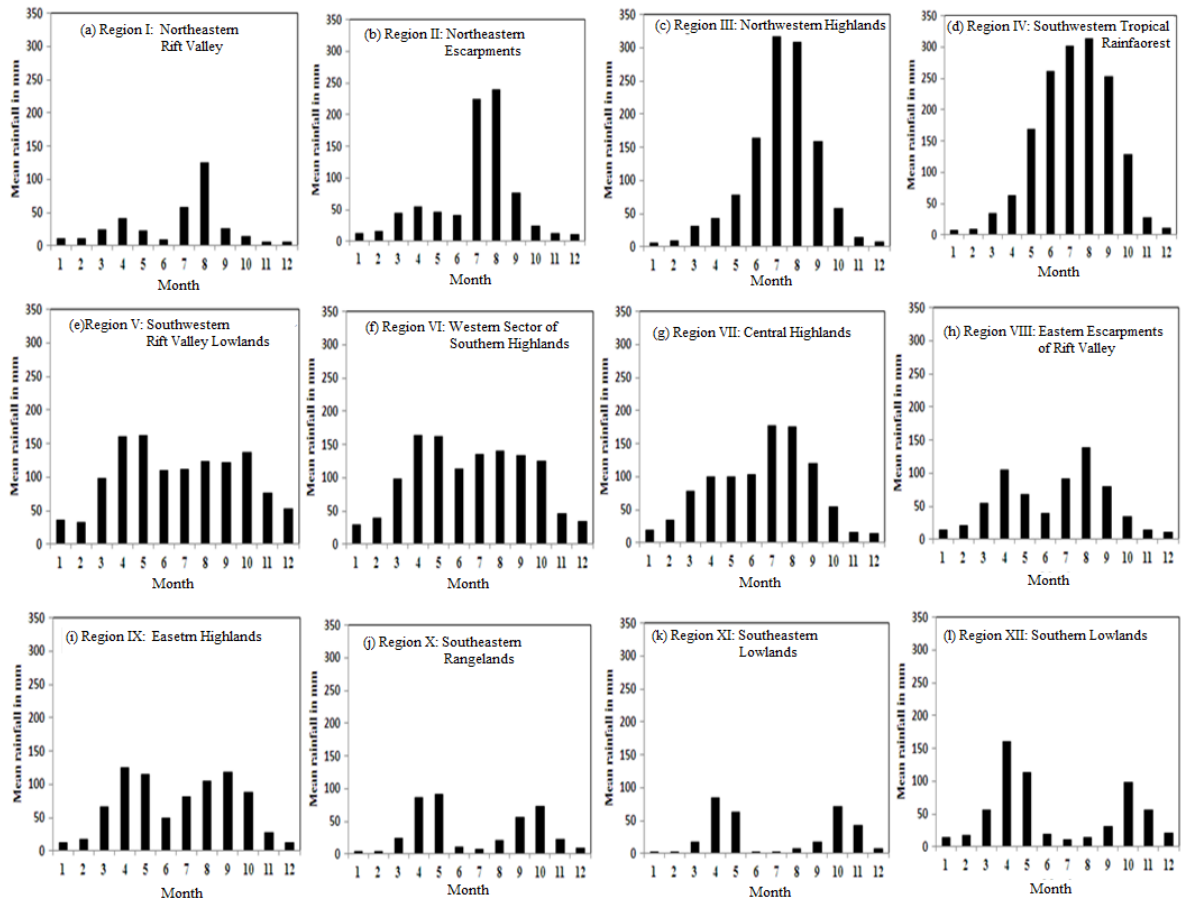


Figure 9. Regional-averaged monthly rainfall climatology (mm/month) for the homogeneous rainfall regions of Ethiopia (see Figure 8) over the period 1983-2010. Area average for each region was computed based on monthly mean of all merged station-satellite rainfall data extracted at random locations of the homogeneous rainfall region. Monthly rainfall climatology computed either from meteorological stations or station-satellite merged rainfall data are reasonably similar.

### 3.6.1. Northeastern Rift Valley and Northeastern escarpments

Northeastern Escarpments and the adjoining lowlands of Northeastern Rift Valley are clustered into two clusters (Region I and II, see Figure 8). Most of the *Kiremt* and *Belg* rainfall amounts and distributions over these

regions are produced under the influence of tropical or mid latitude frontal systems. The Red Sea Convergence Zone (RSCZ) is often associated to the formation of spring and autumn (partially *Bega*) rains over these parts of Ethiopia (Habtemichael and Pedgley, 1966; Tucker and Pedgley, 1977). Moreover, Tucker and Pedgley (1977) suggested the presence of the Afar Convergence Zone (ACZ) between the northwesterlies over the southern Red Sea and southwesterlies over the Gulf of Aden eventually produces convection rain over both sides of ACZ.

The Northeastern Rift Valley (Region I) region is generally categorized as semi-arid. It receives the major and small rains during the *Kiremt* and *Belg* seasons with rainfall maxima occurring in July/August and in March/April (Figure 9a). This region is one of the driest regions in Ethiopia (less than 250mm/year as shown in Figure 3a). Region II, the Northeastern Escarpments, also has the big and small rainy seasons during *Kiremt* and *Belg* season, respectively. But it is different from Region I both in amount and length of rainy seasons. In the Gissila et al. (2004) and Diro et al. (2011) regionalization, the two regions were represented as one cluster. However, previous studies made by Kassahun (1986), Camberlin and Philippon (2002) and Segele et al. (2009) documented that there is a substantial difference in rainfall amounts and rainy season over these parts of Ethiopia. According to our analysis, Region II receives over two-fold of monthly rainfall totals (250mm in July and August, Figure 9b) compared to Region I (over 100 mm in August, Figure 9a). Annual rainfall amounts and seasonal rainfall patterns for Region II are far more stable and higher as compared to Region I (Figure 3). Indeed, the seasonal rainfall cycle of Region II resembles partly the neighboring northwestern Ethiopia during the period when the ITCZ and the associated summer rain-producing systems reach their northern limit (Kassahun, 1987; Segele et al., 2009). The major-rain-producing systems over the region include,

northward advancement of ITCZ and the associated monsoon flow, and southern penetration of mid latitude troughs. The contributions from *Bega* and *Belg* rainfalls are low over the northern tip of Region II and are predominantly influenced by ridge extension from dry Arabian anticyclones (Figures 3 and 4). However, both regions are commonly prone to frequent droughts and often to flash floods. For example, long-lasting unevenly distributed rainfall that occurred during *Kiremt* and *Belg* seasons caused droughts and famines in 1970s, 1980s and 2000s over Region II (not shown here). During *Kiremt* season, when the rain-producing systems approach the regions from western direction, the systems are forced to precipitate along the windward side of northwestern mountain chains and the passages of moist air toward the northeastern Ethiopia becomes very scanty.

### **3.6.2. Northwestern Highlands**

Northwestern Highlands (Region III in Figure 8) extends from northern mountain chains to the northern tip of the country. It mainly receives rain during *Kiremt* season (Figures 3 and 4). This region differs from Region II as its rainfall is characterized by a mono-modal type of seasonal cycle. *Kiremt* rain starts in June and reaches its peak in July and August then withdraws in late September (Figure 9c). Numerous observational studies (e.g., Segele and Lamb, 2005; Romilly and Gebremichael, 2011) indicated that this region experiences extensive *Kiremt* rains while in *Bega* and *Belg* it generally remains dry. In the middle and end of *Kiremt* season, large-scale storms that develop over the Yemeni and northern Ethiopian highlands transverse westward and produce intensive and widespread rains over the region (see Figure 3). Seasonal rainfall averages exceeds 1000 mm in the highlands but getting low over the lowlands with

significant interannual variability dominates throughout (Figure 3 and 4). The major-rain-producing systems over the region are mainly associated with northward advancement of ITCZ. The contributions from *Bega* and *Belg* rainfalls are low and are predominantly influenced by ridge extension from the northern hemisphere high pressure systems. Unlike northeastern Ethiopia, this region is characterized by low rainfall variability, with a long dry period prevails from November to March (Figure 9c).

### **3.6.3. Southwestern Tropical Rainforest**

In the eastern and southern sectors of the southwestern Ethiopia (Region IV, Figure 8), rain falls throughout the year. Maximum rains occur from the middle of March to October without a significant break (Figure 9d). Mean annual rainfall amounts of stations in the region vary between 750mm and 2400 mm (Figure 3a) and on average this region receives 1575 mm. Intra-annual and seasonal rainfall variability are the lowest across the region, except over the western lowlands. Thus, the region is known as the wettest corridor of the country. The presence of tropical rainforests and the proximity of this region to the equatorial moist region initiate convective rainfall over the region. Since the 1980s seasonal and annual rainfalls of the region have decreased as compared to the 1950s and 1960s. The causes for recent declining of rainfall are still unclear. The identification of this region (Figures 3 and 4) is in line with the studies of Gissila et al. (2004) and Diro et al. (2008) while Riddle and Cook (2008) regrouped the southwestern Ethiopia slightly into the northwestern regions and partly into the southwestern regions.

### **3.6.4. Southwestern Rift Valley Lowlands**

The southern outlet of Rift Valley and the peripheral southwest marginal lowlands (Region V, Figure 8) experiences a bimodal rainy season (Figure 9e). This region is located under the passage of moist southerly flow and ITCZ throughout the year. As a result, the rain occurs throughout the year (Kassahun, 1986). However, it sometimes experiences prolonged dry spells whenever the rain producing tropical systems shift northward/southward from the region, particularly in July-August and December-January. Regional rainfall features are generally characterized by rainfall peaks in April and September/October, which support double growing seasons (NMSA 1996). In this region, maximum rainfall occurs in the *Belg* season (500-800 mm) while the second maximum occurs in *Bega* (300-500mm). Unlike the southern and southeastern Ethiopia, a substantial amount of rain also falls in Kiremt.

### **3.6.5. Western Sector of Southern highlands**

This region represents the central Rift Valley (Region VI, Figure 8) and the adjoining high-grounds extending to the foothills of central and southern highlands. It includes the wetter sides of central Rift Valley escarpments, which receive the mean annual rainfall between 1000-1750mm (Figure 3a). The regional rainfall patterns are characterized by continuous rains for two consecutive seasons (*Belg* and *Kiremt*), with a short spells in June (Figure 9f). *Belg* and *Kiremt* seasons are more or less equally important for this region in contrast to Region V, where *Belg* and *Bega* are the main rainy seasons (Figure 9e). Moisture fluxes into the region are mainly from the east except in the *Kiremt* season (Figure 3). Even so, seasonal rainfall in this region is also influenced by tropical as well as mid-latitude systems (Shanko and Camberlin 1998). In contrast to the southern lowlands and highlands, the transition from *Belg* to *Kiremt* rainfall is short.

### **3.6.6. Central Highlands**

The central Ethiopian highland encompasses the areas extending from the central Rift Valley to the Blue Nile valleys (Region VII, Figure 8). Rainfall amounts are usually amplified when the rainy season progresses from June to July. *Kiremt* is the major rainy season in this region with a maximum in July–August (Figure 9g). This region experiences dry climate between November and February. The northward progressions of the southwest monsoon systems create favorable conditions for stable rainy season over this region. Unlike the adjoining Rift Valley and northern regions, where the rain is scanty, this always benefits from the northward advancement and southward retreat of ITCZ (Segele and Lamb, 2005). Besides, the region varies from the nearby high grounds, the semi-arid central Rift Valley region because it receives rainfall mainly from westward and northward swinging of southwest monsoon storms. Conway (2000), for instance argued that rainfall over the Ethiopian Rift Valley shows little association with rainfall over the Central highlands. The dissimilarities between rainfall patterns of these regions are therefore agreed with our findings. Previous studies made by Gissila et al. (2004) and Diro et al. (2008) also demarcated central Ethiopia as a separate homogeneous rainfall regime.

### **3.6.7. Eastern Escarpments of Rift Valley**

The eastern Rift Valley escarpment and the adjoining eastern highlands (Region VIII, Figure 8) experience a similar rainfall cycle. This region represents some of central Rift Valley and the northern fringe of the eastern mountains as well as eastern highlands. The region experiences a bimodal rainfall cycle (Figure 9h), with relatively shorter and weaker rainy

seasons than the northeastern and central highlands. Moreover, the mean monthly rainfall amount is lower in eastern regions than the neighboring central highlands, with rainfall maxima in April and August. This region is known for its vulnerability to extreme rainfall conditions. For instance, the incidence of prolonged 2002 drought (Funk et al., 2005) and 2006 floods could partly be explained as a regional phenomenon. This region is confined and surrounded by lowlands whereby locally induced weather disturbances sometime produce intensive rains and dissipate quickly as a result of limited inflow of moisture. Seasonal variation in moisture transport (Figure 3) toward the region play major role both for the short and long range rainy season (Kassahun, 1987; Jury, 2011). Over this region, rain starts in March and gradually increases in April and May. There is a dry break in June before the major rainy season starts.

The slow southward retreating of rain-bearing systems such as the ITCZ produces rains in September for the region, which differentiate it from the nearby northeastern escarpment. Intra-annual and seasonal rainfall variability is comparatively high compared to Region VII. Rainfall over this region is mainly associated with easterly waves (easterly perturbations) originating in the Arabian Sea and northern Somalia as well as the intensity of southwest monsoon flow (see Figure 3).

### **3.6.8. Eastern Highlands and Southeastern Rangelands**

Southern Highlands (Region IX, Figure 8) represents the Bale Mountains and the adjoining Arsi and Bale highlands, extending into the buffer zones between southeastern rangelands and eastern high-grounds. Rainfall of this region is characterized by a bimodal cycle, with *Belg* as the peak rainy

season (Figure 9i), which contributes 30-55% for annual rainfall totals (Figure 4c). *Kiremt* season also accounts for a substantial percentage for the regional rainfall totals (Figure 4a). Like the south and southeast Ethiopia, *Bega* weather systems (50-300 mm) produce light to moderate rains over the region (Figure 3c). The annual spatial rainfall patterns of the western sector of Region IX are less variable than the nearby regions, but Umer et al. (2007) indicated that rainfall is highly seasonal on the northern slopes of the mountains, with the maximum rainfall occurring between July and September, while mean annual rainfall on the southern slopes of southern highlands is more evenly distributed throughout the year. Southeastern rangelands represent the transition rangelands lying between southeastern lowlands and eastern highlands (Region X, Figure 8). This region is mainly influenced by southward retreat of *Kiremt* systems, and easterly perturbation that induce moisture and rain-bearing clouds from the coast of East Africa. Bi-modal types rains occurring during *Belg* and *Bega* seasons. Both rainy seasons are very short and mostly prevail around April-May and October-November (Figure 9j).

### **3.6.9. Southern and Southeastern Lowlands**

Southeastern and Southern Lowlands (Regions XI and XII, Figure 8) cover extensive portions of agro-pastoral rangelands and lowlands of southeastern and southern Ethiopia. These regions extend from the eastern margin of the southern Rift Valley to the eastern Ethiopia lowlands. The regions experience bimodal seasonal rainfall cycle (Figure 9k and 10l), which exhibit similar rainfall characteristics with other eastern African sub-region. *Belg* and *Bega* seasons account for 60% and 30% of the annual rainfall totals (Figure 4b and 4c). While these regions experience mostly dry weather conditions during the *Kiremt* season as the strong southerly

moisture influx diverged over the lowlands without giving rain (Figure 3). Previous studies also confirmed the uniqueness of these regions (e.g., Korecha and Barnston, 2007; Diro et al., 2008). The Turkana Lake and adjoining regions might be influenced by the Turkana Jet (e.g., Kinuthia and Asnani, 1982; Indeje et al., 2001). Vizy and Cook (2003) indicated that when the southwest monsoon trough weakens, northern Ethiopia dries, in association with a weaker Somali jet, but rainfall is enhanced over southern Ethiopia. The reason for splitting the southern and southeastern Ethiopia into two rainfall regions is based on the observations and the output from cluster analysis (Figure 7b), which show that the southern lowlands receive more rain than the eastern lowlands. Both rainy seasons (*Bega* and *Belg*) also usually start one month earlier over the southern lowlands (Figure 9k and 9l). In addition, advection of clouds from equatorial east Africa produce rain over Region XII. In contrast, southeastern lowlands (Region XI) receive intensive rains, mainly from the formation of tropical depressions along the coastal region of the Horn of Africa. The results of cross correlation analysis among the stations also indicated that the two regions should be separated.

### **3.7. Climatological implications and comparisons with previous findings**

Previous studies have highlighted the need to improve further rainfall classification scheme that represents seasonality and variability at local scale. Our research finding is also broadly consistent with these previous findings, with additional availability of numbers of stations classification techniques we determine further categorization of homogeneous rainfall regimes. We argue that inclusion of all quality-controlled meteorological variables might allow us a further sub-classification to be reached in the long run. The aim of this study

is, therefore, to characterize the spatial and temporal properties of rainfall patterns over Ethiopia and construct annual and seasonal rainfall climatology that are spatially coherent but independent homogeneous rainfall regions. Temporal rainfall patterns are examined to know how sub-continental rainfall anomalies such as the Sahel and all-India, correlate with all-Ethiopia rainfall index with time. On the other hand, to delineate the country into spatial coherent rainfall regions, multivariate statistical techniques namely; Principal Component and Cluster Analyses are applied.

Mean annual and seasonal rainfall totals show regions normally receive low and high rainfalls. Moisture fluxes that show different patterns during each season also explain the presence of distinct seasonal variation over Ethiopia. This study concludes that all-Ethiopia rainfall time series is strongly correlated with both Sahel and all-India summer rains. In this study, Ethiopian rainfall patterns are classified into twelve homogeneous rainfall regions by PCA and CA techniques, while also aided by local climatological knowledge. This study contributes to a better understanding of interannual and seasonal rainfall variations, which are the result of local, regional and local scale meteorological phenomena. The newly constructed spatially-coherent rainfall classification is made to elucidate internal physical differences on Ethiopian rainfall with the vast region that normally has mono-modal or bi-modal type rain.

Unlike the preceding regional rainfall classification made for Ethiopia using a few numbers of stations covering only small portions of the country (e.g., Gissila et al., 2004 used 19 and Diro et al., 2008 and 2011 used 33 and 45 stations); this study uses a larger number of rainfall stations (162 conventional stations and 717 satellite-rainfall-estimate merged gridded

rainfall data) covering major geographical and climatic variations. Moreover, while previous studies were based on simple statistical techniques such as, similarity of annual cycles and interannual correlations of seasonal rainfall, we applied in the current study a series of multivariate statistical techniques to produce spatially-distinct rainfall clusters that could represent independent but spatially-coherent rainfall regions for Ethiopia.

The present study adds several homogeneous rainfall regions to those proposed by Gissila et al. (2004) and Diro et al. (2008 and 2011). This study classifies Ethiopian rainfall patterns into twelve distinct regions while Gissila et al. (2004) identified only five. In contrast, Diro et al. (2008 and 2011) suggested merely two regions for eastern half of Ethiopia while the present study showed that this part of the country could be classified into six homogeneous rainfall regimes. Distinct nature of each rainfall region was further examined based on monthly rainfall climatology (Figure 8). It demonstrates the variation in the onset, length and cessation of each rainy season for each rainfall region. Furthermore, regionally-aggregated standardized rainfall anomalies of *Bega*, *Belg* and *Kiremt* seasons indicate that some past severe droughts like 1984, 1987, and 2002 occurred over many regions, while localized drought and flood years were markedly observed differently (not shown here). Thus, the results presented in this study confirm that much of the large scale meteorological systems known to influence the Ethiopian rainfall distribution are fairly used in justifying the dissimilarities of twelve homogeneous rainfall regions. Besides, the study reveals that local rainfall variations recurrently influencing numerous social and economic practices can be more identified on the present homogeneous rainfall regime than those based on earlier regional classification.

#### 4. Conclusions

Annual and seasonal rainfall climatology of Ethiopia were computed and analyzed for 250 meteorological stations. Besides, thirty stations from the neighboring countries were used to minimize interpolation errors near the Ethiopian border. The inclusion of rainfall data of meteorological stations from the bordering countries and a larger substantial number of inland stations provides more detail to the climatological rainfall characteristics of the country. All-Ethiopian rainfall time series were made for the period 1951-2009. It follows that each of the season contributes 59%, 28% and 13% (*Kiremt*, *Belg* and *Bega*, respectively) to the mean annual rainfall totals. All-Ethiopian *Kiremt* strongly correlates with the Sahel and India summer rainfall, with high correlation coefficients of 0.83 and 0.60, respectively. The result indicates that these regions are widely influenced by similar large scale atmospheric circulation systems. Results from this study therefore, suggest that the scientific findings on the Sahel and India rainfall, which are well documented and more comprehensively studied than that of the Ethiopian rainy seasons, can be beneficial for the understanding of Ethiopia rainfall variability.

Analysis of various clusters on the monthly rainfall data from 162 Ethiopian stations (1971-2000) indicated the presence of distinct spatial rainfall patterns over Ethiopia. PCA was broadly categorized Ethiopia in three major rainfall regions, namely; northeastern, southwest-northwestern and south-southeastern. It identified the dominance of large rainfall dissimilarities and strong seasonality, which separate *Kiremt* rain-benefiting from *Belg* and *Bega* rainfall regimes. The application of CA, on the other hand identified at least twelve distinct rainfall regions for the country. We argue that inclusion of all quality-controlled meteorological

variables might allow us a further sub-classification to be reached in the long run.

Aided by the cluster analysis and the first author's fifteen years of experience as a weather and climate forecaster, we delineated the country into numbers of homogeneous rainfall regions. Based on the merged station-satellite data set as well as by considering the outputs from 162 stations, we classified Ethiopia into twelve homogeneous rainfall regions. The characteristic of each homogeneous rainfall region is the reflection of the typical seasonal cycle that prevails in Ethiopia. Both climatic features and local topographies have been taken into account in discriminating the country's rainfall patterns into homogeneous regions.

The identification of specific rainfall regions adds values in the local seasonal climate forecasting, monitoring of climate variability and change on regional and national scales. Above all, it invites in-depth investigations into the climatic and topographic processes controlling the regional climate of each region both on shorter and longer time scales. Moreover, the mountainous chains that bisect northwestern from the northeastern regions were well replicated in our spatial delineations. However, the topographic barrier that creates the rainfall shadow along the eastern side of the mountain chain during the *Kiremt* rainy season may require further investigation. The formation of the dry corridors of the northern Rift Valley and southeastern lowlands are just two of the interesting regional features, where understanding of the meteorological mechanisms may provide a benefit to realize the impact of rainfall variation on social and economic activities of the region.

Distinct nature of each rainfall region was further examined based on monthly rainfall climatology. It demonstrates the onset, length and cessation of season for each rainfall region. Furthermore, regionally-aggregated standardized rainfall anomalies of *Bega*, *Belg* and *Kiremt* seasons indicate that past severe droughts like 1984, 1987, and 2002 covered occurred substantial portions of Ethiopia, while localized drought and flood incidences were markedly observed differently (not shown here). Thus, the results presented in this study confirm that much of the large scale meteorological systems known to influence the Ethiopian rainfall distribution are fairly used in justifying the dissimilarities of twelve homogeneous rainfall regions. Besides, the study reveals that local rainfall variations recurrently influencing the country's social and economic practices can be more identified on the present homogeneous rainfall regime than those based on earlier regional classification. We have also indicated that inclusion of all quality-controlled meteorological variables, particularly the station-satellite blended rainfall currently available at the grid resolution of 10km allow us to construct spatial coherent and stable rainfall regions in Ethiopia. It is also believed that further detailed spatial analysis of rainfall on various time scales, such as seasonal and high spatial resolution data is needed to obtain finer information for localized societal activities.

In summary, the spatial distributions of Ethiopian rainfall regimes obtained here can be used to analyze past rainfall and also to assess possible future rainfall trends in different parts of the country. As the seasonal cycle is emphasized in the regionalization, we think the regions are well suited for monitoring the impact of rainfall on agricultural productivity, water resources and health services, among others. It can also be used as a reference to evaluate the performance of global and high resolution regional climate models of replicating historical rainfall climatology of each homogeneous rainfall region. We also believe that the rainfall regions can be used for monitoring and prediction of rainfall on seasonal and annual

time scales as well as to develop useful products such as decision support tools at various tempo-spatial scales.

## **Acknowledgements**

This work has been carried out with support from the Ethiopian Malaria Prediction System (EMaPS) project funded by the Norwegian Programme for Development, Research and Education (NUFU), NUFUPRO-2007/10121. The authors would like to thank the National Meteorological Agency of Ethiopia for allowing the first author to carry this research and providing rainfall dataset for Ethiopia.

## References

- Ashraf, M., Lftis J.C., Hubbard K.G. 1997. Application of geostatistics to evaluate partial weather station networks. *Agric. For. Meteorol.*, **84**: 255-271
- Baeriswyl, P.E.A., Rebetez M. 1997. Regionalization of precipitation in Switzerland by means of principal component analysis. *Theor. Appl. Climatol.*, **58**: 31-41
- Block, P. 2011. Tailoring seasonal climate forecasts for hydropower operations. *Hydrol. Earth Syst. Sci.*, **15**: 1355–1368, doi:10.5194/hess-15-1355-2011.
- , Rajagopalan B. 2007. Interannual Variability and Ensemble Forecast of Upper Blue Nile Basin Kiremt Season Precipitation. *J. Hydrometeorol.*, **8**, 3: 327–343.
- Buytaert, W., Celleri R., Willems P., De Bievre B., Wyseure G. 2006. Spatial and temporal rainfall variability in mountainous areas: A case study from the south Ecuadorian Andes. *J. Hydrology*, **329**: 413-421.
- Camberlin, P. 1996. Rainfall anomalies in the source region of the Nile and their connection with the Indian summer monsoon. *J. Climate*, **10**: 1380–1392
- Camberlin, P., Philippon N. 2002. The East African March–May Rainy Season. Associated Atmospheric Dynamics and Predictability over the 1968–97 Period. *J. Climate*, **15**: 1002–1019.
- Comrie, A.C., Glenn EC. 1998. Principal components-based regionalization of precipitation regimes across the southwest United States and north Mexico, with an application to monsoon variability. *Clim. Res.*, **10**: 201-215.

- Conway, D. 2000. The Climate and Hydrology of the Upper Blue Nile River. *Geogr. J.*, **166**: 49-62.
- Dinku, T., Asefa K., Hailemariam K., Grimes D. Connor S. 2011. Improving availability, access and use of climate information. *WMO Bulletin*, **60**, 2.
- Diro, G.T., Black E., Grimes D.I.F. 2008. Seasonal forecasting of Ethiopian Spring rains. *Meteorol. Appl.*, **15**: 73–83.
- , Grimes D.I.F, Black E. 2011. Teleconnections between Ethiopian summer rainfall and sea surface temperature. Part I. Seasonal forecasting. *Clim. Dyn.*, **37**: 103-119.
- Easterling, D.R. 1991. Climatological patterns of thunderstorm activity in South-Eastern USA. *Int. J. Climatol.*, **11**: 213-221.
- Ellouze, M., Azri C., Abida H. 2009. Spatial variability of monthly and annual rainfall data over South Tunisia. *Atmos. Res.*, **93**: 832-839.
- Everitt, B.S. 1979. Unresolved problems in cluster analysis. *Biometrics*, **35**, 1: 169-181.
- Flohn H. 1987. Rainfall teleconnection in the northern and northeastern Africa. *Theor. Appl. Climatol.*, **38**: 191-197.
- Funk, C., Senay G., Asfaw A., Verdirn J., Rowland J., Korecha D., Eilerts G., Michaelsen J. 2005. Recent drought tendencies in Ethiopian and equatorial subtropical Eastern Africa. Vulnerability to Food Insecurity. Factor Identification and Characterization *FEWS/NET Report*, Number 01/2005.
- Gissila, T., Black E., Grimes D.I.F., Slingo J.M. 2004. Seasonal forecasting of the Ethiopian summer rains. *Int. J. Climatol.*, **24**: 1345–1358.

- Gong, X., Richman M.B. 1995. On the application of cluster analysis to growing season precipitation data in North America east of the Rockies. *J. Climate Appl. Meteor.*, **8**: 897-931.
- Habtemichael, A., Pedgley D.E. 1966. Synoptic case-study of spring rains in Eritrea. *Arch. Met. Geoph. Biokl.*, **23**: 285–296.
- Indeje, M., Semazzi F.H.M., Lian X. 2001. Mechanistic model simulations of the East African climate using NCAR regional climate model. Influence of large-scale orography on the Turkana Low-Level Jet. *J. Climate*, **14**: 2710-2724.
- Jackson, I.J., Weinand H. 1995. Classification of tropical rainfall stations: A comparison of clustering techniques. *Int. J. Climatol.*, **15**: 985-994.
- Jobson, J. D. 1992. Applied Multivariate Data Analysis, Vol. II: Categorical and Multivariate Methods. Springer-Verlag, 731 pp.
- Jury, M. R. 2011. Meteorological scenario of Ethiopian floods in 2006–2007. *Theor. Appl. Climatol.*, **104**: 209–219
- Kassahun, B. 1986. Local weather systems over the Red Sea area. Local Weather Systems Prediction for the Red Sea Countries. *Trop. Meteor. Res. Prog. Rep. Series*, **29**, WMO: 1–18.
- , 1987. Weather systems over Ethiopia. *Proc. First Tech. Conf. on Meteorological Research in Eastern and Southern Africa*, Nairobi, Kenya, UCAR, 53–57.
- King'uyu, S.M., Ogallo L.J., Anyamba E.K. 2000. Recent trends of minimum and maximum surface temperatures over Eastern Africa. *J. Climate*, **13**: 2876-2886.
- Kinuthia, J.H., Asnani G.C. 1982. A Newly Found Jet in North Kenya (Turkana Channel). *Mon. Wea. Rev.*, **110**, 11: 1722-1728.

- Korecha, D., Barnston A. 2007. Predictability of June-September rainfall in Ethiopia. *Mon. Wea. Rev.*, **135**, 2: 628-650.
- Littmann, T. 2000. An empirical classification of weather types in the Mediterranean Basin and their interaction with rainfall. *Theor. Appl. Climatol.*, **66**, 161-171.
- Mazzoleni, S., Porto A.L., Blasi C. 1992. Multivariate analysis of climatic patterns of the Mediterranean basin. *Vegetation*, **98**: 1-12.
- Morrison, D.F. 2005. *Multivariate Statistical Methods*, Fourth Ed., Duxbury Advanced Series, Brooks/Cole Thomson Learning, Belmont, USA.
- NMSA 1996. Assessment of drought in Ethiopia. *Meteorological Research Report Series*. Vol.1, No.2, Addis Ababa. pp259.
- Ogallo, L.J. 1988. Relationships between seasonal rainfall in East Africa and the Southern Oscillation. *Int. J. Climatol.*, **8**: 31–43.
- , 1989. The spatial and temporal patterns of the East African seasonal rainfall derived from principal component analysis. *Int. J. Climatol.*, **9**: 145–167.
- Ramos, M. C. 2001. Divisive and hierarchical clustering techniques to analyze variability of rainfall distribution patterns in a Mediterranean region. *J. hydrol.* **57**: 123-138.
- Richman, M. B. 1986. Rotation of Principal Components. *J. climatol.*, **6**: 293-335.
- Riddle, E.E., Cook K.H. 2008. Abrupt rainfall transitions over the Greater Horn of Africa. Observations and regional model simulations. *J. Geophys. Res.*, **113** (D15109): 1-14.

- Romero, R., C. Ramis, and J.A. Guijarro, 1999: Daily rainfall patterns in the Spanish Mediterranean area. An objective classification. *Int. J. Climatol.*, **19**, 95-112.
- Romilly, T. G., Gebremichael, M. 2011. Evaluation of satellite rainfall estimates over Ethiopian river basins. *Hydrol. Earth Syst. Sci.*, **15**: 1505–1514, doi:10.5194/hess-15-1505-2011
- Segele, Z.T., Lamb P.J. 2005. Characterization and variability of Kiremt rainy season over Ethiopia. *Meteor. Atmos. Phys.*, **89**: 153–180.
- , Lamb P.J., Leslie L.M. 2009. Large-scale atmospheric circulation and global sea surface temperature associations with Horn of Africa June–September rainfall. *Int. J. Climatol.*, **29**: 1075–1100.
- Shanko, D., Camberlin P. 1998. The effect of the southwest Indian Ocean tropical cyclones on Ethiopian drought. *Int. J. Climatol.*, **18**: 1373–1378.
- Simmons, A., Uppala S., Dee D., Kobayashi S. 2006/07. ERA-Interim: New EMWF reanalysis products from 1989 onwards. *ECMWF Newsletter* no. **110**: 25-35.
- Soltani, S., Modarres R. 2006. Classification of Spatio-Temporal Pattern of Rainfall in Iran Using A Hierarchical and Divisive Cluster Analysis. *J. Spatial Hydrol.*, **6**, 2: 1-12.
- Tabias, G.Q., Salas J.D. 1985. A comparative analysis of techniques for spatial interpolation of precipitation. *Water Resour. Bull.*, **21**: 365-380.
- Tennant, W.J., Hewitson C.B., 2002. Intra-seasonal rainfall characteristics and their importance to the seasonal prediction problem. *Int. J. climatol.*, **22**: 1033-1048.
- Tucker, M.R., Pedgley D.E. 1977. Summer winds around the southern Red Sea. *Arch. Met. Geoph. Biokl., Ser. B*, **25**: 221-231.

- Umer, M., Lamb H.F., Bonnefille R., Le´zine A.M., Tiercelin J.J., Gibert E., Cazet J.P., Watrin J. 2007. Late Pleistocene and Holocene vegetation history of the Bale Mountains, Ethiopia. *Quaternary Science Reviews*, **26**: 2229–2246.
- Unal, Y., Kindap T., Karaca M. 2003. Redefining the climate zones of Turkey using cluster analysis. *Int. J. Climatol.*, **23**: 1045-1055.
- Viste, E., Sorteberg A., 2012. Moisture transport into the Ethiopian highlands. *Int. J. Climatol.*, Published online in Wiley Online Library, DOI: 10.1002/joc.3409
- Willmott, C.J. 1978. P-mode principal components analysis, grouping and precipitation regions in California. *Arch. Met. Geoph. Biokl., Ser. B*, **26**: 277-295.
- WMO 1986. Guidelines on quality control. *WMO/TD WCP-85*, 56 pp.
- Vizy, E.K., Cook K.H. 2003. Connections between the summer east African and Indian rainfall regimes. *J. Geophys. Res.*, **108** (D16), 4510, doi:10.1029/2003JD003452.

## Paper III

### **Predictability of June–September rainfall in Ethiopia**

Korecha, D. and Barnston, A. (2007)

The manuscript published online in *Monthly Weather Review*, **135**: 628–650.

# **Predictability of June–September rainfall in Ethiopia**

**Diriba Korecha<sup>1</sup>**

**Anthony G. Barnston<sup>2</sup>**

1 National Meteorological Agency, Addis Ababa, Ethiopia

2 International Research Institute for Climate and Society, Palisades, New York

In much of Ethiopia, similar to the Sahelian countries to its west, rainfall from June to September contributes the majority of the annual total, and is crucial to Ethiopia's water resource and agriculture operations. Drought-related disasters could be mitigated by warnings if skillful summer rainfall predictions were possible with sufficient lead time. This study examines the predictive potential for June–September rainfall in Ethiopia using mainly statistical approaches. The skill of a dynamical approach to predicting the El Niño–Southern Oscillation (ENSO), which impacts Ethiopian rainfall, is assessed. The study attempts to identify global and more regional processes affecting the large-scale summer climate patterns that govern rainfall anomalies. Multivariate statistical techniques are applied to diagnose and predict seasonal rainfall patterns using historical monthly mean global sea surface temperatures and other physically relevant predictor data. Monthly rainfall data come from a newly assembled dense network of stations from the National Meteorological Agency of Ethiopia. Results show that Ethiopia's June–September rainy season is governed primarily by ENSO, and secondarily reinforced by more local climate indicators near Africa and the

Atlantic and Indian Oceans. Rainfall anomaly patterns can be predicted with some skill within a short lead time of the summer season, based on emerging ENSO developments. The ENSO predictability barrier in the Northern Hemisphere spring poses a major challenge to providing seasonal rainfall forecasts two or more months in advance. Prospects for future breakthroughs in ENSO prediction are thus critical to future improvements to Ethiopia's summer rainfall prediction.

## **1 Introduction and background**

Ethiopia, located within 3.30°–15°N, 33°–48°E, has three climatological rainy seasons: June–September (called Kiremt), October–January (Bega), and February–May (Belg; Shanko and Camberlin 1998; Seleshi and Demarée 1995; Tsegay 1998, 2001; Gissila et al., 2004). Kiremt rains during June–September (JJAS) account for 50%–80% of annual rainfall totals over the regions having high agricultural productivity and major water reservoirs. Thus, the most severe droughts are usually related to a failure of the JJAS rainfall to meet Ethiopia's agricultural and water resources needs. This study is devoted to Ethiopia's JJAS rainfall climatology, interannual variability, and predictability.

Tropical rainfall varies from daily, interannual, to interdecadal and longer time scales. Following breakthroughs in weather forecasting in the 1950s and 1960s (see Cane 2000), as environmental monitoring capabilities improved, physical modeling of the interannual variability of sea surface temperature (SST) over the eastern tropical Pacific Ocean revealed predictability of the El Niño–Southern Oscillation (ENSO; Cane et al. 1986; Cane and Zebiak 1987; Zebiak and Cane 1987). ENSO predictability then led to potential predictability of seasonal climate over many tropical and some extratropical

regions. Studies have indicated that northern summer rainfall in the Sahel responds partly to ENSO fluctuations (Nicholson and Kim 1997; Nicholson and Selato 2000; Hastenrath 1995; Rowell 2001, among many others). On decadal scales, research has provided evidence and possible explanation for Sahelian drought throughout most of the last quarter of the 1900s (e.g., Hulme 2001). Techniques used at the Met Office, among other global prediction centers, attempt to capture both interannual and interdecadal components of SST forcing. Research devoted to the twentieth-century Sahel drought focused heavily on the impact of regional and global SST anomalies on interdecadal time scales (Folland et al. 1991; Rowell et al. 1995; Ward 1998; Giannini et al. 2003; Janicot et al. 1996; Janicot et al. 2001; Zeng 2003; Paeth and Friederichs 2004). Some studies have addressed the additional influence of land surface forcing (Zeng et al. 1999; Wang et al. 2004).

Sahel droughts have also been studied statistically relative to more regional oceanic and atmospheric factors. Raicich et al. (2003) demonstrated a connection between Indian monsoon and Sahel rainfall regimes and sea level pressure in the Mediterranean area, and Rowell (2003) showed the influence of Mediterranean SSTs on seasonal Sahel rainfall. Osman and Shamseldin (2002) showed that the driest years in central and southern Sudan occur during the warm phase of ENSO and Indian Ocean SST, and proposed empirical rainfall prediction models. Lamb (1977) suggested an extension of Sahel drought toward Ethiopia on the basis of synoptic circulations. In addition, Giannini et al. (2003) attributed the Sahel's recent drying trend to warmer than-average low-latitude waters around Africa, which, by forcing deep convection over ocean, decrease monsoon-related continental convergence and rainfall from Senegal to Ethiopia. Such studies that include Ethiopia could be confirmed using gauge rainfalls from a newly assembled dense station network—data that could be included into the Sahel rainfall indices.

Seasonal rainfall patterns over tropical Africa, like the Indian subcontinent, are modulated partly by monsoonal flows (Bhatt 1989; Camberlin 1997). Ethiopia's rainfall climatology is determined mainly by seasonal changes in large-scale circulation, part of which involves the seasonal north–south movement of the intertropical convergence zone (ITCZ); this resembles what is generally thought to occur in the traditional Sahel region from Sudan to Senegal (Nicholson 1989). The complex orography across Ethiopia shapes the JJAS rainfall patterns spatially and temporally within the season. Year-to-year variability of Ethiopia's JJAS rainfall patterns has been described in terms of onset, cessation, dry spell occurrences, and growing season duration (Segele and Lamb 2005). Kiremt rainfall advances gradually northward across the western half of the country from March to mid-June, progressing more rapidly across the eastern half from mid-June to mid-July. (From March to May, this rainfall is actually considered part of the Belg rainfall regime.) The mean southwestward retreat of rainfall occurs from early September to November.

The mountain ranges are oriented southwest–northeast, with the Rift Valley bisecting Ethiopia. During JJAS, there are southwest monsoon low-level winds over the Arabian Sea, strong cross-equatorial flow along eastern flank of Africa, and southeasterly trade winds south of the equator (Gissila et al. 2004). With these low-level flows, summer storm development is facilitated by the upper-level tropical easterly jet (TEJ), serving also as westward-steering currents.

JJAS rainfall in the region around Ethiopia is controlled by several climatological features in the lower and upper troposphere (e.g., Hastenrath 1991). These include the following: 1) seasonal northward advance of the

ITCZ, persisting over Ethiopia; 2) formation of heat lows over the Sahara and Arabian landmasses; 3) establishment of subtropical high pressure over the Azores, St. Helena, and Mascarene; 4) southerly/southwesterly cross-equatorial moisture flow from the southern Indian Ocean, central tropical Africa, and the equatorial Atlantic; 5) upper-level TEJ flowing over Ethiopia; and 6) low-level jet (Somali jet). Synoptic systems arising from these seasonal circulations have been discussed [Kassahun 1987; Tadesse 1994; (National Meteorological Services Agency) NMSA 1996; Segele and Lamb 2005]. This study will not focus on these local features, per se. In JJAS, convective activity typically develops over the Ethiopian highlands, while southern and southeastern Ethiopia receives little rain. Using a multidecadal history of rainfall over a dense station network (described below), the spatial distribution of mean total JJAS rainfall (Fig. 1, top) shows the greatest rainfall over the highlands of western/west-central Ethiopia, the northeast and southeast lowlands being relatively dry. Southeastern Ethiopia, closer to East Africa, has rainy seasons during March–May and October–November. The distribution of mean number of days having measurable ( $\geq 0.1$  mm) rainfall (not shown), follows a similar pattern<sup>1</sup>, with western and central Ethiopia receiving measurable rainfall 70%–90% of the days. Farther to the northeast rainfall occurs for only 10–30 days, despite JJAS being the main rainy season. Southern/southeastern Ethiopia receives rains only for a few days in September with the southward retreat of the ITCZ. The bottom of Fig. 1 shows the percentage contribution of JJAS rainfall to the annual total rainfall. Figures 2 and 3 show, respectively, the locations of selected stations, and the seasonal march of mean monthly rainfall at four stations with varying longitude within the central ( $8^{\circ}$ – $10^{\circ}$ N) latitude band. This study focuses on the central, western, and northern parts of the country that have their main rainy season in JJAS (although stations in the southern/southeastern portion of this focus area may have a mildly bimodal seasonal distribution).

---

<sup>1</sup> Note that droughts and floods are sometimes declared even when total rainfall or the number of days receiving rain is not very anomalous. This can occur when

seasonal rainfall is grossly unevenly distributed over the season, with long dry or wet spells that may straddle the monthly boundaries.

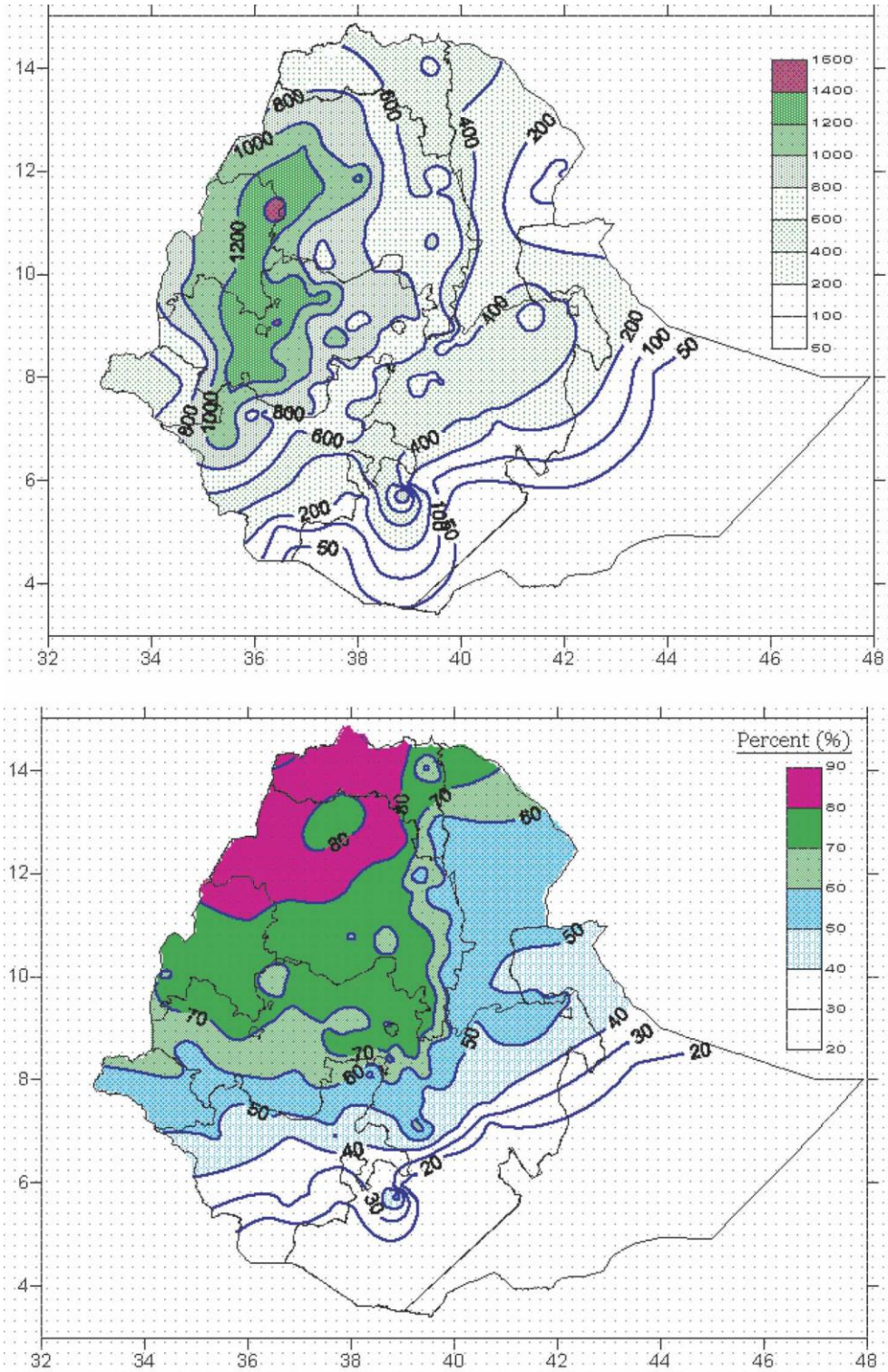


FIG. 1. (top) Total JJAS rainfall climatology (mm) over Ethiopia, 1971–2000 (bottom) Percentage of 1971–2000 mean total annual rainfall contributed by JJAS rainfall.

Ethiopian rainfall in JJAS differs vastly from year to year in timing and total amount. The phase of ENSO has been identified as impacting summer rainfall (Nicholls 1993; Tsegay 1998, 2001; Gissila et al. 2004; Segele and Lamb 2005; Seleshi and Demarée 1995; Bekele 1997), with the same direction of impact as that of the Sahel. The large-scale atmospheric dynamics relevant to Ethiopia, however, differ in some ways from those relevant to regions farther west in the Sahel (Bhatt 1989; Cook 1997). Recently, Gissila et al. (2004) developed an empirical forecast model for Ethiopian summer rainfall using regression with Indian and Pacific SSTs in March, April, and May as potential predictors. Our study aims to quantify the statistical relations between ENSO, and other oceanic and atmospheric phenomena, and JJAS rainfall, a practical objective being to develop models that skillfully anticipate rainfall anomalies prior to rainy season onset, allowing for societal mitigation measures.

We utilize more stations than were available for the above studies, and apply several techniques to quantify rainfall behavior with respect to ENSO and other governing large-scale climate patterns, both averaged over all of Ethiopia and distributed geographically within the country. We assess prospects for implementing statistical techniques for reliable, sustainable climate forecasts, including a forecast for the state of the ENSO by a dynamical model as a potential rainfall predictor. Our datasets and methodologies are described in section 2. ENSO cycles, their implications for predictability of JJAS rainy season, and the predictability of ENSO itself during JJAS, are presented in section 3. Results of diagnostic and predictive rainfall modeling are provided in section 4. Discussion and conclusions are given in section 5.

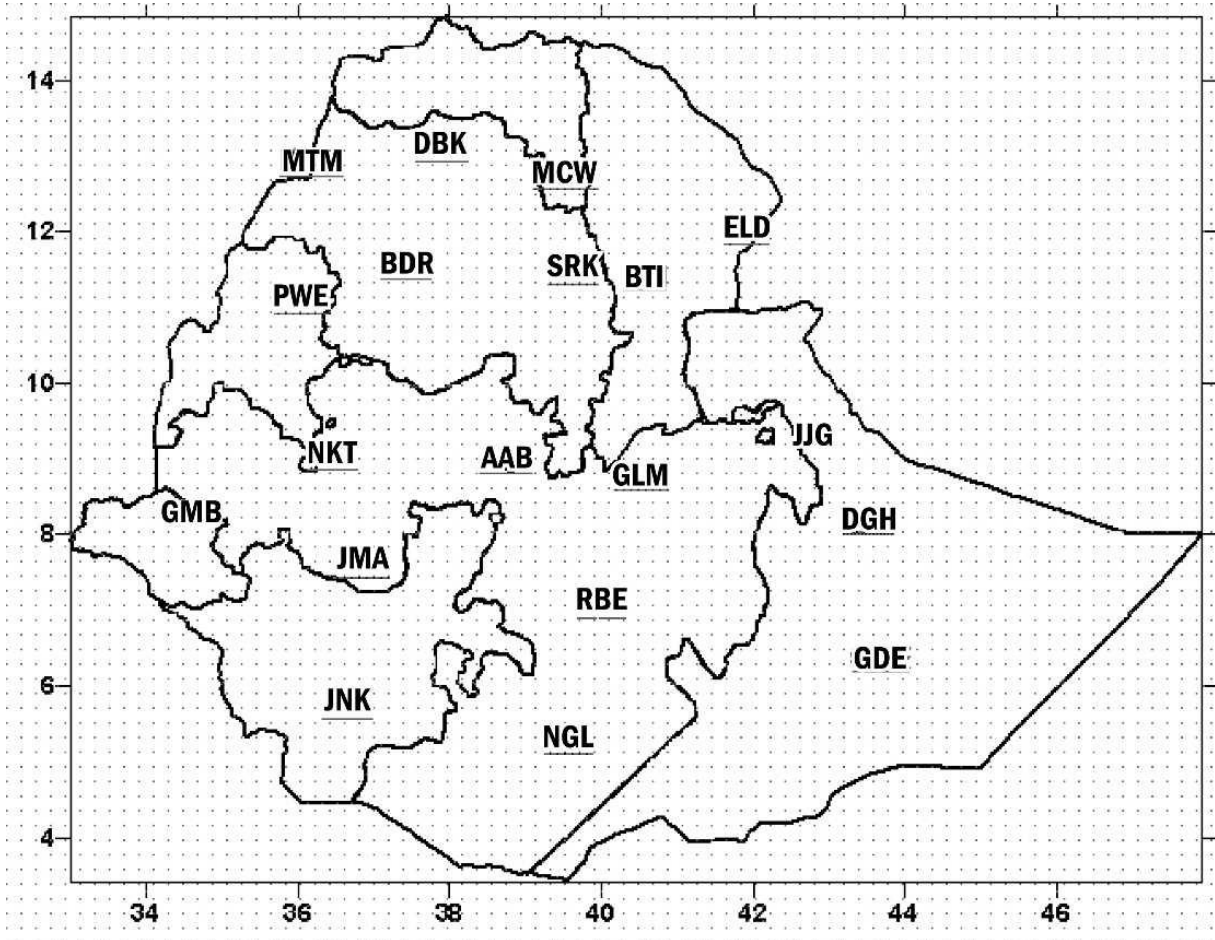


FIG. 2. Locations of selected climatological stations.

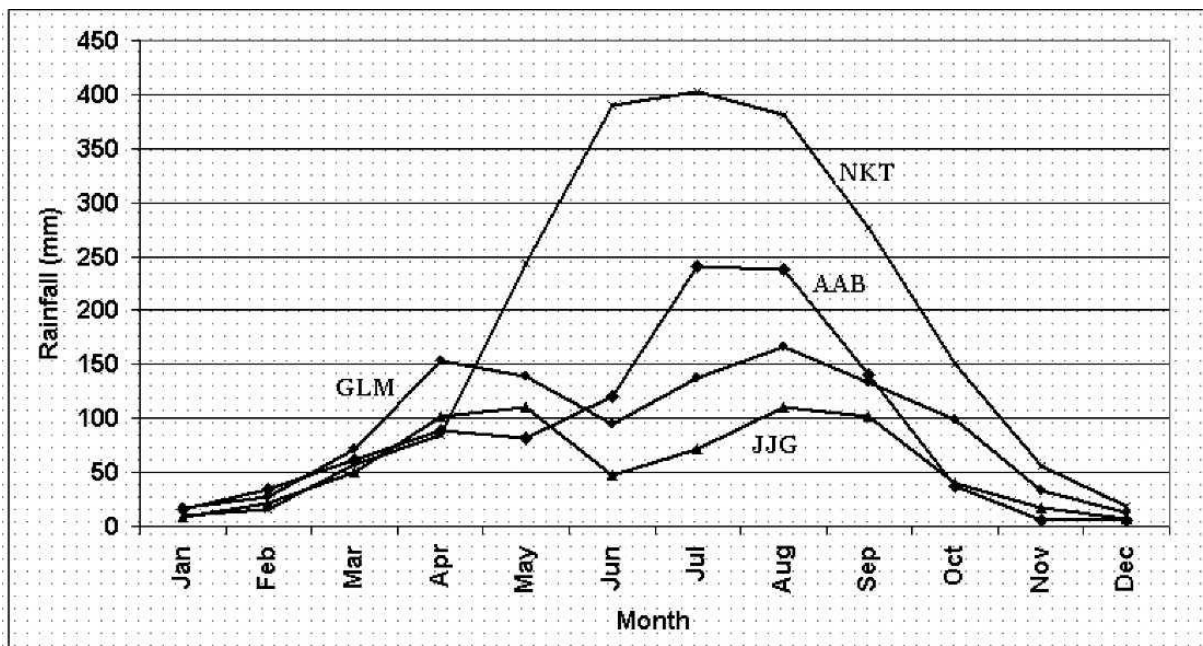


FIG. 3. Time series of long-term mean monthly rainfall (mm), 1970–2000, for selected stations within the central ( $8^{\circ}$ – $10^{\circ}$ N) latitude band. Maximum rainfall occurs in JJAS season, but decreases eastward with bimodal seasonal rainfall patterns more likely over eastern sectors.

## 2 Data and methodology

The rainfall data used for many analyses in this study, obtained from the Ethiopian NMSA, are monthly totals for June–September. Two hundred meteorological stations (Fig. 4a) have periods of records varying from 15 to >50 yr. Nearly half of the full array of stations has records of 30 yr or more since 1961 (Fig. 5). Data from the 1960s are omitted here, due to widespread gaps. A total of 78 stations (Fig. 4b) are used for many of our analyses, usually covering the period 1970–2004<sup>2</sup>. However, only 55 stations, denoted by large circles in Fig. 4b, are used for our all-Ethiopian JJAS rainfall analyses, where stations located in the south and southeast lowlands that are climatologically dry during JJAS are excluded. From 1970 onward, the proportion of missing data is low, with a small number of stations having at most 10% missing data (Fig. 6). Missing months were estimated by interpolation from the relative anomalies of stations within a threshold distance away (typically including 1–4 stations). To assess the maximum sensitivity to including these estimated rainfalls, we compared the time series of the standardized all-Ethiopian average JJAS rainfalls resulting from the “cleaned” 55 stations to that using only the 36 stations having full original records. The two versions of the all-Ethiopian rainfall data correlate 0.91, and the largest absolute differences in standardized rainfalls are near 0.7. This could have a visible, although not major, impact on the results. Omitting 35% of the stations needing any treatment is thought to represent an upper limit of the effect of including stations requiring filling of missing data.

We use global SST from the National Oceanic and Atmospheric Administration/National Climatic Data Center (NOAA/NCDC) Extended Reconstructed Sea Surface Temperature version 2 (ERSSTv2) historical dataset (Smith and Reynolds 2004), with 2° x 2° resolution for 1970–2004. From these SSTs indices are derived, including the Niño-3.4 ENSO index (SSTs averaged over 5°N–5°S, 120°–170°W). The Niño-3.4 index is used to represent the ENSO condition because of its demonstrated importance for ENSO teleconnections (Trenberth and Hoar 1996; Barnston et al. 1997). Retrospective forecasts for Niño-3.4 SST generated by the Lamont-Doherty Earth Observatory’s dynamical ENSO forecast model (current version LDEO5; Chen et al. 2004) were kindly run by D. Chen for the period 1970–2005.

---

<sup>2</sup>A few of the analyses use data spanning only through 2000 or 2002, owing to practical considerations, and this is always noted when it is the case.

In examining diagnostic and predictive aspects of summer Ethiopia rainfall, several linear statistical techniques are employed. Standardized anomalies of the 4-month total rainfalls are used for each station for many analyses, using 1971–2000 as the base period. Standardization places data in all locations in a similar frame of reference for assessing year-to-year rainfall anomalies. The drier stations in the Rift Valley, and eastern or southern Ethiopia, tend to have particularly positively skewed JJAS rainfall distributions, and reduced signal-to-noise ratios due to the few governing non-dry years. Because these south/southeast lowland stations are in seasonally dry zones, they are omitted from the 55-station subset used for the all-Ethiopian rainfall index (Fig. 4b).

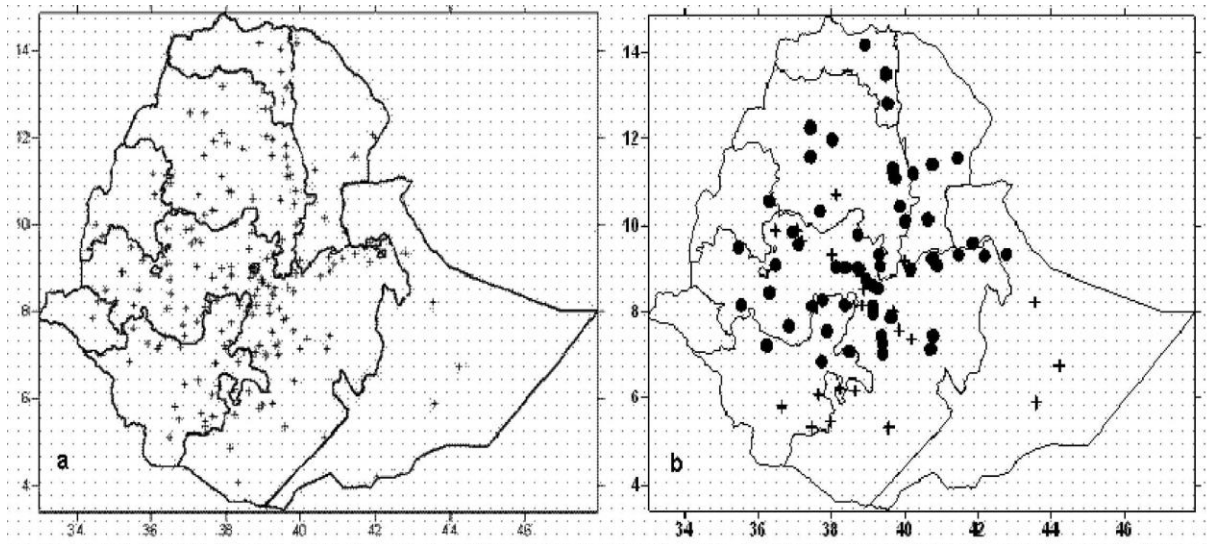


FIG. 4. (left) Locations of the 200 climatological stations over Ethiopia. (right) Same as in (left) but for the 78 stations used in many of the analyses of JJAS rainfall in Ethiopia, 55 of which (larger filled circles) are used for the analyses of all-Ethiopian rainfall.

Simple linear correlation, multiple linear regression, and robust regression techniques<sup>3</sup> are used to develop predictive models for summer Ethiopian rainfall, revealing teleconnections between SST and rainfall. Strategies to predict the ENSO-related summer Niño-3.4 SST anomaly are used as one approach to forecasting consequent Ethiopian rainfall.

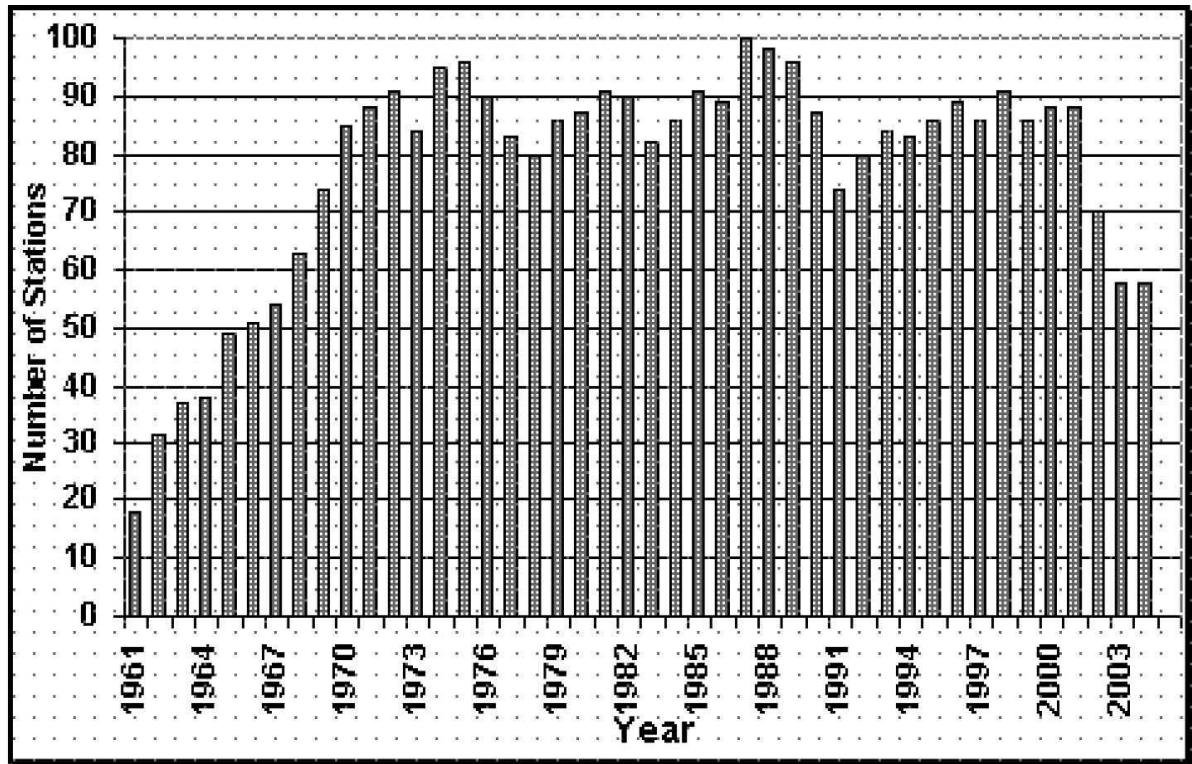


FIG. 5. The number of meteorological stations having non-missing rainfall data during JJAS as a function of year used for analyses of JJAS rainfall anomalies during 1961–2004.

---

<sup>3</sup>Robust regression enables assessment of the sensitivity of results to outlier cases, if any are present.

For prediction of JJAS seasonal rainfall, canonical correlation analysis (CCA) is used, as described in previous studies (e.g., Hotelling 1936; Glahn 1968; Barnett and Preisendorfer 1987; Barnston and Smith 1996; Thiaw et al. 1999). CCA is a multivariate regression that relates patterns in predictor fields (e.g., SST) to patterns in a predictand field (e.g., rainfall). Cross validation (Michaelsen 1987) and retroactive designs are used to minimize inflation of the skill estimates. The SST–rainfall relationships are examined both for

concurrent data and when SST precedes the summer rainfall, as in actual forecasting.

### **3 ENSO and the June–September rainy season over Ethiopia**

The impact of the ENSO variability on global climate has been well documented (Ropelewski and Halpert 1987; Mason and Goddard 2001; Goddard and Dilley 2005, among many others). The ENSO state modulates the rainy seasons in some regions, particularly in the Tropics (Hastenrath 1995). El Niño is associated with drought and forest fires in parts of Australia, Indonesia, Southeast Asia, and southern Africa (Goldammer 1999; Khandekar et al. 2000; Jury 2002). Chances for flooding are enhanced with El Niño during the short rainy season of October–December in East Africa (Ogallo 1988, 1989; Indeje et al. 2000; Philippon et al. 2002).

During JJAS, suppressed rainfall has been observed to accompany El Niño over much of Ethiopia, often with economic catastrophe. Although the importance of ENSO to Ethiopian rainfall is being accepted and incorporated in the NMSA's operational policy<sup>4</sup> more now than previously, it continues to be somewhat underweighted despite widespread documentation of its importance (NMSA 1996; Camberlin 1997; Bekele 1997; Tsegay 1998; Gissila et al. 2004; Segele and Lamb 2005). As shown in Fig. 7 (for 1970 onward), lower tercile all-Ethiopian JJAS seasonal rainfall occurred in 1965, 1972, 1979, 1982, 1984, 1987, 1990, 1991, 1995, 1997, and 2002. More than half of these summers coincided with El Niño events; none occurred during La Niña. Upper tercile rainfall conditions occurred in 1961, 1964, 1970, 1973, 1974, 1975, 1977, 1978, 1981, 1988, 1994, 1996, 1998, 1999, and 2003; more than half of these matched La Niña events, while only one (1994) occurred with El Niño. Below we will assess this connection more

quantitatively, and discuss the potential for issuing useful seasonal rainfall predictions before the onset of summer season rains.

The effect of ENSO on rainfall is seen in composite analyses for selected individual stations by month. JJAS monthly rainfalls are averaged for El Niño, La Niña, or near-neutral conditions, using the classification system of the NOAA/Climate Prediction Center (CPC)<sup>5</sup>. Here, all months of any year are assigned the ENSO phase existing during JJAS of that year, so that impacts of ENSO events occurring during the Belg and Bega seasons are not directly represented. Mean monthly rainfalls seem to be enhanced during La Niña years in regions where JJAS is the major rainy season, due both to greater duration of the rainy season (Segele and Lamb 2005), and increased rainfalls during individual months of the rainy season. Examples of stations from different parts of Ethiopia having a clear ENSO influence are shown in Fig. 8.

Figure 9 illustrates the geographical distribution of the correlation between the SST in the Niño-3.4 index region and Ethiopian JJAS rainfall at the 78 stations, based on 1970–2004, keying SST to individual months prior to summer (Figs. 9a–c) and SST during JAS (Fig. 9d). The association of summer rainfall with ENSO in early pre-summer months (January–April) is weak, and increases as the time of the ENSO state approaches the beginning of the rainfall season. Statistically significant ( $\geq 0.34$ ) negative correlations are found between JJAS rainfall totals and Niño-3.4 SST occurring nearly simultaneously (in JAS) mainly in the northern half of the country but also in the southern highlands and southwest Ethiopia (Fig. 9d). In the climatologically dry southeastern lowlands, associations with ENSO are weak. The moderate negative simultaneous correlations (-0.4 to -0.6 at some locations) imply that rainfall forecasts would have useful skill levels if the summer Niño-3.4 SST could be predicted beforehand. Correlations between

JJAS rainfall and Niño-3.4 SSTs of pre-season months may be of some use only for May, where some correlations are stronger than -0.4. The lack of a stronger relationship between the May ENSO state and rainfall is not surprising, as the ENSO condition may change in either direction between April and June (Tziperman et al. 1998). For example, high Niño-3.4 SST in May could be due to an El Niño that had matured earlier and would likely dissipate before July, or to a newly emerging El Niño that was absent in February and March. Predicting ENSO is known to be difficult during the northern spring. Later we will discuss an indicator of summer ENSO based on the change of the May SST anomaly from that of a few months earlier.

---

<sup>4</sup>Climate prediction in Ethiopia started in 1987 as an experimental innovation (NMSA 1996) after Cane and Zebiak (1987) introduced the first ENSO prediction model. This beginning was a result of research undertaken at NMSA in Ethiopia (Degefu 1987; NMSA 1996). The widespread Ethiopian famines in 1972/73, 1982/83 and 1984/85, confirmed to be drought related, could have been greatly diminished using early warning systems based on probabilistic seasonal rainfall predictions. In the early stages of seasonal prediction, regional synoptic patterns were emphasized (Kassahun 1987; Tadesse 1994). However, the coinciding of drought years with El Niño attracted attention to ENSO as a vital predictor, as anticipating the ENSO state prior to the summer could sharpen the rainfall predictions. In the late 1980s and early 1990s, NMSA added new tools to its initially synoptically based seasonal rainfall predictions such as analogs and ENSO teleconnections, and achieved favorable results in anticipating some drought and flood catastrophes. In summer of 1995 the analog tool was augmented to include ENSO, Atlantic and Indian Ocean SSTs, and large-scale regional circulation patterns. The two to three best analog years were used to suggest the tercile-based seasonal rainfall probabilities as well as the character of the intraseasonal variability, both applied to individual Ethiopian regions.

<sup>5</sup>NOAA defines a nonneutral ENSO state as a departure from normal of the SST in the Niño-3.4 region of magnitude 0.5°C or more, lasting for at least five running three-month periods.

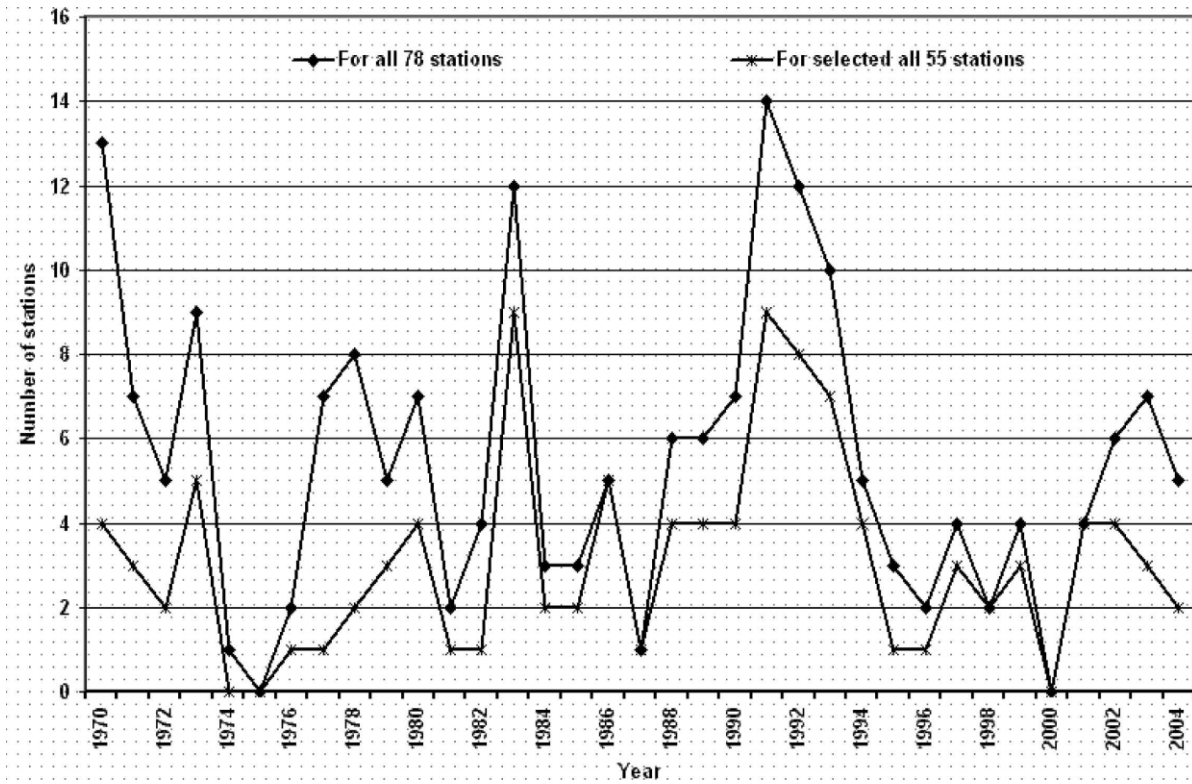


FIG. 6. Number of stations having missing monthly data during JJAS (1970–2004), for the set of 78 stations (upper curve) and the set of 55 stations.

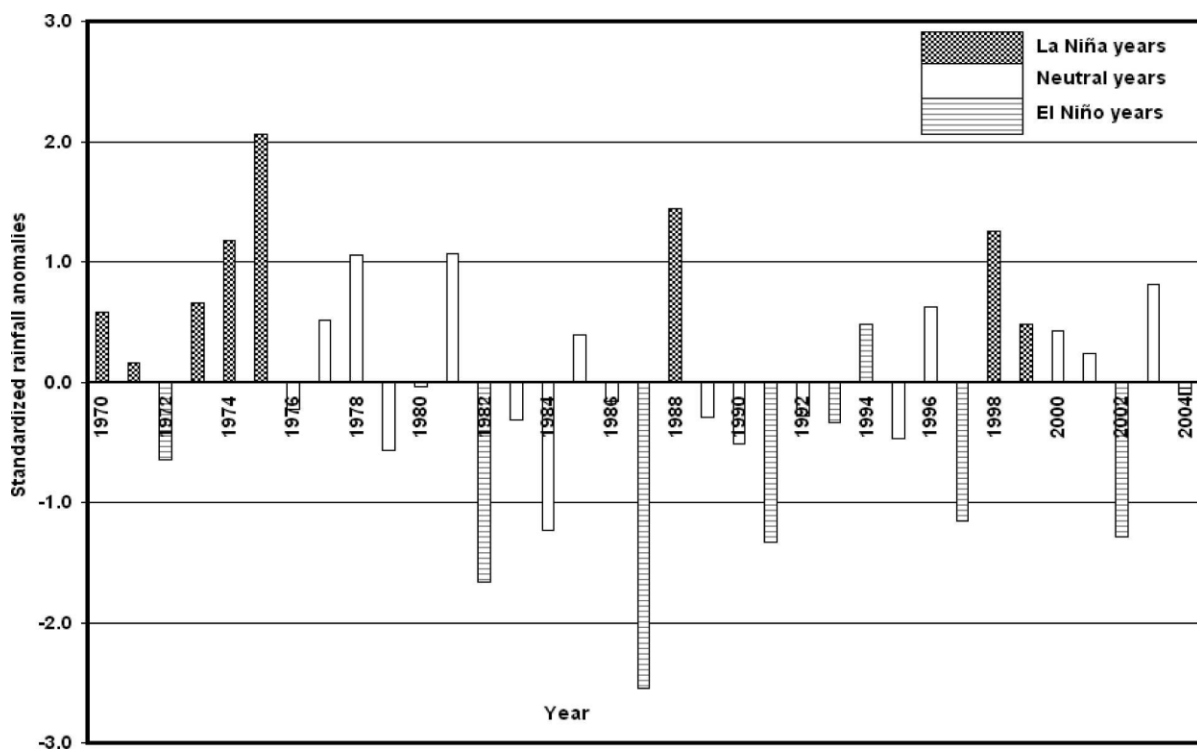


FIG. 7. Standardized JJAS rainfall anomalies of all-Ethiopian rainfalls for the 1970–2004 period. Years having El Niño, La Niña, and neutral conditions during JJAS, based on the NOAA/CPC ENSO classification, are denoted by the patterns inside the bars.

A time series of the all-Ethiopian JJAS rainfall average is derived for 1970–2004, based on the abovementioned 55 stations (Fig. 4b). The time series of the average of the seasonal rainfall totals, are standardized by 1971–2000 rainfall statistics, is shown in Fig. 10. Overall deficient (abundant) rainfall tends to occur during El Niño (La Niña) summers, the four strongest for JJAS being 1972, 1982, 1987, and 1997 (1973, 1975, 1988, and 1999). The correlation with Niño-3.4 SST over 35 yr (1970–2004) is  $-0.76^6$ .

Interestingly, although 1997 marked the strongest El Niño during 1970–2004, the JJAS all-Ethiopian rainfall was only the sixth lowest among the 35 yr. This is explained partly by the modulating roles of other tropical ocean basins in governing Ethiopia's JJAS rainfall. In 1997 the Indian Ocean's delayed warming response to the abnormally warm tropical Pacific (e.g., Goddard et al. 2001) appeared earlier than normal during late northern summer/fall, due both to the seasonally early onset of Pacific warming (April 1997) and the magnitude of that warmth. Thus, in September 1997, with a noticeably warmed western Indian Ocean SST, a north-ward meridional extension of the ITCZ induced widespread rains over Ethiopia. (During most El Niño northern summers, the Pacific, but not yet the Indian Ocean has warmed.) In other severe summer droughts, such as the ENSO-neutral 1984, anomalously warm SST was present in the eastern equatorial Atlantic, with an attendant southward retreat of ITCZ and similar displacement of the monsoon trough (Lamb 1978; Ward 1998; Segele and Lamb 2005).

Furthermore, the upper-tropospheric TEJ (Camberlin 1997) supports Ethiopian rainfall in JJAS (Segele and Lamb 2005). A strong TEJ, which is consistent with above-average SSTs in the northwestern tropical Pacific (and thus, indirectly, with La Niña conditions), was observed in summer 1996, as opposed to a poor TEJ in the dry year of 1984 despite a cool/neutral ENSO state. A comparable positive association between TEJ strength/latitude and Sahel monsoon rainfall was identified by Hastenrath (2000). TEJ and other atmospheric systems may be partly associated with the ENSO state again implying the importance of skillfully predicting the JJAS ENSO condition. How well can the summer ENSO condition be predicted upon completion of May, just in time to anticipate summer rainfall?

<sup>6</sup> It is worth noting that when the rainfall index is computed standardizing at the station level before doing so again for the 55-station average, this correlation is 0.77.

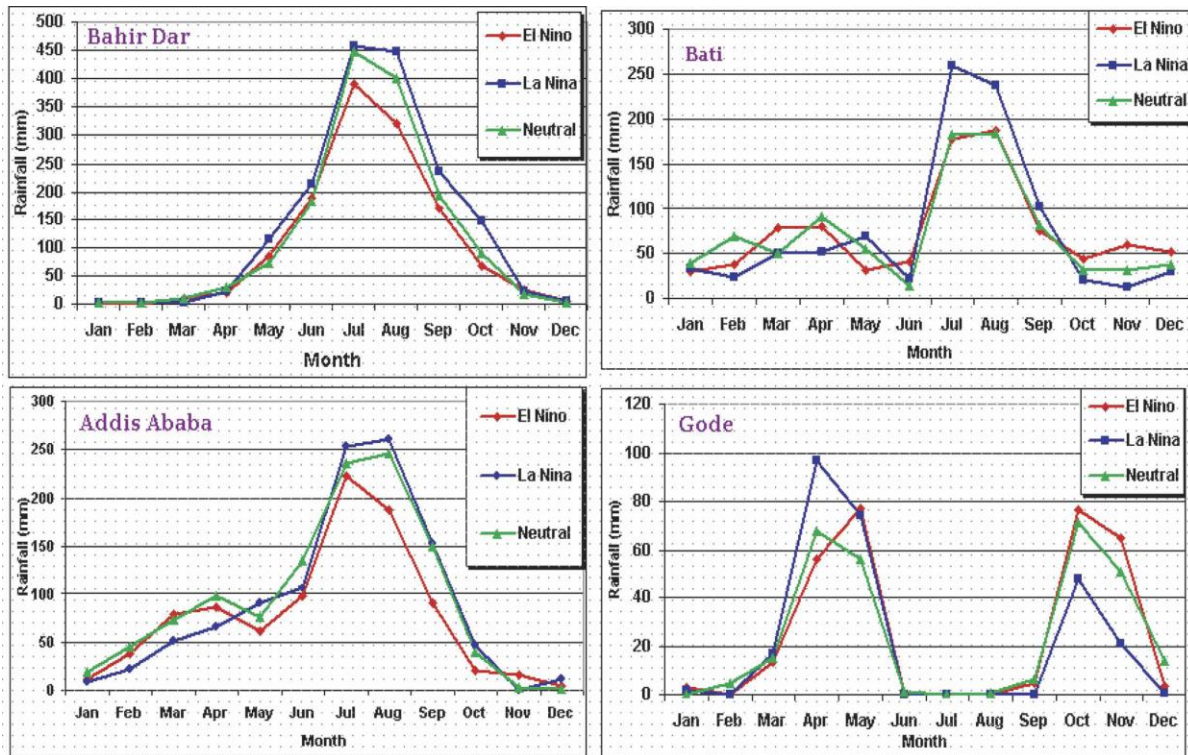


FIG. 8. Seasonal march of mean monthly rainfall amount (mm) composited for years whose JJAS season is classified as El Niño, La Niña, or neutral, for four stations located in the northwest, northeast, central, and southeast portions of Ethiopia, respectively: Bahir Dar (labeled BDR in Fig. 2; northwest), Addis Ababa (AAB; central), Bati (BTI; northeast), and Gode (GDE southeast; influence in both MAM and OND seasons), based on 1970–2004 data.

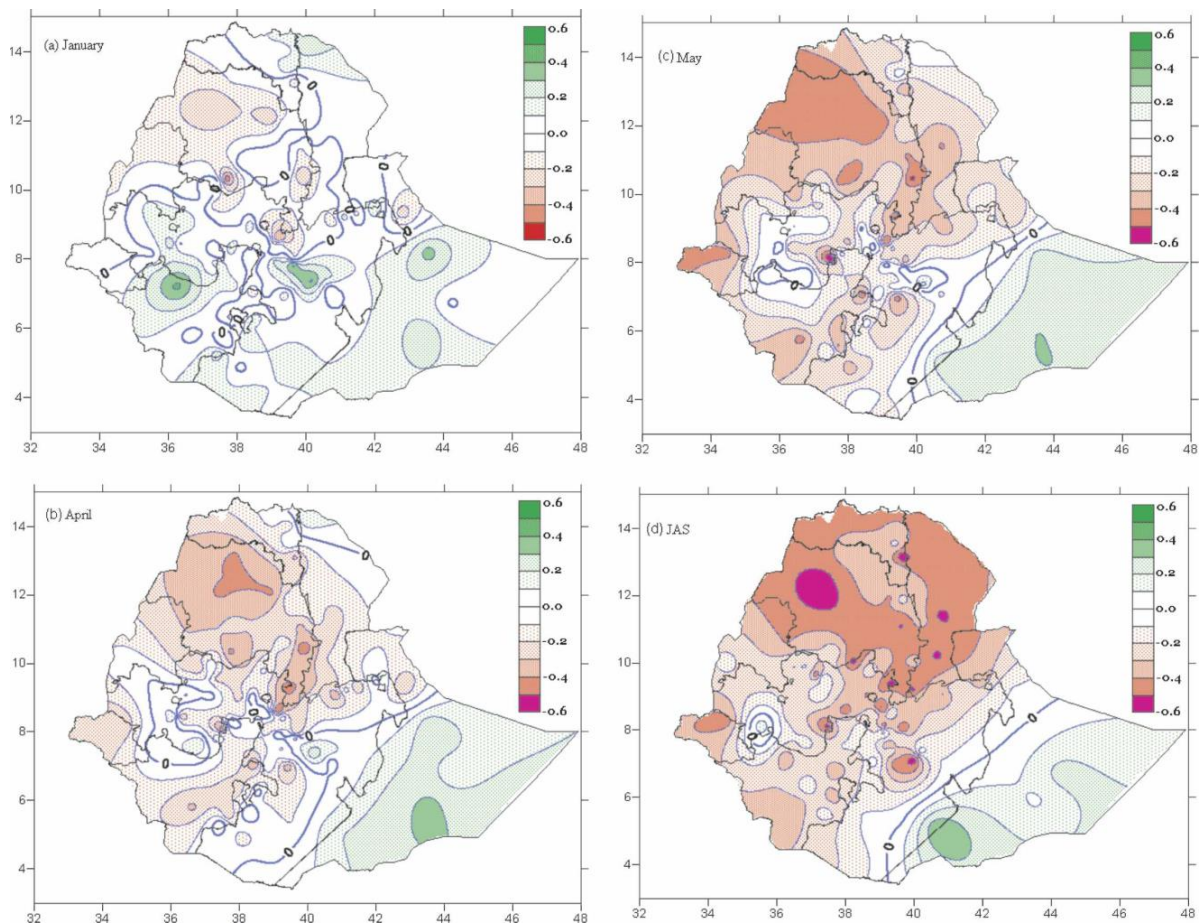


FIG. 9. Spatial distribution of correlation between JJAS rainfall for 78 stations in Ethiopia and Niño-3.4 SST in (a) January, (b) April, (c) May, and (d) JAS. Computed for 1970–2004, values of 0.34 or greater in magnitude are statistically significant at the 95% confidence level.

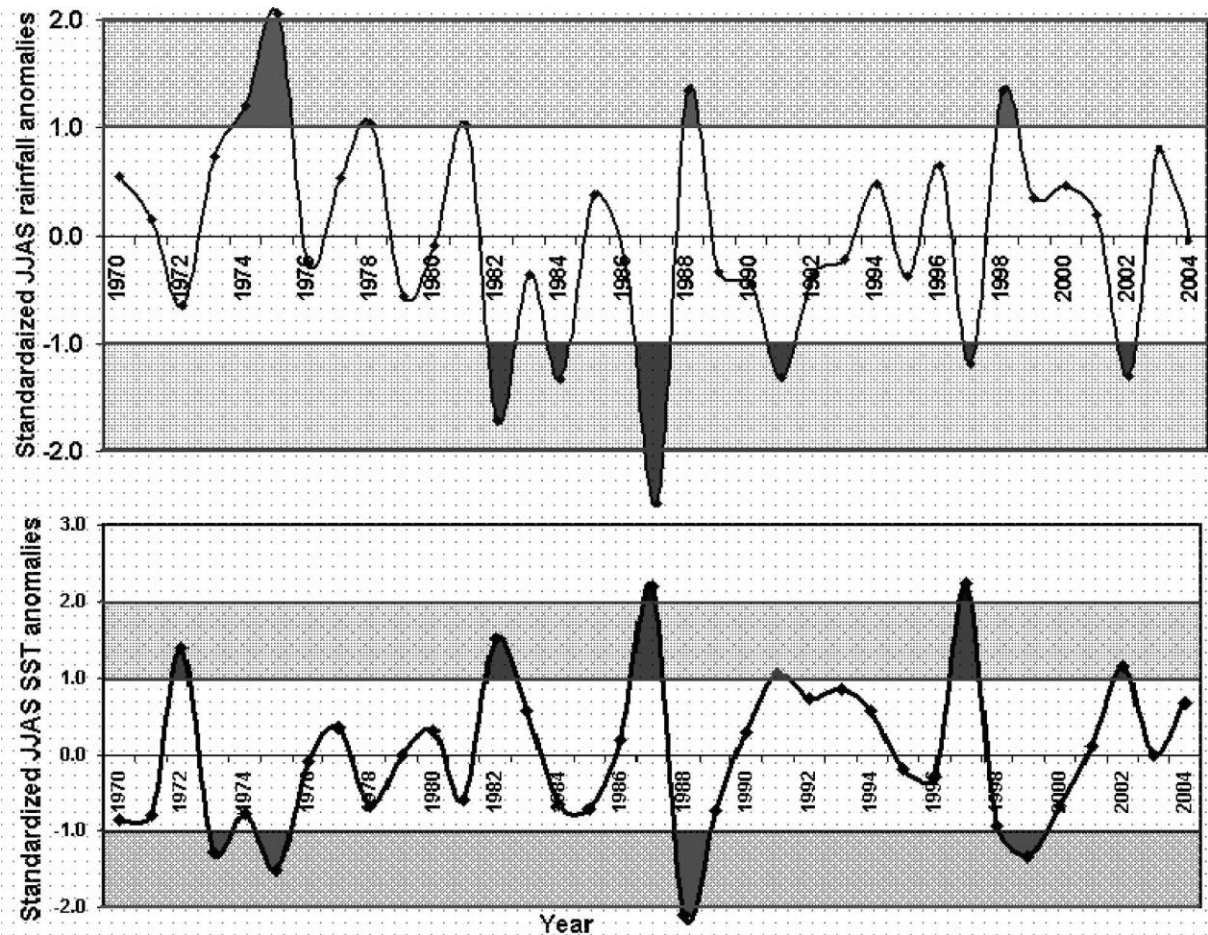


FIG. 10. Standardized JJAS rainfall anomalies of (top) all-Ethiopian rainfalls and (bottom) those of Niño-3.4 SSTs for 1970–2004. Standardization based on 1971–2000 statistics. Correlation between the two is  $\geq 0.76$ .

The strengths of linear relationship between all-Ethiopian JJAS rainfalls and the Niño-3.4 SST index for individual months from January to September, and for JJA and JAS SST, are shown in Table 1 for 1970–2004. Correlations are near  $-0.75$  during the months of the summer rainy season, stronger than correlations presented in Fig. 9d for any individual station, due to the filtering effects of spatial aggregation with respect to the random variability present in single location rainfalls (Gong et al. 2003). Such noise filtering better isolates the ENSO signal. The correlation is moderate ( $-0.59$ ) for the May Niño-3.4 SST, suggestive of some predictability based solely on the May ENSO state. A categorical version of the JJAS simultaneous relationship between ENSO

and rainfall is shown by a contingency table (Table 2). A moderately strong degree of categorical association between the ENSO and rainfall category is clear, with impacts for both El Niño and La Niña. A chi-square test yields >99% statistical significance.

TABLE 1. Correlation, based on 1970–2004, between all-Ethiopian JJAS rainfall and Niño-3.4 SST during monthly or three-month periods prior to and concurrent with the rainfall.

Jan	Feb	Mar	Apr	May	Jun	Jul	JJA	Aug	JAS	Sep
-0.02	-0.12	-0.20	-0.41	-0.59	-0.74	-0.75	-0.76	-0.75	-0.75	-0.72

TABLE 2. Association between the ENSO state and all-Ethiopian JJAS rainfall, based on the 1970–2004 period. Table entries are observed frequencies, followed in parentheses by their inferred conditional probabilities (x100), given the ENSO category. Rainfall categorization is based on the three categories having cutoffs at  $\pm 0.431$  (tercile defining) standardized anomalies. ENSO classification is taken from NOAA/CPC. For the 35 yr of JJAS (1970–2004), 9 (8) years are classified as El Niño (La Niña), and 18 yr as neutral. Significance is assessed using a Chi-square test.

Seasonal Rainfall category	ENSO phase			Significance
	El Niño (9 yr)	Neutral (18 yr)	La Niña (8 yr)	
Dry (10 yr)	6 (67%)	4 (22%)	0 (<5%)	P < 0.01

Normal (12 yr)	2 (22%)	9 (50%)	1 (12%)	
Wet (13 yr)	1 (11%)	5 (28%)	7 (>85%)	

TABLE 3. Autocorrelation ( $\rho_{100}$ ) for the Niño-3.4 SST index for 1970–2004. Correlations of 0.60 or higher for periods during the JJAS rainy season from months prior to JJAS are shown in bold.

	May	Jun	Jul	JJA	Aug	JAS	Sep
Preseason							
Jan	55	25	7	8	-2	0	0
Feb	68	31	10	15	5	7	6
Mar	70	48	25	27	17	20	19
Apr	86	64	49	53	44	47	45
May	100	81	63	70	59	62	61
In season							
Jun		100	89	94	84	87	82
Jul			100	98	96	97	90

If the ENSO state for JJAS could be predicted well in advance, much could be said about the general character of Ethiopia's main rainy season. Since Zebiak and Cane (1987) first established a successful simplified but fully physical coupled ocean–atmosphere model for forecasting ENSO, copious research has been conducted to improve understanding of ENSO and to predict it at several seasons lead (Latif et al. 1998). ENSO forecasts whose lead time traverses the April–June period are known to have lower skill than forecasts whose lead time does not include that period. The seasonal variation of the persistence of tropical Pacific SST anomalies roughly parallels

that of the skill (Wright et al. 1988)—autocorrelation of tropical Pacific SST anomalies at 2–4 months is lowest in boreal spring and highest in fall (Latif et al. 1998). Lag correlations between northern summer tropical Pacific SST from the preceding months represent a lower limit of ENSO-related predictability, and we expect autocorrelations of the ENSO state prior to summer with that of summer to weaken as the lead time increases, paralleling the weakening relationship between all-Ethiopian JJAS rainfall and tropical Pacific SST as the time of the SST retreats from JAS to May, April, etc. Our result (Table 3) confirms declining autocorrelations for pre-summer months, and thus poor relationships using January, February, or March. May is better autocorrelated (0.6–0.7) with the following individual months and the three month mean summer SSTs. Thus, in anticipating the summer ENSO condition based on earlier ENSO conditions, May SST anomalies have moderate utility, April's anomalies are weakly helpful, and earlier anomalies are virtually useless.

Lag correlation for the Southern Oscillation index (SOI), an atmospheric component of ENSO, produces similar results. The SOI may be used in tandem with SST for a more balanced and complete ENSO representation. However, monthly SOI, derived from the sea level pressures of two stations, is “noisier” than the monthly SST index.

Methods to predict the summer ENSO state beyond simple SST autocorrelation could involve dynamical models, or statistical models using physically based predictors. We explore both approaches. The intermediate coupled ocean–atmosphere ENSO prediction model originally developed at Lamont-Doherty Earth Observatory (Zebiak and Cane 1987), with current version LDEO5 (Chen et al. 2004), uses sea level, winds, and SST to initialize the predictions. Hindcasts of Niño-3.4 SSTs for JAS were run using

reconstructed initialization data from a start time of June 1 (i.e., data through May) for each summer from 1970 to 2004. These hindcasts achieve a correlation of 0.9 against observations.

To determine whether a purely statistical model based on observed data through May can attain similar hindcast skill, we develop linear models to predict the JAS ENSO state. Historical records of Niño-3.4 SSTs and SOI over 1951–90 are used to develop the model. Model selection is conducted considering individual or collective SST and SOI values of January to May as predictors, to predict JAS Niño-3.4 SST. Stepwise multiple linear regression is applied to select predictors, stopping when additional predictors no longer significantly enhance predictive skill. The resulting model used three predictors: 1) May SOI, 2) May Niño-3.4 SST, and 3) May Niño-3.4 SST anomaly minus the February–March average Niño-3.4 SST (MFMSST). This model results in a highly significant multiple  $R^2$  of 0.68 (adjusted  $R^2$  of 0.66). The model equation, with standardized variables, is

$$JAS\_SST = 0.116 + 0.486 \times MFMSST - 0.243 \times MaySOI + 0.583 \times MaySST.$$

The time series of hindcasts from LDEO5 and the multiple regression model are shown in Fig. 11. The regression forecasts are shown both within the training period (1951–90) and for an independent (1991–2004) verification period. The statistical model performance is slightly lower than that of LDEO5, as noted from the prediction differences for 1998, 2003, and 2004. The skills of both tools clearly indicate predictive utility for summer ENSO from the end of May. Even this short lead time would be valuable for early warning of a shift in the odds for JJAS rainfall anomalies. In actual practice, the regression tool can be used when more computer-intensive dynamical or more advanced statistical ENSO forecasts are inaccessible.

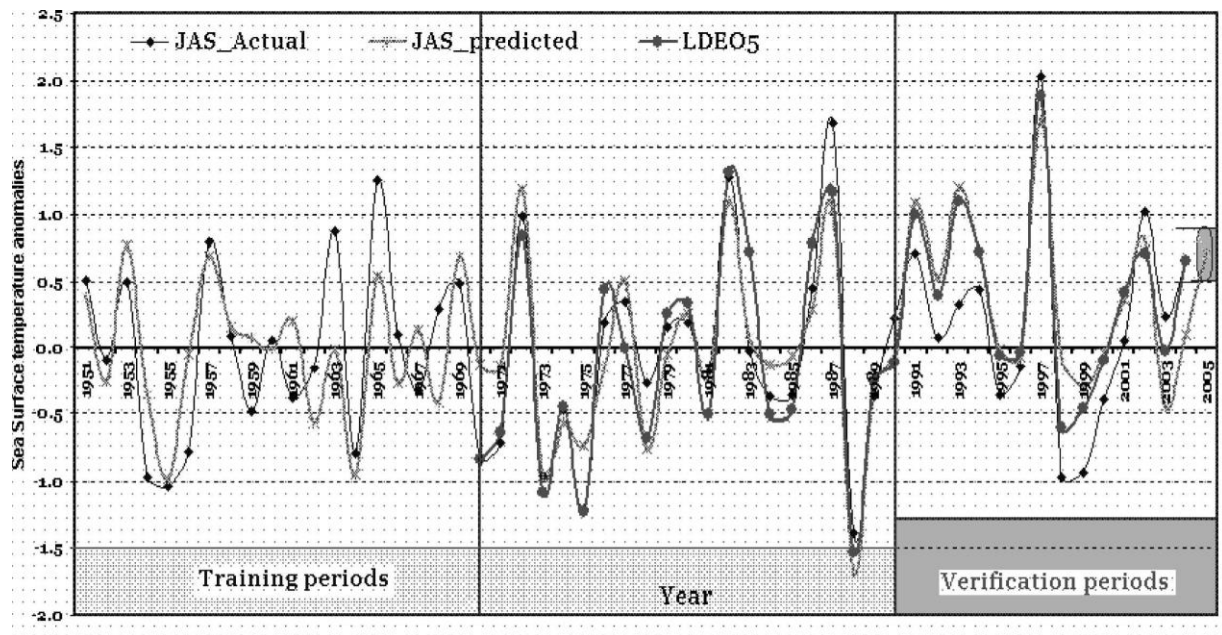


FIG. 11. Time series of the three-month mean (JAS) Niño-3.4 SST anomalies ( $^{\circ}\text{C}$ ) as observed for the periods 1951–2004, the model simulated using LDEO5, and the multiple linear regression model fitted in the present study. LDEO5-predicted SSTs were available for 1970–2004, whereas the multiple linear regression model is built based on 1951–90 and validated for the remaining period.

#### 4 Statistical rainfall predictions

Now we describe results of prediction schemes to forecast Ethiopian rainfall first by exploring patterns of correlation with global SST, then using multiple regression and CCA as tools. We consider the simultaneous (summer) relationships as well as those using the states of the predictors prior to onset of the rainfall season.

Because SST anomalies of the global tropical oceans, particularly ENSO, are known to physically induce shifts from the climatologically expected JJAS

rainfall probability distribution over Ethiopia, we anticipate certain features in the geographical distribution of correlation between all-Ethiopian JJAS rainfall and SST during May (Fig. 12, top) and August (bottom). August is used to represent the summer SSTs, given that SST anomalies usually change slowly. The distribution of correlation with August SST is seen to be roughly an amplified version of that with May SST. This makes sense, as it is the concurrent SSTs that most directly affect Ethiopian summer rainfall, and the May SST anomaly patterns often resemble those of August, given a moderate three-month autocorrelation. If an early warning procedure were based on this tool, updates in June and July would incorporate further evolution in the SST anomaly pattern after May.

The most obvious feature in Fig. 12, both for May and August SST, is ENSO related, with the positive (negative) ENSO phase associated with low (high) seasonal rainfall. The correlation patterns over the Atlantic and Indian Oceans do not show strong features. Some positive correlation between rainfall and May SSTs appear in the off-equatorial western tropical Pacific, the southeast Indian Ocean, and weakly in the equatorial Atlantic. Negative values in the central eastern tropical Pacific are stronger for August than for May SSTs, as are positive correlations near Indonesia and the far eastern Indian Ocean. Weak negative correlations are noted in the subtropical South Atlantic for May SST.

We know that the southwestern Indian Ocean supplies moisture for Ethiopian rainfall during JJAS through a west–east-oscillating Mascarene high pressure center climatologically positioned near the Mascarene Islands during northern summer. The mean summer 1000- and 850-hPa wind flow for the 1970–99 period (Fig. 13) shows Mascarene and St. Helena high pressure, centered near 25°S, 65°E and 25°S, 5°W, respectively.

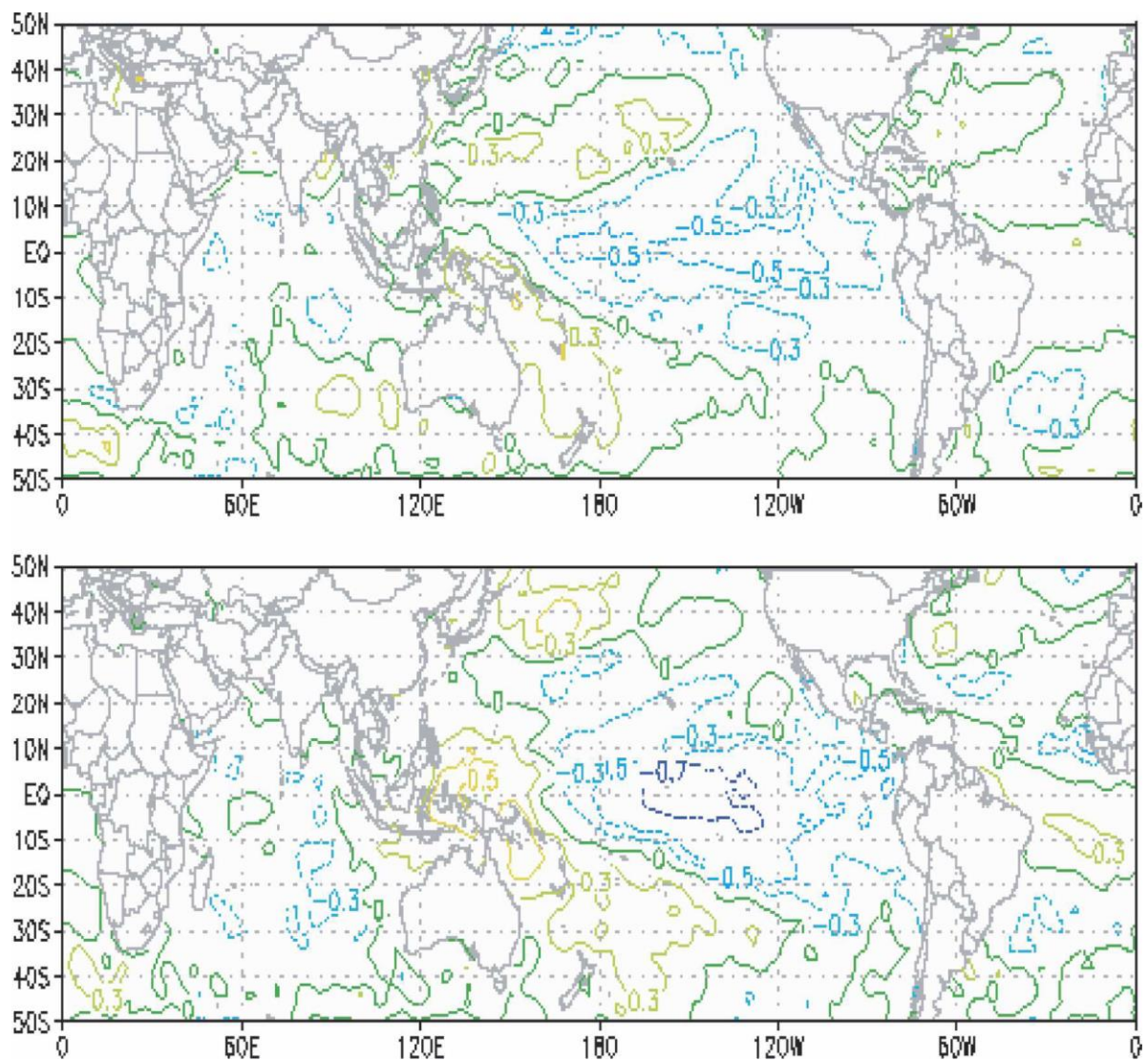


FIG. 12. Correlation between SST anomalies for (top) May and standardized all-Ethiopian JJAS rainfall anomalies observed from 1970–2004. Contour interval is 0.1. (bottom) Same as (top), but for August SST. Correlation magnitudes of 0.34 and more are statistically significant at 95% confidence level.

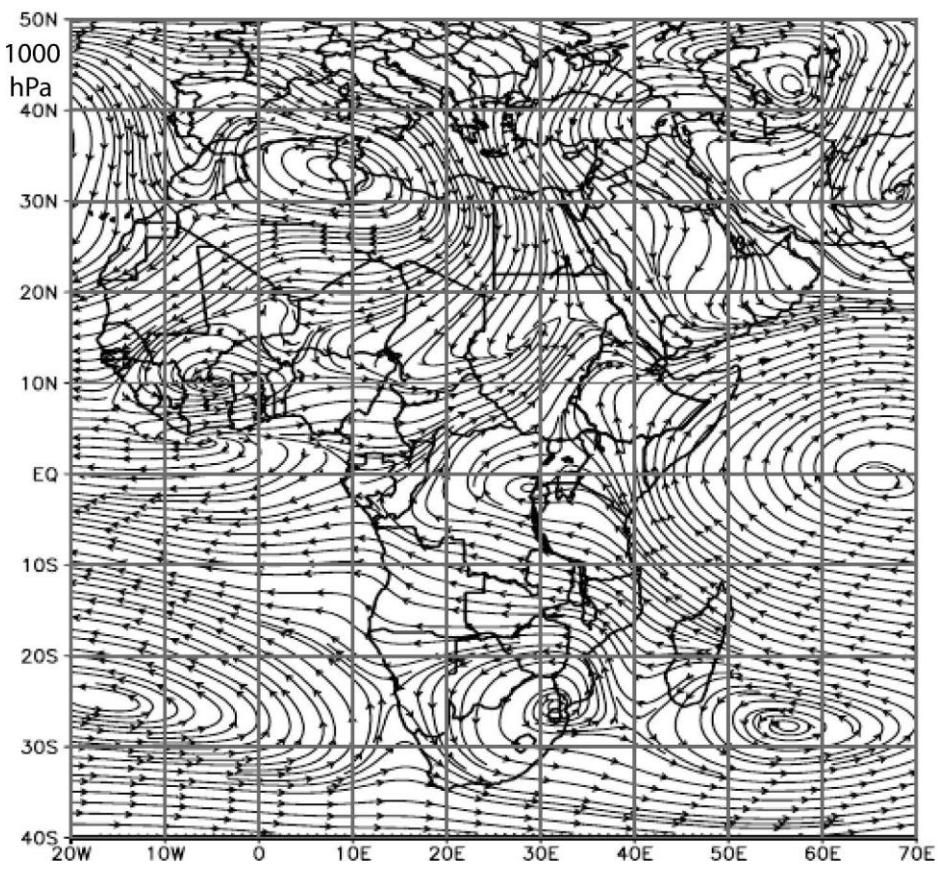
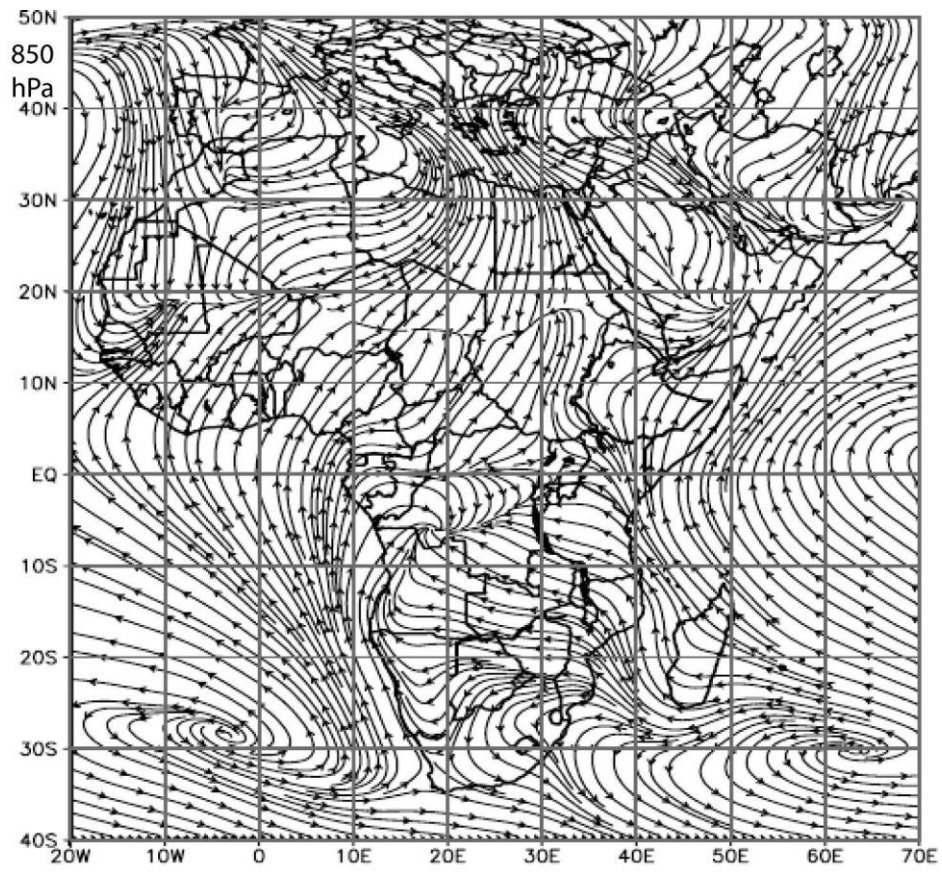


FIG. 13. Mean summer wind flow and locations of prominent seasonal synoptic systems, based on 1970–99, for (top) 850 and (bottom) 1000 hPa, from NCEP–NCAR reanalysis. (Figure contributed by Z. T. Segele.)

The moist air north of the Mascarene high is forced northward through central equatorial Africa, finally reaching northern Ethiopia. The Congo–moist air boundary is a transient quasi-meridional discontinuity formed by converging winds from the Mascarene and St. Helena highs, and pumps moist air toward Ethiopia. A negative SST anomaly near the Mascarene Islands enhances the Mascarene high, increasing cross equatorial moisture flow toward Ethiopia. Weak negative SST correlations appear in the Mascarene high region in Fig. 12.

A weak negative correlation over the equatorial northeast tropical Atlantic, off the West Africa coast, may reflect the SST's role in modulating the strength and extent of the ITCZ's northward migration. Warm SST there encourages airflow (and moisture) both from Atlantic and the central Africa rain forest (Congo–moist air boundary) toward the warm pool, depriving Ethiopia of rainfall. The cloudiness off the coast of West Africa often later causes the positive SST anomalies to become negative.

Positive SST correlations appearing during May and August over the western tropical Pacific, related partly to ENSO, may have consequences for Ethiopian summer rainfall through the 100–200-hPa TEJ. The northwestern tropical Pacific and South China Sea are source regions for TEJ, which tends to be stronger during positive SST anomalies in those waters. Various studies (e.g., Segele and Lamb 2005; Kidson 1977; Ward 1998; Grist et al. 2002) do not directly examine an association of TEJ strength with ENSO, or with JJAS

Ethiopian rainfall. However, Grist et al. (2002) and Ntale et al. (2003) indicate roles for easterly waves and TEJ, linking them to both ocean forcing and seasonal rainfall for West and eastern equatorial Africa, respectively, for their rainy seasons. Formal quantification of the role of TEJ in Ethiopia's Kiremt rainfall, and its association with ENSO, remains open.

All-Ethiopian-average JJAS rainfall can be expressed as a linear combination of atmospheric and oceanic predictors whose values are available upon completion of May. We select this short lead time because much of the rainfall predictability comes from the ENSO state expected during summer, and the evolution of this state is difficult to identify earlier than the end of May. A linear regression model is used, candidate predictors being a selected subset of the available SST data including Niño-3.4 SST, SST over part of the southern, tropical and northern Atlantic sectors, the southwest and northwest Indian Ocean, and the SOI. We consider both May values and the changes of the predictors between February–March and May.

The stepwise regression, after passage of diagnostics related to the fitting and the model assumptions, accepts three predictors: 1) the difference of May minus the February–March SSTs over the south Atlantic in the box defined by 30°–40°S, 15°–30°W (MFM\_SA); 2) the difference of May minus the February–March Niño-3.4 SST (MFM\_Niño-3.4); and 3) May Niño-3.4 SST (May\_Niño-3.4). The regression did not select SSTs in the southwest Indian Ocean, despite its above-mentioned possible role and its importance for rainfall in parts of Ethiopia as illustrated for simultaneous Indian Ocean SST–rainfall correlations in Gissila et al. (2004). Standardizing all variables, the model equation is

All-Eth-RAIN<sub>JJAS</sub>=-0.97 X MFM\_SA - 1.02 X May\_Niño-3.4 - 0.44 X MFM\_Niño-3.4 - 0.06.

All coefficients are statistically significant at the 95% level, and the overall model “goodness of fit” is significant at 99%. The model explains 59% of the total variance of all-Ethiopian JJAS seasonal rainfall ( $R = 0.77$ ); the adjusted  $R^2$  is 0.53 ( $R = 0.73$ ). Diagnostic analysis of the model reveals approximate normality of all variables (including rainfall), minimal serial correlations of the residuals, and only mild outlier presence<sup>7</sup>.

The coefficient estimates remained stable when using cross validation (Michaelsen 1987) and retroactive validation methods (e.g., Barnston et al. 1994) both widely used in climate prediction (e.g., Thiaw et al. 1999; Mutai et al. 1998, Gissila et al. 2004). In cross validation, a model is developed using all years but excluding each single year, in turn, which is predicted and verified in each case. The retroactive method involves partitioning the time series data into a training period and an independent verification period. We use 1970–96 for training and 1997–2004 for verification. Results using both hindcasting techniques are shown in Fig. 14. Models fitted and verified using either cross validation or retroactive techniques performed well on most wet years but underestimated the severity of some dry years. The skill of the cross-validation design is superior to that using the retroactive approach;  $R^2$  values are 0.41 ( $R = 0.64$ ) and 0.26 ( $R = 0.51$ ), respectively. The smaller set of years validated in the retroactive scheme may have rendered its result a less stable estimate of the expected skill. Also, the 1-yr-out style of cross validation can produce still slightly inflated skills, especially when there is high serial correlation in the data (not found in our case). In the cross-validation results, the differences between the model coefficients developed with differing years withheld are small.

7 The low rainfall for 1987 is identified as an influential point (Ramsey and Schafer 2002). Four robust regression alternatives (least trimmed squares regression, least median squares regression, least absolute deviations regression, and maximum likelihood estimates of regression) were applied (Rousseeuw and Leroy 1987) with and without 1987, and comparison of results of the predictor coefficients with those of the original ordinary least squares model indicate that the original model performs entirely satisfactorily without special outlier accommodation.

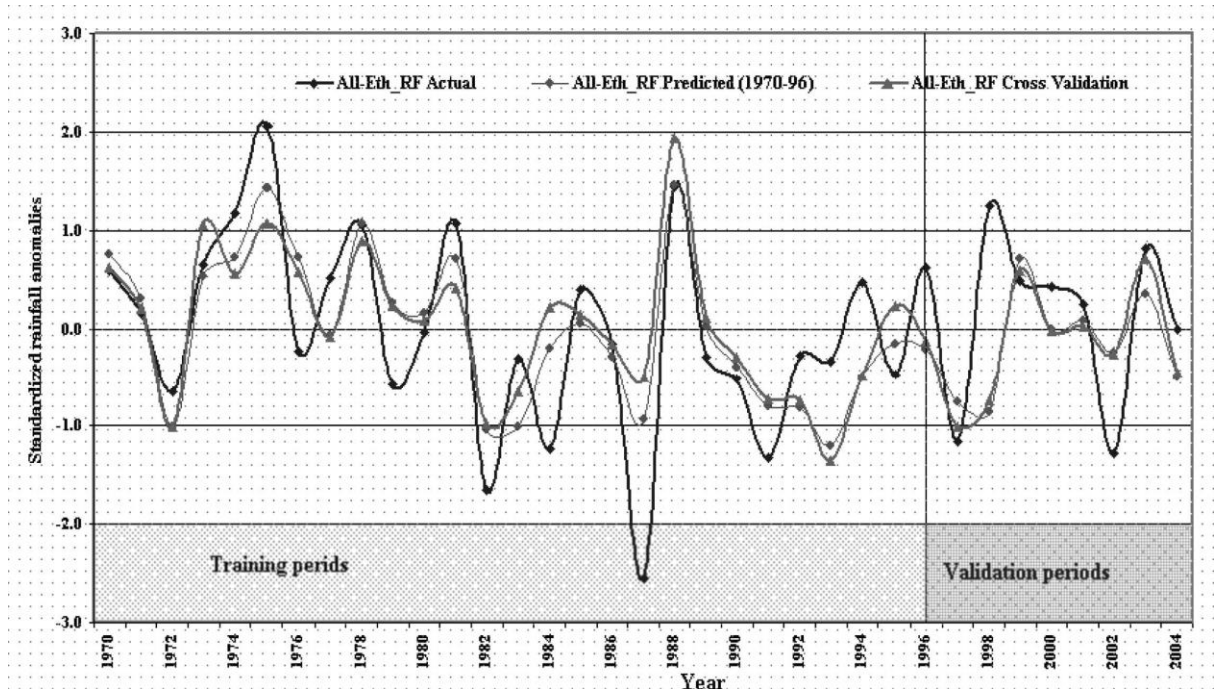


FIG. 14. Predicted and observed all-Ethiopian JJAS standardized rainfall anomalies. The three multiple linear regression predictors, shown in the equation above, include Niño-3.4 SSTs and Atlantic SSTs for the months prior to the beginning of the JJAS rainy season. The retroactive model is fitted to the data series over the training period, and then validated for 1997–2004 (thin gray line). The cross validation model predictions (thicker gray line), and the observations (black line), are shown.

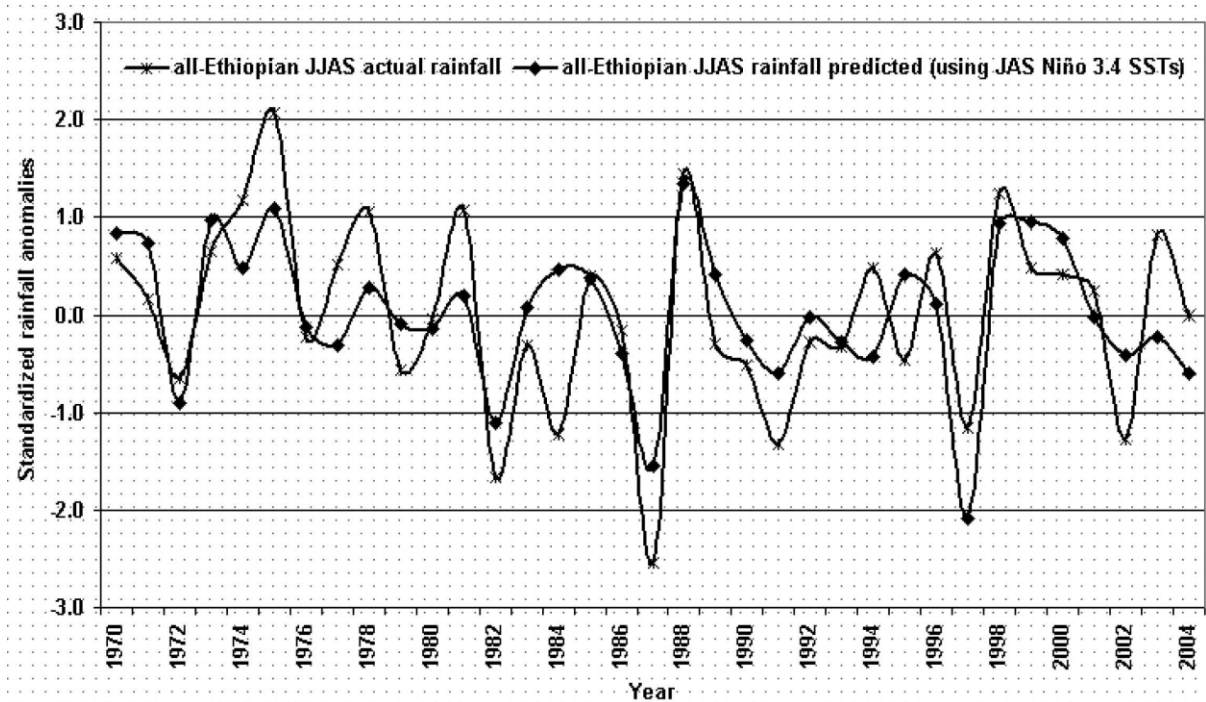


FIG. 15. Model predicted and actual all-Ethiopian JJAS standardized rainfall anomalies. The predictor is JAS Niño-3.4 SST anomalies (JAS\_Niño-3.4) that are fitted to JJAS rainfall by simple linear regression. The regression model is statistically significant with confidence levels of 99%. The JAS Niño-3.4 SSTs alone explain 58% of the total variance of JJAS rainfall.

When fitting the relationship between SSTs and rainfall concurrently in time, the JAS Niño-3.4 SSTs alone explain 58% of the variance of the JJAS all-Ethiopian rainfall (correlation 0.76) far more than any other candidate predictors, and a one-predictor (simple) regression is sufficient (Fig. 15). Gissila et al. (2004) identified the main regions of SST concurrently associated with Ethiopian rainfall as being the western Indian Ocean, the eastern Indian Ocean, and the eastern tropical Pacific. They assumed that these regions would remain important when used predictively, for individual clustering-determined homogeneous geographical sectors of Ethiopia. Our omission of Indian Ocean SST predictors may be attributed to use of a single all-Ethiopian rainfall index, and, more likely, our focus on the predictive rather

than the concurrent SST correlations (top rather than bottom in Fig. 12). Recall that when an ENSO episode develops, typically the Indian Ocean SST anomaly has not yet responded to the growing anomaly in the tropical Pacific during May or June.

Skill in predicting all-Ethiopian JJAS rainfall is also assessed using CCA<sup>8</sup>. CCA identifies linear relationships between predictor and predictand in a manner similar to multiple linear regression, except that CCA is multivariate on both the predictor and the predictand sides and thus accommodates coupled spatial patterns linking the two fields (or two sets of fields). CCA involves eigenanalysis, in that a matrix of correlations between only cross-dataset (predictor–predictand) elements is processed and then subjected to empirical orthogonal function (EOF) analysis. Here, to reduce noise and the potential for over-fitting, the predictor and predictand data individually are pre-orthogonalized using ordinary EOF analysis before applying the CCA, and the CCA then receives the amplitudes of just a few EOFs of the predictor versus a few EOFs of the predictand fields (Barnett and Preisendorfer 1987; Barnston and Smith 1996; Ward 1998; Thiaw et al. 1999). Here we perform CCA starting with 1970–2002 gridded global sea surface temperatures as the predictor field and the set of Ethiopian JJAS standardized individual station rainfall anomalies as the predictand field. Based on skill trials using cross validation, we retain only two modes of predictor and predictand in the pre-orthogonalization, and also two modes in the CCA itself. In two separate

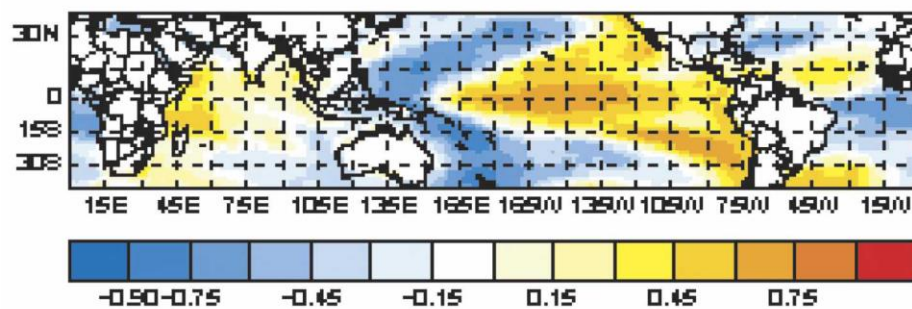
---

<sup>8</sup> A CCA software module called Climate Predictability Tool (CPT) was downloaded from a Web page of the International Research Institute for Climate and Society (IRI) and applied to the global SST and rainfall data used here.

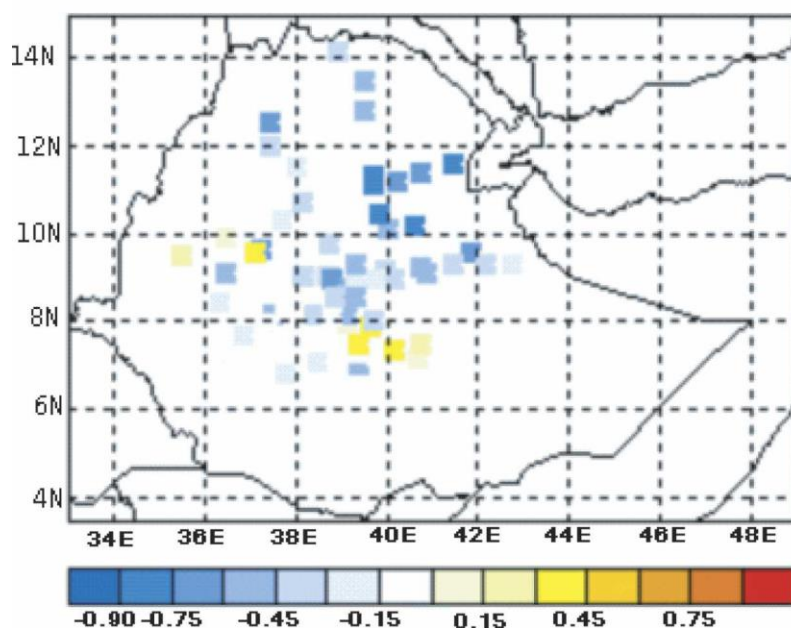
rounds of CCA, we first use May and then use JAS SSTs as the predictor, in each case using JJAS rainfall over Ethiopia as the predictand. Time evolution within the predictor SSTs, as might be captured by the change in SST anomalies from February–March to May, is not incorporated. An advantage of CCA is that *patterns* in the SST field (not just discrete SST index values), are related to *patterns* in the spatial distribution of Ethiopian rainfall anomaly (not just a single Ethiopia average anomaly). If most of the Ethiopian stations tend to have mutually coherent anomalies, as would be the case if they all respond similarly to ENSO, then the benefit of CCA’s pattern accommodation may not be pronounced on the predictand side.

A CCA based on 1970–2002 data between May SSTs and the set of Ethiopia station JJAS rainfalls—a short lead forecast—produces results as shown in Fig. 16. The pattern of May SSTs giving rise to skill in predicting the rainfall pattern over Ethiopia is shown by the spatial loading map for the leading CCA mode (Fig. 16, top). This pattern shows a positive ENSO phase (El Niño), associated with mainly negative JJAS rainfall anomalies over Ethiopia as seen in the predictand loading pattern (Fig. 16, middle). The bottom panel shows the temporal scores of the predictor and predictand associated with this mode. The May SST pattern appears to have good skill in capturing the seasonal rainfall performance observed during strong El Niño years (e.g., 1972, 1982, 1987, and 1997) and the strongest La Niña years (1973, 1975, 1988, and 1998). The canonical correlation, describing the strength of the relationship between the predictor SST patterns and predictand rainfall patterns (i.e., the correlation between the predictor and predictand temporal scores), is 0.55.

### X Spatial Loadings (EOF1)



### Y Spatial Loadings (EOF1)



### Temporal Scores (Mode1)

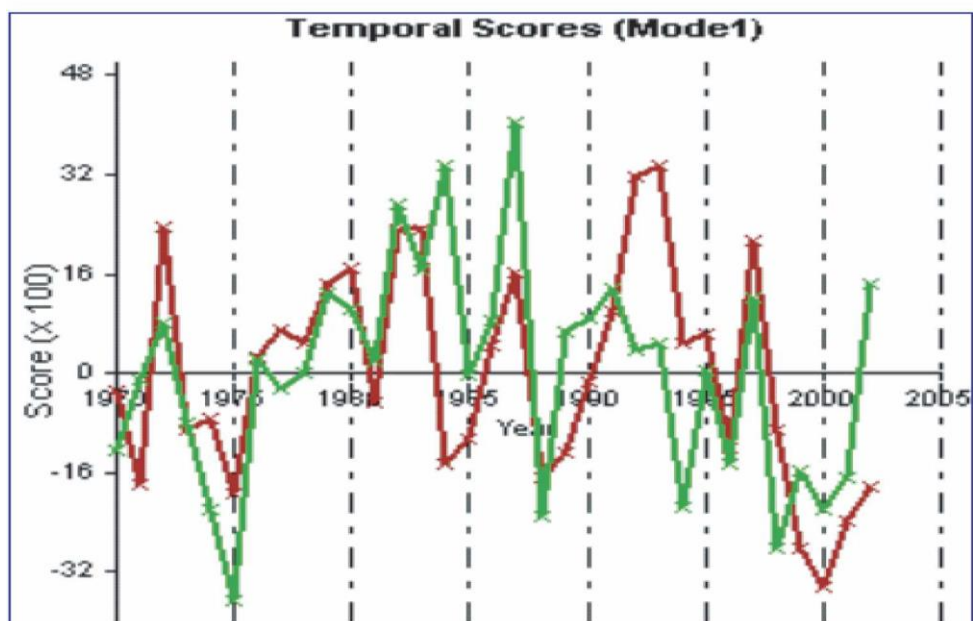
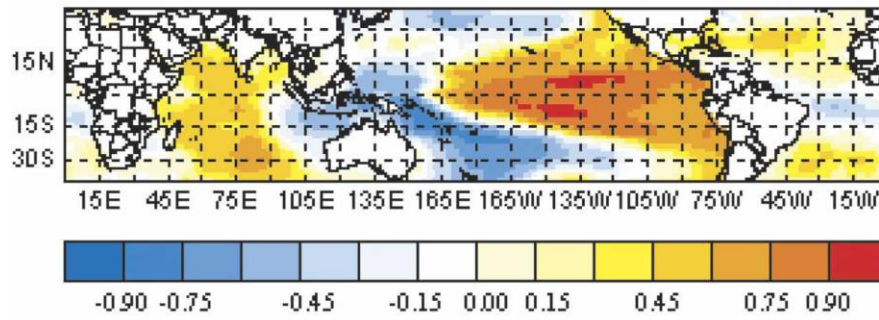


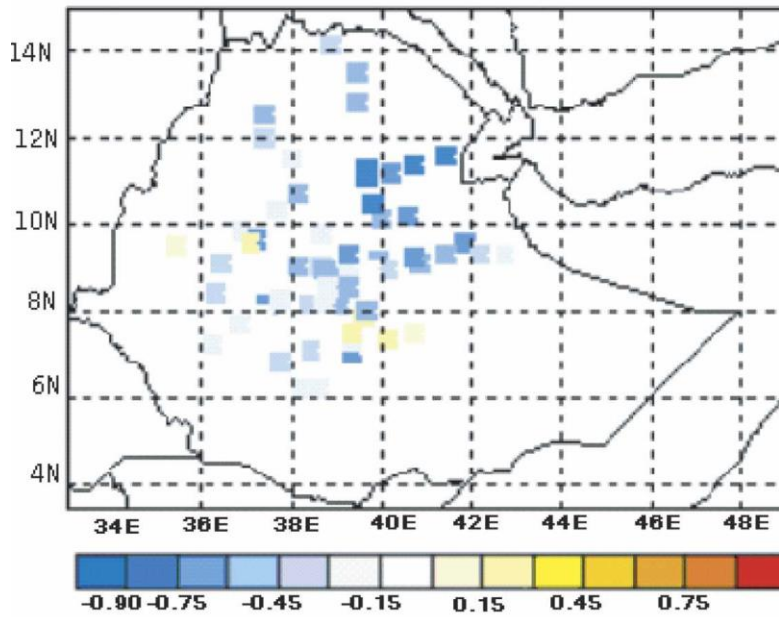
FIG. 16. Spatial loadings of the first CCA mode (called EOF1) for the prediction of (middle) Ethiopian JJAS station rainfall, based on (top) May

SST. (bottom) The time series of the temporal scores of the predictor SSTs (green line) in predicting JJAS rainfall (red line) for this CCA mode. Based on 1970–2002 data.

### X Spatial Loadings (EOF1)



### Y Spatial Loadings (EOF1)



### Temporal Scores (Model)

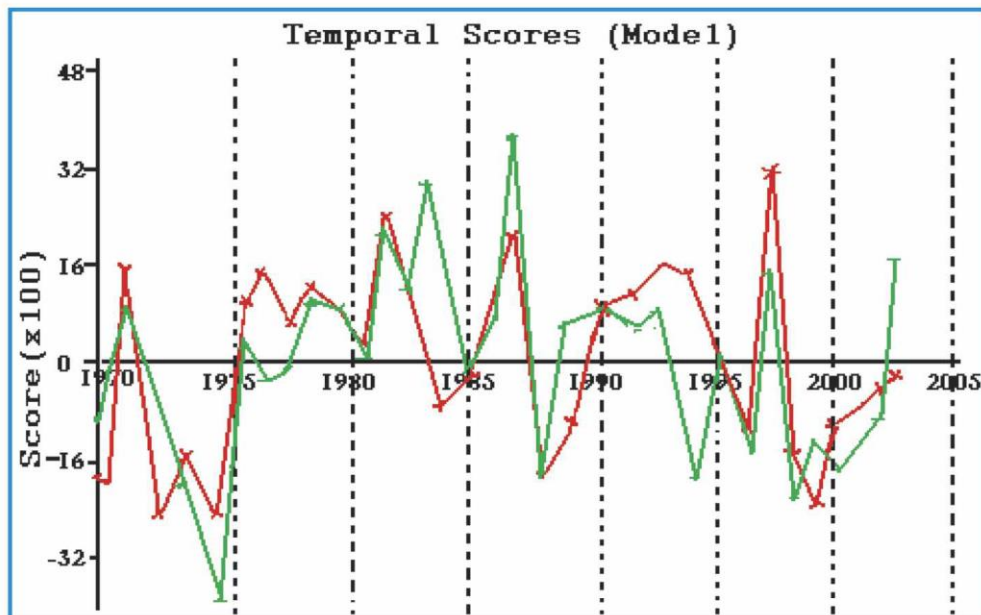


FIG. 17. Same as in Fig. 16 [spatial loadings of (middle) Ethiopian rainfall of (top) SST, and (bottom) temporal scores for each], except that the SST is for JAS.

When the JAS SST field is the “predictor” (Fig. 17), the SST predictor loading pattern has a stronger tropical Pacific ENSO pattern, and includes the Indian Ocean to a greater degree than for May SST. This would be expected, given the lagged response of the Indian Ocean with respect to the tropical Pacific Ocean during ENSO episodes (Goddard and Graham 1999; Goddard et al. 2001). While the predictand rainfall loading pattern is very similar to the result using May SST, a stronger correspondence between predictor and predictand temporal scores is evident (Fig. 17, bottom), with a canonical correlation of 0.70. This implies that the May and JAS SST patterns are associated with nearly the same JJAS rainfall response over Ethiopia, but confidence is greater for JAS SSTs. Inclusion of the second CCA mode (not shown) does not improve predictive skill materially, as mode 2 accounts for far less variance than mode 1 for both May and JAS SST predictors. The morphologically similar result seen for concurrent SST–rainfall patterns and the lagged relationship suggests again that the Ethiopian rainfall anomaly pattern is primarily related to the accompanying summer ENSO state, and that successful rainfall prediction depends critically on prediction of that ENSO state from an earlier time. The regression results for predicting ENSO, presented above, demonstrated the need to ascertain the direction of change of ENSO from an earlier month (e.g., February or March) to May, to determine whether the May ENSO condition is in a growth stage or a dissipative stage relative to the previous 1-yr ENSO cycle.

The temporal scores for the leading CCA predictor mode using either the May or JAS SST field against Ethiopia’s JJAS rainfall station network were each

used separately as the single predictor in a simple regression with the all-Ethiopian rainfall as a scalar predictand. The two simple linear regression models generate predicted rainfall time series as shown in Fig. 18. The predictions generated from the 1-mode CCA using JAS SST bear close resemblance with the results for multiple regression using a few scalar predictors (Fig.15). This indicates that the summer ENSO state is close to being the optimum single predictor for JJAS Ethiopian rainfall, whether the rainfall is described in a single index or as a more detailed anomaly pattern across the stations, and whether ENSO is captured in a single SST index or as a detailed spatial pattern. By contrast, the May SST pattern of the leading CCA mode predicts the all-Ethiopian JJAS rainfall anomalies much less well than the multiple regression whose result was shown above in Fig. 14. This shows that the May ENSO state alone, even as a detailed SST spatial pattern, cannot lead to as skillful a JJAS rainfall prediction as the May ENSO state plus other critical quantities most importantly, the change of the ENSO state between an earlier month and May. A CCA that uses both the February–March SST and the May SST as temporally “stacked” predictor fields might match or exceed the multiple regression skill; such a CCA design could be explored in future research.

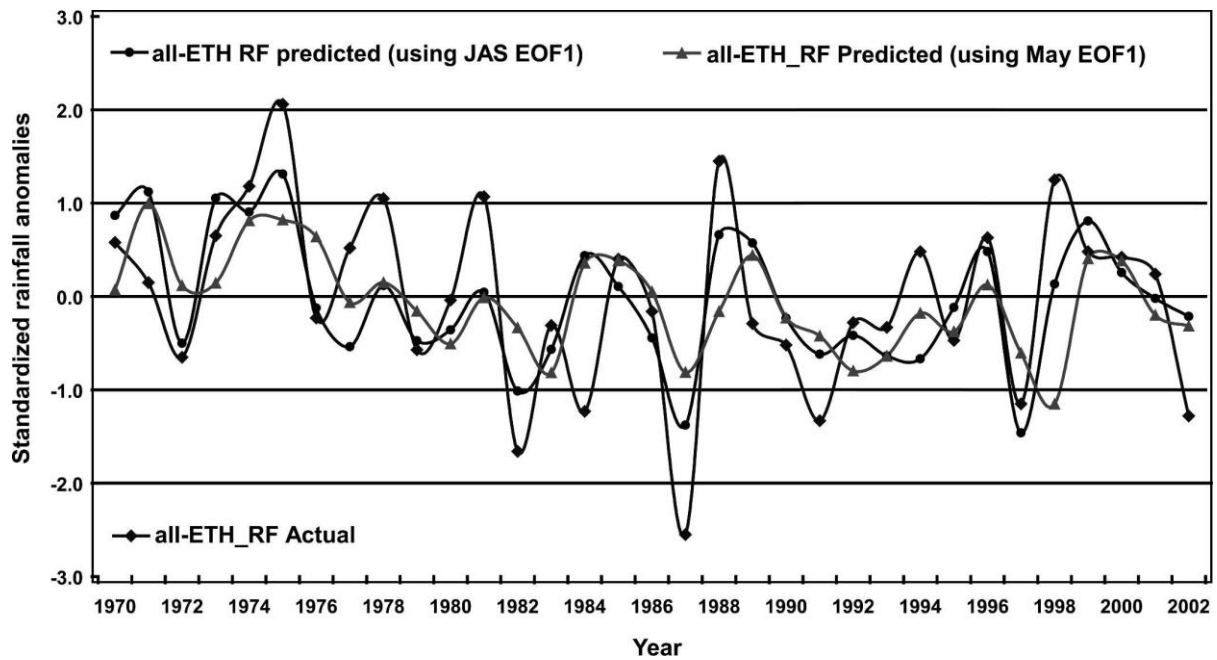


FIG. 18. Model simulated (lines with circles and triangles) and observed (line with diamonds) all-Ethiopian JJAS standardized rainfall anomalies, based on May and JAS CCA mode 1. The simple linear regression is fitted over 1970–96. The skills, expressed as percentages of total variance explained, of all-Ethiopian JJAS rainfall are 25% (May) and 49% (JAS).

#### 4 Discussion and conclusions

In most of Ethiopia, adequate rainfall during the main rainy season (JJAS) is essential for major societal operations such as hydropower generation, agricultural irrigation, and drinking water. This study examines the potential for predictions of JJAS rainfall with a lead time sufficient for proactive risk management.

A rainfall climatology is derived from a newly assembled dense network of Ethiopian stations for the 1970–2004 period. Previous studies suggested that ENSO-related SST anomalies have a predictable and physically based effect

on Ethiopian JJAS rainfall. Here, using the new station rainfalls, we examine the potential to predict JJAS Ethiopian rainfall based on the climate state prior to the onset of the rainy season using statistical techniques, and exploring the skill of statistical methods and one dynamical method to predict the all-important summer ENSO state.

A moderately strong teleconnective relationship between the northern summer ENSO state and concurrent JJAS Ethiopian seasonal rainfall is demonstrated, La Niña (El Niño) associating with enhanced (suppressed) summer rainfall across much of the country. Six out of the nine El Niño years in the 1970–2004 period have been in the dry tercile of the all-Ethiopian JJAS rainfall distribution, while seven out of the eight La Niña years have been in the wet tercile. The ENSO response is strongest over the northern half of the country where the rainfall patterns often depend on the northward advance of the ITCZ during northern summer (Segele and Lamb 2005; Tsegay 2001; Fraedrich et al. 1997). A relationship between the seasonal oscillation of ITCZ and ENSO, and consequences for Ethiopia's JJAS rainfall, has been suggested (Degefu 1987; Seleshi and Demarée 1995; Segele and Lamb 2005).

One linkage scenario involves a weakening and retreating of ITCZ as El Niño episodes begin maturing during late northern summer; the converse would occur in the case of La Niña. In particular, the northward protruding meridional arm of ITCZ associated with rainfall in central and northern Ethiopia, depending on cross-equatorial northward flow of moist air, may be affected by ENSO.

It is found possible to use the presummer ENSO state, and its direction and rate of evolution, as a simple statistical precursor for the ENSO state during the coming summer season, and consequently the summer seasonal rainfall.

Because of the changeable and uncertain evolution of the ENSO state during northern spring season (the ENSO “predictability barrier”), the strength of association between ENSO and JJAS rainfall decreases sharply as the time of the ENSO state retreats to progressively earlier months—particularly from May backward. The May ENSO state alone provides some indication of the summer Ethiopian rainfall, but the temporal change of May SST from a few months earlier is an essential additional predictor for JJAS ENSO (and hence rainfall), discriminating between growing and decaying ENSO episodes. The LDEO5 intermediate dynamical ENSO prediction model is found to produce skillful ENSO forecasts for the northern summer season using initialized SST data through the end of May. Simple statistical models based on historical Niño-3.4 SST index and SOI in May, and the change from several months earlier, are also shown to produce skillful forecasts of the July–September (JAS) Niño-3.4 SSTs. This simple model could be used in the absence of significant resources and would be further enhanced by merging it with outputs from dynamical ENSO forecasting models such as LDEO5 or others. The northern spring barrier is more than halfway traversed by the end of May and a moderately skillful summer forecast can be made at this short lead time. When and if ENSO can be better predicted through this difficult time of year, longer lead forecasts could be made for Ethiopian summer rainfall.

Rainfall teleconnections to SST regions other than the tropical Pacific are considerably weaker and of smaller spatial scale, and include the Indian and Atlantic Oceans both during and preceding summer.

Multiple linear regression and CCA models are developed to predict JJAS rainfall directly, without predicting the summer ENSO state explicitly. Multiple regression is applied to all-Ethiopian JJAS rainfall, using SST indices and SOI as predictors. The stepwise design selected May Niño-3.4 SSTs, its recent time derivative, and the recent time derivative of SSTs in the subtropical South Atlantic, explaining 59% of the interannual all-Ethiopian JJAS rainfall variance. Pertinent to the key role of the ENSO state to occur during the summer season, the JAS Niño-3.4 SSTs can be used as an alternative “predictor” (after being predicted earlier) that alone would have a better predictive skill score than the above three precursor variables do together. Of course, operational use of this latter model unrealistically requires perfect forecasts for the Niño-3.4 SST. Again we conclude that ENSO predictability is currently the missing requirement for more skillful rainfall forecasts at longer lead times.

The CCA defines spatial pattern relationships between global SST and JJAS Ethiopia station rainfalls. The simultaneous SST–rainfall patterns strongly confirm the impact of ENSO, and indicate a lesser role for SSTs near the source regions of monsoonal low-level systems near southwest India and in South Atlantic. These conclusions also apply to the CCA using leading May SSTs.

In summary, this study’s main finding is that the northern summer ENSO condition is overwhelmingly the single most important factor governing the JJAS rainfall across Ethiopia, excluding the southern/southeastern lowlands. SST anomalies in the Atlantic and Indian Oceans appear to matter far less. More regional climate and weather processes were not investigated here, but could be tied into this larger scale. Skillful predictions of Ethiopian summer rainfall hinge upon the best possible forecasts of the summer ENSO state

from an earlier time. Useful summer rainfall predictions are thus potentially achievable using global dynamical or statistical models. Further study may extend knowledge to more regional scales, particularly using regional models that reproduce large-scale processes (e.g., ITCZ, middle- and upper-troposphere circulations), and downscale for local land surface variations. In the meantime, existing statistical modeling techniques, aided by statistical or dynamical predictions of the summer ENSO state, allow for improved use of seasonal rainfall forecasts for sustainable, dependable early warning systems so critically important to societal operations.

## **Acknowledgments**

The authors appreciate the helpful comments of the anonymous reviewers, as well as those of Z. T. Segele and W. Thiaw. Z. Segale kindly offered Fig. 13 to us. We are grateful to Mark Cane for directing the Climate and Society Masters program that enabled the Korecha–Barnston collaboration underlying this study, to Dake Chen for a special hindcast run of the LDEO-5 ENSO forecast model, and to Simon Mason for developing the CPT, which contained the user-friendly CCA package used in this study. This paper is funded by a Cooperative Agreement NA050AR431004 from the National Oceanic and Atmospheric Administration. The views expressed herein are those of the authors and do not necessarily reflect the views of NOAA or any of its sub-agencies.

## **References**

Barnett, T. P., and R. Preisendorfer, 1987: Origins and levels of monthly and seasonal forecast skill for U.S. surface air temperatures determined by canonical correlation analysis. *Mon. Wea. Rev.*, **115**, 1825–1850.

- Barnston, A. G., and T. M. Smith, 1996: Specification and prediction of global surface temperature and precipitation from global SST using CCA. *J. Climate*, **9**, 2660–2697.
- , and Coauthors, 1994: Long-lead seasonal forecasts—Where do we stand? *Bull. Amer. Meteor. Soc.*, **75**, 2097–2114.
- , M. Chelliah, and S. B. Goldenberg, 1997: Documentation of a highly ENSO-related SST region in the equatorial Pacific. *Atmos.–Ocean*, **35**, 367–383.
- Bekele, F., 1997: Ethiopian use of ENSO information in its seasonal forecasts. *Internet J. Afr. Studies*, No. 2. [Available online at <http://www.ccb.ucar.edu/ijas/ijasno2/bekele.html>.]
- Bhatt, U. S., 1989: Circulation regimes of rainfall anomalies in the African–South Asian Monsoon Belt. *J. Climate*, **2**, 1133–1144.
- Camberlin, P., 1997: Rainfall anomalies in the source region of the Nile and their connection with the Indian summer monsoon. *J. Climate*, **10**, 1380–1392.
- Cane, M. A., 2000: Understanding and predicting the world's climate system. *Applications of Seasonal Climate Forecasting in Agricultural and Natural Ecosystems—The Australian Experience*, G. Hammer, Ed., Kluwer Academic Publishers, 29–50.
- , and S. E. Zebiak, 1987: Deterministic prediction of El Niño events. *Atmosphere and Oceanic Variability*, H. Cattle, Ed., Roy. Meteor. Soc., 153–182.
- , ———, and S. C. Dolan, 1986: Experimental forecasts for El-Niño. *Nature*, **321**, 827–832.
- Chen, D., M. A. Cane, A. Kaplan, and S. E. Zebiak, 2004: Predictability of El Niño over the past 148 years. *Nature*, **428**, 733–735.
- Cook, K. H., 1997: Large-scale atmospheric dynamics and Sahelian precipitation. *J. Climate*, **10**, 1137–1152.

- Degefu, W., 1987: Some aspects of meteorological drought in Ethiopia. *Drought and Hunger in Africa: Denying Famine a Future*, M. H. Glantz, Ed., Cambridge University Press, 23–36.
- Folland, C., J. Owen, M. N. Ward, and A. Colman, 1991: Prediction of seasonal rainfall in the Sahel region using empirical and dynamical models. *J. Forecasting*, **10**, 21–56.
- Fraedrich, K., J. Jiang, F.-W. Gerstengarbe, and P. C. Werner, 1997: Multiscale detection of abrupt climate changes: Application to River Nile flood levels. *Int. J. Climatol.*, **17**, 1301–1315.
- Giannini, A., R. Saravana, and P. Chang, 2003: Oceanic forcing of Sahel rainfall on inter-annual to inter-decadal time scales. *Science*, **302**, 1027–1030.
- Gissila, T., E. Black, D. I. F. Grimes, and J. M. Slingo, 2004: Seasonal forecasting of the Ethiopian summer rains. *Int. J. Climatol.*, **24**, 1345–1358.
- Glahn, H. R., 1968: Canonical correlation and its relationship to discriminant analysis and multiple regression. *J. Atmos. Sci.*, **25**, 23–31.
- Goddard, L., and N. E. Graham, 1999: Importance of the Indian Ocean for simulating rainfall anomalies over eastern and southern Africa. *J. Geophys. Res.*, **104**, 19 099–19 116.
- , and M. Dilley, 2005: El Niño: Catastrophe or opportunity. *J. Climate*, **18**, 651–665.
- , S. J. Mason, S. E. Zebiak, R. E. Ropelewski, R. Basher, and M. A. Cane, 2001: Current approaches to seasonal-to-interannual climate predictions. *Int. J. Climatol.*, **21**, 1111–1152.
- Goldammer, J. G., 1999: Forests on fire. *Science*, **284**, 1782–1783.
- Gong, X., A. G. Barnston, and M. N. Ward, 2003: The effect of spatial aggregation on the skill of seasonal precipitation forecasts. *J. Climate*, **16**, 3059–3071.

- Grist, J. P., E. S. Nicholson, and A. I. Barcilon, 2002: Easterly waves over Africa. Part II: Observed and modeled contrasts between wet and dry years. *Mon. Wea. Rev.*, **130**, 212–225.
- Hastenrath, S., 1991: *Climate Dynamics of the Tropics*. Kluwer Academic Publishers, 488 pp.
- , 1995: Recent advances in tropical climate prediction. *J. Climate*, **8**, 1519–1532.
- , 2000: Interannual and longer term variability of upper-air circulation over the tropical Atlantic and West Africa in boreal summer. *Int. J. Climatol.*, **20**, 1415–1430.
- Hotelling, H., 1936: Relations between two sets of variates. *Biometrika*, **28**, 321–377.
- Hulme, M., 2001: Climate perspectives on Sahelian desiccation: 1973–1998. *Global Environ. Change*, **11**, 19–29.
- Indeje, M. H., M. F. Semazzi, and L. J. Ogallo, 2000: ENSO signals in East African rainfall seasons. *Int. J. Climatol.*, **20**, 19–46.
- Janicot, S., V. Moron, and B. Fontaine, 1996: Sahel droughts and ENSO dynamics. *Geophys. Res. Lett.*, **23**, 515–518.
- , S. Trzaska, and I. Pocard, 2001: Summer Sahel–ENSO teleconnection and decadal time scale SST variations. *Climate Dyn.*, **18**, 303–320.
- Jury, M. R., 2002: Economic impacts of climate variability in South Africa and development of resource prediction models. *J. Appl. Meteor.*, **41**, 46–55.
- Kassahun, B., 1987: Weather systems over Ethiopia. *Proc. First Tech. Conf. on Meteorological Research in Eastern and Southern Africa*, Nairobi, Kenya, UCAR, 53–57.
- Khandekar, M. L., T. S. Murty, D. Scott, and W. Baird, 2000: The 1997 El Niño, Indonesian forest fires and the Malaysian smoke problem: A deadly combination of natural and manmade hazards. *Nat. Hazards*, **21**, 131–144.

- Kidson, J. W., 1977: African rainfall and its relation to the upper air circulation. *Quart. J. Roy. Meteor. Soc.*, **103**, 441–456.
- Lamb, H. H., 1977: Some comments on the drought in recent years in the Sahel–Ethiopia zone of North Africa. *Drought in Africa*, D. Dalby, R. J. Harrison-Church, and F. Bazzaz, Eds., Vol. 2, School of Oriental and African Studies, 33–37.
- , 1978: Large-scale tropical Atlantic surface circulation patterns associated with Sub-Saharan weather. *Tellus*, **30**, 240–251.
- Latif, M., and Coauthors, 1998: A review of the predictability and prediction of ENSO. *J. Geophys. Res.*, **103**, 14 375–14 393.
- Mason, S. J., and L. Goddard, 2001: Probabilistic precipitation anomalies associated with ENSO. *Bull. Amer. Meteor. Soc.*, **82**, 619–638.
- Michaelsen, J., 1987: Cross-validation in statistical climate forecast models. *J. Climate Appl. Meteor.*, **26**, 1589–1600.
- Mutai, C. C., M. N. Ward, and A. W. Colman, 1998: Towards the prediction of the East Africa short rains based on sea-surface temperature-atmosphere coupling. *Int. J. Climatol.*, **18**, 975–997.
- Nicholls, N., 1993: What are the potential contributions of El Niño–Southern Oscillation research to early warning of potential acute food-deficit situations? *Workshop on Usable Science: Food Security, Early Warning and El Niño*, M. H. Glantz, Ed., National Center for Atmospheric Research, 169–177.
- Nicholson, S. E., 1989: Long-term changes in African rainfall. *Weather*, **44**, 46–56.
- , and J. Y. Kim, 1997: The relationship of the El Niño–Southern Oscillation to African rainfall. *Int. J. Climatol.*, **17**, 117–135.
- , and J. C. Selato, 2000: The influence of La Niña on African rainfall. *Int. J. Climatol.*, **20**, 1761–1776.
- NMSA, 1996: Climatic and agroclimatic resources of Ethiopia. National Meteorological Services Agency of Ethiopia, Meteorological Research Report Series, Vol. 1, No. 1, 1–137.

- Ntale, H. R., T. Y. Gan, and D. Mwale, 2003: Prediction of East African seasonal rainfall using simplex canonical correlation analysis. *J. Climate*, **16**, 2105–2112.
- Ogallo, L. J., 1988: Relationships between seasonal rainfall in East Africa and the Southern Oscillation. *Int. J. Climatol.*, **8**, 31–43.
- , 1989: The spatial and temporal patterns of the East African seasonal rainfall derived from principal component analysis. *Int. J. Climatol.*, **9**, 145–167.
- Osman, Y. Z., and Y. A. Shamseldin, 2002: Quantitative rainfall prediction models for Central and Southern Sudan using El Niño–Southern Oscillation and Indian Ocean Sea Surface Temperature indices. *Int. J. Climatol.*, **22**, 1861–1878.
- Paeth, H., and P. Friederichs, 2004: Seasonality and time scales in the relationship between global SST and African rainfall. *Climate Dyn.*, **23**, 815–837.
- Philippon, N. P., P. Camberin, and N. Fauchereau, 2002: Empirical predictability study of October–December East African rainfall. *Quart. J. Roy. Meteor. Soc.*, **128**, 2239–2256.
- Raicich, F., N. Pinardi, and A. Navarra, 2003: Teleconnections between Indian monsoon and Sahel rainfall and the Mediterranean. *Int. J. Climatol.*, **23**, 173–186.
- Ramsey, F. L., and W. D. Schafer, 2002: *The Statistical Sleuth: A Course in Methods of Data Analysis*. 2<sup>nd</sup> ed. Duxbury, 742 pp.
- Ropelewski, C. F., and M. S. Halpert, 1987: Global- and regional scale precipitation patterns associated with the El Niño–Southern Oscillation. *Mon. Wea. Rev.*, **115**, 1606–1626.
- Rousseeuw, P. J., and A. M. Leroy, 1987: *Robust Regression and Outlier Detection*. John Wiley & Sons, Inc., 360 pp.
- Rowell, D. P., 2001: Teleconnection between the tropical Pacific and the Sahel. *Quart. J. Roy. Meteor. Soc.*, **127**, 1683–1706.

- , 2003: The impact of Mediterranean SSTs on the Sahelian rainfall season. *J. Climate*, **16**, 849–862.
- , C. K. Folland, K. Maskell, and M. N. Ward, 1995: Variability of summer rainfall over tropical North Africa (1906–92): Observations and modeling. *Quart. J. Roy. Meteor. Soc.*, **121**, 669–704.
- Segele, Z. T., and P. J. Lamb, 2005: Characterization and variability of Kiremt rainy season over Ethiopia. *Meteor. Atmos. Phys.*, **89**, 153–180.
- Shanko, D., and P. Camberlin, 1998: The effect of the southwest Indian Ocean tropical cyclones on Ethiopian drought. *Int. J. Climatol.*, **18**, 1373–1378.
- Seleshi, Y., and G. R. Demarée, 1995: Rainfall variability in the Ethiopian and Eritrean highlands and its links with the Southern Oscillation Index. *J. Biogeogr.*, **22**, 945–952.
- Smith, T. M., and R. W. Reynolds, 2004: Improved extended reconstruction of SST (1854–1997). *J. Climate*, **17**, 2466–2477.
- Tadesse, T., 1994: The influence of the Arabian Sea storms/depressions over the Ethiopian weather. *Proc. Int. Conf. on Monsoon Variability and Prediction*, WCRP-84 and WMO Tech. Doc. 619, Geneva, Switzerland, World Meteorological Organization, 228–236.
- Thiaw, W. M., A. G. Barnston, and V. Kumar, 1999: Predictions of African rainfall on the seasonal timescale. *J. Geophys Res.*, **104**, 31 589–31 597.
- Trenberth, K. E., and T. J. Hoar, 1996: The 1990–1995 El Niño–Southern Oscillation event: Longest on record. *Geophys. Res. Lett.*, **23**, 57–60.
- Tsegay, W., 1998: El Niño and drought early warning in Ethiopia. *Internet J. Afr. Studies*, No. 2. [Available online at <http://www.ccb.ucar.edu/ijas/ijasno2/georgis.html>.]
- , 2001: The case of Ethiopia: Impacts and responses to the 1997-98 El Niño event. *Once Burned, Twice Shy? Lessons Learned from the 1997-98 El Niño*, M. H. Glantz, Ed., United Nations University Press, 88–100.

- Tziperman, E., M. A. Cane, S. E. Zebiak, Y. Xue, and B. Blumenthal, 1998: Locking of El Niño's peak time to the end of the calendar year in the delayed oscillator picture of ENSO. *J. Climate*, **11**, 2191–2199.
- Wang, G., E. A. B. Eltahir, J. A. Foley, and D. Pollard, 2004: Decadal variability of rainfall in the Sahel: Results from the coupled GENESIS-IBIS atmosphere–biosphere model. *Climate Dyn.*, **22**, 625–637.
- Ward, M. N., 1998: Diagnosis and short-lead time prediction of summer rainfall in tropical North Africa at interannual and multidecadal time scales. *J. Climate*, **11**, 3167–3191.
- Wright, P. B., J. M. Wallace, T. P. Mitchell, and C. Deser, 1988: Correlation structure of the El Niño–Southern Oscillation phenomenon. *J. Climate*, **1**, 609–625.
- Zebiak, S. E., and M. A. Cane, 1987: A model El Niño–Southern Oscillation. *Mon. Wea. Rev.*, **115**, 2262–2278.
- Zeng, N., 2003: Drought in the Sahel. *Science*, **302**, 999–1000.
- , J. D. Neelin, and C. J. Tucker, 1999: Enhancement of interdecadal climate variability in the Sahel by vegetation interaction. *Science*, **286**, 1537–1540.

## Paper IV

### **Recent drought and precipitation tendencies in Ethiopia**

Viste, E., Korecha D., Sorteberg, A. (2012)

Last version of manuscript published in *Theoretical and Applied Climatology*, 2012.

The final publication is available at

[www.springerlink.com/content/r84166851504x2h2/](http://www.springerlink.com/content/r84166851504x2h2/).

# Recent drought and precipitation tendencies in Ethiopia

Ellen Viste<sup>1</sup>, Diriba Korecha<sup>1,2</sup>, Asgeir Sorteberg<sup>1,3</sup>

1 Geophysical Institute, University of Bergen, Bergen, Norway

2 National Meteorological Agency, Addis Ababa, Ethiopia

3 Bjerknes Centre for Climate Research, University of Bergen, Bergen, Norway

## Abstract

In 2011, drought in the Horn of Africa again made news headlines. This study aims to quantify the meteorological component of this and other drought episodes in Ethiopia since 1971. A monthly precipitation data set for 14 homogeneous rainfall zones was constructed based on 174 gauges, and the standardized precipitation index was calculated on seasonal, annual, and biannual time scales. The results point to 2009 as a year of exceptionally widespread drought. All zones experienced drought at the annual scale, although in most zones, previous droughts were more extreme. Nationally, 2009 was the second driest year, surpassed only by the historic year 1984. Linear regression analysis indicates a precipitation decline in southern Ethiopia, during both February–May and June–September. In central and northern Ethiopia, the analysis did not provide evidence of similar tendencies. However, spring droughts have occurred more frequently in all parts of Ethiopia during the last 10–15 years.

# 1 Introduction

As reported by news media and aid organizations, the recent drought in the Horn of Africa has had devastating consequences. The year leading to June 2011 has been claimed to be the driest in 60 years in some regions of Somalia, northern Kenya, and southern Ethiopia (USAID/FEWS 2011). Considering Ethiopia, how does the recent meteorological situation compare with previous droughts? In a gauge-based precipitation data set for 14 Ethiopian rainfall zones during 1971–2011, 2009 was the second driest year nationally, surpassed only by the catastrophic 1984 drought.

In southern Ethiopia, the data indicate that there has been a general decline in precipitation during this period. Ethiopia is frequently portrayed as a drought-stricken country, both in the media and the scientific literature (McCann 1990). A brief Internet search for drought in Ethiopia during 1999–2011 produced hits at news media and aid organizations for every year, except 2001 (e.g., Bhalla 2000; Addis 2009; CERF 2006; Nebehay 2011). As many of these reports are spot interviews in local communities, two factors may distort the meteorological information provided: the climatic diversity of Ethiopia and the difference between meteorological, hydrological, agricultural, and socioeconomic drought.

In the news media, the words famine and drought are used almost interchangeably (McCann 1990), not taking into account that famines are as much social as natural disasters (Sen 1981; Torry 1986; Webb et al. 1992; Conway and Schipper 2011; Broad and Agrawala 2000). Webb et al. (1992), referring to Harrison (1988), noted that although 21 countries in Sub-Saharan Africa experienced a severe drought in 1984/1985, only a handful of these

countries suffered famine. Drought-related famine is the result of several factors, where the lack of precipitation is only the first (Webb et al. 1992). This means that famine, in itself, cannot be taken as evidence of drought, while it is also not possible to assess the role of societal conditions without knowledge of the extremeness of the precipitation deficits.

The fact that the mean annual precipitation in parts of the Ethiopian highlands exceeds 2,000 mm (Griffiths 1972) may make the impression of Ethiopia as dry countries seem paradoxical. In the other end of the scale, arid/semiarid regions in the lowland receive a meager 300 mm. From the conditions on the ground, it may be difficult to distinguish between a dry climatology and drought in the sense of abnormally little precipitation. The strong seasonality of precipitation adds to the confusion. A dry summer season has more severe effects in the north than in the south, where not much rain can be expected to fall at that time of the year (Griffiths 1972; Korecha and Barnston 2007). In this study, the term drought is reserved for precipitation deficits that are outside of the normal range. It does not take into account that some regions may have generally dry or frequently varying conditions.

The incomplete link between precipitation and water availability also blurs the picture. In addition to hydrological factors such as evaporation and runoff, social constructions affect the amount of available water per capita (Mishra and Singh 2010). Due to the high population density, there are regions in the Rift Valley and the central Ethiopian highlands that must be considered extremely water-limited, despite annual precipitation of more than 1,000 mm (Funk et al. 2005).

Such increasing water demands may be interpreted as a reduction in precipitation. Farmers in northern Ethiopia claim to have shifted to more drought-resistant crops due to declining rainfall during the last couple of generations (Meze-Hausken 2004). However, there is little evidence for precipitation trends in this region, neither in seasonal precipitation amounts nor in the frequency and intensity of extreme events (Meze-Hausken 2004; Seleshi and Camberlin 2006; Seleshi and Zanke 2004; Bewket and Conway 2007). On the other hand, precipitation declines in southern and eastern Ethiopia have been documented, most strongly for the spring season (Seleshi and Camberlin 2006; Seleshi and Zanke 2004; Williams and Funk 2011; Funk et al. 2008).

Using gauge observations through May 2011, we present updated trend analyses for two separate regions: southern Ethiopia, which relies most strongly on the spring (February–May) rains, and central and northern Ethiopia, where the summer (June–September) is the main rainy season. In addition, the aim of this study has been to quantify the meteorological severity and rank of historic drought episodes. The standardized precipitation index (McKee et al. 1993) is used as a drought measure in each of 14 Ethiopian rainfall zones. Drought-related famines in Ethiopia have been documented from 253BC till the 1990s (Degefu 1987; Webb and Braun 1994; Webb et al. 1992) and supplemented by precipitation studies for the last decades (Korecha and Barnston 2007; Segele and Lamb 2005; Seleshi and Zanke 2004; Williams and Funk 2011), as well as local and regional drought studies (Gebrehiwot et al. 2011; Bewket and Conway 2007; Edossa et al. 2010). But a regional and nationwide comparison of the precipitation during different drought episodes is still missing. We will discuss the following years: 1972–1975, 1984, 1987, 1990–1992, 1999–2000, 2002–2003, and 2008–2011, with emphasis on the most recent event.

## **2 Data and methods**

The 14 homogenous rainfall zones described in Korecha and Sorteberg (submitted to the International Journal of Climatology, 2012) were used to represent different parts of Ethiopia. Monthly precipitation for each zone was calculated for 1972–2011, and the standardized precipitation index (McKee et al. 1993) was used to identify droughts during this period. The standardized precipitation index (SPI) is a statistical measure indicating how unusual an event is, making it possible to determine how often droughts of a certain strength are likely to occur. SPIs may also be compared directly between different locations. However, the practical implication of an SPI-defined drought, the deviation from the normal amount of precipitation, will vary from one place to another. In order to address this question, the percentage of the normal amount of precipitation was also calculated for periods of SPI-defined drought.

All drought measures were calculated based on accumulated precipitation at several time scales. Long-time drought was considered at time scales of 12 and 24 months, and the 4-month indices for May and September were used to describe the spring and summer seasons, respectively.

### **2.1 Precipitation data**

### **2.2 Gauge-based zone precipitation**

Korecha and Sorteberg (submitted to the International Journal of Climatology, 2012) identified 14 homogeneous rainfall zones covering all of Ethiopia, and details of the different zones may be found there. In Fig. 1, these zones are

plotted in a vegetation map. Ethiopia is located in the inner part of the Horn of Africa, within 3–15° N and 33–48° E, with Eritrea to the north, Djibouti to the east, Sudan to the west, Kenya to the south, and Somalia to the south and east. The Ethiopian plateau, constituting most of the green area in the vegetation map, is divided by the Rift Valley, running southwest–northeast, from zone I through parts of zones XA, IX, VIII, VII, and XII-B.

For each zone, a time series of monthly precipitation for January 1970–May 2011 was made, based on monthly data for 238 gauge stations obtained from the National Meteorological Agency of Ethiopia. First, the monthly climatology of each station was calculated and averaged over the stations in the zone to produce the zone climatology. Similarly, station anomalies were calculated for each month in the record, using the fraction of the climatological values at each station, and these values were averaged to produce a time series of zone anomalies. The anomaly series was then multiplied by the zone's climatology to obtain a time series of monthly precipitation in the zone. When calculating the climatology of the zones, only stations having data for at least 50 % of each calendar month during the reference period 1971–2000 were used. For stations to be used in the subsequent anomaly calculations, the corresponding requirement was set to 70 %. As a result, 174 stations were used in the climatology, and 132 stations in the time series. Due to the spread of observations, shown in Fig. 1, the number of stations differs from zone to zone and month to month, ranging from one in the southwestern lowlands (zone V) to a maximum of 40 in the central highlands (zone IX).

When calculating the climatology of the zones, only stations having data for at least 50% of each calendar month during the reference period 1971–2000 were used. For stations to be used in the subsequent anomaly calculations, the corresponding requirement was set to 70 %. As a result, 174 stations

were used in the climatology, and 132 stations in the time series. Due to the spread of observations, shown in Fig. 1, the number of stations differs from zone to zone and month to month, ranging from one in the southwestern lowlands (zone V) to a maximum of 40 in the central highlands (zone IX).

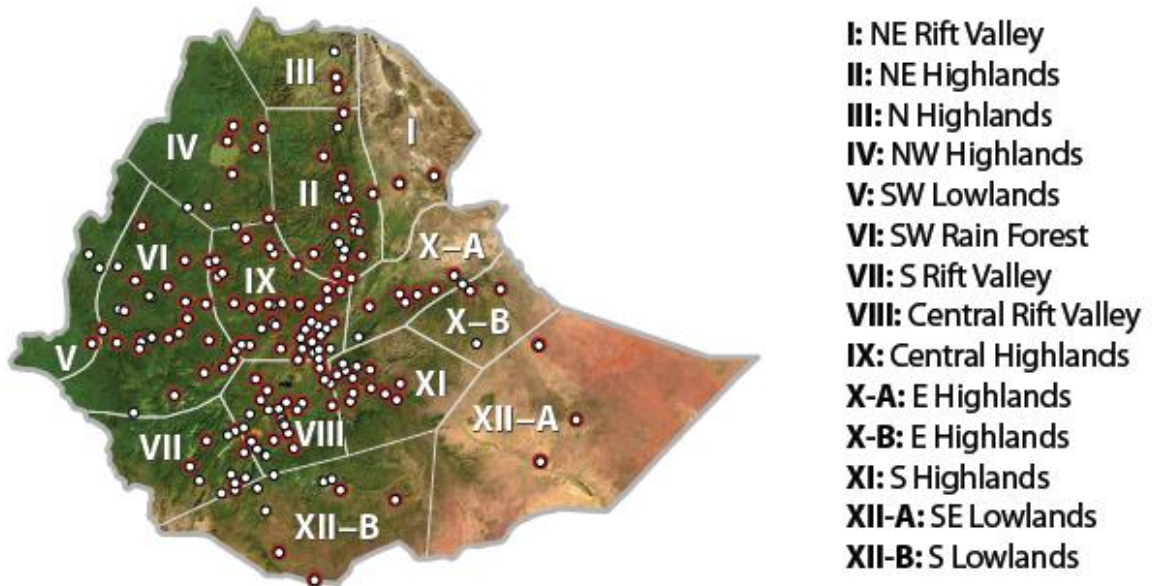


Fig. 1 Ethiopian climate zones and stations (markers: white used for climatology, red for time series). Background satellite photo: NASA/  
www.maplibrary.org

In five cases of single months with missing data in one of the zones, the anomaly fraction from that neighbor zone with the most similar seasonal cycle was used to estimate monthly precipitation for this zone. The main purpose of this filling was to avoid long-lasting gaps in the accumulated 12- and 24-month precipitation used in the SPI calculations. Apart from this, missing data were not adjusted.

Precipitation trends for 1971–2010 were calculated for two regions: One consisting of the zones where the northern hemisphere summer, June–

September, is the main rainy season and one of zones where spring, February–May, is the main rainy season. For each of these regions, and nationally, the monthly precipitation in each zone was weighted by the area of the zone and averaged to produce the regional mean precipitation. For each region, and for the country as a whole, trend analysis was performed for the summer and spring seasons used to define the regions, as well as for the fall season, October–December.

Trend lines were estimated by linear regression, using the least squares method, and the slope of the regression line tested at the 0.05 level of statistical significance. Bootstrapping was also used to calculate a mean slope value and the 95% confidence interval. Two nonparametric tests were applied to test the significance of the slope: the Spearman's rho test and the Mann–Kendall test. As the power of these tests in detecting trends is similar (Yue et al. 2002), and no practical differences between them appeared in our results, only the outcome of Spearman's rho test will be shown.

### **2.1.2 Global Precipitation Climatology Project**

Data from the Global Precipitation Climatology Project (GPCP) (Adler et al. 2003; Huffman et al. 2009) was used for comparison with the zone data in selected years. This is a merged data product that incorporates precipitation estimates from satellite microwave and infrared data and surface rain gauge observations. Version 2.2 of the monthly data, with a resolution of 2.5° latitude and longitude, was used.

### **2.3 ERA-Interim reanalysis data**

ERA-Interim reanalysis data were used to describe anomalies in the moisture flux field in the spring and summer of 2009. ERA-Interim is produced by the European Centre for Medium-Range Weather Forecasts at a resolution of about  $0.75^\circ$  latitude and longitude, with 60 vertical levels and a 4-D variational assimilation system (Simmons et al. 2006; Uppala et al. 2008; Berrisford et al. 2009). The ERA-Interim vertically integrated moisture flux was calculated by the Climate Analysis Section at the National Center for Atmospheric Research, using methods described in Trenberth et al. (2002).

### **2.4 Classifying drought using the standardized precipitation index**

The SPI (as described by McKee et al. 1993) was used to define drought periods. Requiring only precipitation as input, the SPI covers a variety of time scales and allows comparison of drought severity both between periods in time and between different locations. Drying soil is the result of several factors, where precipitation is only the first. More complicated drought indices, like the Palmer Drought Severity Index (Palmer 1965) may be favored in regions where the variability in evapotranspiration is high. On the other hand, the introduction of evapotranspiration rates introduces another element of uncertainty into the calculations (Lloyd-Hughes and Saunders 2002). It is important to acknowledge that drought conditions may be modified by evapotranspiration, but as the variability of precipitation is often greater than the variability of evapotranspiration (Ntale and Gan 2003), drought indicators based purely on precipitation give a good overall view of the situation. In regions like Ethiopia, where the access to data is limited, there are good reasons for choosing a precipitation-based drought measure.

McKee et al. (1993) defined the following four drought categories: mild drought (SPI between 0 and -0.99, occurring 24 % of the time), moderate drought (SPI between -1.00 and -1.49, occurring 9.2 % of the time), severe drought (-1.50 to -1.99, occurring 4.4 % of the time), and extreme drought (SPI -2.00 or less, occurring 2.3 % of the time). A drought event may then be defined as a period during which the SPI is continuously negative and reaches a value of -1 or less at one or more time steps. Drought begins when the SPI first falls below zero and ends with the first positive value (McKee et al. 1993). The SPI may be calculated at any time scale, depending on which effect of drought one wishes to detect. Edwards and McKee (1997) suggested using 3-month accumulated precipitation in the SPI for a short-term or seasonal drought index, a 12-month SPI for an intermediate-term drought index, and 48 months for a long-term index. In this study, SPIs were calculated for intermediate- to long-term periods of 12, 24, and 48 months. To assess seasonal drought, the 4-month accumulation was calculated for May and September, as this is the most commonly used of the definitions of the spring and summer seasons in Ethiopia.

### **2.3.1 Defining and calculating the SPI**

A simple way to describe precipitation anomalies, is to use a standard Z-score,

$Z = \frac{x - \bar{x}}{s}$ , where  $x$  is the observed precipitation value, and  $\bar{x}$  and  $s$  the mean and standard deviation, respectively, over a defined period.  $Z$  is the number of standard deviations that the observation is from the normal, assuming that the observations are normally distributed.

Precipitation is normally not normally distributed, and McKee et al. (1993) proposed a simple solution to this problem by applying a gamma transformation to the distribution. First, the gamma distribution is fitted to the observed precipitation. The SPI values are then assumed to be normally distributed and are found by comparing two cumulative distribution functions: that of the gamma-distributed precipitation and the normally distributed SPI values. The SPI of a specific observation of precipitation is the standard deviation of the normal curve at the same cumulative probability level as the precipitation.

This principle is illustrated in Fig. 2. The left panel shows a histogram made from example observations of precipitation, as well as the gamma probability function fitted to the distribution. The panel in the middle shows the corresponding empirical and theoretical cumulative probability distributions. To the right is a graph of the cumulative probability of the normal distribution. The SPI of a specific precipitation value is found by going from the gamma cumulative distribution function (CDF) to the normal CDF at the same cumulative probability level (arrow). The SPI is then the number of standard deviations from the mean of the normal distribution.

The procedure described in Edwards and McKee (1997) was used for calculating SPIs, using monthly zone precipitation as input. To determine the SPI for a specific zone, precipitation was summed over the time scale of interest, separately for each month—up to and including this month. For, e.g., a 3-month SPI, each value in the input record is the sum of this month and the two previous months. A gamma distribution is then fitted to the set of three-monthly values of accumulated precipitation.

The gamma probability distribution function is defined as

$$g(x) = \frac{x^{\alpha-1} e^{-x/\beta}}{\beta^\alpha \Gamma(\alpha)} \text{ for } x > 0, \text{ where } x \text{ is precipitation, } \alpha \text{ the shape parameter, } \beta \text{ the scale}$$

parameter and  $\Gamma(\alpha)$  the gamma function,

$$\Gamma(\alpha) = \int_0^\infty e^{-t} t^{\alpha-1} dt$$

The corresponding cumulative probability of a specific amount of precipitation,  $x$ , occurring for a given month and time scale is given by

$$G(x) = \int_0^x g(x) dx$$

The gamma distribution parameters were calculated as maximum likelihood estimates using Matlab.

As the gamma distribution is defined only for  $x > 0$ , any observations of zero precipitation must be treated separately. Let  $q$  be the probability of a zero, defined as the ratio of the number of zeros to the total number of observations. Then, the cumulative probability of a specific amount of precipitation is given by

$$H(x) = q + (1 - q)G(x)$$

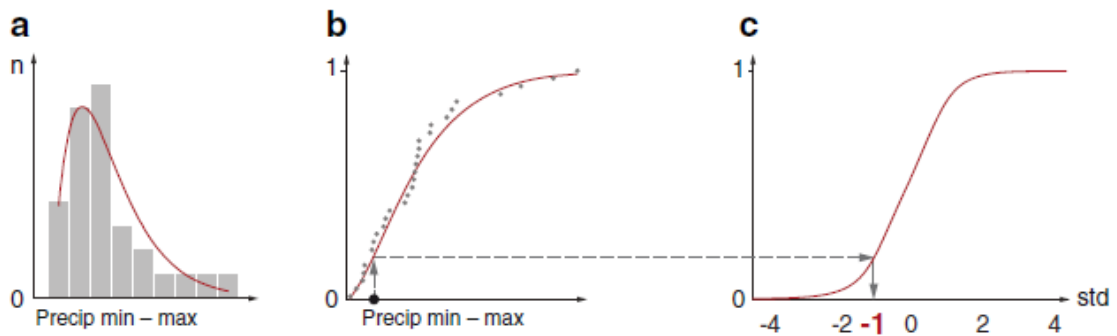


Fig. 2. Calculating the SPI. a) Bar histogram of a sample distribution of monthly precipitation, with the number of occurrences in each of nine equally spaced precipitation classes. The red curve is the gamma probability distribution function fitted to these data. b) The empirical cumulative

probability distribution of the same data (markers), with the corresponding cumulative distribution function (CDF) of the fitted gamma function (red curve). c CDF of the standard normal distribution. As indicated by the arrows in b and c, the SPI of a specific precipitation value may be found graphically by locating the gamma CDF value corresponding to this precipitation and go to the same level of the normal CDF (horizontal arrow). The SPI is then the standard deviation of the normal distribution at this level, found at the horizontal axis; in the example equal to  $-1$ . This is equivalent to fitting a gamma function to the data and then assumes that the SPI describing them is normally distributed.

### **2.3.2 Representativeness of the SPI as a measure of drought**

The SPI benefits from being simple to calculate, depending only on precipitation, but the method also has some shortcomings. The main ones are that it is a purely statistical measure, that it depends on the assumptions of gamma distributed precipitation and normal-distributed SPIs, and that records with low climatological precipitation may give misleading results.

As described by McKee et al. (1993), the SPI is uniquely related to probability. This is one of its main benefits, as specific values will be reached at specific frequencies, allowing comparison across time and space. The assumption that the SPI values are normally distributed further implies that wet and dry periods, as well as wet and dry climates, will be represented in a similar way. On the other hand, this also means that the SPI may not be used to identify regions that are more drought-prone than others. The frequency of extreme drought is the same for all regions, wet or dry.

The SPI may be altered by fitting other distribution functions than the gamma function to the precipitation data. Guttman (1999), testing various functions (two-parameter gamma, three-parameter Pearson type III, three-parameter generalized extreme values, four-parameter kappa, and five parameters Wakeby), concluded that the Pearson type III was the best universal model, as it performed well for both wet and dry events. For dry events, however, their assessment showed that there was little difference in the number, duration, intensity, or regional variation of the events as portrayed by the distributions compared.

Ntale and Gan (2003) compared different drought indices for East Africa, concluding that a modified SPI was the best indicator for monitoring East African droughts. Their modifications included replacing the gamma distribution with a plotting position formula to describe the cumulative probability distribution of precipitation. Finding the normality assumption of the SPI to be a less good approximation on time scales of 6 months or shorter, they used the Pearson type III distribution to describe the SPIs. The downside of this procedure is that it generates a drought classification in which the SPI range of each category varies with the time scale of the drought.

In dry regions, and regions where precipitation is predominantly seasonal, the statistical nature of the SPI may produce results that are easily misinterpreted, or have limited value, especially on shorter time scales. In the highlands of Ethiopia, the northern hemisphere summer is the main rainy season, whereas the northern hemisphere winter is mainly dry (Griffiths 1972; Korecha and Barnston 2007). In a running 3-month SPI, small absolute deviations in winter precipitation will generate more extreme SPI fluctuations than larger absolute deviations in summer precipitation. The implications of a

lack of rain during summer are clearly much more severe. On the other hand, even though the SPI is theoretically unbounded, the existence of zeros in the precipitation records introduces a lower bound (Wu et al. 2007).

According to Guttman (1999), the number of data points also limits the range of the SPI, and SPIs with time scales longer than 24 months may be unreliable. McKee et al. (1993) recommended using record containing at least 30 years of data when calculating the SPI. Comparing scale of ~30 and ~100 years, Wu et al. (2005) concluded that different lengths of records could give different results, especially for long time scales and especially when evaluating the severity of severe droughts. Despite the limitations of the gamma-based SPI, there are good reasons for using it as a drought indicator, one of them being that it is easily calculated and easily interpreted. An analysis of the physical meaning of the parameters ( $\alpha$  and  $\beta$ ) in the gamma distribution in African climates is presented in Husak et al. (2007). Regions are described on a monthly basis as either scale-dominated, with variable rain and more extreme events, or shape-dominated, with consistent rain and fewer extreme events. Overall and for all months, they find the gamma distribution to be suitable for roughly 98 % of the cells in a  $0.1^\circ$  grid over Africa.

### **3 Regional variations and the seasonal precipitation cycle**

In Ethiopia, the elevation ranges from 130 m below sea level in the dry Denakil depression in the northeastern lowlands (zone I, Fig. 1) to 4,550 m above sea level on Ras Dashen in the northern highlands (zone III). The climatological variation is correspondingly large, both in total precipitation

amounts and in the seasonality of the precipitation. As shown in Fig. 1, the vegetation goes from arid/semiarid in the lowlands in the southeastern lowlands (zone XII-A) and northeastern Rift Valley (zone 1), to lush green in the highlands and part of the Rift Valley cutting through them, from the southwest to the northeast. The vegetation map reflects the distribution of precipitation. As shown in Fig. 3, the annual precipitation ranges from less than 300 mm in the northeastern and southeastern lowlands (zones I and XII-A) to more than 1,700 mm in the southwestern rain forest (zone VI).

The seasonal precipitation cycle varies mainly from the southeast to the northwest, as seen by comparing the seasonal share of the annual precipitation, in the lower panel in Fig. 3. The northern hemisphere spring season, February–May, plays a role in most of the country, with shares of the annual precipitation ranging from 12 % in the northwestern highlands (zone IV) to 62 % in the southeastern lowlands (zone XII-A). In the three southernmost zones, spring is the wettest season. The spring rains are important not just for the spring crops, accounting for 5–15 % of the national food crop, but also for improving pasture for livestock and for the planting of long-season crops that are harvested in September–December (Degefu 1987; Funk et al. 2003; McCann 1990). The interannual variability of the spring rains is higher than the summer rains, and on resource poor farms, the spring crop may be what determines whether the annual productivity reaches the critical margin (McCann 1990).

June–September is the main rainy season in the rest of the country, contributing to more than 70 % of the annual precipitation in the north and northwest (Fig. 3). About 85–95 % of the Ethiopian food crop is produced in this season (Degefu 1987). In the northern highlands (zone III), a substantial part of the annual precipitation falls in July–August (Fig. 3). This is the time

when the tropical rain belt associated with the intertropical convergence zone is at its northernmost position, above northern Ethiopia and Eritrea (Leroux 2001; Degefu 1987).

The only region where June–September cannot be considered a rainy season, is in the southern and southeastern lowlands (zones XII-A and XII-B). In addition to spring, October–November is important in the south and southeast, providing 20–26 % of the annual precipitation. The actual amount of precipitation falling in October–November is as high, or higher, in parts of the highlands as in the dry lowlands. Still, in the highlands, both the spring and the summer precipitation exceed that of October–November (Fig. 3). Together with December–January, this is mainly a harvest season (Degefu 1987).

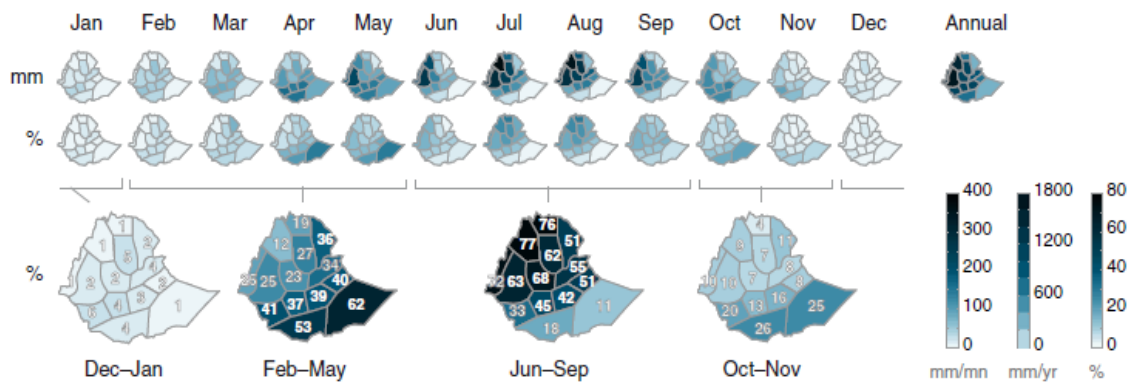


Fig. 3 The seasonal precipitation cycle in Ethiopian rainfall zones: 1971–2000 monthly mean precipitation [in millimeters] (first row; left color bar), annual [in millimeters] (first row; middle color bar), and monthly (second row) and seasonal (third row) percentage of annual precipitation (right color bar and white numbers in the seasonal maps)

During December–January, no part of the country receives more than 6 % of the annual precipitation, in several zones as little as 1 % (Fig. 3). The rain that occasionally falls during these months is important for grazing cattle and the absence such rainfall in 1983–1984 marked the beginning of catastrophic 1984 drought (Degefu 1987). However, as these months are generally dry, they constitute a barrier between the growth seasons. Thus, it is practically meaningful to consider the 12-month accumulated precipitation at the end of the year as a collective drought measure for the year.

#### **4 Comparison of drought episodes**

Drought has occurred at different times in different parts of Ethiopia. This is partly a result of the variation in the seasonal precipitation cycle; as discussed in Section 3, the impact of missing rain during spring or summer is not the same in all zones. Webb et al. (1992) identifies the southern, southeastern, and northeastern parts of Ethiopia as most often affected by drought and famine. This is equivalent to zones I, II, VII, XII-A, and XII-B and parts of VII, X-A, XB, and III. Three factors are mentioned as differing in these regions, compared to the rest of the country: population pressure, agro-ecological resource base, and climate (Webb et al. 1992). In the first part of this section, the standardized precipitation index is used to assess the severity of drought episodes during 1972–2011. Then, the most severe year during the last decade, 2009, is discussed in more detail.

When discussing drought, precipitation anomalies during seasons with low mean precipitation in each zone will not be taken into account. This does not mean that less than normal precipitation at this time of the year is without consequences, e.g., for specific crop types, but that precipitation deficiencies during the dominant rainy seasons have a much larger impact. The timing of

the onset and cessation as well as the frequency and duration of dry spells during the season also have an impact on the effect of Ethiopian droughts (Segele and Lamb 2005). This question has not been addressed, as only monthly precipitation data were available.

#### **4.1 Severity of drought episodes since 1971**

Mild drought occurred in parts of the Rift Valley and the northeastern highlands at the end of 1971. But 1971 was not particularly dry, and data for this year have not been included in Fig. 4, showing the 12-month SPI in December in each of the zones during 1972–2010. The rank of the SPI is the same as the rank of the annual precipitation. As the maps indicate, well-known drought episodes are associated with different degrees of severity on the SPI classification scale described in Section 2.3. Some years, like 1984, 2002, and 2009, were dry in most of Ethiopia, whereas other episodes, like the drought in the south in 1999–2000, affected more limited regions. Similar to the annual values in Figs. 4, 5, and 6 show 4-month SPI values in May and September, representing spring and summer, respectively.

SPI values are statistical expressions of the severity of a drought, relative to how unusual each drought level is. It is not possible to infer anything about the amount of missing water from SPI values. As a measure of the precipitation deficiency, Fig. 7 shows the percentage of the annual precipitation corresponding to the annual SPI droughts in Fig. 4. The relative reduction of precipitation in unusually dry years is higher in dry zones like the northeastern Rift Valley (I) and the southern (XII-B) and southeastern (XII-A) lowlands than in precipitation-rich zones like the central highlands (IX) and the southwestern rain forest (VI). For example, the year 1984 was the driest

in the record in both the northeastern Rift Valley (I) and the northeastern highlands (II); the northeastern highlands being most extreme on the SPI scale (Fig. 4). Still, the relative reduction in precipitation (Fig. 7) was larger in the northeastern Rift Valley, which received only 18 % of the annual mean precipitation this year, compared to 59 % in the northeastern highlands.

The following sections describe selected drought periods, with reference to Figs. 4, 5, 6, and 7. SPI maps for every month at time scales of 3, 4, 6, 9, 12, and 24 months have also been examined, but are not shown. When discussing seasonal drought, the 4-month time scale for May (spring) and September (summer) is used, unless otherwise specified.

#### **4.1.1 1972–1975**

The 1972–1975 drought may mainly be considered a combination of distinct episodes, and most of Ethiopia experienced moderate, severe, or extreme drought at some stage. The most extreme single season was the spring of 1973, which was severely or extremely dry in a band crossing the country from the southwest to the northeast. In 6 of the 14 zones, this was one of the three driest spring seasons during 1972–2011 (Fig. 5). The following summer was not particularly dry, but 1973 still ended up among the one–five driest years in four zones—in the eastern highlands (XIIA), the driest, with 63 % of the annual mean precipitation (Fig. 7). In half of the zones, this was the second drought year in a row. In 1974 and 1975, seasonal drought occurred in some zones, but the wet summer of 1975 led to above-normal precipitation in most of the country, except in the southeast.

### 4.1.2 1980–1982

During the early 1980s, drought occurred in different parts of the country at different times. In 1980, the southeastern lowlands (zone XII-A) experienced severe drought at all the time scales considered, with extreme drought at time scales of 6–24 months. As shown in Fig. 4, this was the driest year in this zone. The summer of 1982 was severely dry in the northern (III), northwestern (IV), northeastern (II), and central (IX) highlands, making this the driest year in the northwestern highlands (IV; Fig. 6).

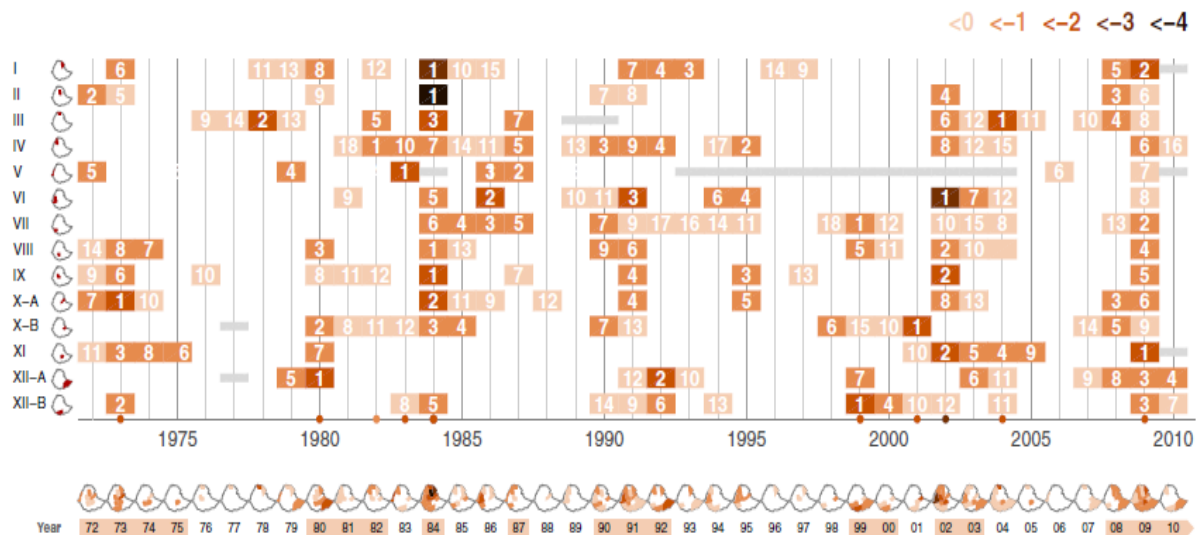


Fig. 4 Severity of droughts on the annual scale, as time series and maps for Ethiopian rainfall zones. Data: 12-month SPI for December during 1972–2010, showing only years when there was an SPI-defined drought, as described in the text. The small maps to the left show the location of the zones, in red. For each zone, annual SPI values are presented as a row of rectangles, with colors indicating the severity of drought relative to the SPI scale in the upper right corner. Gray horizontal bars represent missing values. The white numbers in the

rectangles show the rank of each year among the driest for each zone. The colored dots at the horizontal axis mark years when at least one zone was at its driest during the record. The row of maps below the set of zone time series summarizes the situation for the country from year to year. Well-known drought years have been marked with orange under these maps.

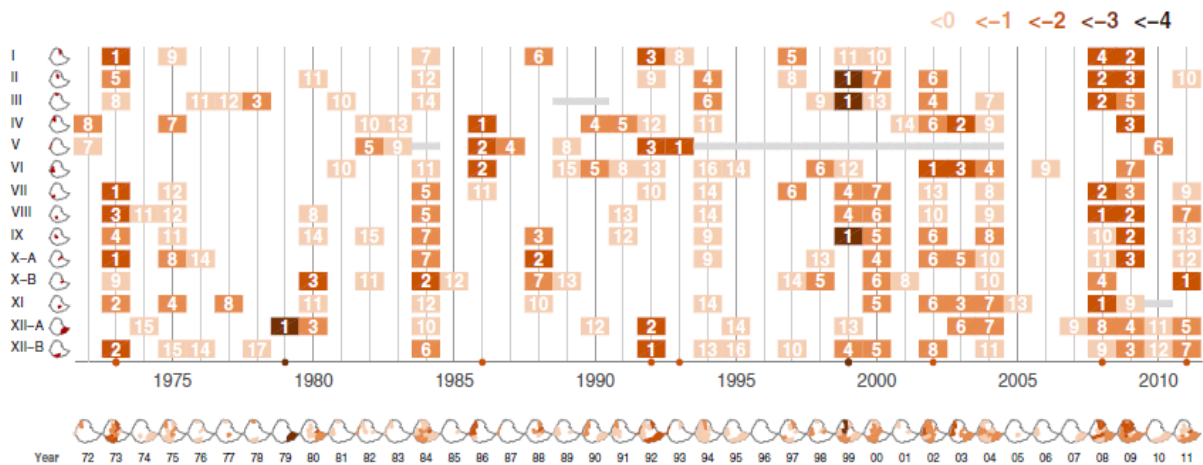


Fig. 5 Severity of spring droughts, as time series and maps for Ethiopian rainfall zones. Data: 4-month SPI for May (i.e., based on February–May accumulation) during 1972–2011, showing only years when there was an SPI-defined drought, as described in the text. The small maps to the left show the location of the zones, in red. For each zone, spring SPI values are presented as a row of rectangles, with colors indicating the severity of drought relative to the SPI scale in the upper right corner. Gray horizontal bars represent missing values. The white numbers in the rectangles show the rank of each spring among the driest for each zone. The colored dots at the horizontal axis mark springs when at least one zone was at its driest during the record. The row of maps below the set of zone time series summarizes the situation for the country from year to year.

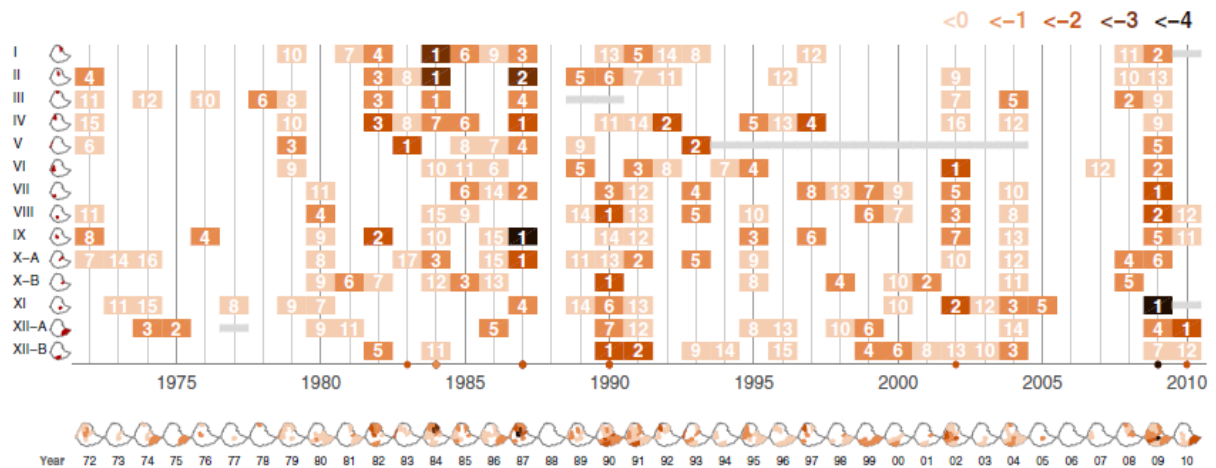


Fig. 6 Severity of summer droughts, as time series and maps for Ethiopian rainfall zones. Data: 4-month SPI for September (i.e., based on June–September accumulation) during 1972–2010, showing only years when there was an SPI-defined drought, as described in the text. The small maps to the left show the location of the zones, in red. For each zone, summer SPI values are presented as a row of rectangles, with colors indicating the severity of drought relative to the SPI scale in the upper right corner. Gray horizontal bars represent missing values. The white numbers in the rectangles show the rank of each summer among the driest for each zone. The colored dots at the horizontal axis mark summers when at least one zone was at its driest during the record. The row of maps below the set of zone time series summarizes the situation for the country from year to year.

### 4.1.3 1984

Webb et al. (1992) noted that when severe drought hit Ethiopia in 1984, the famine was already under way, as a result of dry episodes during the previous years. Although 1983 was close to normal in most of Ethiopia, a dry season in the winter of 1983–1984 caused problems for livestock and led to pastoralist movements as early as January 1984 (Degefu 1987). Segele and Lamb (2005) also extensively demonstrated the severity of the 1984 drought over Ethiopia, particularly during the summer season.

As shown in Figs. 4, 5, and 6, the drought in 1984 was severe in the northeastern half of the country, while all zones were affected at the seasonal level. In half of the zones, 1984 was among the three driest years, being the driest in the northeastern Rift Valley (zone I), the northeastern highlands (II), the central highlands (IX), and the central Rift Valley (VIII). The northeastern Rift Valley (I) received only 18 % of its mean annual precipitation (Fig. 7), by far the highest relative deviation in any zone during 1972–2010. The severity of the 1984 drought was strengthened as all the three rainy seasons were dry in those parts of the country where they are effective. April and August were the most extreme months, and a dry October contributed to the mild–moderate drought in the south.

Degefu (1987) gives an account of the development of the 1984 drought in Ethiopia, including a description of the atmospheric circulation during spring and summer. In the spring season, the interaction between tropical lows and middle latitude low pressure systems was hindered by pressure anomalies over the Sahara and the Arabian Peninsula. In general, wave activity was reduced (Degefu 1987). The ERA-Interim wind field at 700 and 850 hPa suggests that the transport of air and moisture from the equatorial Indian Ocean toward Ethiopia in April was reduced, and the vertical velocity at 500 hPa indicates reduced convection/increased subsidence over the Horn of Africa (not shown). The tropical cyclone Kamisy, which developed over the southern Indian Ocean in April 1984, has been blamed for disturbing the normally northwestward flow of moisture (Shanko and Camberlin 1998).

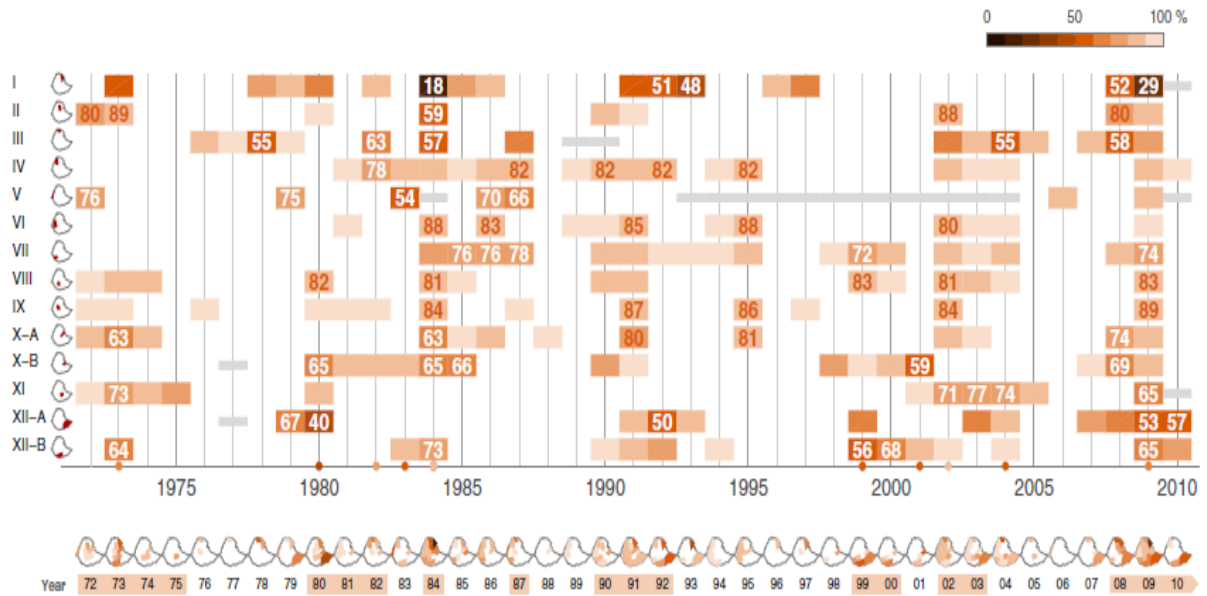


Fig. 7 Percentage of annual mean precipitation during SPI-defined, 12-month scale drought periods, as time series and maps for Ethiopian precipitation zones, during 1972–2010. Only years when there was an SPI-defined drought, as described in the text, are shown. The small maps to the left show the location of the zones, in red. For each zone, the percentage of the annual mean in each year is shown as a row of rectangles, colored relative to the scale in the upper right corner. The percentage values for the five driest years in each zone are repeated as white numbers inside the rectangles. Gray horizontal bars represent missing values. The colored dots at the horizontal axis mark years when at least one zone was at its driest. The row of maps below the set of zone time series summarizes the situation for the country from year to year. Well-known drought years have been marked with orange under these maps.

During the summer season, many of the characteristic atmospheric circulation anomalies during dry Ethiopian summers (Segele et al. 2009) may be seen in the reanalysis fields, e.g., in August the low-level East African jet was weaker than normal, causing less transport of moisture from the Indian Ocean. Easterly anomalies in the 700- and 850-hPa winds to the west of

Ethiopia signifies reduced transport from Central Africa, and southerly anomalies above northern Ethiopian and the southern Red Sea indicates less transport from the north. Convection was reduced, not only in Ethiopia, but in a band reaching across the Sahel and into the Atlantic Ocean. GPCP anomaly maps for July and August (not shown) show that the rain-belt above Africa was reduced or deflected southward.

#### **4.1.4 1987**

In 1987, the wettest spring season during 1972–2011 was followed by the all-over driest summer season (Fig. 6). This episode can be characterized as a summer drought in the highlands, reaching extreme levels on the 4-month scale. This was primarily caused by missing rain in July. Followed by a dry fall, and then a dry spring in 1988, the drought reached extreme levels also on the 12-month scale in May 1988. A wet summer then ended the drought on all scales below 12 months. According to Webb et al. (1992), the spring crops were destroyed by locust invasions, and this may have exacerbated the effect of the consecutive summer drought.

#### **4.1.5 1990–1992**

During 1990–1992, all zones experienced moderate, extreme, or severe drought on the seasonal or annual level. The years 1990 and 1991 were dry in all of Ethiopia, with the exception of a small positive deviation in the northeastern Rift Valley (I) in 1990. A severely dry spring in 1992 followed, causing extreme drought on the 12-month scale in the southern (XII-B) and southeastern (XII-A) lowlands, as well as in the northeastern Rift Valley (I) and the northwestern highlands (IV). In the southern lowlands (XII-B), the spring of 1992 was the worst during 1972–2011, and in the southeastern lowlands (XII-A) the second worst (Fig. 5). These zones get 50–60 % of the

annual precipitation in spring (Fig. 3). As a result, the southeastern lowlands (XII-A) received only 50 % of the mean annual precipitation in 1992 (Fig. 7).

#### **4.1.6 1999–2000**

The years 1998, 1999, and 2000 were all dry in the south, mainly due to dry spring seasons. In January–February 1999, the three southwestern zones (VII, VIII, and XII-B) already experienced mild to moderate drought on the 12-month time scale. Though 1992 was comparable at some time scales, the worst drought in the southern lowlands (XIIB) occurred in 1999–2000. The year 1999 was the driest year during 1972–2010 in this zone, and severe drought occurred at all time scales at some stage. Similarly, the combination of 1999 and 2000 made this the driest period on the 24-month time scale.

The spring season in 1999 was dry in all of Ethiopia in both years, and as shown in Fig. 5, seasonal drought occurred in most of the country. In the Northern (III), Northeastern (II), and central highlands (IX), the 1999 spring was the driest during the record. Summer and fall were wet in the highlands, leading to normal or above normal annual precipitation in the northern half of the country. The spatial anomaly pattern for 2000 is strikingly similar to that of 1999, with a dry spring followed by a wet summer in the north, this time with a wet fall season everywhere, except in the southwest.

#### **4.1.7 2002–2003**

Due to a dry spring followed by a dry summer, 2002 became one of the driest years during 1972–2011. In the southwestern rain forest (VI), this was the driest year, and in the central Rift Valley (VII), the central highlands (IX), and the southern highlands (XI) the second driest (Fig. 4). After a dry spring in 2003, a wet summer brought some relief, but 2003 was also drier than

normal. In the southwestern rain forest (VI), the drought was extreme at all-time scales from 3 to 24 months and at some time scales also in adjacent zones and in the southern highlands (XI). At the 12-month scale, moderate to severe drought persisted in most of the highlands and the central Rift Valley from June–July 2002 through July 2003.

#### **4.1.8 2008–2011**

Figure 5 displays a visual cluster of dry spring seasons during the last decade. This is in accordance with Williams and Funk (2011), linking decreasing precipitation in East Africa in March–June with an eastward displacement of the circulation above the Indian Ocean. The drought from 2008 until the present has been characterized by the repetition of dry spring seasons. Dry springs affect all of Ethiopia, causing the largest relative precipitation deficits in the south, where this is the main rainy season (Fig. 3). Except for a wet intermezzo in 2006, and 3 years with just above-normal values in one of the zones, the southern (XII-B) and southeastern (XII-A) lowlands have been drier than normal in every year from 1998 through 2010 (Fig. 4). During this period, only 1998, 2005, and 2006 did not experience some degree of drought in at least one of these zones (Fig. 4). This set the stage for the recent drought.

Among the recent years, 2009 stands out as the driest, being among the three driest years during 1972–2010 in 5 of the 14 zones. In the southern highlands (XI), this was the driest year in the record, and in the northeastern Rift Valley (I) and the southern Rift Valley (VII), the second driest year. As shown in Fig. 5, the spring season was dry in both 2008 and 2009, with the exception of the westernmost part. In most of the country, at least one of these springs was among the three driest during 1972–2011. Then came the summer of 2009, the driest or second driest in 5 of the 14 zones.

As shown in Fig. 4, 2009 was the only year during 1972–2011 when drought occurred on the annual scale in all of Ethiopia, in most zones ranging from moderate to severe. In most zones, more extreme levels of drought were reached during other years, but the drought was never as widespread, neither on annual nor on seasonal levels (Figs. 5 and 6).

The year 2010 was also dry in the south, ending with mild to moderate drought on the 12-month time scale in December (Fig. 4). For the rest of Ethiopia, the picture is mixed. The drought in the south continued with a dry spring in 2011 (Fig. 5), and at the end of the record in May 2011, the drought in the southern and southeastern lowlands (XIIB and XII-A) was still severe on time scales of 12 and 24 months. In the eastern highlands (X-B), the 2011 spring was the driest during 1972–2011.

Though confirming the existence of extreme to severe drought in southern Ethiopia in 2010–2011, the zone aggregated precipitation data do not confirm the extremeness previously reported (USAID/FEWS 2011); the driest year in 60 years. The driest 12-month periods in the southern and southeastern lowlands (zones XII-A and XII-B) occurred in 1992 and 2000, respectively. This does not exclude the possibility of local conditions in 2011 being even worse than at the zone level.

## **4.2 A closer look at 2009**

In Section 4.1, 2009 was found to be the driest among the recent years, while 1984 must be said to be the driest year during 1972–2010. The droughts in Ethiopia in the 1970s and 1980s were part of a drought belt ranging from the West African Sahel to the Horn of Africa, a typical African drought pattern

(Flohn 1987; Nicholson 1986; Mattsson and Rapp 1991). However, there is no one-to-one correspondence between precipitation anomalies in the Sahel and the Horn of Africa (Flohn 1987), and 2009 does not appear to be a typical example of this kind of situation. In this section, we will briefly discuss some of the large-scale features associated with the 2009 drought.

#### **4.2.1 Continental drought: 2009 compared with 1984 and 2002**

Figure 8 shows the large-scale drought patterns in the three driest years in Ethiopia: 1984, 2002, and 2009. SPI values based on the GPCP data set demonstrate quite distinct patterns for these 3 years. Whereas the 1984 drought covered a latitudinal belt across Africa, including the Sahel and northern Ethiopia, the 2009 drought struck Ethiopia and the regions to the southwest: northwestern Kenya, Uganda, South Sudan, and parts of the Central African Republic and the Democratic Republic of the Congo. The year 2002 was dry in Ethiopia and West Africa, but without the consecutive trans-African belt characterizing 1984. Even though both the spring and the summer season were dry in both 1984 and 2009 (Section 4.1), the large-scale patterns in Fig. 8 reflect the fact that in 1984 the summer was the most extreme season, whereas the spring was particularly dry in 2009. The 1984 drought follows the northern hemisphere summer rain belt, whereas the core of the 2009 drought is located farther south, covering the Horn of Africa and the northern part of East Africa. In these regions, the February–May season is at least as important.

As the rank map in the lower left corner shows, 2009 was the driest or second driest year in most of Ethiopia in the GPCP data; more severe than both 1984 and 2002. The discrepancy between the gauge-based zone data described in this study and the satellite-based, gauge-adjusted GPCP data set may have

several causes. The GPCP data benefit from having satellite-based data in regions where observations are generally scarce, like the southwestern and southeastern lowlands (zones V and XII-B; Fig. 1). On the other hand, the number of Ethiopian gauges with freely available data is very limited, implying that anomalies at these stations may be given too much weight in other parts of Ethiopia. As there are large local variations in rainfall in Ethiopia, the quality of the GPCP and similar data sets is lower than it would have been if more ground observations had been included (Dinku et al. 2007).

#### **4.2.2 Atmospheric moisture transport in 2009**

Atmospheric circulation anomalies indicate that deflections of the transport of moisture to Ethiopia contributed to the drought in 2009 (Fig. 9). During the northern hemisphere winter, the low-level flow along the coast of East Africa is northeasterly. In spring, a southerly flow begins, developing into the Somali or East African low-level jet in summer (Findlater 1969a, b, 1977; Riddle and Cook 2008). In April, this jet is still under development, with a southeasterly flow reaching the coast of Kenya and Tanzania, while the flow in the northern Indian Ocean is still mainly northeasterly, entering the coast of the Horn of Africa from the east. As shown in Fig. 9a, the convergence zone that covers most of Ethiopia in April occurs as this easterly flow meets the southeasterly flow bringing moisture from the southern and equatorial Indian Ocean. Figure 9c shows how southwesterly anomalies deflected moisture away from the coast of East Africa in April 2009. This is a result of similar anomalies in the low-level wind field, seen at 700 and 850 hPa (not shown). The anomalies hinder both the flow from the southeast and the east, resulting in a divergence anomaly covering most of Ethiopia. The convergence anomaly to the southwest of Ethiopia is due to the northeasterly anomaly in this region, the result of a strengthening of the 700-hPa wind field (not shown).

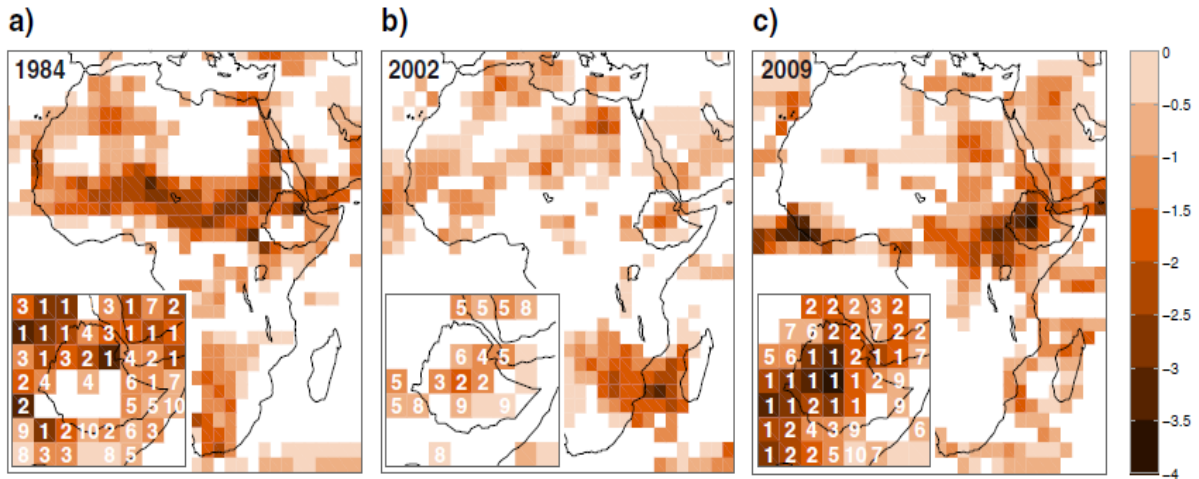


Fig. 8 Continental SPI distribution in 1984, 2002, and 2009. Twelve-month SPI of GPCP V2.2 in December 1984 (a), 2002 (b), and 2009 (c). The small, inset maps show the rank among the driest years during 1979–2010, for a region surrounding Ethiopia.

During the northern hemisphere summer, air masses from the Indian Ocean, Central Africa, and the Red Sea region flow toward Ethiopia (Mohamed et al. 2005; Korecha and Barnston 2007; Levin et al., 2009; Segele et al. 2009; Viste and Sorteberg 2011). As shown in Fig. 9b, this causes strong moisture convergence above the Ethiopian highlands. Reduced precipitation may occur either if less moisture is available in the highlands or due to reduced convergence and ascent. Figure 9d shows reduced convergence above large parts of Ethiopia in July–August 2009, as well as in a zone to the southwest, reaching from Ethiopia across the continent to the Gulf of Guinea. There is a large belt of easterly anomalies in the moisture flux in this region, as well as in the transport into the continent from the Indian Ocean through the Turkana Channel in southern Ethiopia and northern Kenya. More moisture than normal entered both Ethiopia and the rest of the continent in this region, but the easterly anomaly farther west was stronger, leading to divergence. The inflow of moisture from the Red Sea to Ethiopia was also reduced.

The moisture transport anomalies in April and July–August 2009 were in line with previously documented conditions that reduce precipitation Ethiopia. The transport in April was similar to the transport in the driest spring seasons discussed by Williams and Funk (2011), whereas easterly anomalies in the July–August transport above Central Africa are known to cause reductions in the inflow of moisture to the Ethiopian highlands (Segele et al. 2009; Williams et al. 2011; Viste and Sorteberg 2012). The question remains whether these—or other relevant atmospheric anomalies—were connected or whether the dry spring in 2009 being followed by a dry summer was just an unfortunate random combination. We did not find indications of any consistent statistical relationship between precipitation or drought conditions in the spring and the summer season. Over all, dry spring seasons were as often followed by wet summers as by dry summers. However, Williams et al. (2011) found that precipitation variability in the Greater Horn of Africa during summer has been increasingly influenced by circulation anomalies caused by a warming of the southern tropical Indian Ocean. Based on similarities in spatial patterns of precipitation trends during spring and summer, they suggested that there may be a common mechanism behind suppressed precipitation in both seasons. If this is the case, and the associated circulation anomalies continue to occur, the probability of two-season droughts may increase.

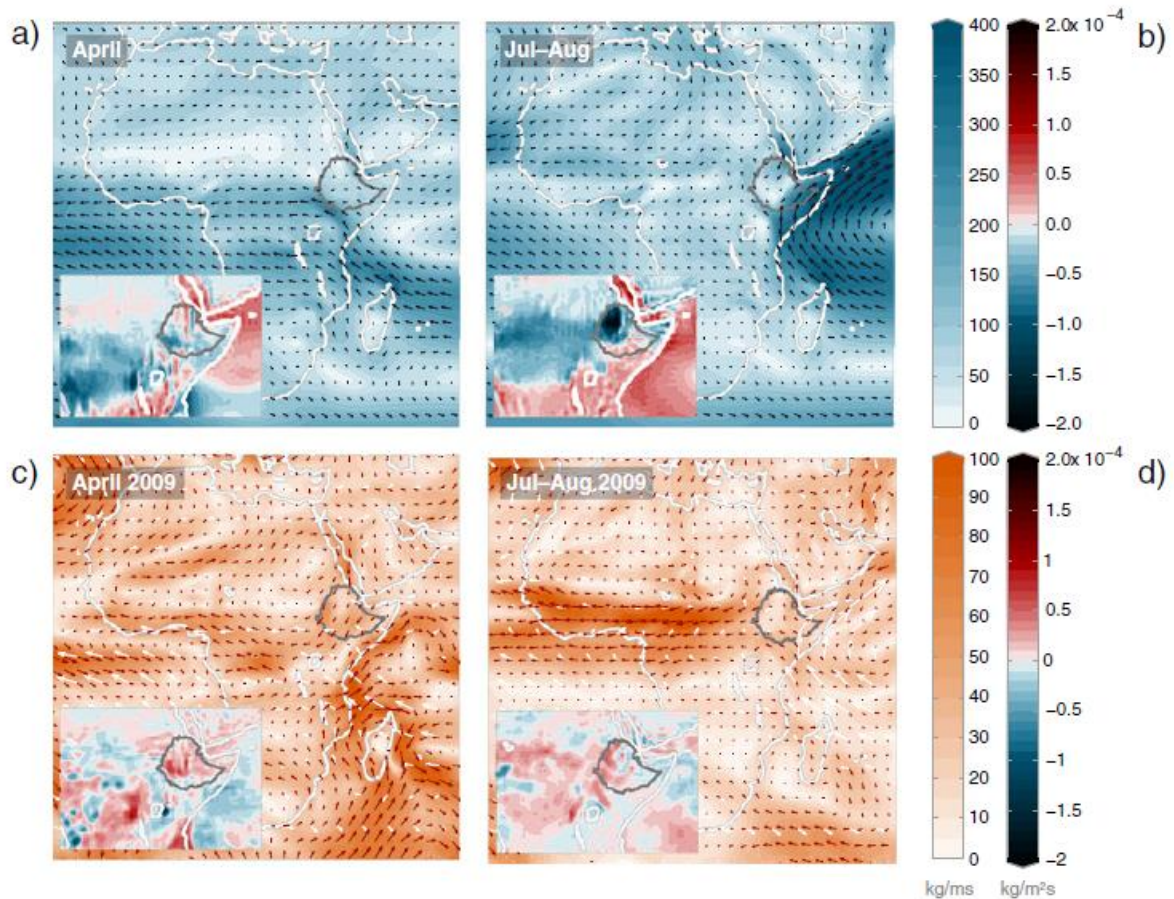


Fig. 9 Moisture flux anomalies in 2009. ERA-Interim vertically integrated moisture flux and moisture flux divergence (small, inset maps): 1981–2010 mean values in April (a) and July–August (b) and deviations from this mean in April 2009 (c) and July–August 2009 (d). The white background arrows in c and d represent the mean flux shown in a and b, respectively

## 5 Trends in seasonal precipitation

Precipitation trends in Ethiopia have been the subject of several studies, with sometimes contrasting conclusions (Conway 2000; Seleshi and Zanke 2004; Funk et al. 2003; Shang et al. 2011; Bewket and Conway 2007). In the data set used in this study, trend analysis indicates that rainfall in southern Ethiopia has decreased from 1971 till the present, both annually and in the

northern hemisphere spring and summer seasons. No clear trends could be detected in central and northern Ethiopia.

The 14 rainfall zones were categorized into two regions, depending on whether February–May or June–September contributes most to the annual precipitation. As shown in Fig. 3, the “spring region” thus consists of the three southernmost zones (VII, XII-A, and XII-B), whereas the rest of Ethiopia make up the “summer region”. The regional precipitation, shown in Fig. 10, was calculated as area weighted averages of the zones in each region. As described in Section 2.1.1, trends were calculated using linear regression and the significance was tested with bootstrapping and the nonparametric Spearman's rho test. In Fig. 10, trend lines are shown in those cases where the null hypothesis of no trend could not be rejected at the 0.05 significance level. In the remaining cases, the p values of the various tests were too high. Statistical test results are given in Table 1. In general, there was good correspondence between the results of the different statistical tests applied.

In the spring region, the February–May precipitation has declined with 2.6 mm/year during 1971–2010. Comparing the expected values in 1971 and 2010, this amounts to a reduction of 30 %. This is in line with Williams and Funk (2011), who found a general decrease in the March–June precipitation in East Africa during 1979–2009 compared to 1950–1979. In addition to the decline in the main rainy season in the spring region, Fig. 10 also shows a reduction of almost equal magnitude (2.2 mm/year) in the drier June–September season, amounting to a reduction of more than 50 %. The total annual reduction in the spring region is 32% (5.4 mm/year). Previously, a decline in precipitation has been documented for individual gauge stations in southern, southwestern, and southeastern Ethiopia during 1965–2002, but mainly during June–September from 1982 (Seleshi and Zanke 2004).

Investigating extreme rainfall events in the same data, Seleshi and Camberlin (2006) reported decreasing trends in extreme rainfall intensity during both February–May and June–September at the same stations.

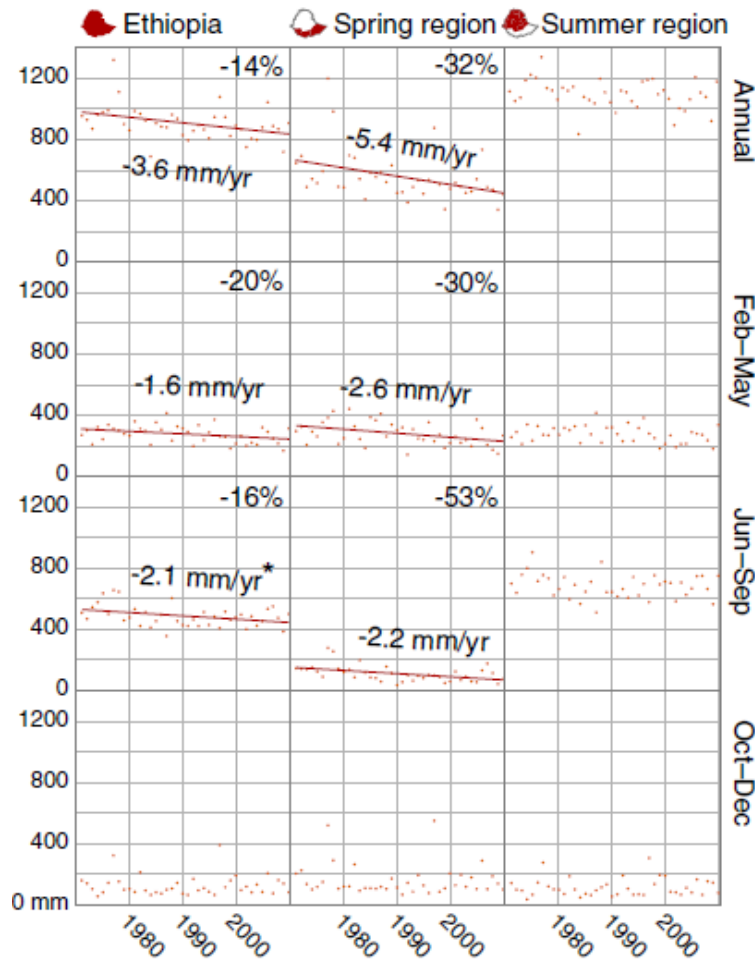


Fig. 10 Precipitation trends. Annual and seasonal regional precipitation of 1971–2010; nationally and for regions where the spring/summer contributes most to the annual precipitation. Linear regression trend lines and slope values are shown when statistically significant ( $p < 0.05$ ) and also passing Spearman's rho test and the bootstrap test. Exception: the national June–September trend (marked with asterisk) passed all criteria, except Spearman's rho test. The percentage in the upper right corner marks the change in the expected value over the period, comparing the trend line values in the first and last year.

The results of most previous studies do not show any clear signs of changing rainfall patterns in central and northern Ethiopia (Seleshi and Camberlin 2006; Seleshi and Zanke 2004; Bewket and Conway 2007; Cheung et al.2008). The results of this study are similar: The hypothesis of no trend in this region could not be rejected at the 0.05 % significance level, neither annually nor in any of the seasons. However, Fig. 5 demonstrates a visual clustering of dry seasons during the last 10–15 years in this part of the country, as well as in the south. The frequency of spring droughts was higher in this period than in the previous decades.

Table 1 Ethiopian precipitation trends in 1971–2010 [in millimeters per year]

	Linear regression trend and 95 % CI	Bootstrap mean trend and 95 % CI	Linear regression $R^2$	Linear regression	Spearman p
National, annual	-3.6 [-6.4 -0.7]	-3.6 [-6.5 -0.9]	0.14	0.016	0.006
National, MAM	-1.6 [-3.1 -0.1]	-1.6 [-3.1 -0.3]	0.11	0.037	0.044
National, JJAS	-2.1 [-4.0 -0.3]	-2.1 [-4.1 -0.3]	0.13	0.023	0.057
National, OND	0.1 [-1.8 2.0]	0.1 [-1.8 1.7]	0.00	0.921	0.877
Spring region, ann	-5.4 [-9.7 -1.1]	-5.5 [-10.4 -1.6]	0.15	0.014	0.002
Spring region, MAM	-2.6 [-4.6 -0.6]	-2.5 [-4.6 -0.7]	0.15	0.013	0.014
Spring region, JJAS	-2.2 [-3.5 -0.9]	-2.2 [-3.5 0.9]	0.23	0.002	0.001
Spring region, OND	-0.7 [-3.6 2.1]	-0.7 [-3.4 1.8]	0.01	0.606	0.545
Summer reg, ann	-2.1 [-4.7 0.5]	-2.0 [-4.9 0.6]	0.07	0.110	0.133
Summer region, MAM	-1.2 [-2.7 0.3]	-1.2 [-2.7 0.1]	0.06	0.121	0.121
Summer region, JJAS	-1.3 [-3.5 0.9]	-1.3 [-3.4 0.9]	0.04	0.239	0.333
Summer region, OND	0.3 [-1.4 2.0]	0.3 [-1.3 1.7]	0.00	0.726	0.665

Linear trend slope and 95 % confidence interval determined by regression (first data column) and bootstrap (second column), with p values from the regression (third column) and Spearman's rho test (fourth column) on the national level and in regions dominated by spring and summer precipitation ann annual, MAM March–May, JJAS June–September, OND October–December.

The decline in precipitation in the southern part of the country is large enough to produce trends on the national level, despite the lack of trends in central and northern Ethiopia. The annual change during 1971–2010 was  $-3.6$  mm/year, a reduction of 14 % over the period. This was a result of a reduction of 1.6 mm/year in February–May and 2.1 mm/year in June–September. No

trends could be seen in any of the regions in October–December. Contrasting the lack of trends in other studies, Conway (2000) found that the rainfall over the Upper Blue Nile Basin in the Ethiopian highlands had decreased markedly from the mid-1960s to the late 1980s. As pointed out by Bewket and Conway (2007), the use of different time periods in the analyses is most likely the main reason for discrepancies between trend studies in the central and northern highlands. The dry years of the 1980s were followed by recovering rainfall in 1990s. Thus, it is more likely that a negative trend will be detected in a time series ending in the late 1980s or early 1990s, than in the late 1990s. Over the more than hundred years from 1898 to 2002, Conway and Bewket (2004) found no trend in precipitation in Addis Ababa, though they also noted that the lack of spatial correlation means that this record may not be used to infer anything about other parts of the Ethiopian highlands.

The main result (not shown) of changing the period in our analysis from 1971–2010 to 1981–2010 was that significant trends occurred only in February–May, and then in both the spring and summer regions, as well as nationally. The reduction in the spring region was as high as 4.3 mm/year (37 %), in the summer region 2.6 mm/year (24 %), and nationally 3.2 mm/year (29 %).

## **6 Conclusions**

Analysis of gauge-based precipitation data for 14 Ethiopian climatic zones during 1971–2011 justifies the international concern about the recent dryness. Some of the last years have been among the driest in this period, and in southern Ethiopia, precipitation has declined, both in the spring (February–May) and the summer season (June–September). Dry spring seasons have characterized the period since 1999, affecting most of Ethiopia.

The largest relative precipitation deficits have appeared in the south, where this is the main rainy season. The rest of the country has also experienced extremely dry springs during the last decade, but no general, long-lasting trend can be assumed based on this data set. The spring seasons of 2008 and 2009 were extremely dry in about half of the zones, and in 2009, the dry spring was followed by a dry summer. As a result, 2009 was one of the few years with drought conditions in all of Ethiopia, both on seasonal and annual scales. On the national level, 2009 was the second driest year in the record, after 1984, and drier than 2002. In the southern highlands, 2009 was the driest year in the record, whereas in the rest of the country, previous droughts were more extreme. In the northeastern Rift Valley, the annual amount of precipitation was as low as 29 % of the mean this year, compared to 18 % in 1984. Fluctuations of this size were not experienced in any other zones, receiving at least 50 % of the annual mean precipitation in the driest year. In the central highlands, the annual precipitation was never less than 84 % of the mean.

In the three southernmost zones, where the spring season is the most important rainy season, linear regression showed a decline in precipitation both in the spring (2.6 mm/year), the summer (2.2 mm/year), and annually (5.4 mm/year). This is in accordance with previous studies (Seleshi and Camberlin 2006; Seleshi and Zanke 2004; Williams and Funk 2011; Funk et al. 2008).

In the rest of the country, those zones where the summer rains are most important, the linear regression analysis does not give us a reason for suggesting a corresponding decrease, neither on seasonal nor annual scale. This is in accordance with studies using records that ended in 2002/2003. However, signs of the decline in spring precipitation during 1979–2009 found

by Williams and Funk (2011) are present, as there has been a cluster of dry spring seasons during the last 10–15 years. Not only were the spring seasons of 2008–2011 among the driest during this period, but with the exception of 2001, almost nationwide spring droughts also occurred during 1999–2004.

The spatial drought pattern from year to year varies, to a large extent reflecting the variation in the seasonal precipitation cycle between the zones. Ethiopian precipitation exhibits great spatial variation, both in the average year, and when it comes to interannual variability. This affects the drought patterns. In a few years, mainly 1984 and 2009, drought conditions prevailed in all of Ethiopia, on both seasonal and annual time scales. In most historic drought years, the problem was of a more local or regional character, affecting only some parts of the country, and not necessarily in the same season. Due to this variation, there were no years without at least mild annual drought in at least one zone. Together with the severe effect of even small precipitation deficits on the mainly rain-fed agriculture (World Bank 2005), this helps to build the picture of Ethiopia as specifically drought-prone.

If the tendency of dry springs persists in the future, the risk of serious drought years may increase in all of Ethiopia; in the south because the spring is the main rainy season. In northern and central Ethiopia, where the summer is the main rainy season, the outcome is less obvious. But unless physical mechanisms act against it, an increase in spring droughts increases the probability of the occasional dry summer having been preceded by a dry spring. As a result, droughts may more frequently last throughout the agricultural growth season, as in the two driest years during 1971–2010: 1984 and 2009.

## Acknowledgment

This work has been carried out with support from the University of Bergen. It has also received support from the Bjerknes Centre for Climate Research and the Ethiopian Malaria Prediction System project funded by the Norwegian Programme for Development, Research and Education (NUFU). We thank the National Meteorological Agency of Ethiopia for providing the precipitation data, Tagel Gebrehiwot for valuable information about the data, and an anonymous reviewer for constructive suggestions.

## References

- Addis K (2009). Drought and famine: Ethiopia's cycle continues. <http://www.time.com/time/world/article/0,8599,1915544,00.html>. Accessed 14 October 2011
- Adler RF, Huffman GJ, Chang A, Ferraro R, Xie P-P, Janowiak J, Rudolf B, Schneider U, Curtis S, Bolvin D, Gruber A, Susskind J, Arkin P, Nelkin E (2003). The version-2 Global Precipitation Climatology Project (GPCP) monthly precipitation analysis (1979-present). *J. Hydrometeorol.* 4(6):1147–1167
- Berrisford P, Dee D, Fielding K, Fuentes M, Kållberg PW, Kobayashi S, Uppala SM (2009). The ERA-Interim archive. ERA report series, vol 1. ECMWF, Reading
- Bewket W, Conway D (2007). A note on the temporal and spatial variability of rainfall in the drought-prone Amhara region of Ethiopia. *Int. J. Climatol.* 27(11):1467–1477
- Bhalla N (2000). Children die in Ethiopian drought. <http://news.bbc.co.uk/2/hi/africa/696160.stm>. Accessed 20 December 2011

- Broad K, Agrawala S (2000). Climate: the Ethiopia food crisis—uses and limits of climate forecasts. *Science* 289(5485):1693–1694
- CERF (2006) CERF in Ethiopia (2006). Central Emergency Response Fund. <http://ochaonline.un.org/Default.aspx?tabid01755>. Accessed 20 December 2011
- Cheung WH, Senay GB, Singh A (2008). Trends and spatial distribution of annual and seasonal rainfall in Ethiopia. *Int. J. Climatol.* 28 (13):1723–1734
- Conway D. (2000). The climate and hydrology of the Upper Blue Nile River. *Geogr J* 166(1):49–62
- Conway D. Bewket CMW (2004). Over one century of rainfall and temperature observations in Addis Ababa, Ethiopia. *Int. J. Climatol.* 24(1):77–91
- Conway D, Schipper ELF (2011). Adaptation to climate change in Africa: challenges and opportunities identified from Ethiopia. *Glob Environ Chang* 21(1):227–237. doi:10.1016/j.gloenvcha.2010.07.013
- Degefu W (1987). Some aspects of meteorological drought in Ethiopia. In: Glantz MH (ed) *Drought and hunger in Africa. Denying famine a future*. Press Syndicate of the University of Cambridge, Cambridge
- Dinku T, Ceccato P, Grover-Kopec E, Lemma M, Connor SJ, Ropelewski CF (2007). Validation of satellite rainfall products over East Africa's complex topography. *Int J Remote Sensing* 28(7):1503–1526
- Edossa D, Babel M, Das Gupta A (2010). Drought analysis in the Awash River Basin, Ethiopia. *Water Resour. Manag.* 24(7):1441–1460. doi:10.1007/s11269-009-9508-0
- Edwards DC, McKee TB (1997). Characteristics of 20th century drought in the United States at multiple time scales. Atmospheric science paper. Colorado State University, Dept. of Atmospheric Science, Fort Collins, Colorado
- Findlater J (1969a). Interhemispheric transport of air in the lower troposphere over the western Indian Ocean. *Q. J. R. Meteorol. Soc.* 95(404):400–403

- Findlater J (1969b). A major low-level air current near the Indian Ocean during the northern summer. *Q. J. R. Meteorol. Soc.* 95(404):362–380
- Findlater J (1977). Observational aspects of the low-level cross equatorial jet stream of the western Indian Ocean. *Pur. Appl. Geophys.* 115(5):1251–1262
- Flohn H (1987). Rainfall teleconnections in northern and northeastern Africa. *Theor. Appl. Climatol.* 38(4):191–197
- Funk C, Asfaw A, Steffen P, Senay GB, Rowland J, Verdin J (2003). Estimating Meher crop production using rainfall in the 'long cycle' region of Ethiopia. FEWS-NET Special Report. USGS/FEWS/USAID
- Funk C, Senay G, Asfaw A, Verdin J, Rowland J, Korecha D, Eilerts G, Michaelsen J, Amer S, Choularton R (2005). Recent drought tendencies in Ethiopia and equatorial-subtropical eastern Africa. FEWS NET, vol 1.
- Funk C, Dettinger MD, Michaelsen JC, Verdin JP, Brown ME, Barlow M, Hoell A (2008). Warming of the Indian Ocean threatens eastern and southern African food security but could be mitigated by agricultural development. *PNAS* 105:11081–11087
- Gebrehiwot T, van der Veen A, Maathuis B (2011). Spatial and temporal assessment of drought in the northern highlands of Ethiopia. *Int. J. Appl. Earth Obs. Geoinf.* 13(3):309–321. doi:10.1016/j.jag.2010.12.002
- Griffiths JF (ed) (1972). Ethiopian highlands, vol 10. World survey of climatology. Elsevier, Amsterdam
- Guttman NB (1999). Accepting the standardized precipitation index: a calculation algorithm. *JAWRA J. Am. Water Resour. Assoc.* 35(2):311–322.
- Harrison GA (ed) (1988). Famine. Biosocial Society Symposium Series, vol 1. Oxford University Press, New York
- Huffman GJ, Adler RF, Bolvin DT, Gu G (2009). Improving the global precipitation record: GPCP version 2.1. *Geophys Res. Lett.* 36 (L17808).

- Husak GJ, Michaelsen J, Funk C (2007). Use of the gamma distribution to represent monthly rainfall in Africa for drought monitoring applications. *Int. J. Climatol.* 27(7):935–944.
- Korecha D, Barnston AG (2007). Predictability of June-September rainfall in Ethiopia. *Mon. Weather Rev.* 135(2):628–650
- Leroux M (2001). *The meteorology and climate of tropical Africa*, 2<sup>nd</sup> ed. Springer, Chichester
- Levin NE, Zipser EJ, Cerling TE (2009). Isotopic composition of waters from Ethiopia and Kenya: insights into moisture sources for eastern Africa. *J. Geophys. Res.* 114(D23306).
- Lloyd-Hughes B, Saunders MA (2002). A drought climatology for Europe. *Int. J. Climatol.* 22(13):1571–1592.
- Mattsson JO, Rapp A (1991). The recent droughts in Western Ethiopia and Sudan in a climatic context. *Ambio* 20(5):172–175
- McCann JC (1990) A great agrarian cycle? Productivity in highland Ethiopia, 1900 to 1987. *J. Interdiscip. Hist.* 20(3):389–416
- McKee TB, Doesken NJ, Kleist J (1993). The relationship of drought frequency and duration to time scales. Paper presented at the Eighth Conference on Applied Climatology, Anaheim, California, 17–22 January 1993
- Meze-Hausken E (2004). Contrasting climate variability and meteorological drought with perceived drought and climate change in northern Ethiopia. *Clim. Res.* 27:13–31
- Mishra AK, Singh VP (2010). A review of drought concepts. *J. Hydrol.* 391(1–2):202–216.
- Mohamed YA, van den Hurk BJJM, Savenije HHG, Bastiaanssen WGM (2005). Hydroclimatology of the Nile: results from a regional climate model. *Hydrol. Earth Syst. Sci.* 9:263–278
- Nebehay S (2011). Worst drought in 60 years hitting Horn of Africa: U.N. <http://www.reuters.com/article/2011/06/28/us-africa-drought-idUSTRE75R2JQ20110628>. Accessed 20 December 2011

- Nicholson SE (1986). The spatial coherence of African rainfall anomalies: interhemispheric teleconnections. *J. Climate Appl. Meteorol.* 25(10):1365–1381.
- Ntale HK, Gan TY (2003). Drought indices and their application to East Africa. *Int. J. Climatol.* 23(11):1335–1357.
- Palmer WC (1965). Meteorological drought, vol 45. U.S. Weather Bureau Research Paper Washington, D.C.
- Riddle EE, Cook KH (2008). Abrupt rainfall transitions over the Greater Horn of Africa: observations and regional model simulations. *J. Geophys. Res.* 113(D15109):14
- Segele ZT, Lamb PJ (2005). Characterization and variability of Kiremt rainy season over Ethiopia. *Meteorog. Atmos. Phys.* 89(1):153–180
- Segele ZT, Lamb PJ, Leslie LM (2009). Large-scale atmospheric circulation and global sea surface temperature associations with Horn of Africa June-September rainfall. *Int. J. Climatol.* 29(8):1075–1100
- Seleshi Y, Camberlin P (2006). Recent changes in dry spell and extreme rainfall events in Ethiopia. *Theor. Appl. Climatol.* 83:181–191
- Seleshi Y, Zanke U (2004). Recent changes in rainfall and rainy days in Ethiopia. *Int. J. Climatol.* 24(8):973–983
- Sen A (1981). Poverty and famines: an essay on entitlement and deprivation. Oxford University Press, Oxford
- Shang H, Yan J, Gebremichael M, Ayalew SM (2011). Trend analysis of extreme precipitation in the northwestern highlands of Ethiopia with a case study of Debre Markos. *Hydrol. Earth Syst. Sci.* 15 (6):1937–1944.
- Shanko D, Camberlin P (1998). The effects of the Southwest Indian Ocean tropical cyclones on Ethiopian drought. *Int. J. Climatol.* 18 (12):1373–1388
- Simmons AJ, Uppala SM, Dee D, Kobayashi S (2006). ERA-Interim: new ECMWF reanalysis products from 1989 onwards. *ECMWF News* 110:25–35

- Torry W (1986). Economic development, drought, and famines: some limitations of dependency explanations. *GeoJournal* 12(1):5–18.
- Trenberth KE, Stepaniak DP, Caron JM (2002). Accuracy of atmospheric energy budgets from analyses. *J. Climate* 15(23):3343–3360
- Uppala SM, Dee D, Kobayashi S, Berrisford P, Simmons AJ (2008). Towards a climate data assimilation system: status update of ERA-Interim. *ECMWF Newsletter*. ECMWF, Reading
- USAID/FEWS (2011). East Africa: past year one of the driest on record in the eastern Horn.
- Viste E, Sorteberg A (2011). Moisture transport into the Ethiopian highlands. *Int J Climatol*. doi:10.1002/joc.3409
- Viste E, Sorteberg A (2012). The effect of moisture transport variability on Ethiopian summer precipitation. *Int. J. Climatol*. doi:10.1002/joc.3566
- Webb P, Braun J (1994). *Famine and food security in Ethiopia*. Wiley, New York
- Webb P, Braun Jv, Yohannes Y (1992). *Famine in Ethiopia: policy implications of coping failure at national and household levels*. Research Reports, vol 92. International Food Policy Research Institute, Washington, D.C.
- Williams A, Funk C (2011). A westward extension of the warm pool leads to a westward extension of the Walker circulation, drying eastern Africa. *Clim. Dyn.* 37(11–12):2417–2435.
- Williams A, Funk C, Michaelsen J, Rauscher S, Robertson I, Wils T, Koprowski M, Eshetu Z, Loader N (2011). Recent summer precipitation trends in the Greater Horn of Africa and the emerging role of Indian Ocean sea surface temperature. *Climate Dynamics*.
- World Bank (2005). *Well-being and poverty in Ethiopia. The role of agriculture and agency*. Poverty Reduction and Economic Management 2 (AFTP2). World Bank

- Wu H, Hayes MJ, Wilhite DA, Svoboda MD (2005). The effect of the length of record on the standardized precipitation index calculation. *Int. J. Climatol.* 25(4):505–520.
- Wu H, Svoboda MD, Hayes MJ, Wilhite DA, Wen F (2007). Appropriate application of the standardized precipitation index in arid locations and dry seasons. *Int. J. Climatol.* 27 (1):65–79.
- Yue S, Pilon P, Cavadias G (2002). Power of the Mann–Kendall and Spearman's rho tests for detecting monotonic trends in hydrological series. *J. Hydrol.* 259(1–4):254–271.